



**Dissecting the role of Complex I ROS
production via forward and reverse electron
transport in the brain of *Drosophila
melanogaster***

Charlotte Graham

Doctor of Philosophy
Institute for Cellular and Molecular
Biosciences
Newcastle University

Acknowledgements

First of all, I would like to thank my supervisor, Professor Alberto Sanz, who provided me with this opportunity. Thank you for your guidance and support over the last four years. I am extremely grateful for the chance to be part of your lab and the skills you have taught me.

Secondly to Dr Joao Passos and Dr Gabi Saretzki, who were both part of my annual progression panel. Thank you for the valuable advice and support, at our meetings.

Thank you to my lab group, Rhoda, Filippo, Elise and Becca. I am very lucky to have had such a close friendship with my colleagues. Because of all of you, I have so many great memories that I can take away from my PhD. In addition, you have always been there to help me when things in the lab weren't going to plan. I will miss our daily lunch breaks, Filippo's pranks (I think) and our office chats. A special thanks to Rhoda, who has become my "lab big sister" over these past 4 years and helped me overcome many hurdles, in and outside of work. Even when I didn't believe in myself, you were always there to tell me otherwise, along with the best advice I could have hoped for. Thanks also goes to the other fellow PhD students in CAV, who have contributed to my time here including James, Lucy and George.

In the first few weeks of my PhD I was introduced to Beth, Tass, Sarah, Emma and Jess, the "PhD girls". I am so thankful that we all stayed in touch and that we have been able to share this experience with each other. I have lost count of the number of times they have cheered me up after a bad day (mostly with wine and good food). With you guys I knew that I wasn't alone during these 4 years.

A special thanks to Jennah, who I met during my masters, I knew straight away I had made a friend for life. Thank you for your words of wisdom throughout my PhD, especially the 'PhD survival package' you sent me in the final months, when I needed it the most.

To my best friends Rebs and Richard, who I've known for over ten years, thank you for always being there for me and making me laugh, a lot, when I was feeling down. Being part of Reb's wedding in the final months of my PhD gave me something to

look forward to and I will cherish those memories forever. Richard, thank you for always being at the end of the phone when I needed you.

To everyone I have lived with throughout my PhD including Andy, Sarah, Corrie and Rachel. Thank you for being there when I got home from work, especially after a bad day of experiments, and cheering me up. Andy, you always knew the right thing to say and even though we don't live in the same city anymore, I am forever grateful for our friendship, even when you 'rustle my jimmies'. To Sarah, who is still willing to live with me, even after our undergraduate years at the University of Manchester and now during my time at Newcastle University. I have so many fond memories with you over the past four years. Thank you for our weekend trips to Ikea, adventures around Northumberland and nights out to Cosy Joes, which kept me going and gave me something to look forward to.

Last but not least, I would like to thank my family, Mum, Dad and my brother, David. Everything that has happened over these past four years has only made me realise how truly lucky I am, to have such an amazing and supportive family around me. You have never doubted me once and because of that you make me feel like I can achieve anything. Thank you for everything that you have done and continue to do for me. I hope you know how appreciative I am and how much I love you all (as well as Max, our dog).

Abstract

The dual nature of reactive oxygen species (ROS) is a widely recognised paradox. For many years, mitochondrial ROS were characterised as the main cause of ageing and chronic ROS production was documented in many age-related diseases. In contrast, recent studies have described ROS as signalling molecules essential for maintaining cellular homeostasis.

Further experimentation has revealed that the extent of ROS production, as well as the location, can be important in determining the behaviour of ROS. The best example is the process known as Reverse Electron Transport (RET). RET is associated with a large increase in site-specific ROS production at CI and is responsible for stimulating key signalling pathways that control stress adaptation and cellular fate. Additionally, the expression of the alternative NADH dehydrogenase, Ndi1, which promotes ROS-RET, leads to extension of lifespan in *Drosophila melanogaster*. Exploring ROS-RET signalling may be instrumental in understanding the role of ROS in health and disease.

In the following chapters, I investigate the mechanisms behind ROS-RET. I use *ex vivo* ROS measurements in the brain of *Drosophila melanogaster* to demonstrate that ROS-RET occurs under physiological conditions when flies are exposed to heat stress. I describe in detail how manipulation of the electron transport chain affects the occurrence of ROS-RET. My results reveal that the entry of electrons through CI and CII is essential for ROS-RET to occur. However, blocking the exit of electrons (CIII-CIV) increases ROS production but not via ROS-RET. Finally I have performed a genome-wide RNAi screen, taking advantage of the alternative oxidase (AOX) that suppresses ROS-RET, where I have found new candidate genes responsible for regulating mitochondrial ROS levels.

In summary, I provide evidence of how ROS-RET can be regulated *in vivo* including its physiological stimulation, factors essential for its generation and new genes involved in its regulation.

List of Abbreviations

ATP	Adenosine triphosphate
AKG	alpha-ketoglutarate
AOX	Alternative oxidase
ASK1	Apoptosis signal-regulating kinase 1
ATPIF1	ATPase inhibitory factor 1
BDSC	Bloomington <i>Drosophila</i> Stock Centre
BNE	Blue Native Electrophoresis
BSA	Bovine serum albumin
<i>C.elegans</i>	<i>Caenorhabditis. elegans</i>
Ca ²⁺	Calcium
CAC	Citric acid cycle
CI	Complex I
CII	Complex II
CIII	Complex III
CIV	Complex IV
CN	Cyanide
CO	Carbon monoxide
CoQ	Ubiquinone
CoQH ₂	Ubiquinol
cpYFP	Circularly permuted Yellow Fluorescent Protein
CV	Complex V
Cyt C	Cytochrome C
cyt c1	Cytochrome c1
<i>daGAL4</i>	<i>daughterless-Gal4</i>
DAH	Dahomey
	Database for Annotation, Visualization and Integrated
DAVID	Discovery
DCF	2',7'-dichlorofluorescein
DHE	Dihydroethidium
DHODH	Dihydroorotate dehydrogenase
DHRSX	dehydrogenase/reductase X-linked
DMSO	Dimethylsulfoxide

ECM	extracellular matrix
	Ethyleneglycol-bis(2-amino-ethylether)-N,N,N',N'-tetracetic acid
EGTA	acid
ER	Endoplasmic reticulum
ETC	Electron transport chain
ETF-QO	Electron-transferring-flavoprotein dehydrogenase
EtOH	Ethanol
FADH ₂	Flavin adenine dinucleotide
FCCP	Carbonyl cyanide-p-trifluoromethoxyphenylhydrazone
Fe-S	Iron-sulphur
FMN	Flavin mononucleotide
G3P	glycerol-3-phosphate
G3PDH	Glycerol-3-phosphate dehydrogenase
GO	Gene Ontology
GOF	Gain-of-function
GS	GeneSwitch
GSH	Glutathione
GSSG	Glutathione disulphide
H ₂ DCF	2',7'-dichlorodihydrofluorescein diacetate
H ₂ F	Dihydrofluorescein
H ₂ O ₂	Hydrogen peroxide
H ₂ S	Hydrogen sulphide
HIF-1	Hypoxia-inducible factor
HO ₂ ·	Hydroperoxyl radical
HS	Heat stress
Hyper	Hydrogen Peroxide protein
IMM	Inner mitochondrial membrane
IMS	Intermembrane space
I _Q	Ubiquinone-binding site
IR	Ischemia-reperfusion
KCl	Potassium Chloride
KCN	Potassium cyanide
KH ₂ PO ₄	Potassium Phosphate
KOH	Potassium Hydroxide

LCMS	Liquid chromatography MS
LDLs	Low-density lipoproteins
LOF	Loss-of-function
LOX	Lipoxygenases
LPS	Lipopolysaccharides
LS	Leigh Syndrome
MAO	Monoamine oxidases
MAPK	Mitogen-activated protein kinase
MFRTA	Mitochondrial free radical theory of ageing
Mitohormesis	Mitochondrial hormesis
MPTP	1-methyl-4-phenyl-1,2,3,6-tetrahydropyridine
MRP	Mitochondrial ribosomal proteins
MS	Mass spectrometry
mtDNA	Mitochondrial DNA
NaAc	Sodium Acetate
NADH	Nicotinamide adenine dinucleotide
Nde1	NADH dehydrogenase external 1
Nde2	NADH dehydrogenase external 2
Ndi1	NADH dehydrogenase internal 1
NO	Nitric oxide
NOS	Nitric oxide synthase
NOX	NADPH oxidases
O ₂	Oxygen
O ₂ ⁻	Superoxide anion
OH ⁻	Hydroxyl radical
OMM	Outer mitochondrial membrane
Orp1	Oxidant receptor peroxidase 1
OSCP	Oligomycin sensitivity-conferring protein
OXPPOS	Oxidative phosphorylation
PBS	Phosphate Buffered Saline
P _i	Inorganic phosphate
PI3K-Akt	Phosphoinositide-3-kinase-Akt pathway
pmf	Proton motive force
PUFAs	Polyunsaturated fatty acids

QH-	Ubisemiquinone radical
RCS	Reactive carbonyl species
RET	Reverse electron transport
RNAi	RNA interference
RNS	Reactive nitrogen species
roGFP	Redox-oxidation Green Fluorescent Protein
ROS	Reactive oxygen species
rRNAs	ribosomal RNAs
RU486	Mifepristone
SDH	Succinate dehydrogenase
SDR	short-chain dehydrogenase/reductase
SOD	Superoxide dismutase
TIM23	Translocase of the inner membrane 23
Tko	Technical knockout
TMPD	N,N,N',N'-Tetramethyl-p-phenylenediamine dihydrochloride
TOM	Translocase of the outer membrane
TPP	Tri-phenyl-phosphonium
tRNAs	transfer RNAs
Trx2	Thioredoxin 2
<i>tubGS</i>	<i>tubulin-Gene-Switch</i>
UAS	Upstream activator sequence
VDRC	Vienna <i>Drosophila</i> Resource Centre
$^1\text{O}_2$	Singlet oxygen

Table of Contents

Acknowledgements	iii
Abstract	i
List of Abbreviations	ii
Table of Contents	vi
List of Figures	x
List of Tables	xiii
Chapter 1 Introduction	1
1.1 Overview of Mitochondria.....	1
1.1.1 Origins and evolution of mitochondria.....	2
1.1.2 Structure and function of the mitochondria	2
1.1.3 The electron transport chain (ETC).....	5
1.1.4 Mitochondrial mobile electron carriers	6
1.1.5 Complex I (CI)	7
1.1.6 Complex II (CII).....	8
1.1.7 Complex III (CIII).....	9
1.1.8 Complex IV (CIV)	11
1.1.9 The Chemiosmosis Theory.....	12
1.1.10 ATP Synthase	13
1.1.11 Alternative respiratory enzymes; AOX and Ndi1	14
1.2 Reactive Oxygen Species (ROS).....	17
1.2.1 Antioxidants.....	20
1.2.2 Oxidative stress	21
1.2.3 ROS as signalling molecules.....	23
1.2.4 Cellular ROS	26
1.2.5 Mitochondrial ROS.....	28
1.2.6 Methods of measuring mitochondrial ROS levels; resolution vs physiological relevance.....	31
1.2.7 The physiological relevance of site-specific ROS production at CIII.....	36
1.2.8 The physiological relevance of site-specific ROS production via Reverse Electron Transport (RET) at CI	38
1.3 Mitochondrial ROS and age-related diseases	41
1.3.1 Historical importance of MFRTA; evidence for and against	43

1.3.2 The concept of hormesis	44
1.3.3 Importance of studying mitochondrial ROS signaling.....	45
1.4 <i>Drosophila melanogaster</i> as a model system.....	46
1.4.1 Advantages of using <i>Drosophila</i> as a model organism	48
1.4.2 GAL4/UAS system to control gene expression.....	49
1.4.3 Genetic screening	51
1.4.4 <i>Drosophila</i> and ageing studies	51
1.4.5 Studying mitochondrial function in <i>Drosophila</i>	52
1.5 Aims	54
Chapter 2 Materials and Methods	56
2.1 Reagents.....	56
2.2 Fly Husbandry.....	59
2.2.1 Preparation of the fly food	64
2.2.2 Addition of ETC inhibitors to the fly food.....	65
2.2.3 Heat Stress model	65
2.2.4 Lifespan Experiments	66
2.2.5 Genome-Wide RNAi Screen.....	66
2.3 Quantitative real-time PCR (qPCR)	69
2.3.1 RNA Extraction.....	69
2.3.2 cDNA Synthesis	69
2.3.3 q-PCR using the Standard Curve Method	70
2.4 High-Resolution Respirometry measurements.....	73
2.5 ROS Measurements in the <i>Drosophila</i> Brain.....	75
2.6 Statistical Analysis.....	76
Chapter 3 Heat Stress Induces ROS-RET physiologically in <i>Drosophila melanogaster</i>	77
3.1 Reverse Electron Transport	77
3.1.1 RET Under Physiological Conditions	77
3.1.2 Validating RET at Complex I	80
3.2 Results	83
3.2.1 Heat stress increases ROS production	83
3.2.2 Heat Stress changes the way CI produces ROS.....	88
3.2.3 Dissipating proton motive force with FCCP prevents RET during heat stress.	91
3.2.4 ROS produced during heat stress originates from mitochondria	95

3.2.5 Heat stress cannot stimulate RET in old flies	99
3.2.6 Intermittent induction of ROS-RET and its effect on lifespan	101
3.2.7 Heat stress does not extend lifespan in <i>Drosophila melanogaster</i>	104
3.3 Discussion.....	108
Chapter 4 Effect of limiting the entry of electrons into the mitochondrial ETC on ROS-RET	112
4.1 Manipulating the Redox State of CoQ	112
4.2 Reduction of CI activity	114
4.3 A fully functional CI is required for ROS-RET	116
4.4 Reduction of CII activity	120
4.5 CII is required for triggering ROS-RET	122
4.6 Discussion.....	126
Chapter 5 Effect of limiting the exit of electrons from the mitochondrial ETC on ROS-RET	128
5.1 Halting the exit of electrons	128
5.2 Maintaining a High Proton Motive Force.....	129
5.3 Decreasing Complex III activity	131
5.4 The effect of decreasing CIII activity on ROS-RET signalling.....	133
5.4.1 The CIII inhibitor, myxothiazol, does not trigger ROS-RET in the brain of <i>Drosophila melanogaster</i>	133
5.4.2 Genetic depletion of CIII does not stimulate ROS-RET.....	138
5.5 Decreasing Complex IV activity	140
5.6 Inhibition of CIV increases ROS production but does not trigger ROS-RET ..	142
5.6.1 Pharmacological inhibition of CIV increases ROS production.	142
5.6.2 Genetic depletion of CIV elevates ROS production but does not trigger ROS-RET	145
5.7 Reduction of CV activity	149
5.8 Genetic inhibition of CV triggers ROS-RET	152
5.8.1 Oligomycin specifically inhibits CV without initiation of a ROS-RET signal.	152
5.8.2 Genetic depletion of CV, using <i>ATPSynthase-δ-KD</i> line increases ROS via RET.....	157
5.8.3 Alpha-ketoglutarate (AKG) is not a CV inhibitor in <i>Drosophila melanogaster</i>	160
5.8.4 J147 does not significantly alter mitochondrial respiration in <i>Drosophila melanogaster</i>	162

5.9 Discussion.....	165
Chapter 6 A Genome-Wide RNA Interference screen to identify genes involved in the regulation of ROS-RET.....	170
6.1 The importance of genome-wide RNA interference screens	170
6.2 The use of the alternative oxidase; AOX	170
6.3 Hypothesis behind the screen	173
6.4 Screening strategy.....	175
6.5 Analysis of the identified hits	177
6.6 Selection criteria of candidate genes	191
6.7 Effect of knocking down candidate genes on brain mitochondrial ROS levels	193
6.8 AOX rescues the knockdown of genes that induce RET-dependent and RET-independent ROS	196
6.9 Discussion.....	202
Chapter 7 General Discussion.....	206
7.1 Introduction	206
7.2 Main findings and contributions to the field.....	208
7.3 Future Work	217
7.4 Final Conclusions	221
References	223

List of Figures

Figure 1.1 Diagram of mitochondria.....	4
Figure 1.2 Schematic diagram of the ETC.	6
Figure 1.3 Diagram displaying the structure of Complex I.	8
Figure 1.4 Diagram displaying the structure of Complex II.	9
Figure 1.5 Diagram displaying the structure of Complex III.	11
Figure 1.6 Diagram displaying the structure of Complex IV.....	12
Figure 1.7 Diagram displaying the structure of ATP Synthase.	14
Figure 1.8 Schematic diagram showing the expression of alternative respiratory enzymes, Ndi1 and AOX.....	17
Figure 1.9 Schematic diagram demonstrating the sites of ROS production from CI and CIII of the ETC.	30
Figure 1.10 Diagram of the Drosophila life cycle.....	48
Figure 1.11 Schematic diagram of the GAL4-UAS and GeneSwitch GAL4 (GS) system.....	50
Figure 3.1 Schematic diagram illustrating the differences in ROS production at CI during forward (FET) and reverse (RET) electron transport.	79
Figure 3.2 The effects of rotenone during FET and RET.....	81
Figure 3.3 The effect of FCCP in normal conditions.	82
Figure 3.4 Diagram demonstrating the ROS measurement protocol.	85
Figure 3.5 ROS measurements of flies subjected to heat stress over a 6 hour time course.	86
Figure 3.6 ROS measurements of flies subjected to 4 hours of heat stress.	87
Figure 3.7 The effect of rotenone on ROS production in normal conditions.	89
Figure 3.8 The effect of rotenone on ROS production during heat stress.....	90
Figure 3.9 The effect of FCCP on ROS production in non-stressed conditions.....	93
Figure 3.10 The effect of FCCP on ROS production during heat stress.	94
Figure 3.11 Diagram depicting the role of antioxidants inside the mitochondria.....	96
Figure 3.12 The effect of SOD2 overexpression on ROS production during heat stress.	97
Figure 3.13 The effect of mitochondrial-catalase expression on ROS production during heat stress.....	98

Figure 3.14 The effect of heat stress on ROS production in young and old flies.....	100
Figure 3.15 Diagram outlining the 3 different groups of the lifespan experiments as well as the 4 conditions used during the lifespan experiments and how this was applied on a weekly basis.	103
Figure 3.16 The effect of heat stress throughout the Drosophila lifespan.....	106
Figure 3.17 Comparison of the different groups from Drosophila lifespans.	107
Figure 4.1 Schematic diagram indicating the RNAi constructs used to target CI subunits.....	115
Figure 4.2 Effect of ND-75-KD on ROS production in non-stressed conditions and during heat stress.	118
Figure 4.3 Effect of ND-42-KD on ROS production in non-stressed conditions and during heat stress.	119
Figure 4.4 Schematic diagram showing the methods of CII inhibition used.....	121
Figure 4.5 Effect of malonate on ROS production in non-stressed conditions and during heat stress.	124
Figure 4.6 Effect of SdhD-KD on ROS production in non-stressed conditions and during heat stress.	125
Figure 5.1 Schematic diagram indicating the binding site of myxothiazol and the RNAi construct used to target the CIII UQRC-Q subunit.	132
Figure 5.2 The effect of myxothiazol on respiration.	135
Figure 5.3 The effect of myxothiazol (10, 50, 100 μ M) on ROS production in non-stressed conditions and during heat stress.	136
Figure 5.4 The effect of myxothiazol (500 μ M, 1 mM) on ROS production in non-stressed conditions and during heat stress.	137
Figure 5.5 The effect of UQCR-Q-KD on ROS production in non-stressed conditions and during heat stress.....	139
Figure 5.6 Schematic diagram indicating the binding site of CN and the RNAi construct used to target the CIV levy subunit.	141
Figure 5.7 The effect of CN on ROS production in non-stressed conditions and during heat stress	143
Figure 5.8 The effect of CN on ROS production in combination with the uncoupler, FCCP and the CIII inhibitor, myxothiazol.....	Error! Bookmark not defined.
Figure 5.9 The effect of levy-KD on ROS production in non-stressed conditions and during heat stress.....	147

Figure 5.10 The effect of levy-KD on ROS production in combination with the uncoupler, FCCP and the CIII inhibitor, myxothiazol.	148
Figure 5.11 Schematic diagram indicating the binding sites of oligomycin and AKG and the RNAi construct used to target the CV ATPsyn δ subunit.....	151
Figure 5.12 High-resolution respirometry measurements showing the inhibitory effect of oligomycin.....	154
Figure 5.13 The effect of oligomycin on ROS production in non-stressed conditions.	155
Figure 5.14 The effect of oligomycin in high concentrations and after 3 days in non-stressed conditions.....	156
Figure 5.15 The effect of ATPSyn δ -KD on ROS production in non-stressed conditions and during heat stress.	159
Figure 5.16 High-resolution respirometry demonstrating the effect of AKG on State 3 and 4 respiration.....	161
Figure 5.17 High-resolution respirometry demonstrating the effect of AKG on State 3 and 4 respiration, in comparison to oligomycin.	163
Figure 5.18 The effect of ATPIF1-OE on ROS production in non-stressed conditions and during heat stress.....	164
Figure 6.1 Schematic diagram showing how the expression of AOX by-passes CIII and CIV.....	172
Figure 6.2 Schematic diagram showing how the expression of AOX can manipulate ROS production from the ETC and rescue lethal phenotypes in KD lines.	174
Figure 6.3 Diagram displaying the strategy of the genome-wide RNAi screen.....	176
Figure 6.4 Schematic diagram of STRING analysis showing protein interactions between the 41 confirmed hits.....	190
Figure 6.5 ROS measurements of 12 candidate genes in normal conditions (25°C).	195
Figure 6.6 Characterisation of VhaPPA-1-1-KD flies.	199
Figure 6.7 Characterisation of Ppn-KD flies.	200
Figure 6.8 Characterisation of Cchl-KD flies.	201
Figure 7.1 The effect of CI ROS production in young versus old flies.....	211
Figure 7.2 Diagram displaying the ROS-RET signal.....	222

List of Tables

Table 2.1 List of chemical reagents.	56
Table 2.2 List of fly stocks.	61
Table 2.3 List of fly food ingredients.	64
Table 2.4 List of ETC inhibitors and their concentrations	65
Table 2.5 List of reagents used during cDNA synthesis.	70
Table 2.6 List of reagents used for qPCR.	71
Table 2.7 List of Primers.	72
Table 2.8 List of fluorophores used to measure ROS.	75
Table 6.1 Number of genes screened indicating lethal genes and lethal genes rescued by AOX.	179
Table 6.2 Functional Annotation Clustering Analysis of lethal genes.	180
Table 6.3 OXPHOS genes screened indicating the number of lethal genes (when knocked-down) and rescued by AOX.	183
Table 6.4 OXPHOS genes rescreened indicating the number of lethal genes (when knocked-down) and rescued by AOX.	183
Table 6.5 Confirmed candidate genes rescued by AOX.	184
Table 6.6 Functional Annotation Clustering Analysis of lethal genes rescued by AOX.	189

Chapter 1 Introduction

1.1 Overview of Mitochondria

Mitochondria are essential cytosolic organelles found in most eukaryotic cells. The primary role of mitochondria is the production of energy, in the form of adenosine triphosphate (ATP). ATP is popularly known as the cellular 'energy currency', as it is instrumental in allowing cells to perform all fundamental biological processes. Hence, mitochondria are most commonly referred to as the 'powerhouses of the cell' and are present in all human cell types, except for mature erythrocytes (Cedikova *et al.*, 2016). Additionally, mitochondria are responsible for other vital cellular functions and in the last two decades, have also been shown to participate in cellular signalling (Chandel, 2014), as I shall discuss below. The mitochondrial density of a cell varies between specific cell types, depending on the total energy demand. For example, mitochondria are more abundant in cells that require a continuous supply of energy, such as brain and muscle cells, which are metabolically highly active (van der Blik *et al.*, 2017). Most cells heavily rely on the energy that mitochondria generate to maintain cellular homeostasis. This includes the brain, the central organ of our nervous system, responsible for controlling our basic physiological functions, as well as being the centre of our consciousness that makes us human (Stefanatos and Sanz, 2018).

Given that mitochondria possess such an integral role in energy production within our cells, it is no surprise that the occurrence of mitochondrial dysfunction is associated with a wide range of diseases. There are two types of disease related to mitochondrial dysfunction, (i) mitochondrial diseases that are a consequence of mutations in mitochondrial proteins (Wallace, 1999) and (ii) diseases where mitochondrial dysfunction occurs independently of mutations in genes encoding mitochondrial proteins (Wallace, 2005). A few examples of the latter group includes; diabetes, metabolic syndrome and many neurodegenerative diseases, such as Parkinson's disease (Lane *et al.*, 2015). In addition, the link between mitochondria and ageing is well established and the accumulation of defective mitochondria is one of the hallmarks of the ageing process (Lopez-Otin *et al.*, 2013). For these reasons, mitochondrial research is at the forefront of current scientific agenda (Picard *et al.*, 2016). Scientists are focusing on attempting to elucidate the mechanisms behind

mitochondrial dysfunction, which could lead to the discovery of future therapeutics and solutions to facilitate healthy ageing (Sun *et al.*, 2016) (Cedikova *et al.*, 2016).

1.1.1 Origins and evolution of mitochondria

The origin of mitochondria began approximately 1.5 billion years ago, as single prokaryotic cells that were engulfed by primordial eukaryotic cells and later became dependent on each other, forming a symbiotic relationship (Margulis, 1975). Subsequently, the endosymbiont evolved into pleomorphic structures possessing a double membrane and their own circular double-stranded DNA, known today as mitochondria (Roger *et al.*, 2017). Over the millions of years of evolution, mitochondria have retained a small fraction of their genetic system. In humans, mitochondria are responsible for encoding 1% of mitochondrial proteins, amounting to 37 genes. The mitochondrial DNA encodes 13 core hydrophobic subunits of the respiratory chain, along with 22 transfer RNAs (tRNAs) and 2 ribosomal RNAs (rRNAs), required for mitochondrial protein synthesis (Anderson *et al.*, 1981). The nuclear DNA currently encodes the majority of mitochondrial proteins, as the original mitochondrial genes have been transferred over to the nucleus. Mitochondrial proteins encoded by the nuclear genome are synthesised in the cytoplasm and then imported into mitochondria via specific translocation machinery, involving mitochondrial-targeting sequences (Kang *et al.*, 2018). Since the endosymbiotic event, mitochondria have evolved into dynamic organelles and developed a range of vital cell signalling processes. The close relationship developed over time, between mitochondria and the rest of the cell, is crucial for maintaining cellular homeostasis (Malina *et al.*, 2018).

1.1.2 Structure and function of the mitochondria

The fundamental structure of mitochondria encompasses a double membrane, which defines two aqueous compartments (Figure 1.1). Individually, these 4 components each have their distinct roles in the production of energy (McCarron *et al.*, 2013). The outer mitochondrial membrane (OMM), which resembles eukaryotic membranes in function and biochemical composition, separates the contents of the mitochondria from the cytosol. It functions in regulating the passage of proteins and small molecules in and out of the mitochondria (Crompton, 1999). This is predominantly mediated by the Translocase of the outer membrane (TOM) complex, which resides

in the OMM and governs the transport of larger polypeptides, through the recognition of mitochondrial targeting sequences (Hill *et al.*, 1998) (Endo and Yamano, 2010). Also present are a family of porins, which allow smaller (<10 kDa) proteins and ions to freely diffuse across the membrane (Weeber *et al.*, 2002). Unlike the OMM, the inner mitochondrial membrane (IMM) is only permeable to small-uncharged molecules such as oxygen, carbon dioxide and water. In order to complete the transport of nascent mitochondrial proteins, the translocase of the inner membrane 23 (TIM23) family, is present to facilitate the final steps of the TOM complex (Wiedemann and Pfanner, 2017). The IMM assists with the generation of energy as it accommodates the electron transport chain (ETC), necessary for oxidative phosphorylation (OXPHOS). It forms characteristic folds known as cristae, to establish a high surface area, thereby increasing the abundance of the respiratory chain and the yield of energy production (Cogliati *et al.*, 2016).

Another key component involved in the production of energy is the intermembrane space (IMS), formed in-between the OMM and the IMM. Transportation of protons across the IMM to the IMS, by respiratory complexes within the ETC, allows the creation of an electrochemical proton gradient, which drives ATP synthesis (Berry *et al.*, 2018). Due to the permeability of the OMM, the IMS is chemically equivalent to the cytoplasm, unlike the mitochondrial matrix, (the second aqueous compartment), which is enclosed by the IMM (Mannella *et al.*, 2001). The matrix is a dense environment and residence to many enzymes involved in the citric acid cycle (CAC) and β -oxidation, as well as the mitochondrial DNA (mtDNA). The CAC results in the oxidation of pyruvate and amino acids, whilst β -oxidation predominantly oxidises fatty acids. The circular mtDNA found in the mitochondrial matrix is stored into structures known as nucleoids. Nucleoids are spherical structures lacking a membrane and filled with a protein network, which function to regulate mitochondrial DNA transcription and replication and protect the mtDNA from damage (Lee and Han, 2017). Additionally, the mitochondrial matrix possesses nuclear-encoded ribosomes, necessary for the transcription and translation of the mitochondrial proteome (Mai *et al.*, 2017). The matrix is also required for the maintenance of the electrochemical proton gradient across the IMM. Here, the matrix is kept at a high pH of ~ 7.8 , in comparison to the IMS, which is kept at $\sim 7.0-7.4$, to make proton translocation into the IMS favourable (Porcelli *et al.*, 2005).

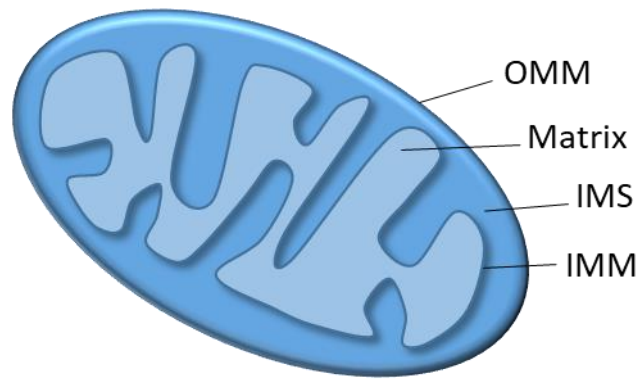


Figure 1.1 Diagram of mitochondria

This diagram highlights the double membrane structure which mitochondria possess (OMM (outer mitochondrial membrane) and IMM (inner mitochondrial membrane), giving rise to the two aqueous compartments (IMS (intermembrane space) and matrix).

The complex structural architecture of mitochondria is responsible for the diverse array of biological processes that occur within these organelles. One of the major processes occurring in mitochondria is OXPHOS, which in many cell types supplies most of the cellular ATP (Mookerjee *et al.*, 2017). OXPHOS receives electrons from CAC and β -oxidation, two other metabolic processes that occur within the mitochondria (Bratic and Trifunovic, 2010). During β -oxidation, fatty acids transported into the mitochondrial matrix are oxidised by a 4-step reaction, to ultimately produce acetyl-CoA. Acetyl-CoA can then be further oxidised by CAC, leading to the production of reducing equivalents, used to feed electrons into the respiratory chain (Sajnani *et al.*, 2017). The central role of mitochondria in OXPHOS, CAC and β -oxidation highlight their importance. However, they also contribute to a wide range of other biochemical reactions, for example the ornithine cycle. This process is responsible for converting ammonia into urea, in which the first two steps occur within the mitochondria. Additionally, mitochondria are also essential for the production of iron-sulphur clusters that are involved in electron transfer processes, in the mitochondria and other cellular compartments (Lill, 2009). Without mitochondria and consequently iron-sulphur clusters, essential cellular processes, such as nuclear DNA replication or transcription, cannot occur (Stehling and Lill, 2013).

Mitochondria are also pivotal for maintaining and regulating calcium (Ca^{2+}) homeostasis. Ca^{2+} is sequestered in the mitochondrial matrix and used for signalling

purposes. The release of Ca^{2+} from mitochondria can influence different cell survival pathways, such as apoptosis and autophagy (Rizzuto *et al.*, 2012). Furthermore, mitochondria have also been reported to play a role in numerous signalling pathways including growth factor signalling, hypoxic and immune responses and processes of cellular differentiation and migration through the production of reactive oxygen species (ROS), discussed in detail below (Tait and Green, 2012).

1.1.3 The electron transport chain (ETC)

The primary function of mitochondria is the production of energy through the process of OXPHOS. In many cell types, this is the primary source of ATP generation, covering an approximate 80% of cellular energy demand (Papa *et al.*, 2012). The synthesis of ATP requires the intricate arrangement of four individual complexes (complex I, II, III, and IV) collectively known as the ETC and the mitochondrial ATP synthase (complex V). These five complexes are embedded into the IMM, and each possesses its own distinct functions, which co-operatively orchestrate the generation of energy (Rutter *et al.*, 2010). The first four complexes (complexes I – IV) participate in the step-wise transfer of electrons to the final electron acceptor, which in aerobic organisms is oxygen.

Electrons enter the ETC via reducing equivalents from CAC or β -oxidation, such as NADH (nicotinamide adenine dinucleotide) and FADH_2 (flavin adenine dinucleotide), which function to shuttle electrons to complexes I and II (CI and CII), respectively. Other sites of electron entry include the glycerol-3-phosphate dehydrogenase (G3PDH), which also donates electrons directly to the Coenzyme Q (CoQ) pool (Mracek *et al.*, 2013). Additionally, the electron-transferring-flavoprotein dehydrogenase (ETF-QO) and dihydroorotate dehydrogenase (DHODH) are also involved in the reduction of CoQ. Once electrons are donated to CI and CII, they are transferred down the chain to CoQ. Complex III (CIII) then passes the electrons, from the CoQ pool, further down the chain to the next electron carrier, cytochrome C (Cyt C). From here complex IV (CIV) receives the electrons from Cyt C and passes them to oxygen, which acts as a final electron acceptor. These continuous redox reactions are also coupled with the transport of protons from the matrix, into the IMS, by three of the respiratory complexes (CI, CIII and CIV). The movement of protons across the IMM contributes to the production of a proton motive force (pmf), which promotes the

fifth complex (CV) to carry out the final reaction of ATP synthesis (Figure 1.2) (Berry *et al.*, 2018).

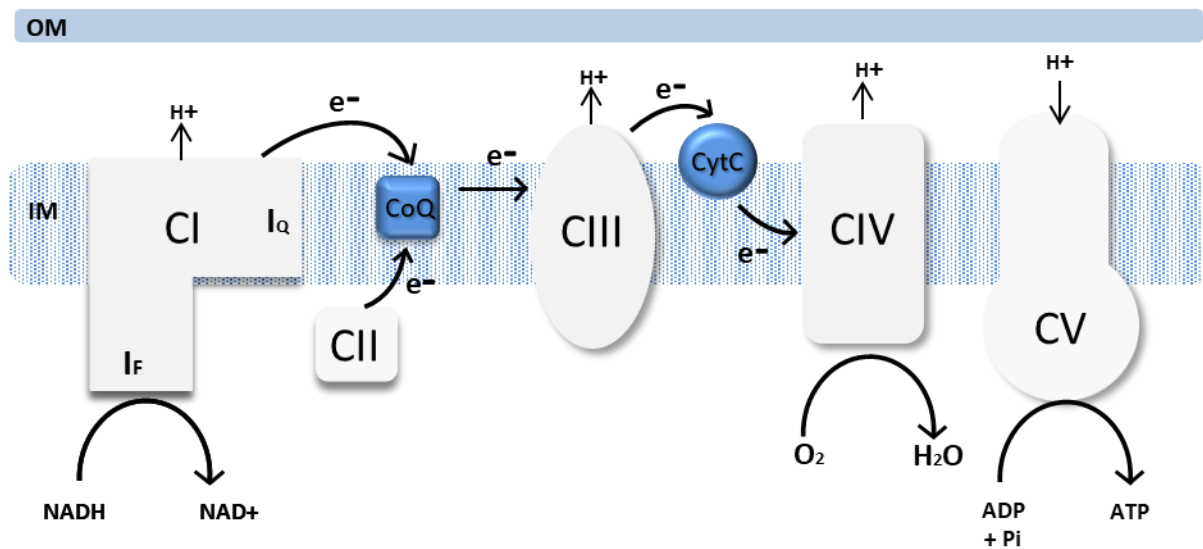


Figure 1.2 Schematic diagram of the ETC.

Diagram displaying the 5 individual complexes involved in OXPHOS. Additionally, it highlights the flow of electrons down the chain and the transport of protons into the IMS.

1.1.4 Mitochondrial mobile electron carriers

Two mobile electron carriers accomplish the transfer of electrons between the ETC complexes: CoQ and Cyt C. CoQ is a lipid-soluble cofactor, which resides in the IMM and can freely diffuse across the membrane. It accepts electrons from CI and CII, as well as the several other mitochondrial dehydrogenases, mentioned previously and transfers them onto respiratory CIII (Quinzii and Hirano, 2010). In its oxidised state (CoQ, ubiquinone) receives electrons, whereas in its reduced state (CoQH₂, ubiquinol) it donates electrons. The latter allows CoQ to function as an antioxidant within the mitochondria and other cellular compartments (Hernandez-Camacho *et al.*, 2018). However, under its radical intermediate form (CoQ \cdot , semiquinone) it also exists as a pro-oxidant. CoQ is involved in a wide range of other cellular pathways (Lenaz, 2001), therefore mutations in the genes involved in its synthesis, lead to a deficit of CoQ and cause severe mitochondrial disorders (Quinzii and Hirano, 2010). The function of CoQ is central for the production of ATP in the mitochondria. Hence, it has been proposed to be involved in the detection of metabolic alterations via changes in the redox state of the ETC (Guaras *et al.*, 2016). Later, I will discuss how changes in the CoQH₂:CoQ ratio alter the generation of mitochondrial ROS.

The other mobile electron carrier of the ETC is Cyt C that transfers electrons between CIII and CIV. Similarly to CoQ, Cyt C is found either oxidised or reduced. Cyt C is a central regulator of apoptosis and its release from the mitochondrion, to the cytosol, has the potential to trigger cell death (Kluck *et al.*, 1997). It has been proposed that only the oxidised form can trigger caspase activation and cell death (Pan *et al.*, 1999), therefore sensing of the ETC redox state, by Cyt C, can be coupled with the regulation of apoptosis. However, other reports indicate that both forms, oxidised and reduced, trigger apoptosis (reviewed in (Brown and Borutaite, 2008)). Finally, in parallel to CoQ, Cyt C can also act as an antioxidant scavenging superoxide (Pasdois *et al.*, 2011), or as a pro-oxidant promoting the formation of superoxide (Giorgio *et al.*, 2005).

1.1.5 Complex I (CI)

CI, otherwise known as NADH:ubiquinone oxidoreductase, is the first and largest component of the ETC. It carries out the oxidation of NADH, receiving two electrons, which are subsequently donated to CoQ. Alongside the transfer of electrons, it also transports a total of four protons across the IMM to the IMS, contributing to the pmf (Figure 1.3) (Rhooms *et al.*, 2019) (Zhu *et al.*, 2016) (Sharma *et al.*, 2009). This multi-domain respiratory enzyme is composed of 45 subunits, which amounts to a weight of 980 kDa. Of these 45 subunits, 7 are encoded by mtDNA, whilst the remainder are nuclear-encoded (Wirth *et al.*, 2016). 14 out of the 45 subunits are core subunits, which are involved in the transfer of electrons from NADH to CoQ, whereas the rest are accessory subunits. A small number of the accessory subunits are assembly factors, required for the complete assembly of CI (McKenzie and Ryan, 2010). However the role of these subunits is yet to be characterised (Carroll *et al.*, 2006). Electron microscopy has revealed that CI occupies an L-shaped structure, where the embedded long arm spans the IMM and the short arm protrudes into the mitochondrial matrix (Parey *et al.*, 2018) (Sanchez-Caballero *et al.*, 2016). The hydrophilic matrix domain of CI is the site of electron donation, where the soluble carrier; NADH, binds and catalyses the reduction of a flavin mononucleotide (FMN), situated at the top of the complex. Following oxidation of NADH, the electrons are passed through CI via a series of redox reactions, involving 7 subunits containing Fe-S clusters. This transfer of electrons occurs until they reach the ubiquinone-binding site (I_Q), located near the hydrophobic membrane-bound domain. The binding of CoQ

at this site allows the complete transfer of electrons and subsequent reduction of CoQ to CoQH₂ (Parey *et al.*, 2018) (Murphy, 2009). The traditional CI chemical inhibitors, rotenone and piericidin A, are both able to target and prevent the binding of CoQ to CI (Parey *et al.*, 2018) (Sharma *et al.*, 2009). Accompanying the electron transfer through the hydrophilic region is the transport of protons to the IMS, occurring within the hydrophobic domain of CI. Within the hydrophobic arm, there are 7 core mtDNA encoded subunits, which all participate in the translocation of protons across the IMM (Brandt *et al.*, 2003). It has been proposed that the energy produced, as a result of the redox reactions during electron transfer, is able to power a conformational change in the hydrophobic domain, allowing the passage of protons (Sazanov, 2014). CI can be sectioned into three different zones based on their distinct activities. The first is the N module, which partakes in the electron flow through CI, starting at the FMN site. The second is the Q module, involving the ubiquinone-binding site where the reduction of CoQ occurs. The final module, which regulates the movement of protons across the membrane, is defined as the P module (Mimaki *et al.*, 2012).

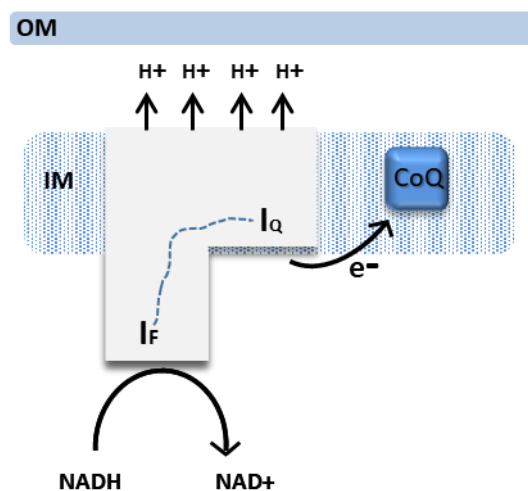


Figure 1.3 Diagram displaying the structure of Complex I.

Electrons from NADH are transferred to the I_F site of CI and are passed through the complex to the I_Q site, indicated by the dotted line). At the I_Q site ubiquinone binds and accepts the electrons. In addition, CI is responsible for the transport of 4 protons across the IMM, to the IMS.

1.1.6 Complex II (CII)

The second member of the ETC, CII, is the enzyme succinate dehydrogenase (SDH). CII is by far the simplest of the respiratory complexes, formed by four subunits

(SDHA, SDHB, SDHC and SDHD), all of which are nuclear-encoded. It is anchored into the IMM by the two smaller subunits, SDHC and SDHD. The remaining two peripheral subunits, SDHA and SDHB, are situated in the mitochondrial matrix (Cecchini, 2003) (Bowman and Birch-Machin, 2016). SDH possesses a dual functionality, as it is the only complex involved in both OXPHOS and CAC. Its functional role is catalysing the oxidation of the small metabolite succinate, an intermediate from the CAC, into fumarate (Cecchini, 2003). This reaction releases two electrons, which are then donated to the CoQ pool. Since this complex does not participate in the movement of protons to the IMS, it does not contribute to the pmf. The overall mechanism of CII begins with the reduction of covalently bonded FAD group, associated with subunit SDHA. From here, the electrons are sequentially passed through subunit SDHB, via three integral Fe-S clusters ([2Fe-2S], [4Fe-4S] and [3Fe-4S]). The final transfer of electrons occurs when CoQ binds to the membrane-bound domain of CII, forming CoQH₂ (Figure 1.4) (Rutter *et al.*, 2010). CII inhibitors are categorized under two distinct classes, dependent on their targeted binding site. These include either the succinate-binding site or the ubiquinone-binding site of CII. A highly recognised inhibitor of CII, is malonate, which competes with succinate to bind to the FAD co-enzyme (Kim, 2002).

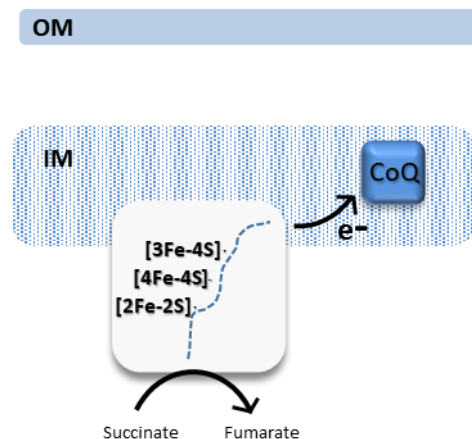


Figure 1.4 Diagram displaying the structure of Complex II.

Succinate is oxidised to form fumarate and electrons are passed through CII via 3 Fe-S clusters, indicated by the dotted line, until being passed to ubiquinone.

1.1.7 Complex III (CIII)

Coenzyme Q:cytochrome c oxidoreductase also referred to as bc₁ complex or CIII is the third respiratory enzyme in the ETC. It continues the flow of electrons down the

chain, by oxidising CoQH₂ and subsequently reducing Cyt C, through the transfer of two electrons. In parallel to electron transfer, it also transports four protons across the membrane, contributing to generate the pmf (Xia *et al.*, 2013). In total, there are 11 subunits that constitute a fully assembled dimeric CIII, one of which is encoded by mtDNA (Murphy, 2009). Three of the subunits form a catalytic core, namely cytochrome c1, cytochrome b and the Rieske iron-sulphur protein. The redox reactions are achieved via the presence of haem groups within the cytochrome c1 and b subunits as well as the [2Fe-2S] cluster within the Rieske protein. Additionally, CIII possesses two quinone (Q) binding sites, Q_o and Q_i, which are instrumental for the movement of electrons and protons through the complex (Crofts, 2004). The Q_o site is situated towards the IMS and is responsible for accepting electrons from CoQH₂, in addition to the translocation of four protons into the IMS. The Q_i site is orientated towards the matrix side of the membrane, where it acquires two protons from the matrix and two electrons to reduce CoQ. The movement of electrons and protons throughout CIII, relies on the completion of the Q cycle, involving the two mentioned Q sites. The electron transfer within CIII is split into two steps, therefore the whole process and complete reduction of Cyt C, requires two rounds of the Q cycle (Xia *et al.*, 2013). The cycle proceeds with the binding of CoQ to the Q_o site, which subsequently gains two electrons and two protons. From here, the 2 electrons are passed through two distinct pathways, whilst the two protons are shuttled directly to the IMS. The first electron is transferred to the Rieske iron-sulphur cluster and then sequentially passed to the haem group in cytochrome c1 (cyt c1). Cyt C present in the membrane is then able to bind to cyt c1 within CIII and receive this electron, becoming partially reduced. In this same cycle, the second electron obtained from CoQH₂, is passed down to two haem groups of cytochrome b, cytochrome bL and cytochrome bH. At the Q_i site, a bound CoQ accepts this electron along with a proton retrieved from the matrix, to become partially reduced. This cycle is then repeated once more to allow the complete oxidation of CoQ at the Q_o site, as well as the full reduction of both Cyt C and CoQ (at the Q_i site) (Larosa and Remacle, 2018). This process transports a total of four protons to the IMS, as well as removing two additional protons from the matrix, therefore CIII is able to greatly contribute to the pmf (Crofts, 2004). The most recognised inhibitors of CIII are antimycin A, myxothiazol and stigmatellin. Antimycin A targets the Q_i site of CIII (Murphy, 2009), whereas the latter two are able to bind to the Q_o site of the enzyme (Zhang *et al.*, 1998).

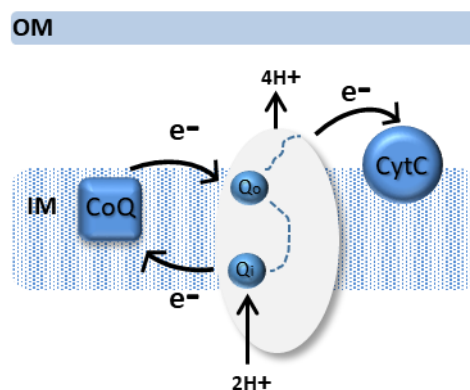


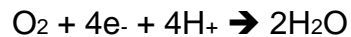
Figure 1.5 Diagram displaying the structure of Complex III.

Ubiquinone binds to the Q_o site of CIII and transfers 2 electrons. The first electron is passed through CIII until it reaches the cyt c1 and is sequentially transferred to Cyt c. The second electron is passed onto the Q_i site of CIII, which is then used to reduce ubiquinol. The complete reduction of Cyt C requires two cycles and subsequently transports four protons to the IMS.

1.1.8 Complex IV (CIV)

CIV, also known as cytochrome c oxidase, is the final enzyme involved in the transport of electrons within the ETC. Its role is to catalyse the oxidation of Cyt C, transferring the electrons to the final electron acceptor oxygen and terminating the flow of electrons. It is also the third complex where electron transport is coupled with proton translocation across the IMM to the IMS. Mammalian CIV is composed of 13 subunits, in which the three largest (COX I, COX II and COX III) are encoded by mtDNA (Timon-Gomez *et al.*, 2018). CIV exists as an active dimer embedded into the membrane and consists of 3 distinct regions, I, II and III (Li *et al.*, 2006). I and II are involved in coordinating the redox reactions carried out by CIV, whilst region III stabilises the structure. The electron transfer reactions are achieved by the presence of metal centres, in the catalytic site of the enzyme. Within region I resides a haem group, haem a, as well as a binuclear centre formed by haem a₃ and the copper centre, CuB. Incorporated into region II is another copper centre referred to as CuA (Shimada *et al.*, 2017). The first step in the mechanism of CIV is the interaction between reduced Cyt C and the CuA centre of region II. Here the transfer of electrons occurs from the haem group within Cyt c to the prosthetic copper centre. CuA then shuttles the electrons through the two haem groups of region I, reaching the second copper centre, CuB. The binuclear centre is the site of water formation where molecular oxygen (O_2) is split into 2 monooxygen and reduced. The complete

reaction requires 4 Cyt C molecules to donate four electrons to O₂, along with four protons retrieved from the matrix. The overall reaction catalysed by CIV is:



Additionally, a further four protons are transported into the IMS from the matrix (Figure 1.6) (Kim *et al.*, 2009). Inhibitors of CIV, such as cyanide (CN), carbon monoxide (CO), nitric oxide (NO) and hydrogen sulphide (H₂S) all target the oxygen-binding binuclear centre (Pearce *et al.*, 2008) (Dorman *et al.*, 2002).

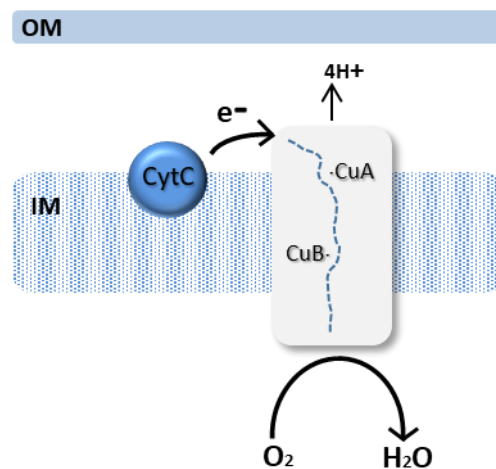


Figure 1.6 Diagram displaying the structure of Complex IV.

Cyt C binds and transfers electrons to CIV. Electrons are passed through the complex via two copper centres (indicated by the dotted line), until reaching the final electron acceptor, O₂, to form water. CIV is also involved in the translocation of four protons into the IMS.

1.1.9 The Chemiosmosis Theory

In the 1960's Peter Mitchell proposed the chemiosmosis theory, describing the mechanism of how ATP is produced within the mitochondria (Mitchell, 1961). Today this theory is widely accepted and explains the molecular mechanisms that drive OXPHOS. The theory states that an established electrochemical proton gradient across the IMM, acts as stored energy that can drive the synthesis of ATP. The pmf is generated through the translocation of protons across the membrane, leading to a positively charged IMS. As previously discussed, the production of this proton gradient is coupled to electron transfer and accomplished by three components of the ETC, CI, CIII and CIV. The movement of protons down the gradient, into the matrix,

creates an energy potential, which is then harnessed, by the enzyme ATP synthase, to catalyse the phosphorylation reaction and synthesise ATP (Morelli *et al.*, 2019).

The electrochemical proton gradient is used to generate the pmf that is required for the production of energy, by mitochondria. The pmf is produced with the energy released from transferring electrons between the four respiratory complexes, as described in detail below. Pmf has two components, namely, the mitochondrial membrane potential and the pH gradient (Brand and Nicholls, 2011). Changes to the pmf can affect all the other cellular processes, where the mitochondrion is involved, for example, redox and calcium homeostasis, proteostasis and metabolic reactions. Thus, the pmf has a strong influence on the signalling occurring between the mitochondria and the rest of the cell (Berry *et al.*, 2018).

1.1.10 ATP Synthase

ATP Synthase, otherwise known as CV, is the fifth complex involved in OXPHOS. It is an IMM proton pump that catalyses the synthesis of ATP from ADP and inorganic phosphate (P_i). CV consists of 15 subunits, which are arranged into two central domains, F_0 and F_1 (Walker, 2013), (Neupane *et al.*, 2019). The F_0 domain occupies a hydrophobic ring-like structure, bound to the IMM and is comprised of approximately 8 identical subunits, called the c subunit. The F_1 region extends outwards into the mitochondrial matrix and is assembled by 5 subunits, α , β , γ , δ and ϵ . Nearest to the membrane is the primary stalk formed by the subunits γ , δ and ϵ , which are attached to a hexamer of 3 alternating α and β subunits. Also attached is the peripheral stalk which connects the F_0 and F_1 domains and is comprised of subunits a, b, d, F6 and oligomycin sensitivity-conferring protein (OSCP) as well as the accessory subunits e, f, g and A6L (Figure 1.7) (Jonckheere *et al.*, 2012). The role of the F_0 domain is to pump protons through the complex, whilst the F_1 domain forms the catalytic head, where the ATP synthesis occurs. CV is able to synthesise ATP by harnessing energy from the electrochemical proton gradient. The energy released from this gradient, fuels the rotation of CV and catalyses the production of energy (Stock *et al.*, 1999). The first step in the mechanism of CV, is the passing of protons through subunit c, of the membrane bound region, which deposits the protons into the mitochondrial matrix. The movement of these protons causes the F_0 domain of CV to rotate 120° . This rotation stimulates the rotary mechanism of the central stalk, specifically the γ subunit, which induces conformational changes within

the catalytic region of F_1 . Within the $3\alpha 3\beta$ hexamer, three catalytic sites bind the substrate (ADP and P_i) and through a series of three conformational changes (open, loose and tight), ATP is released (Figure 1.7) (Stock *et al.*, 1999) (Senior *et al.*, 2002). A well-studied inhibitor of CV is the antibiotic oligomycin, which binds to the F_0 region, therefore preventing the passage of protons through the enzyme, consequently inhibiting ATP synthesis (Symersky *et al.*, 2012).

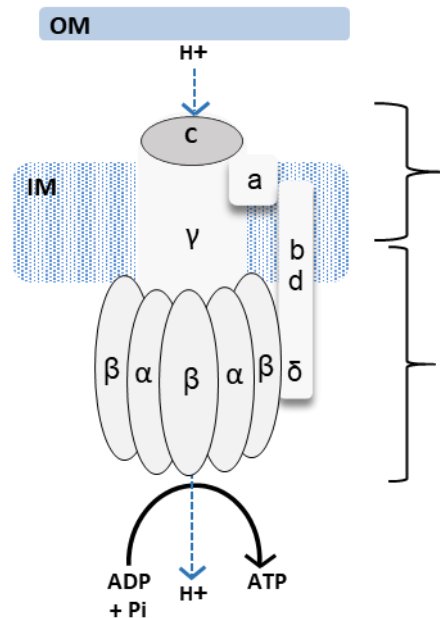


Figure 1.7 Diagram displaying the structure of ATP Synthase.

The membrane bound region, F_0 and peripheral region, F_1 are outlined. Protons move from the IMS through the c subunit of CV into the matrix, indicated by the dotted line. The movement of protons causes a rotary motion the catalytic head, consisting of α and β subunits, which catalyse the production of ATP.

1.1.11 Alternative respiratory enzymes; AOX and Ndi1

In addition to the five basic respiratory complexes of the OXPHOS system, seen in mammalian mitochondria, many organisms such as plants, fungi and bacteria, also express alternative respiratory enzymes (McDonald, 2009) (Saari *et al.*, 2019). Alternative enzymes can also be found in animals, including some chordates such as *Ciona intestinalis* but not in humans or flies (McDonald *et al.*, 2009) (McDonald and Gospodaryov, 2019). The expression of these alternative respiratory systems, in the aforementioned organisms, evolved as a survival response to toxins present in the surrounding environment that targeted the ETC (McDonald *et al.*, 2009) (McDonald and Gospodaryov, 2019). Alternative enzymes function to bypass interrupted electron flow that may have occurred as a result of damage to the standard ETC

components, or environmental stresses that inhibit CI, CIII or CIV (Saari *et al.*, 2019). Therefore this evolutionary trait, of possessing alternative respiratory enzymes, protects mitochondria from dysfunction, by overcoming the stress of limited electron flow. This protective mechanism allows the maintenance of mitochondrial energy production (Saari *et al.*, 2019), as well as the maintenance of mitochondrial processes coupled with OXPHOS, such as synthesis of Fe-S clusters or nucleotides and one-carbon metabolism reactions (Schiff *et al.*, 2012). For unknown reasons, alternative respiratory enzymes became redundant in most animals, (including humans and flies), during evolution and therefore have been removed from their genomes (McDonald *et al.*, 2009) (McDonald and Gospodaryov, 2019).

There are two classes of alternative respiratory enzymes, the alternative NADH dehydrogenases and the alternative oxidases, which all possess the ability to recover electron flow at specific points of the ETC. Most organisms possess both types of enzymes at the same time (McDonald and Gospodaryov, 2019). However, unlike the standard respiratory complexes, they do not pump protons into the IMS and therefore do not contribute to the pmf, directly. Thus, these alternative respiratory systems cannot fully restore ATP synthesis. Another characteristic feature is their structural simplicity consisting of a single polypeptide, encoded by the nuclear genome, in contrast to the complex multi-subunit structures that form the standard ETC components. This contributes to their quick and easy assembly, with less opportunity of becoming damaged (Saari *et al.*, 2019).

The Alternative Oxidase (AOX), found in plant and fungi mitochondria, is able to reduce O₂ to water through the direct transfer of electrons from CoQ, thus bypassing CIII and CIV. AOX is a small integral dimeric polypeptide, bound to the matrix facing side of the IMM, where it is activated by accumulation of CAC intermediates and a highly reduced CoQ pool (Figure 1.8) (Vanlerberghe, 2013) (Fernandez-Ayala *et al.*, 2009). Upon activation, a conformational change within its structure elevates its affinity for CoQH₂, beyond that of CIII. Due to its alternative pathway of electron flow, independently of CIII and CIV, AOX also confers cyanide resistance (Hakkaart *et al.*, 2006). To take advantage of these systems, scientists have been able to express AOX in the mitochondria of higher eukaryotes, mainly from the tunicate *Ciona intestinalis* (Hakkaart *et al.*, 2006) but also from the fungus *Aspergillus nidulans* (Perales-Clemente *et al.*, 2008). In mammalian cells and *Drosophila melanogaster*,

the co-expression of AOX was shown to partially rescue the lethal phenotype caused by knocking down CIII/CIV subunits or inhibiting CIII/CIV with antimycin and cyanide, respectively (Rajendran *et al.*, 2019) (Dogan *et al.*, 2018) (Szibor *et al.*, 2017) (Sanz *et al.*, 2010a) (Kemppainen *et al.*, 2014) (Fernandez-Ayala *et al.*, 2009). In addition, AOX has been described to rescue pathological phenotypes that are not caused by CIII or CIV inhibition, in *Drosophila melanogaster*. A non-extensive list includes: (i) mutations in the antioxidant gene, *dj-1 β* (Fernandez-Ayala *et al.*, 2009), (ii) knock down of the catalytic subunit of the mtDNA polymerase (Humphrey *et al.*, 2012), (iii) accumulation of β -amyloid protein in the fly brain (El-Khoury *et al.*, 2016) or (iv) disruption of Jun N-terminal kinase signalling during development (Andjelkovic *et al.*, 2018). All of these phenotypes are associated with elevated levels of ROS and/or oxidative stress. AOX is a powerful tool to reduce mitochondrial ROS levels when ectopically expressed in mammals and insects, which I will discuss in detail later in this thesis.

The second class of alternative respiratory enzymes is the alternative NADH dehydrogenases. Examples that belong to this group are the NADH dehydrogenase internal 1 (Ndi1), NADH dehydrogenase external 1 (Nde1) and the NADH dehydrogenase external 2 (Nde2). This class of rotenone-insensitive enzymes transfers electrons directly to the CoQ pool through the oxidation of NADH, subsequently bypassing CI (Matus-Ortega *et al.*, 2015). Ndi1 is found in plants, fungi and the mitochondria of some animals (Gospodaryov *et al.*, 2014), embedded into the IMM, facing the matrix (Figure 1.8) (Bahadorani *et al.*, 2010). In some species of fungi such as *Saccharomyces cerevisiae*, CI has been completely lost during evolution and Ndi1 is the only NADH dehydrogenase located in the mitochondrial matrix (Yagi *et al.*, 2006). In parallel to AOX, Ndi1 (from *Saccharomyces cerevisiae*, *Ciona intestinalis* and *Aspergillus nidulans*) has been inserted into the genome and subsequently expressed in the mitochondria, of mouse and human cells, as well as flies (Yagi *et al.*, 2006) (Gospodaryov *et al.*, 2014) (Perales-Clemente *et al.*, 2008). Ndi1 expression confers resistance to CI inhibitors (e.g. rotenone or metformin), in mammalian cells and fruit flies (Seo *et al.*, 1998) (Seo *et al.*, 2004), as well as rescuing the lethal phenotype caused by the knockdown of CI subunits (Bai *et al.*, 2001) (Park *et al.*, 2007) (Marella *et al.*, 2010) (Cho *et al.*, 2012) (Wheaton *et al.*, 2014). The therapeutic use of Ndi1 has been strongly explored in models of Parkinson's disease, since CI dysfunction is one of the hallmarks of this disease

(Schapira *et al.*, 1990). In fact, Ndi1 has been shown to rescue fly and mouse models of Parkinson's disease (Seo *et al.*, 2006) (Barber-Singh *et al.*, 2009) (Sanz *et al.*, 2010b) (Vilain *et al.*, 2012). Finally, expression of Ndi1 either from *Saccharomyces cerevisiae* or *Ciona intestinalis*, has been shown to extend lifespan in fruit flies (Bahadorani *et al.*, 2010) (Sanz *et al.*, 2010b) (Hur *et al.*, 2013) (Gospodaryov *et al.*, 2014).

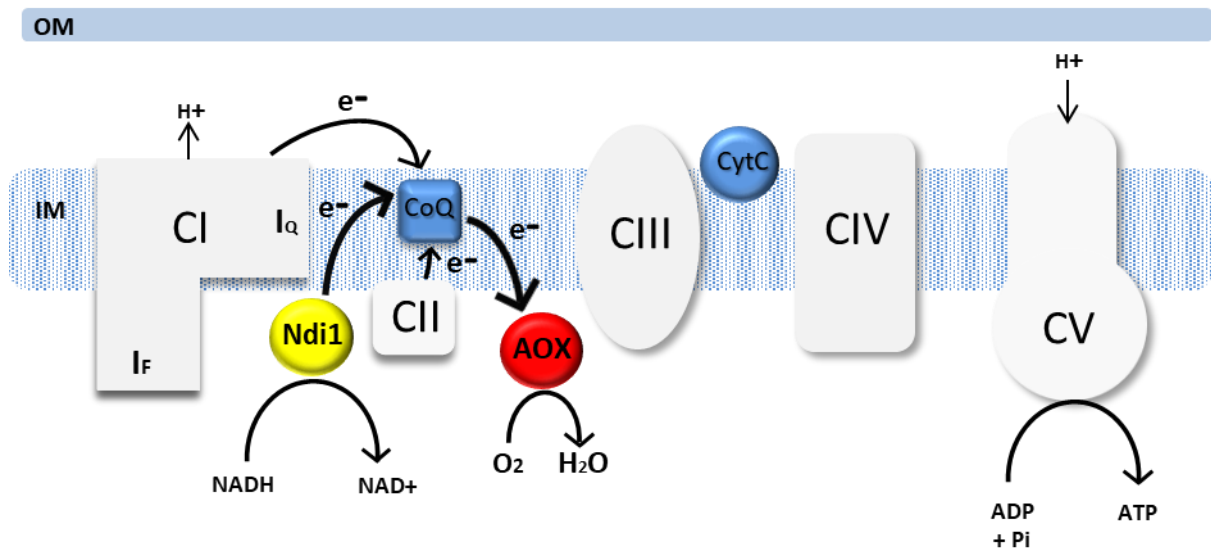


Figure 1.8 Schematic diagram showing the expression of alternative respiratory enzymes, Ndi1 and AOX.

Ndi1 and AOX are both expressed within the matrix facing side of the IMM. Ndi1 directly reduces NADH to NAD⁺ and transfers electrons to the CoQ, thereby bypassing CI. AOX takes electrons directly from the CoQ pool and reduces O₂ into H₂O.

1.2 Reactive Oxygen Species (ROS)

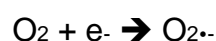
Free radicals are atoms or molecules with one or more unpaired electrons, rendering them highly unstable. As a result of this instability, they are able to take single electrons from molecules around them. When produced within biological systems, free radicals can cause injury, known as oxidative damage (Pamplona and Barja, 2007). The most common free radicals found in cells are derived from O₂ and known as reactive oxygen species (ROS). Another group derived from nitrogen, referred to as reactive nitrogen species (RNS) and reviewed in (Pacher *et al.*, 2007), are also abundant. However, during this thesis, I focus primarily on ROS. O₂ is an oxidant due to the presence of two unpaired electrons with parallel spins in its external orbital (Magder, 2006); therefore, O₂ accepts electrons one at a time. The incomplete

reduction of O₂ mainly occurs during processes consisting of univalent electron transfer, such as OXPHOS (Barja, 1999). Accordingly, ROS are formed when O₂ is incompletely reduced with 1, 2 or 3 electrons. ROS represent a large group of molecules, all possessing different stabilities and half-lives. Examples of ROS include the free radicals: superoxide anion (O₂^{•-}), hydroxyl radical (OH^{•-}), singlet oxygen (¹O₂) and hydroperoxyl radical (HO₂[•]). However, not all ROS are free radicals such as the non-radical entity hydrogen peroxide (H₂O₂) (Lambert and Brand, 2009).

ROS are abundantly generated by mitochondria, however, they are also produced in large amounts in other cellular compartments, such as peroxisomes and cytosol, discussed in detail below. It has been well established that cells require a basal level of ROS, acting as signalling messengers, to maintain cellular homeostasis (Murphy, 2009). Endogenous antioxidants scavenge the excess ROS and detoxify them into less reactive products. When ROS overwhelm the antioxidant defence mechanisms and start to deviate from the optimum cellular levels, they can inflict damage onto their nearby surroundings (Hekimi *et al.*, 2011). Here they react with other components of the cell, resulting in oxidative damage to proteins, DNA and lipids (Ray *et al.*, 2012). In recent years, there has been a rise in research behind the mechanisms of ROS production and the delicate balance between their beneficial or destructive behaviour.

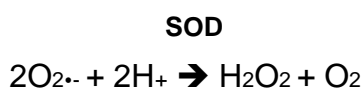
There are numerous types of ROS that can be produced, however, in this section, I will focus on discussing the three most common forms of ROS produced, as a result of electrons leaking from the ETC (Scialo *et al.*, 2013). These specifically include superoxide, hydrogen peroxide and hydroxyl radical.

The most common type of ROS, produced by the ETC (Esterhazy *et al.*, 2008), is superoxide (O₂^{•-}), which is generated during the univalent reduction of oxygen:



This reaction is the first to yield ROS, in the form of superoxide, which can subsequently be converted into a variety of other oxidative molecules, via a cascade of downstream chemical reactions. Superoxide is highly reactive, due to the presence of an unpaired electron and consequently has a short half-life (Esterhazy *et*

al., 2008). This form of ROS is able to react with the Fe-S and modify cysteine groups, within proteins. Superoxide on its own can non-enzymatically dismutate into H₂O₂ (Paulsen and Carroll, 2010). However, this is a very slow process therefore, cells have evolved specialised antioxidant enzymes, belonging to the family of superoxide dismutases (SOD), which specifically target superoxide. SOD converts superoxide into the less reactive H₂O₂ by the following reaction:



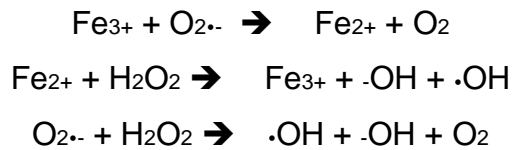
The activity of SOD is highly efficient (due to its low K_m for superoxide) and scavenges free superoxide, almost immediately (Sheng *et al.*, 2014) at a rate of ~10⁹ M⁻¹s⁻¹ compared to the spontaneous dismutation of superoxide (~10⁵ M⁻¹s⁻¹).

Hydrogen peroxide (H₂O₂) is produced when O₂ receives two electrons. Given that H₂O₂ is not a free radical, it is more stable and possesses a longer half-life (~1 ms), in comparison to superoxide (Bak and Weerapana, 2015). H₂O₂ is considered to be the most abundant cellular ROS (Bienert *et al.*, 2006). Due to its stability and neutral charge, it can move between cellular compartments and interact with biomolecules far away from its site of production (Lee *et al.*, 2011). H₂O₂ is the product of a dismutase reaction involving two molecules of superoxide, which is usually achieved by the activity of SOD (Wang *et al.*, 2018). There are three families of antioxidants responsible for metabolising H₂O₂, namely catalases, glutathione peroxidases and peroxiredoxins, which catalyse the following reaction;



The hydroxyl radical (·OH) is produced when O₂ is incompletely reduced with three electrons. It is the most reactive form of ROS and for this reason, is considered the most toxic. The reactivity of the hydroxyl radical is so high and unpredictable that there is no enzymatic antioxidant dedicated to its detoxification, in contrast to superoxide or H₂O₂ (Sciabo *et al.*, 2013). Unlike superoxide and H₂O₂, it can directly interact with DNA, inflicting damage, which subsequently leads to DNA mutations. The hydroxyl radical is produced via a two-step reaction involving the encounter of

both superoxide and H₂O₂. These reactions are known as the Haber-Weiss and Fenton reactions, which utilise ferrous ions as a metal catalyst (Lipinski, 2011).



1.2.1 Antioxidants

Antioxidants include a wide range of systems dedicated to the removal of oxidants from cells and exist as either enzymes or non-enzymatic organic molecules. Cells have specialised enzymatic systems dedicated to maintaining ROS at non-toxic levels. In 1969, McCord and Fridovich discovered the first enzymatic antioxidant dedicated to detoxifying superoxide in cells, called SOD (McCord and Fridovich, 1969). This was a historical discovery as it confirmed the production of superoxide *in vivo* and prompted the development of the Free Radical Theory of Ageing, proposed by Denman Harman (Harman, 1956). The term antioxidant covers a broad range of enzymes and molecules; however in this section I will focus on the enzymes involved in the specific detoxification of superoxide and H₂O₂.

As previously mentioned, SOD is involved in the dismutation of superoxide into H₂O₂ and O₂. There are three distinct isoforms of mammalian SOD, which differ according to their roles, metal association and subcellular location. (Hayyan *et al.*, 2016). The first is SOD1 (CuZnSOD), which is in charge of managing cytosolic superoxide levels. The second is the manganese-containing SOD2, found exclusively within mitochondria. The final SOD, better known as ECSOD, which is also associated with Cu and Zn ions, is localised to the extracellular matrix to protect surrounding tissues from high levels of superoxide (Sheng *et al.*, 2014).

Detoxification of H₂O₂ into innate water molecules can occur via three different families of enzymes (reviewed in (Veal *et al.*, 2007)). The first is catalase, predominantly situated in the peroxisomes, whose activity results in the conversion of H₂O₂ into water and O₂. In addition, there are two other major families of enzymes, which participate in the degradation of H₂O₂, including glutathione peroxidases and peroxiredoxins. These enzymes are located in the cytosol, mitochondria and other cytosolic compartments, such as nuclei, according to their specific isoforms. The

glutathione peroxidases require the presence of 2 reduced glutathione (GSH) molecules (Mailloux, 2018). This reaction involves the reduction of H_2O_2 forming a glutathione disulphide (GSSG) and water (Handy and Loscalzo, 2012). The reduction of GSSG, to restore the pools of GSH and continue the detoxification of H_2O_2 , is catalysed by glutathione reductase, which acquires electrons from NADPH to complete the reaction (Mailloux, 2018). The peroxiredoxins, use a similar mechanism to glutathione peroxidase, where the reduction of H_2O_2 occurs in the presence of another co-substrate, thioredoxin 2 (Trx2) (Handy and Loscalzo, 2012). Within the active site of peroxiredoxins are 2 conserved cysteine residues, which are responsible for the reduction of H_2O_2 . Following the degradation of H_2O_2 the oxidised cysteine residue forms an intermolecular disulphide bridge, with the second cysteine residue. Trx2 then sequentially restores the reductive state of peroxiredoxins. Trx2 can then be reactivated by thioredoxin reductase, using the reductive properties of NADPH. It has been widely established that peroxiredoxins are the major family of enzymes involved in the detoxification of H_2O_2 (Mailloux, 2018). In addition to the removal of H_2O_2 , glutathione peroxidases are also implicated in the detoxification of lipid peroxides (Ursini and Bindoli, 1987).

1.2.2 Oxidative stress

The accumulation of ROS in cells is associated with the damage to proteins, DNA, and lipid membranes (Pamplona and Barja, 2007). As previously discussed, cells have evolved antioxidant systems whose primary function is to prevent oxidative damage (Pamplona and Costantini, 2011). However, when antioxidants become overwhelmed with high levels of oxidants, oxidative stress occurs. If it is not controlled, oxidative stress will inflict oxidative damage that may cause permanent molecular damage (Sies, 1997). Accumulation of oxidative damage has been shown during ageing (Forster *et al.*, 1996) (Gan *et al.*, 2012) (Akila *et al.*, 2007) and in many degenerative diseases (D'Amico *et al.*, 2013) (Navarro *et al.*, 2009) (Du *et al.*, 2009). It is clear that oxidative stress is deleterious and happens during ageing, as well as age-related diseases but it remains to be established whether it is a cause or a consequence. Here, I will focus on the damage that can be instigated by superoxide, H_2O_2 and hydroxyl radical.

Superoxide cannot directly damage proteins, but it can attack Fe-S clusters, which results in the release of iron and H_2O_2 , as well as disruption of protein activity

(Esposito *et al.*, 2013). Therefore the attack of Fe-S by superoxide can result in the generation of hydroxyl radicals, via Fenton reactions, which accelerate oxidative damage. Ageing and age-related diseases are characterised by an increase in ROS levels (both superoxide and H₂O₂), free iron and oxidative damage (Massie *et al.*, 1985) (Massie *et al.*, 1983) (Hofer *et al.*, 2008) (Forster *et al.*, 1996) (Gan *et al.*, 2012) (Akila *et al.*, 2007) (Seo *et al.*, 2008). It is possible to speculate that the age-related increase in superoxide causes the release of iron. Increased iron levels, together with accumulation of superoxide and H₂O₂, would produce the hydroxyl radical, which in turn would initiate the oxidative damage, observed in old individuals. Supporting the former hypothesis, are the observations from feeding an enriched iron diet to *Caenorhabditis elegans*, which increased oxidative stress (Valentini *et al.*, 2012). Furthermore, in a *Drosophila* model of Alzheimer's disease, chelating free iron or reducing ROS levels restored lifespan to normal (Rival *et al.*, 2009), which further supports the role of iron and hydroxyl radical in triggering oxidative stress.

ROS with high reactivity, such as hydroxyl radical and peroxynitrite, are able to attack any biological molecule, of the cell. These specific types of ROS can react with lipid membranes, initiating lipid peroxidation (Bielski *et al.*, 1983). Polyunsaturated fatty acids (PUFAs), within membranes, are particularly sensitive to oxidative attack, due to the presence of structural double bonds (Pamplona *et al.*, 1996). Lipid peroxidation has two main characteristics; first of all, it operates as a chain reaction where oxidised fatty acids perform electrophilic attacks on non-oxidised fatty acids to take their electrons, causing the oxidation of the attacked fatty acids. Secondly, reactive carbonyl species (RCS) are generated as by-products of lipid peroxidation. These RCS can spread oxidative damage long distances from their site of generation (reviewed in (Pamplona, 2011)). Lipid peroxidation is stopped by the presence of fat-soluble antioxidants such as vitamin E (Wang and Quinn, 2000) or the neutralisation of lipid hydroperoxides, by glutathione peroxidases (Ursini and Bindoli, 1987).

The most harmful consequence of ROS is damage inflicted onto DNA. This is due to the fact that DNA contains the information needed to synthesise all cellular components and cannot be replaced, once it is irreversibly damaged (Sanz *et al.*, 2006). *In vitro*, hydroxyl radical, peroxynitrite and other highly reactive free radicals, can attack DNA directly and cause different lesions including: single- and double-strand breaks, point mutations and deletions. mtDNA has been proposed to be

particularly vulnerable to oxidative damage due to its proximity to the ETC, which is supported by data demonstrating that levels of oxidative damage detected in mtDNA, are higher than in nuclear DNA (Richter *et al.*, 1988). Similarly, mtDNA accumulates mutations at a higher rate in comparison to nuclear DNA (Ladoukakis and Zouros, 2017). Mutations in mtDNA increase during ageing and have been linked to the onset of ageing and age-related diseases (Greaves *et al.*, 2012) (Su *et al.*, 2018). However, some studies indicate that mutations in mitochondria are not caused by oxidative damage but by errors during replication and subsequent clonal expansion (Larsson, 2010) (Lefevre-Borg *et al.*, 1988) (Kauppila *et al.*, 2018).

Free radicals can inflict damage to proteins in a heterogeneous manner (reviewed in (Stadtman, 2006) (Stadtman and Levine, 2003)). For example, oxidative damage can affect the whole protein (e.g. protein fragmentation and cross-linking with other proteins) or specific amino acids. As I have discussed above, proteins containing Fe-S clusters are particularly sensitive to oxidative attack by superoxide (Imlay, 2006). Additionally, cysteine and methionine are the two amino acids more prone to oxidative modifications (Stadtman *et al.*, 2003) (Held and Gibson, 2012). These modifications can be either irreversible or reversible. Irreversible oxidation reactions include the carbonylation of several amino acid residues, nitration of tyrosine residues and the over-oxidation of cysteine forming sulfinic and sulfonic acids, all of which have been implicated in oxidative damage (Cai and Yan, 2013). Overall, ageing is characterized by the accumulation of oxidised proteins (Forster *et al.*, 1996), which can be caused either by the increase in oxidative stress associated with ageing or by an age-related decline in the mechanisms of protein quality control (Sohal and Weindruch, 1996) (Higuchi-Sanabria *et al.*, 2018).

1.2.3 ROS as signalling molecules

Over the past decade, the role of ROS as cellular signalling messengers has been under a lot of scrutiny, within the scientific community (Holmstrom and Finkel, 2014). In light of the overwhelming amount of evidence that exists today, ROS are now widely recognised as redox signalling molecules that can orchestrate multiple different signalling pathways, essential for maintaining cellular health and viability.

The general mechanism of signal transduction is through ROS-mediated redox reactions, with key cysteine residues (Ray *et al.*, 2012). Both superoxide and H₂O₂

can react with the thiol groups of cysteine, to induce oxidative modifications. Cysteine residues are highly conserved and account for only 2% of amino acid content (Bak and Weerapana, 2015). In addition, they are the only amino acid to possess a thiol functional group; collectively making cysteine residues unique and effective for signal transduction (Kettenhofen and Wood, 2010). Oxidative modifications to the thiol groups within cysteine residues can induce structural changes, which alters protein activity. As previously mentioned, these cysteine oxidation reactions can be either irreversible, where they are predominantly associated with damage, or reversible, where they are involved in redox signalling. Reversible modifications of the cysteine residues can include S-sulfenation, S-nitrosylation, S-glutathionylation and disulphide bond formation. These redox-related modifications can alter the catalytic activity and function of the protein, to initiate specific signalling pathways, within the cell, discussed in detail below (Paulsen and Carroll, 2010).

S-sulfenation of cysteine residues yields the formation of the sulfenic acid. Following this reaction, sulfenic acid can then be oxidised further to produce more stable forms of oxidative modifications, both reversible (i.e. S-glutathione) and irreversible (i.e. sulfinic and sulfonic acid). Thus, the formation of sulfenic acid can lead to divergent downstream consequences (Poole *et al.*, 2004). S-sulfenation is mostly achieved through the interaction with H₂O₂, however, can also occur through oxidation with peroxynitrite and other forms of ROS (Cai and Yan, 2013). This form of cysteine oxidation has been associated with numerous signalling pathways, involving the activity of various proteins and transcription factors, such as Fos and Jun (activator protein-1) (Claiborne *et al.*, 1999), as well as Nf-κB (Pineda-Molina *et al.*, 2001). For example, some studies have reported that the formation of sulfenic acid within aldose reductase, provides protection against cardiac ischemia reperfusion in rats (Kaiserova *et al.*, 2006). In addition, S-sulfenation is needed for the initiation of T-cell growth and proliferation (Michalek *et al.*, 2007). Protein S-nitrosylation is carried out by RNS, such as NO and peroxynitrite. This modification can occur on tyrosine, serine and threonine residues, as well as cysteine residues. There is evidence that S-nitrosylation can provide cardio-protection during ischemia reperfusion (Murphy *et al.*, 2012) (Sun *et al.*, 2007). However, the excessive nitrosylation of specific proteins has also been observed in multiple diseases, such as neurodegenerative disorders and cardiovascular disorders (reviewed in (Foster *et al.*, 2009)). S-glutathionylation occurs as a result of ROS and RNS, during oxidative stress. It can also be achieved

by the endogenous antioxidant glutathione, under low GSH/GSSG ratios. This form of modification leads to a mixed disulphide bond and can protect proteins from downstream irreversible oxidative modifications, to form sulfinic and sulfonic acids (Cooper *et al.*, 2011). Similarly to other types of cysteine oxidation, glutathionylation has been implicated in both physiological and pathological processes. In terms of cell signalling, glutathionylation has been shown to regulate proteins kinases such as mitogen-activated protein kinase (MAPK) (Templeton *et al.*, 2010) as well as transcription factors, including Nf- κ B (Reynaert *et al.*, 2006). These support the role of glutathionylation in a wide range of processes such as proliferation, differentiation and apoptosis. However, this oxidative modification has also been associated with neurodegenerative disease, cancer and type 2 diabetes (Cooper *et al.*, 2011). Disulphide bond formation through ROS or RNS in proteins is different to the mixed disulphide produced during glutathionylation, between proteins and GSH. Disulphide bonds are produced between two cysteine residues, within the structure of a protein, causing structural and functional changes, which can regulate cellular stress responses. For example, a disulphide bond created in Keap1, in response to oxidative stress, leads to the activation of NF-E2-related factor 2, which elevates the expression of antioxidants (Cai and Yan, 2013).

The two forms of ROS that are predominantly associated with redox signalling are H₂O₂ and superoxide. This is due to their higher stabilities, compared to other more harmful ROS entities, such as the hydroxyl radical. Additionally, H₂O₂ and superoxide predominantly target proteins or Fe-S groups within proteins and cannot directly target DNA and lipids, in contrast to the hydroxyl radical. H₂O₂ is particularly effective as a signalling molecule as it can diffuse across membranes and travel long distances, from where it was originally produced, due to its long half-life (Bak and Weerapana, 2015). The activity of superoxide as a signalling molecule is subject to controversy, due to its chemical properties. The short half-life of superoxide means that it is not able to travel far and therefore reacts primarily with proteins in close proximity to its site of generation (Wang *et al.*, 2018). However, recent studies have discovered channels within the OMM of the mitochondria, specifically for the transport of superoxide, thus supporting its role as a signalling molecule, (Hayyan *et al.*, 2016).

The first encounter of ROS as a signalling molecule was during the 1990s, where an increase in cellular proliferation was detected, upon addition of H₂O₂, triggered by the

activation of pathways regulated by NF- κ B (Schreck *et al.*, 1991). NF- κ B is involved in a wide range of cellular survival pathways, including immune responses, autophagy, proliferation, differentiation and apoptosis. Since then, the interaction between ROS and other signalling pathways has been extensively studied. Specific pathways include, the MAPK cascade, which is able to regulate many critical cellular processes, through downstream phosphorylation events, such as survival, cell growth, differentiation and cell death (Dhillon *et al.*, 2007). The hypoxia inducible factor (HIF-1), which is stabilised by ROS, is primarily involved in triggering a response under low oxygen conditions and promotes cellular survival (Jung *et al.*, 2008). As I mentioned above, the Keap1-Nrf2-ARE signalling pathway, regulated by ROS-mediated-oxidation of cysteine residues, is involved in the activation of an antioxidant response to counteract oxidative stress. The phosphoinositide-3-kinase-Akt pathway (PI3K-Akt), is also activated by ROS to initiate downstream processes responsible for protein synthesis, cell proliferation and cell growth. In addition, ROS can also participate in the regulation of Ca²⁺ ions through the opening of channels, such as mPTP (in the IMM) (Zhang *et al.*, 2016). Recently, there has been evidence that H₂O₂ can also induce redox signalling through peroxiredoxins or the co-substrate thioredoxin, which are able to relay the signal directly to target proteins (Netto and Antunes, 2016).

1.2.4 Cellular ROS

As discussed above, mitochondria are an important source of ROS; however there are also enzymes that reside in the cytoplasm and distinct cellular compartments that contribute to the generation of ROS. These can be categorised according to their location within the cell, for example (i) the plasma membrane, (ii) cytosol, (iii) peroxisome and (iv) endoplasmic reticulum (Brown and Borutaite, 2012), discussed in detail below.

One of the most prevalent non-mitochondrial sources of ROS originates from the plasma membrane generated by the trans-membrane NADPH oxidases, otherwise known as the NOX family. In mammals, there are seven tissue specific NOX isoforms in total, all with the primary role of producing ROS (superoxide or H₂O₂) (Krause, 2004). In fact, NOX are the only family of enzymes whose primary function is the generation of ROS (Drummond *et al.*, 2011), whereas in other enzymes it can be argued that ROS are produced as by-products. One of the main roles of NOX-

derived ROS is triggering an innate immune response. For example, in macrophages the integral NOX enzymes can produce and release a burst of superoxide outside of the cell, which can target and kill harmful microbes (Panday *et al.*, 2015). Within the cytosol there are the NO synthase (NOS) enzymes and lipoxygenases (LOX). In normal conditions, NOS enzymes are responsible for the production of the essential signalling molecule, NO. Conversely, under conditions of limited substrate or cofactor availability, the enzyme's activity can shift to the production of superoxide (Xia and Zweier, 1997). In addition, studies have revealed that cytosolic superoxide and H₂O₂ can promote further ROS production by NOS, by shifting NO production to superoxide production (Sun *et al.*, 2010). Cytosolic LOX enzymes catalyse the oxidation of the unsaturated fatty acid arachidonic acid, released from the plasma membrane. A by-product of this redox reaction is the formation of superoxide. Further research has shown a possible interaction between the metabolites produced by LOX and the NOX enzymes, in which these LOX metabolites trigger ROS production from NOX (Cho *et al.*, 2011b). Also found in the cytosol are the xanthine oxidase enzymes, typically involved in the metabolism of hypoxanthine, to produce uric acid. However, due to their oxidase properties, they are also able to participate in the direct transfer of electrons to oxygen, leading to the generation of superoxide, H₂O₂ and NO. ROS produced as a result of Xanthine oxidase enzymes possess both negative and positive consequences. For example, the activity of xanthine oxidase has been reported to be higher in carcinogenic tissues compared to healthy tissue. In this model, it was been proposed that ROS produced by xanthine oxidase has promoted the progression of cancer by stimulating cell proliferation. However, ROS produced via xanthine oxidases has also been associated with cell signalling, including pathways linked to apoptosis and cell differentiation (Battelli *et al.*, 2016).

Peroxisomes are small cytosolic organelles, residence to many enzymes that are involved in catalysing the oxidation of substrates such as long-chain fatty acids, polyamines or D-amino acids. During these metabolic reactions, electrons from the oxidised substrates are passed to O₂ to form ROS (Sandalio *et al.*, 2013). A few examples of enzymes, present in the peroxisome that generate ROS, include acyl-CoA oxidase (for β -oxidation of fatty acids), urate oxidase, xanthine oxidase and D-amino acid oxidase (Schrader and Fahimi, 2006). To neutralize the high amounts of H₂O₂ generated, the antioxidant catalase is highly expressed in the peroxisome (Schrader and Fahimi, 2006). Another subcellular compartment, involved in the

production of ROS, is the endoplasmic reticulum (ER). Amongst many of the ROS generating enzymes found in the ER, is the cytochrome P450 heme-containing polypeptide, which resides in the ER membrane. These enzymes are responsible for the oxidation of a broad range of substrates, in which the acquired electrons are simultaneously passed to oxygen (Zangar *et al.*, 2004). Oxidative enzymes such as Ero1 and the NOX family are important for the production of ROS, to achieve folding of newly-synthesised nascent proteins, through the formation of disulphide bonds (Yoboue *et al.*, 2018). Overall, there are multiple ways, in which ROS can be produced in the cytosol, excluding the mitochondria. Similarly to mitochondrial ROS, these have also been linked to signalling pathways as well as numerous disease pathologies (Zhang *et al.*, 2016).

1.2.5 Mitochondrial ROS

Mitochondria have been considered for a long time as the main generators of ROS (Barja, 2019). However, this is due to the lack of comprehensive studies measuring ROS generation from different sources in the same experimental conditions (Sanz, 2016). A recent study by Martin Brand's laboratory addressing this question showed that in C2C12 human myoblasts only 45% of the ROS produced by the cells come from the mitochondrion (Wong *et al.*, 2019). Similarly, previous studies have suggested that peroxisomes produce higher levels of ROS than mitochondria, in the liver (reviewed in (Brown and Borutaite, 2012)).

In any case, mitochondria are one of the most important generators of ROS within the cell. Furthermore, mitochondrial ROS remain the most studied and the only free radicals that have shown a direct connection with ageing and age-related diseases, in multiple independent studies and several animal species, including humans (reviewed in (Sanz, 2016) (Barja, 2019) (Wallace, 2005)). Given that respiration requires a vast amount of the overall O₂ supply, the mitochondrial matrix is rich in O₂, which is therefore vulnerable to reduction via escapee electrons from the ETC. The extent of electrons leaking from the ETC during OXPHOS is unclear, particularly *in vivo*. Early estimations suggested that, during normal conditions, 1-4% of electrons leak and generate ROS (Barja, 2007). However, a more conservative updated estimation reduces this amount, to less than 0.1% of electrons (Larosa and Remacle, 2018). Within the mitochondria, there are 11 acknowledged sites where electrons can escape and reduce O₂, with one electron to produce superoxide (reviewed in (Wong

et al., 2017)). However, only CI and CIII have been shown to produce ROS under relevant physiological conditions, where independent approaches, such as chemical and genetic *in vivo* inhibition of the complex have been utilised to confirm the source of ROS (reviewed in (Murphy, 2009) (Stefanatos and Sanz, 2011) (Wong *et al.*, 2019), (Chandel, 2010) (Weinberg *et al.*, 2015) (Sanz, 2016) (Chouchani *et al.*, 2016)).

Within CI, there are two established sites of ROS production, namely the I_F (Chouchani *et al.*, 2016) and the I_Q (Treberg *et al.*, 2011) sites. A minority of reports have also suggested the Fe-S N₂ cluster of CI, as a site of ROS production (Genova *et al.*, 2001) (Herrero and Barja, 2000). The I_F site represents the FMN region of CI, where NADH binds and donates two electrons. The I_Q site is the site where CoQ binds to and receives two electrons, from CI. All the sites in CI contribute to the generation of mitochondrial matrix superoxide (Zhao *et al.*, 2019). Inhibitors of the I_Q site within CI, such as rotenone and piericidin A, both lead to an increase in superoxide production at the I_F site. This is the consequence of a highly reduced I_F site, when the downstream electron flow is blocked, which increases the NADH/NAD⁺ ratio and leads to the increased production of superoxide (Murphy, 2009). Superoxide production at the I_Q site has been proposed to occur during the process of reverse electron transport (RET) when the CoQ pool is highly reduced (Murphy, 2009). However, others have proposed that only the I_F site produces ROS in both a forward and reverse direction (Pryde and Hirst, 2011). Strong support for the I_Q site comes from the development of a new class of antioxidants calls S1QELs (suppressors of site I_Q electron leak) (Brand *et al.*, 2016). S1QELs scavenge superoxide exclusively produced at the I_Q site and have been shown to protect against ischemia-reperfusion (IR), *in vivo* (Brand *et al.*, 2016). As I will discuss in detail below, IR is characterised by the production of ROS by CI via RET (Brand *et al.*, 2016) and therefore the protection of S1QELs against IR injury, supports the I_Q site as the location of electron leakage.

At present, there is only one recognised site of electron leakage and superoxide production within CIII, the Q_o site, where $CoQH_2$ binds and undergoes oxidation (Muller *et al.*, 2003) (Muller *et al.*, 2004). At this site, superoxide can be deposited into both the matrix and the IMS. Mitochondria from rat and mouse skeletal muscle, showed that around 63% and 50% of superoxide ends in the matrix, respectively (Treberg *et al.*, 2010) (Muller *et al.*, 2004). The inhibitor antimycin A binds to the Q_i site of CIII and leads to a dramatic increase in superoxide production at the Q_o site. This is due to an accumulation of electrons upstream of the Q_i site, leading to the formation of a ubisemiquinone radical ($QH\cdot$) and the univalent reduction of O_2 (Murphy, 2009). Another condition, which is known to affect superoxide generation at the Q_o site is the mitochondrial membrane potential. It has been proposed that RET also occurs within CIII when electrons, at the Rieske iron-sulphur cluster, move back towards the Q_o site and produce superoxide (Bleier and Drose, 2013).

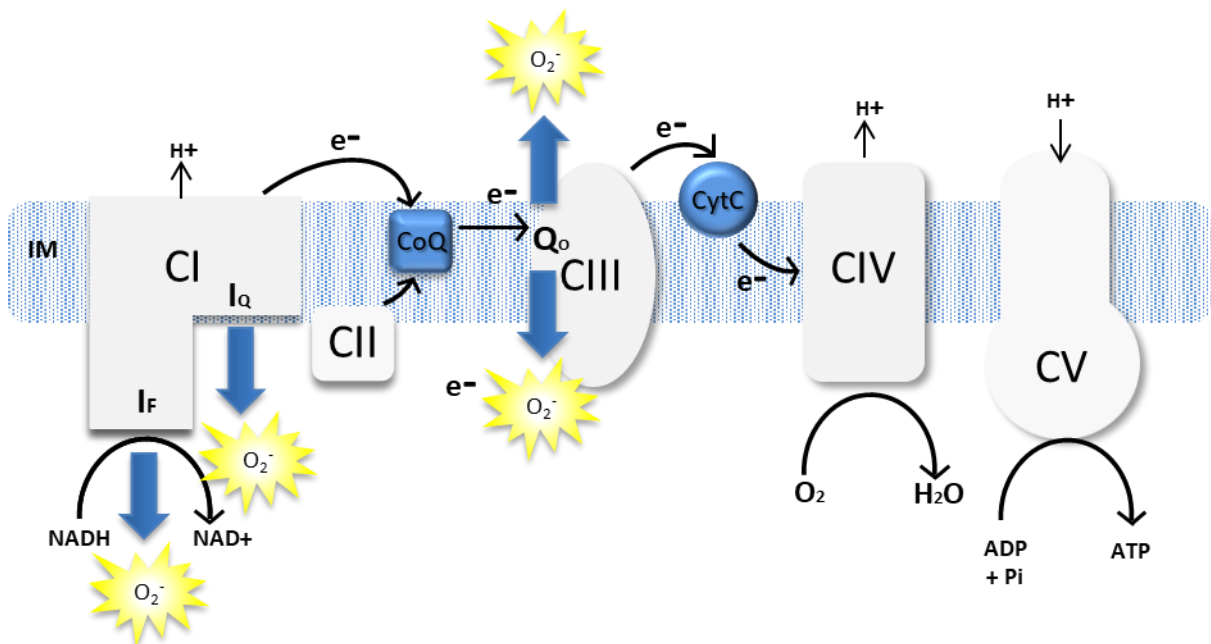


Figure 1.9 Schematic diagram demonstrating the sites of ROS production from CI and CIII of the ETC.

CI possesses two sites (I_q and I_F) which both generate ROS into the mitochondrial matrix. CIII has one site of ROS production (Q_o), which is capable of producing ROS in both the matrix and IMS.

CII is usually overlooked as an important generator of ROS (Drose, 2013). However, mutations in CII that increase superoxide generation have been related to cancer (Ishii *et al.*, 2005), neurodegeneration (Ackrell, 2002) and reduced lifespan (Walker *et al.*, 2006). Electrons can leak from the IIF site of CII, where the FAD cofactor oxidises

succinate, when both CI and CIII are inhibited (Quinlan *et al.*, 2012). Superoxide production from II_F can occur with electrons flowing in forward or reverse direction but superoxide is always directed to the mitochondrial matrix. Aside from the major respiratory complexes, mitochondrial superoxide generation can also occur via NADH/NAD⁺ linked enzymes, collectively known as 2-oxoacid dehydrogenase complexes. During the oxidation of their specific substrates, this group of enzymes form ROS at their flavin sites. These metabolic enzymes include alpha-ketoglutarate dehydrogenase, pyruvate dehydrogenase, branched-chain-2-oxoacid dehydrogenase and 2-oxoadipate dehydrogenase (Quinlan *et al.*, 2014). Another group of enzymes that can generate ROS include those that interact with the CoQ pool. For example, G3PDH, DHODH and ETF:CoQ, which all participate in the reduction of CoQ. G3PDH oxidises G3P and feeds the electrons directly to the CoQ pool. The Q binding site of this enzyme has been proposed to be the site of superoxide production (Mracek *et al.*, 2014). The DHODH enzyme executes the oxidation of dihydro-orotate and subsequently donates the electrons to CoQ. Similarly to G3PDH, superoxide can be generated at the CoQ binding site (Hey-Mogensen *et al.*, 2014). Lastly, the ETF:QO passes electrons to the CoQ, derived from β oxidation of fatty acids. Studies suggest that superoxide production occurs as a result of the singular electron transfer from the flavin site to the CoQ binding site (Watmough and Fremman, 2010).

In addition, there are two other reported families of proteins that contribute to the production of mitochondrial ROS. The first is the p66^{Sch} adaptor protein, which upon cytosolic stress signals is imported to the mitochondria, where it mediates the direct reduction of O₂ molecules with electrons from Cyt C (Kaludercic and Giorgio, 2016). The final example is the mitochondrial monoamine oxidases (MAO) found in the OMM (Edmondson, 2014). These enzymes catalyse the oxidation of amines, which consequentially produces a significant amount of ROS, associated with a few disease pathologies, such as Parkinson's disease (Fitzgerald *et al.*, 2014).

1.2.6 Methods of measuring mitochondrial ROS levels; resolution vs physiological relevance

Measuring ROS levels is challenging due to their high reactivity and short half-lives. For these reasons, the hydroxyl radical, which is extremely reactive and unstable, is the hardest form of ROS to study. This is particularly true for *in vivo* measurements;

thus the majority of studies regarding mitochondrial ROS production have been performed using *in vitro* techniques and mainly in isolated mitochondria. The use of isolated mitochondria has revealed important evidence surrounding how and where ROS can be produced. For example, the ETC complexes, where electrons leak from specific sites to incompletely reduce oxygen and generate ROS. However, *in vitro* studies cannot provide information about how ROS are produced *in vivo* and which enzymes generate ROS, in relevant physiological circumstances.

The use of isolated mitochondria has many drawbacks; however it has been extremely useful in allowing the high-resolution study of how mitochondrial ROS are generated (Sanz, 2016). Through these high-resolution techniques, it has been possible to identify specific enzymes and the sites within those enzymes, where ROS are produced. For example, it has facilitated the distinction between the production of ROS through forward electron transport or RET. High-resolution is achieved by the use of specific substrates and inhibitors to manipulate the redox state of the ETC and the pmf (Wong *et al.*, 2018). Using this approach, it is possible to study the sites of ROS production, exclusively at CI, by feeding mitochondria with CI-linked substrates (e.g. pyruvate and glutamate), in combination with rotenone. The major disadvantage of using isolated mitochondria is the lack of physiological relevance, caused by removing mitochondria from the cell for ROS measurements. Under these circumstances, mitochondria lose the ability to interact with other intracellular components and are exposed to unnaturally high levels of O₂. Thus, measurements are performed using saturated concentrations of substrates that are rarely observed *in vivo*. Working with cells *in vitro* eliminates certain disadvantages that isolated mitochondria possess (Sanz, 2016). However, the conditions under which cells are generally cultured i.e. high O₂ and glucose levels also limits the physiological relevance of ROS measurements. The following two examples illustrate the limitations of using cells to study mitochondrial ROS. Firstly, fibroblasts from muscle biopsies of patients suffering from mitochondrial diseases, in some cases, have no mitochondrial phenotypes, when cultured *in vitro* (Rodenburg, 2011). Secondly, human fibroblasts become senescent after a few rounds of replication, when cultured in high O₂ levels (20%). This phenotype is dependent on the levels of mitochondrial ROS and can be prevented when they are reduced (Passos *et al.*, 2007). However, senescence does not occur in the same fibroblasts if they are cultured under

physiological O₂ levels (~3%) (Busutil *et al.*, 2003). These examples further emphasise why *in vitro* experiments should be interpreted with caution.

In vivo ROS measurements are much more limited in number and current studies using *in vivo* techniques possess two major drawbacks (Wang *et al.*, 2013). First of all, they lack the resolution achieved by studies using isolated mitochondria and secondly the conflict surrounding the quantification *versus* visualisation of ROS levels. In this section, I will briefly discuss different approaches available to overcome these disadvantages and allow high-resolution *in vivo* ROS measurements.

It is possible to measure ROS *in vivo* in the presence or absence of specific inhibitors, to increase the resolution of the measurements. The inhibitors are fed or injected into the animal model, to determine where and how ROS are produced. The typical example is the administration of rotenone to prevent RET (Scialo *et al.*, 2016a) (Chouchani *et al.*, 2014a). Here one of the main problems is the toxicity of the drug for the animal, the difficulties of targeting specific tissues or cell types and undesirable side effects of the inhibitor. To obtain tissue specificity, genetic approaches can be used to target specific subunits of the respiratory complexes, leading to reduced levels of the specific complex. An example of this is the knockdown of CI subunits to prevent RET, in *Drosophila* (Scialo *et al.*, 2016a) or the knockdown of CIII subunits to abolish ROS production at the Q_o site (Diebold *et al.*, 2019). Finally, the use of alternative respiratory enzymes allows the redox state of the CoQ pool to be manipulated, which subsequently leads to an increase or decrease, in the production of superoxide (Scialo *et al.*, 2017). In summary, chemical and genetic inhibition of the respiratory complexes, as well as the expression of alternative respiratory enzymes, increases the resolution of mitochondrial ROS measurements, performed *in vivo* or *ex vivo*.

One method of measuring ROS *in vivo* and *ex vivo* is using microscopy, which allows the visualisation of ROS that can be subsequently quantified. However, the quantification of ROS levels using microscopy can be quite challenging (Xu and Xu, 2016). On the other hand, techniques available for allowing the precise quantification of ROS, such as, Mass Spectrometry (MS), measure the reduced and oxidised state of a ROS probe but they do not allow the visualisation of ROS, *in vivo*. An example is the MitoB/MitoP method, developed by the laboratory of Mike Murphy in Cambridge,

which takes advantage of a ratiometric approach to precisely detect H₂O₂, in the mitochondrial matrix (Cocheme *et al.*, 2011). An advantage of this technique is the reduction of experimental variability that may occur through autoxidation of the probe or differential accumulation, within the mitochondria. However, one of the drawbacks of MitoB/MitoP and other approaches that rely on MS for detection, is that they are highly invasive and require a significant amount of sample.

The visualisation of ROS levels can be achieved using chemical probes, which fluoresce once oxidised and can be measured using fluorescence microscopy. However, the use of fluorescent probes can be impossible to correlate with real values of ROS levels and ROS levels are usually reported as arbitrary units. Alternatively, the oxidation of the same probes can be measured by flow cytometry (Kauffman *et al.*, 2016) or using liquid chromatography together with MS (LC-MS) (Zielonka *et al.*, 2009). These methods make quantification more reliable and reproducible between experiments.

There are many different fluorescent probes for specific types of ROS (reviewed in (Xu and Xu, 2016)). The probes most commonly used are 2',7'-dichlorodihydrofluorescein diacetate (H₂DCF), for total ROS levels and dihydroethidium, for superoxide. H₂DCF belongs to a group of cell-permeable compounds called dihydrofluorescein (H₂F). Once H₂DCF enters cells, the acetate group, which allows the entry of H₂DCF into the cell, is cleaved via cellular esterases. Upon oxidation H₂F is converted to the highly fluorescent 2',7'-dichlorofluorescein (DCF). H₂DCF is normally used to measure H₂O₂ within cytosolic compartments of cells. The main advantage of this probe is its high sensitivity. However, H₂DCF has low specificity towards peroxides, as it also reacts with other ROS and RNS. In addition, it also has high autoxidation rates (Kalyanaraman *et al.*, 2012). Another fluorescent probe is Dihydroethidium (DHE), which is commonly used to detect superoxide (Robinson *et al.*, 2006). The variant of DHE, known as MitoSOX, allows DHE to be targeted to mitochondria using tri-phenyl-phosphonium (TPP). MitoSOX has become the most popular probe to detect mitochondrial ROS. However, DHE and therefore MitoSOX, have many drawbacks including lack of specificity, where other ROS and RNS are also able to oxidise MitoSOX. Additionally, MitoSOX increases fluorescence upon intercalation into DNA, both nuclear and mitochondrial, as well as the potential of auto-oxidation, thus is not always a direct indicator of

superoxide and can produce misleading results (Zielonka and Kalyanaraman, 2010). The lack of specificity can be addressed by using MS to allow the specific detection of 2-hydroxyethidium, which is formed as a result of superoxide oxidation (Zhao *et al.*, 2003). Despite all these problems, MitoSOX remains a quick and inexpensive way of studying mitochondrial superoxide levels, particularly considering the lack of reliable alternatives for measuring superoxide. Recently, an improved version of MitoSOX, called MitoNeoD, has been developed (Shchepinova *et al.*, 2017). It has been reported that MitoNeoD can overcome the two main problems of MitoSOX previously discussed, including the lack of specificity and increased fluorescence upon intercalation into DNA.

To achieve *in vivo* ROS measurements, using the probes discussed above, they can be either fed or injected into the animal model. However, due to their high autoxidation rates, this can be challenging and increases variability, thus reducing reproducibility among experiments (Sanz, 2016). A partial solution is to use these probes *ex vivo*, taking advantage of their cell permeability. Alternatively, it is possible to utilise genetically encoded fluorescence detectors that can be expressed in specific tissues or cells (Sanz, 2016). For the detection of H₂O₂, the two most commonly used options are the redox-oxidation Green Fluorescent Protein (roGFP) (Albrecht *et al.*, 2011) and Hydrogen Peroxide protein (Hyper) (Choi *et al.*, 2001). Unfortunately, there is no reliable alternative for specifically measuring superoxide. The circularly permuted Yellow Fluorescent Protein (cpYFP) was previously proposed as a superoxide sensor (Wang *et al.*, 2008), however, has since been shown not to specifically detect superoxide (Muller, 2009). All of these aforementioned methods are ratiometric detectors, similar to MitoB/MitoP. In these cases, the ratiometric system is based on two different excitations wavelengths, one for the oxidised and the other for the reduced form of the protein. Here, the fluorescent protein is fused to a peroxide sensor, which confers their specificity and determines their sensitivity. Genetically encoded sensors have an important advantage over chemical probes, as they can be targeted to specific organelles within the cell. For example, the laboratory of Tobias Dick has produced roGFP proteins fused to the oxidant receptor peroxidase 1 (Orp1, roGFP-Orp1), which detects H₂O₂, in the mitochondria or the cytosol (Albrecht *et al.*, 2011). roGFP allows fixation of the samples, which increases the potential number of samples examined and *in vivo* estimations of ROS levels. Genetically encoded sensors are generally

more specific but less sensitive, in comparison to chemical probes. However, new and more sensitive roGFP probes fused to peroxiredoxin proteins have been developed to detect basal levels of H₂O₂, in both the mitochondria and cytosol (Morgan *et al.*, 2016). Another disadvantage of the genetically encoded sensors *versus* the chemical probes, is that they require the transformation of cells or whole animals. This could be technically challenging and very expensive, in the case of mice and other mammal models.

Finally, it is recommended to confirm the specificity of any ROS signal measured. ROS measurements could be repeated in the presence of specific antioxidants that must reduce the intensity of the signal. For example, during the detection of superoxide, the overexpression of SOD would significantly reduce the signal. Conversely, overexpression of catalase must reduce a H₂O₂ signal without altering any superoxide signal being measured.

All the probes and sensors described above have advantages and disadvantages that need to be considered carefully. The use of chemical probes offers a quick, sensitive and inexpensive way of detecting ROS levels and allows performing multiple experiments, in parallel. However, they possess issues with the specificity of the ROS detected and are prone to technical artefacts. Genetically encoded sensors are more specific but less sensitive and require complex systems of expression that increase the time and resources invested in ROS measurements, thus limiting the number of experiments. Therefore the use of one or another approach will depend on the experimental design and the resources available.

1.2.7 The physiological relevance of site-specific ROS production at CIII

It is now apparent that ROS can behave as signalling molecules in cells, as well as contributing to oxidative damage. It has been established that 'good' ROS participate in signalling and have low or moderate reactivity, i.e. H₂O₂ and superoxide. In contrast to 'bad' ROS, which are highly reactive and cause oxidative damage, e.g. hydroxyl radical or peroxynitrite. The physiological effect of ROS is determined by three factors, namely (i) where and when they are produced, (ii) the amount generated and (iii) the type of ROS (Sanz, 2016). As discussed before, ROS involved in signalling are produced at specific times and places, in moderate amounts and have low reactivity. Conversely, oxidative stress is characterised by uncontrolled

production of ROS, with high reactivity that leads to oxidative damage. As mitochondria have a central role in metabolism, a lot of research has focused on this organelle as a potential site for the creation of signalling ROS messengers. As discussed above, the two major sites of ROS production detected in isolated mitochondria, are respiratory complexes I and III (Wong *et al.*, 2017). Thus, both CI and CIII derived ROS have been implicated in vital physiological processes, as well as being associated with ageing and age-related diseases, by *in vivo* studies (Stefanatos and Sanz, 2018).

CI possesses two sites that generate ROS into the mitochondrial matrix (St-Pierre *et al.*, 2002). An intriguing mechanism of CI is that it can produce ROS, with electrons flowing in both a forward and reverse direction (Robb *et al.*, 2018). Paradoxically, reports showing a role of CI ROS in cellular signalling indicate that ROS are mostly produced in the reverse direction. I will discuss in detail the mechanism and physiological pathways behind ROS produced via RET (ROS-RET), in the following section. In this section, I will focus on the physiological relevance of ROS produced by CIII.

So far, only the Q_o site of CIII has been shown to produce ROS (Brunelle *et al.*, 2005). CIII ROS production is bidirectional, with approximately half of the ROS being generated into the IMS and the other half into the mitochondrial matrix (Treberg *et al.*, 2010) (Muller *et al.*, 2004). The production of ROS into the IMS can be particularly useful for transmitting mitochondrial information directly to the cytosol. Here the ROS act as signalling messengers and have the potential to interact with a vast array of redox-regulated proteins (reviewed in (Sena and Chandel, 2012)). Studies from the laboratory of Navdeep Chandel have established an association between ROS generated at the Q_o site of CIII and multiple physiological processes (Schieber and Chandel, 2014). For example, Chandel's work has shown that CIII ROS are required to stabilise HIF-1 α , in response to hypoxia (Chandel *et al.*, 2000). Upon CIII inhibition, using the Q_o site inhibitors myxothiazol and stigmatellin, or the genetic depletion of the Rieske-iron sulphur protein, the stabilisation of HIF-1 α was prevented, thus supporting the role of CIII ROS production within this process (Brunelle *et al.*, 2005) (Bell *et al.*, 2007). In addition, CIII derived ROS has also been shown to regulate the differentiation of adipocytes from mesenchymal stem cells. This process requires an increase in OXPHOS, which subsequently increased

electron leak and superoxide production at CIII (Tormos *et al.*, 2011). Suppressing the increased ROS levels, using similar techniques described earlier, prevented differentiation, therefore demonstrating its dependence on the production of ROS. Finally, CIII derived ROS have also been affiliated with the activation of T cells (Sena *et al.*, 2013) as well as TGF- β signalling (Jain *et al.*, 2013).

ROS produced at CIII have also been associated with negative effects during pathological situations. For example, a link between air pollution and ROS has been suggested, which promotes death of alveolar epithelial cells (Soberanes *et al.*, 2009). In this model, ROS produced at the Q_o site of CIII were responsible for triggering apoptosis, by activation of the redox-sensitive kinase ASK1 (Apoptosis signal-regulating kinase 1). It is known that air pollution causes the release of pro-inflammatory cytokines, such as IL-6, which induces lung inflammation. The release of IL-6 by alveolar macrophages occurs in response to the increase in ROS produced by CIII (Soberanes *et al.*, 2019). Furthermore, in a Kras-driven mouse model of lung cancer, CIII derived ROS were shown to be required for both proliferation and tumorigenesis in cancer cells (Weinberg *et al.*, 2010). The anti-proliferative effects of metformin on cancer may be caused by the inhibition of ROS generated by CIII (Wheaton *et al.*, 2014). Accordingly, expression of Ndi1 in metformin-treated cells restores both ROS production at CIII (but not at CI) and the proliferation capacity of the cells, when injected into mice (Wheaton *et al.*, 2014).

1.2.8 The physiological relevance of site-specific ROS production via Reverse Electron Transport (RET) at CI

In 1961, Chance and Hollunger demonstrated that feeding the CII-linked substrate, succinate, to isolated mitochondria resulted in the reduction of NAD⁺ back to NADH, a process that they termed reverse electron transport (RET) (Chance and Hollunger, 1961). For many years, RET was dismissed as an *in vitro* artefact. However, in the last 10 years, evidence has accumulated supporting the occurrence of RET *in vivo*, thus re-establishing its scientific interest. RET is a phenomenon observed at CI of the respiratory chain, where electrons move in the reverse direction back to CI, from CoQH₂. Coinciding with the process of RET, there is a significant rise in ROS production from CI. The exact site of electron leak during RET is unclear, and both the I_F and I_Q sites have been proposed as the source of ROS (Pryde and Hirst, 2011) (Quinlan *et al.*, 2013). For RET to occur there are two required conditions: a highly

reduced CoQ pool and a high pmf, both of which are essential to make the reverse flow of electrons possible. Previous studies have shown that the use of the inhibitor, FCCP, to abolish the polarised membrane prevented the occurrence of RET (Robb *et al.*, 2018). Additionally, preventing the binding of CoQ to CI, via targeted I_Q site inhibitors, such as rotenone, also prevents the process of RET. In each case, the dramatic increase in ROS associated with RET, was also abolished. ROS-RET has since been recognised in a number of physiological processes, discussed in detail below (Scialo *et al.*, 2016a).

The physiological occurrence of ROS-RET was first reported during IR (Paraidathathu *et al.*, 1992) (Lesnefsky *et al.*, 2004) (Chen *et al.*, 2006). A paper from Michael Murphy's laboratory at Cambridge (Chouchani *et al.*, 2014a) showed that O₂ starvation during ischemia leads to the rapid accumulation of succinate. During reperfusion and restoration of O₂, CII starts metabolising the abundant supply of succinate, leading to a highly reduced CoQ pool and sustained high membrane potential. In combination, these two conditions, stimulate RET and the extensive production of ROS associated with it (Chouchani *et al.*, 2014a).

Since 2014, ROS-RET has been implicated in many other physiological processes (Scialo *et al.*, 2017). In contrast to the IR model, ROS produced during RET in these cases are not detrimental. Instead they have been shown to play an essential role in activating specific signalling pathways, required for maintaining cellular homeostasis. For example, the differentiation of myoblasts into myotubes requires the generation of ROS-RET (Lee *et al.*, 2011). Genetically silencing CI subunits or culturing cells in rotenone, prevented differentiation. The role of ROS during this process was further confirmed by adding antioxidants, which also prevented cellular differentiation. Another function of ROS-RET is the regulation of CI levels and its integration into respiratory supercomplexes (Guaras *et al.*, 2016). When cells were cultured in a sugar-rich medium, rotenone increased ROS production, indicating forward electron flow. However, when fatty acids were used as the primary fuel to supply electrons to mitochondria, ROS-RET was observed, indicating the reverse flow of electrons (Guaras *et al.*, 2016). Interestingly, the occurrence of ROS-RET caused oxidation of CI subunits, which subsequently reduced both CI levels and its integration into supercomplexes. This demonstrates an adaptation affecting the assembly of supercomplexes, depending on the type of substrates available for oxidation. When

electrons from the oxidation of substrates enter the ETC downstream of CI, the complex is degraded and supercomplexes are restructured, to favour CIII/CIV association versus CI/CIII/CIV (Cogliati *et al.*, 2013).

Altering the respiration rate to the levels of O₂ in the blood is an essential task. In mammals, cells located in the carotid body are responsible for this process. When O₂ levels are low, the chemoreceptors of the carotid body trigger a response that increases the respiration rate. The former response requires both the activity of CI and the presence of ROS, to occur (Fernandez-Aguera *et al.*, 2015) (Arias-Mayenco *et al.*, 2018). In the absence of CI, the presence of rotenone or high concentrations of antioxidants, the cells of the carotid body are unable to respond to changes in O₂ levels and mouse models cannot increase respiration, during hypoxia. Furthermore, CI ROS seems to also play an essential role in the immune response, similarly to CIII derived ROS. Macrophages react to the presence of pathogenic bacteria by triggering a pro-inflammatory response, characterised by the generation of several types of cytokines. This immune response requires mitochondrial ROS, which is triggered by exposing or injecting lipopolysaccharides (LPS) in macrophages and experimental animals, respectively (West *et al.*, 2011). A comprehensive study from the laboratory of Luke O'Neill at Trinity College has shown that the metabolism of macrophages is reprogrammed, in the presence of bacteria. Mitochondrial respiration was manipulated to produce ROS instead of ATP and these ROS triggered the expression of pro-inflammatory cytokines. The pro-inflammatory response was abolished in the presence of rotenone, FCCP or expressing AOX, indicating that ROS were produced by RET.

Finally, our laboratory has shown that ROS-RET can also be induced *in vivo* by the expression of the alternative Ndi1, described before. RET is stimulated by the expression of Ndi1, due to the direct transfer of electrons from the oxidation of NADH, to the CoQ pool. Thus, leading to a highly reduced CoQ and a dramatic increase in ROS, observed in the fly brain (Scialo *et al.*, 2016a). As expected, this increase in ROS was abolished by blocking the I_Q site with rotenone or by dissipating the membrane potential with FCCP. In addition, preventing the reduction of CoQ with AOX or knocking down subunits of CI, also abolished ROS, supporting RET as the source. Surprisingly, Ndi1-induced ROS-RET has also been shown to significantly extend the lifespan of *Drosophila melanogaster*, irrespective of diet or the

background (Sanz *et al.*, 2010b) (Scialo *et al.*, 2016a) (Bahadorani *et al.*, 2010) (Hur *et al.*, 2013)). Furthermore, NDX, an alternative NADH dehydrogenase found in *Ciona intestinalis*, has also been reported to lead to lifespan extension (Gospodaryov *et al.*, 2014). Due to the fact that Ndi1 can bypass CI, it can rescue CI subunit mutations (Sanz *et al.*, 2010b) (Cho *et al.*, 2012), thus, Ndi1 expression protects mitochondrial function against the effects of ageing and several other stress conditions. Evidence, in support of the former, includes the increase in mitochondrial respiration in old flies expressing Ndi1 (Sanz *et al.*, 2010b), as well as an increase in mitochondrial ATP production, in models of Parkinson's disease (Vilain *et al.*, 2012). More surprisingly, Ndi1 can also protect against the knockdown of *Sod2*, which increases mitochondrial superoxide levels (Scialo *et al.*, 2016a). In the *Sod2-KD* model, flies expressing Ndi1 lived longer and their mitochondria respired more efficiently than the controls, despite having higher levels of mitochondrial ROS. This indicates that ROS-RET can act as a signal, which activates pro-survival pathways over the background noise of ROS, caused by knockdown of *Sod2* or the age-related progressive increase in ROS.

In light of the recent evidence, there has been speculation that ROS-RET plays a pivotal role in signal transduction and maintaining cellular homeostasis. ROS-RET is connected to two central components of metabolism, including both the redox state of the CoQ pool (which provides information about electron flow through the ETC) and the pmf (which is essential in regulating mitochondrial ATP production). In addition, ROS generated during the process of RET can be modulated in intensity and duration. For these reasons, ROS-RET is an ideal signalling system responsible for communicating information from the mitochondria, to the rest of the cell (reviewed in (Scialo *et al.*, 2017)). Thus, research dedicated to understanding the mechanisms behind ROS-RET, may be pivotal in understanding the role ROS play in health and disease.

1.3 Mitochondrial ROS and age-related diseases

The ageing process is a universal phenomenon in all animals, characterised by inevitable deterioration, which ultimately leads to death (Lopez-Otin *et al.*, 2013). Over the past decade, the importance of researching the mechanisms behind ageing has been established by the evident increase of the elderly population, which currently shows no indication of slowing down. Coinciding with the ageing population

is the corresponding increase of age-related disease prevalence (LeBrasseur *et al.*, 2015). Excessive mitochondrial ROS production has been repeatedly implicated in the ageing process and has also been observed in numerous age-related pathologies (Vos *et al.*, 2010). This is particularly observed in neurodegenerative diseases such as Alzheimer's and Parkinson's diseases (Kim *et al.*, 2015). In Alzheimer's disease, enhanced oxidative stress has been reported, resulting in damaged neurons, within the brain. In addition, different studies have shown decreased levels of antioxidants in patients of Alzheimer's disease (Zhao and Zhao, 2013). Parkinson's disease has been associated with a decrease in the activity of respiratory CI, which leads to excessive production of ROS (Schapira, 2008). This was later supported by the parkinsonism phenotype induced by the CI inhibitors, 1-methyl-4-phenyl-1,2,3,6-tetrahydropyridine (MPTP) or rotenone (Betarbet *et al.*, 2000). Although both these neurodegenerative disorders present an increase in oxidative stress, it is still unclear if mitochondrial ROS is the cause or consequence of Alzheimer's and Parkinson's disease (Kim *et al.*, 2015). Elevated mitochondrial ROS production can also be observed in the pathology of cancer (Rodic and Vincent, 2018). It has previously been established that DNA damage induced by oxidative stress can increase the risk of cancer (Moloney and Cotter, 2018). Recently, mitochondrial ROS have also been shown to possess a regulatory role in cancer progression. Here, the cancer cells can maintain ROS at precise concentrations, enough to stimulate growth and proliferation but low enough to avoid apoptosis and autophagy. Therefore allowing the rapid growth and progression associated with cancer cells (Idelchik *et al.*, 2017). Type II diabetes is another age-related disorder, where patients have been identified to have increased ROS production. It has been proposed that the sustained ROS-dependent activation of downstream insulin signalling pathways, can lead to insulin resistance (Abdul-Ghani *et al.*, 2009). A final example of heightened mitochondrial ROS production is in cardiovascular diseases. Here it has been shown that the oxidation of low density lipoproteins (LDLs), by ROS, is a direct cause of atherosclerosis (Panth *et al.*, 2016).

In most of these cases, the source of ROS observed in these pathologies has not been investigated. For example if the ROS are generated at specific sites, such as CI or CIII, or produced non-specifically, as a result of a defective metabolism. Answering this question may help the development of more specific therapies that prevent oxidative stress, without altering redox signalling.

1.3.1 Historical importance of MFRTA; evidence for and against

In the 1950's Denman Harman proposed the free radical theory of ageing, describing free radicals as the primary cause of ageing (Harman, 1956). This was later modified in 1972 to the mitochondrial free radical theory of ageing (MFRTA), which characterised mitochondria as biological clocks. In this updated version of the theory, free radicals produced exclusively in the mitochondria accumulate, leading to oxidative stress, which induces the ageing process (Harman, 1972). Since this theory was first introduced, extensive research exploring the relationship between ageing and mitochondrial ROS has been instigated. The evidence from these studies has accumulated, both supportive and contradictory (reviewed in (Sanz *et al.*, 2006) (Sanz and Stefanatos, 2008) (Barja, 2019)). Although this theory is still popular, it does not take into consideration the recent advancements surrounding the role of ROS in redox signalling ((Lapointe and Hekimi, 2010) (Sanz, 2016)). Below I describe in detail the evidence for and against the MFRTA.

The first line of evidence, supporting the MFRTA, revealed a positive correlation between ROS and age, (Toroser *et al.*, 2007) (Sanz *et al.*, 2010a) (Cocheme *et al.*, 2011) as well as a correlation between short-lived animals and higher ROS levels, compared to long-lived species (Barja *et al.*, 1994). This was further supported by an increase in oxidative stress and mitochondrial dysfunction, a classic hallmark of ageing in old individuals and short-lived species (Chistiakov *et al.*, 2014). Additionally in many age-related diseases, such as Parkinson's disease (Kim *et al.*, 2015), cancer (Idelchik *et al.*, 2017), cardiovascular diseases (Garcia *et al.*, 2017b) and diabetes (Abdul-Ghani *et al.*, 2009), high levels of ROS and oxidative stress could be detected. All the previously described evidence, supporting the MFRTA, are observational in nature and based on correlations. Contradictory evidence started to accumulate when alternative experimental approaches were used, to test the predictions of the theory. The experimental manipulation of antioxidant levels brought about inconsistent data, which began to challenge the integrity of MFRTA. Studies were able to demonstrate that the overexpression of antioxidants and the administration of non-enzymatic antioxidants, such as vitamin E and C, to decrease ROS levels showed no beneficial effects on longevity (Ernst *et al.*, 2013). Furthermore, diminishing antioxidant levels did not shorten lifespan as expected either (reviewed in (Sanz *et al.*, 2006)). For example in *C.elegans*, the knockdown of

all SOD enzymes, did not lead to a decrease in longevity, despite a rise in superoxide levels (Van Raamsdonk and Hekimi, 2012) (Yang *et al.*, 2007) (Van Raamsdonk and Hekimi, 2009) (Yang *et al.*, 2007) (Doonan *et al.*, 2008). Similarly, in a heterogeneous SOD2 knockdown mouse model, no effect on lifespan was observed, although mice suffered from higher levels of ROS and oxidative damage (Van Remmen *et al.*, 2003). Additionally, in *Drosophila melanogaster* it has been demonstrated that the overexpression of MnSOD and the expression of a mitochondrial targeted catalase have no effect or negative effects on lifespan, respectively (Mockett *et al.*, 2010). The direct manipulation of mitochondrial ROS production was then used to test the validity of the MFRTA. Reducing the production of superoxide from the ETC did not extend lifespan in fruit flies (Sanz *et al.*, 2010a). In fact, in flies and worms an increase in mitochondrial ROS was shown to extend lifespan (reviewed in (Ristow and Schmeisser, 2011) (Sanz, 2016) (Hekimi *et al.*, 2011)). For example the *clk-1* mutation in worms, targeting CoQ, increased both mitochondrial ROS and lifespan (Wong *et al.*, 1995). In addition, administration of CI inhibitors, rotenone or paraquat, as well as mutations in ETC subunits, were associated with an increase in ROS production, which positively affected longevity in worms (Yang and Hekimi, 2010). In *Drosophila melanogaster*, there is no positive effect on lifespan associated with feeding rotenone or paraquat (Scialo *et al.*, 2016a). However mutations in CI, which increase ROS in the muscle (Owusu-Ansah *et al.*, 2013) and the aforementioned expression of Ndi1, which increases mitochondrial ROS production, both extend lifespan. All these manipulations that increase ROS and extend lifespan are reverted by overexpression or administration of antioxidants, showing that these beneficial effects are ROS dependent.

Despite the accumulation of contradictory evidence, overall, the MFRTA has been pivotal in advancing the field of ageing and ROS. Research surrounding this theory has enabled a deeper understanding of the physiological processes that ROS participate in, providing the tools to understand the dual role that ROS play in redox signalling and oxidative stress.

1.3.2 The concept of hormesis

It has been established that damaged mitochondria produce higher levels of ROS and accumulate during ageing. Paradoxically to this, are studies demonstrating that boosting mitochondrial ROS levels, in young individuals, extends lifespan. The

concept of hormesis has been used to provide an explanation for these contradictory facts. Hormesis is defined as an adaptive response in which mild stress in early life will induce resistance to higher levels of stress, in later life. In the case of mitochondrial ROS, increasing their levels would stimulate protective survival mechanisms to counteract the stress and produce antioxidant systems, capable of removing the ROS signal (Luna-Lopez *et al.*, 2014). Mitochondrial hormesis is known as mitohormesis (Yun and Finkel, 2014) and has been used to explain how mitochondrial ROS regulate lifespan (Ristow and Schmeisser, 2011). From the point of view of mitohormesis, the exposure of ROS in early life can induce the expression of antioxidants that protect against oxidative stress, in later life (Schulz *et al.*, 2007). The problem with this explanation is that fails to explain why the overexpression of the same antioxidants does not extend lifespan, as discussed previously. Additionally, mitohormesis also fails to explain why ROS produced at different sites can impose different downstream effects, through targeting distinct physiological pathways (Luna-Lopez *et al.*, 2014).

1.3.3 Importance of studying mitochondrial ROS signaling

It has been well established that cells rely on healthy and active mitochondria to provide cellular energy, as well as maintaining cellular homeostasis, through the activation of numerous signalling pathways. At the forefront of mitochondrial signalling is the controlled production of mitochondrial ROS, a by-product of OXPHOS. Mitochondrial ROS can diffuse across the double membrane, as signalling messengers, in response to stress and regulate the redox state of key cysteine residues in target proteins. Once homeostasis has been restored, antioxidant systems are activated to remove the ROS signal (Shadel and Horvath, 2015). However, the unregulated and excessive production of mitochondrial ROS has been implicated in a wide range of pathologies, including the ageing process. It appears that during early life mitochondrial ROS protects cells and promotes cell viability, which is ultimately lost in later life, where ROS drives oxidative stress. It has been shown that three factors can determine the behaviour of ROS. Firstly, the type of ROS, in which low reactive molecules such as H₂O₂ participate in signalling and highly reactive molecules as the hydroxyl radical, cause oxidative damage. Secondly, the location and duration of ROS production. As previously discussed, ROS produced by CI activate different downstream targets, in comparison to ROS produced by CIII. Similarly, ROS produced in response to stress can help cells to

cope with that stress, whereas ROS produced continually will cause oxidative stress. Finally, the amount of ROS produced, where low amounts modulate the activity of signalling pathways and high amounts contribute to ageing and the onset of age-related diseases (Hekimi *et al.*, 2011).

One of the important unanswered questions in the field of redox biology, is how ROS signalling is lost during ageing and how oxidative stress takes a leading role (Stefanatos and Sanz, 2018). The two major sites of mitochondrial ROS production within the mitochondria are CI and CIII, which can both regulate superoxide production depending on the electron flow through the ETC and the pmf. As I discussed for ROS-RET, changing ROS levels in response to alterations in mitochondrial respiration, is one of the characteristics that makes mitochondrial ROS suitable to participate in redox signalling. However, mitochondria fail to communicate information in the presence of a dysfunctional ETC, which is observed during ageing and in mitochondrial diseases. For example, in *Drosophila*, CI levels and activity declines in aged flies, compared to early adulthood (Scialo *et al.*, 2016a). It has been previously shown that CI inhibition prevents RET (Scialo *et al.*, 2016a), therefore the reduction of CI activity during ageing would gradually lead to the inhibition of RET and the alteration of any physiological processes, which ROS-RET regulate. It is possible that during early life, ROS are produced specifically through regulated processes, which are ultimately lost during ageing. Thus, in later life, there is a switch in ROS production, to create non-specific, unregulated ROS, which drives the oxidative stress, we see in older individuals (Stefanatos and Sanz, 2018). To understand how ROS signalling fails, it is essential to measure mitochondrial ROS levels across all ages and test whether the place, time and intensity of ROS, changes during ageing. In the future, this could be central to developing treatments, which ameliorate age-related diseases and facilitate healthy ageing.

1.4 *Drosophila melanogaster* as a model system

The common fruit fly, also known as *Drosophila melanogaster*, was first introduced to scientific research as a model organism in the 1900s. Since then, research on *Drosophila* has contributed to understanding further, a wide range of scientific topics such as ageing, behaviour, genetics and human disease (Fernandez-Moreno *et al.*, 2007). A total of six Nobel prizes have been awarded to researchers working with fruit flies, most recently being in 2017 (Guo *et al.*, 2016).

The *Drosophila* genome consists of only 4 pairs of chromosomes; X/Y, II, III and IV. Although due to the notably small size of chromosome 4, the majority of genes are encoded on the first three chromosomes (Kaufman, 2017). In 1910, Thomas Hunt Morgan discovered the *Drosophila* white-eyed mutant (Morgan, 1910), which was the catalyst for the deep understanding of fruit fly genetics we hold today (Fernandez-Moreno *et al.*, 2007). At present, the entire fruit fly genome, of approximately 13,600 genes, has been characterised, making them an obvious choice for carrying out genetic studies (Adams *et al.*, 2000). One of the advantages of using *Drosophila melanogaster* as a model organism is the existence of public stock centres where fly lines carrying drivers, transgenes or mutations, are available for the whole community. Two of the most important stock centres are the Bloomington *Drosophila* Stock Centre (BDSC, <https://bdsc.indiana.edu/>) and the Vienna *Drosophila* Resource Centre (VDRC, <https://stockcenter.vdrc.at/control/main>).

The life cycle of *Drosophila melanogaster* is short, consisting of an approximate 10-day developmental period, categorised into 4 distinct stages: embryo, larva, pupa and adult. The *Drosophila* life cycle begins with the fertilisation of an embryo encased in an egg, which undergoes embryogenesis for 24 hours. From embryos, they develop into larvae, starting with the first instar larva, which feeds on the carbohydrate-protein-based food media. Following on from first instar larva, they moult into second instar larva, which burrow into the culture medium and enter a second moulting phase. The mature 3-day-old third instar larvae start to migrate up the surfaces of the containers and here they develop into pupae. During pupation, metamorphosis occurs to develop fully formed adult flies, from the coordinated assembly and maturation of imaginal disks and histoblasts, present in the larvae. After a pupation period of 4 days, the adult flies eclose from their pupae and can survive for an approximate 2 – 3 months at 25°C (Figure 1.10). As *Drosophila* are poikilothermic, their rate of development and longevity can be controlled using temperature. At 25 °C, it will take an average of 10 days to produce adult flies however at a lower temperature of 18 °C, the process is much slower, taking up to 20 days (Fernandez-Moreno *et al.*, 2007).

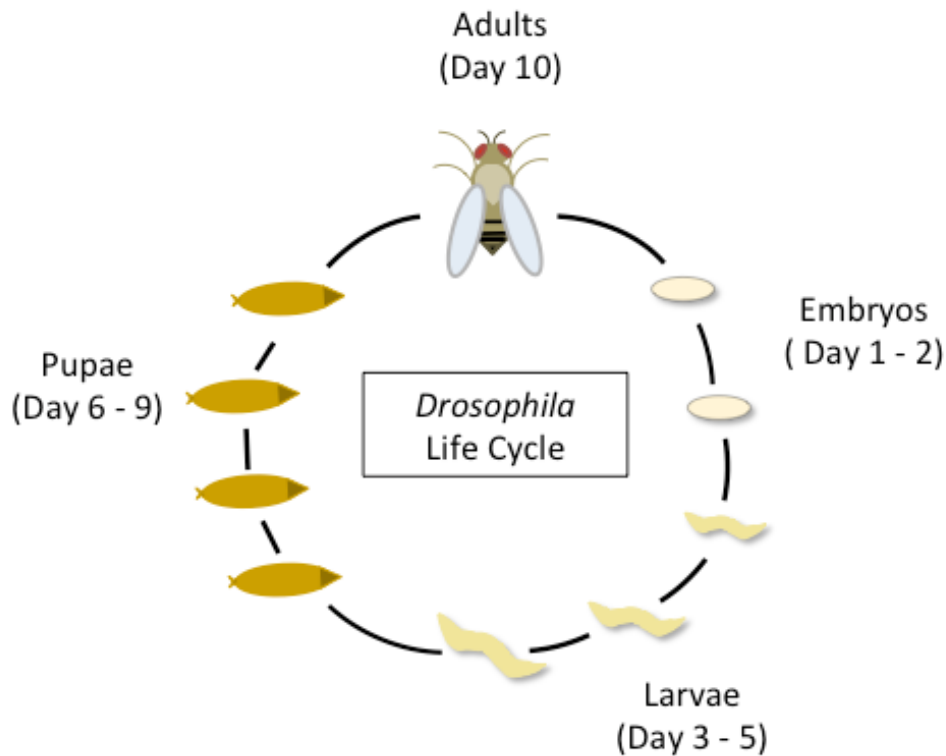


Figure 1.10 Diagram of the *Drosophila* life cycle.

The *Drosophila* life cycle is categorised into four stages, including embryos, larvae, pupae and adults.

1.4.1 Advantages of using *Drosophila* as a model organism

There are many reasons that make the fruit fly an advantageous model organism. The first is that they allow *in vivo* experimentation to study an entire organism, therefore can overcome the limitations associated with *in vitro* studies, such as the artificial conditions in which cells are cultured. Secondly, working with *Drosophila* is cost-effective due to their low maintenance costs. In addition, fruit flies have a short lifespan, when compared to the average 3-year lifespan of mice, and produce a high number of offspring. Furthermore, fruit flies are small 3 mm long invertebrates, available in much higher numbers than bigger animals and can be reared in confined spaces, allowing many biological repeats in a short time frame, to confirm results (Hirth, 2010). One of the tools that makes *Drosophila* an extremely valuable model organism is its powerful genetics. Since their first introduction to laboratories more than 100 years ago, scientists have been able to map out the entire fly genome and develop an extensive range of genetic techniques, allowing the effortless manipulation of targeted genes (Sun *et al.*, 2013). There are two defined categories of genetic manipulation: (i) loss-of-function (LOF) and (ii) gain-of-function (GOF). LOF

includes the partial or complete removal of a targeted gene, whilst GOF involves strategies to increase the expression of a specific gene. There are different strategies that individually or in combination allow modification of gene expression in *Drosophila*, including the use of (i) P-element insertional mutagenesis, (ii) gene silencing through RNA interference (RNAi), (iii) FLP-FRT recombination, (iv) CRISPR-Cas9 genome editing and (v) PhiC31 mediated site-specific recombination (reviewed in (Cooley *et al.*, 1988) (Theodosiou and Xu, 1998) (Bier *et al.*, 2018) (Gao *et al.*, 2008) (Heigwer *et al.*, 2018)). Another advantage is the similarity of the human and fly genome, where 75% of disease-related genes in *Drosophila* possess homologues in humans (Pandey and Nichols, 2011). This offers the potential to study the effects of human diseases in flies, to elucidate their biological mechanisms and discover future therapies.

1.4.2 GAL4/UAS system to control gene expression

The GAL4/UAS (upstream activator sequence) system is a highly used tool that allows the manipulation of targeted gene expression in *Drosophila* (Brand and Perrimon, 1993). The basis of this system consists of two elements; the first is the functional incorporation of the yeast GAL4 transcription factor and secondly the presence of a UAS sequence which GAL4 binds to, neither of which are endogenously present in fruit flies (Scialo *et al.*, 2016b). Each of these components is distributed between two separate lines. The yeast transcription factor GAL4 is expressed in the presence of a promoter, whilst the targeted gene is expressed downstream of the UAS sequence. When these two lines are crossed the transcription factor GAL4 is able to bind to the UAS, thus driving expression of the downstream gene of interest. The resulting progeny will express the transgenes of interest (Figure 1.11). This system allows the spatial and temporal control of gene expression depending on the chosen promoter. To achieve spatial control, the promoter can be either ubiquitous or tissue-specific.

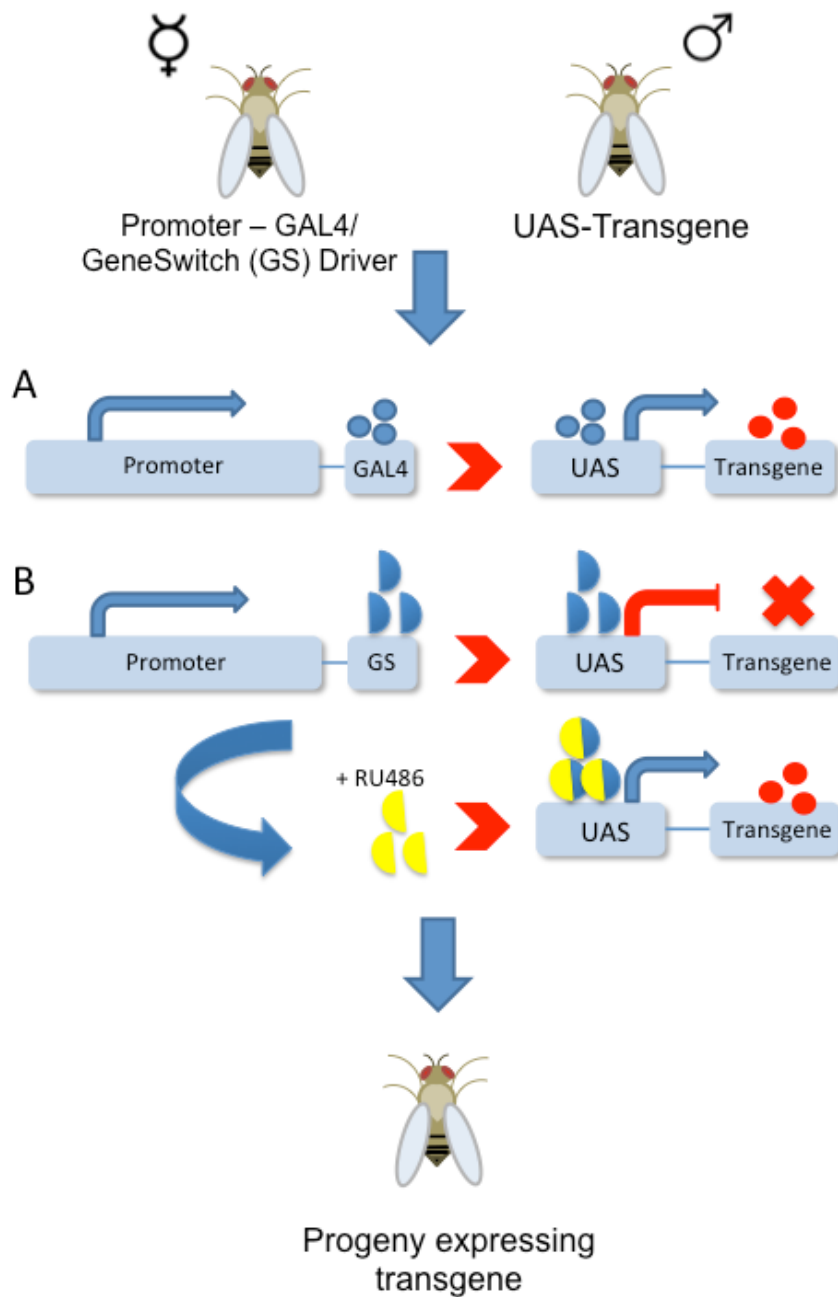


Figure 1.11 Schematic diagram of the GAL4-UAS and GeneSwitch GAL4 (GS) system.

(A) GAL4-UAS system; Virgin female flies carrying the GAL4 promoter are crossed with male flies carrying the transgene. This leads to the binding of GAL4 to the UAS-transgene, resulting in the expression of the transgene. **(B) GeneSwitch GAL4 (GS) system;** Similarly to GAL4-UAS virgin female flies are crossed with male transgene flies however the GAL4 transcription factor is only induced in the presence of RU-846 leading to the expression of the transgene.

The GeneSwitch GAL4 (GS) system is a modified GAL4 protein that is only active in the presence of the synthetic progesterone analogue, mifepristone (RU486). This allows control over when and where the modified expression is activated (Nicholson *et al.*, 2008). Thus, in theory, it allows work with an identical background in both experimental and control group where the only difference is the presence of RU486 in the fly food. However, GS has many drawbacks including its leakiness, where the transgene can be expressed even in the absence of RU486 (Poirier *et al.*, 2008). GS is particularly problematic when working with RNAi transgenes designed for depleting endogenous *Drosophila* genes (Scialo *et al.*, 2016b). In the former case, genes are also depleted in the control, (without RU486) when strong drivers are used. Therefore GS requires appropriate controls and confirmation that the control group has normal levels of expression of the gene of interest.

1.4.3 Genetic screening

Further demonstrating the advantages of *Drosophila*'s genetic tool kit is the ability of performing large-scale genetic screens, to characterise gene function and their respective biological mechanism (Perrimon *et al.*, 2010). In *Drosophila*, the most common method used to perform screens is the targeted silencing of genes using RNA interference (RNAi). This is achieved by the integration of double-stranded RNAs, transported in a transgenic vector. These double-stranded RNAs cause targeted degradation of individual mRNA strands, thereby inhibiting gene expression (Mohr, 2014). RNAi provides an *in vivo* genetic platform to observe links between genotype and phenotype easily. This genetic technology has enabled the execution of large scale, unbiased, high-throughput genetic screens allowing the analysis of approximately 12,500 gene targets, equating to 91% of the *Drosophila* genome (Heigwer *et al.*, 2018). To date, genetic screens in *Drosophila* have played an essential role in understanding metazoan development, circadian rhythm, cellular signalling pathways and a range of disease mechanisms (Mohr *et al.*, 2010).

1.4.4 *Drosophila* and ageing studies

Drosophila melanogaster is a convenient model for the research of ageing and age-related diseases. The most valid reason is the short lifespan, of approximately 2-3 months, (depending on genetic background and temperature where flies are cultured), making them ideal candidates for carrying out *in vivo* lifespan studies

quickly and easily (Sun *et al.*, 2013). Their short lifespan allows ageing researchers to quickly identify genetic mutations, drugs or environmental interventions that can lead to the extension or reduction of longevity, within a whole organism. Thus, making fruit flies extremely valuable within ageing studies (He and Jasper, 2014). The powerful genetics of *Drosophila* allows manipulating the expression of any gene suspected to be implicated in the ageing process (Clancy *et al.*, 2001) or expressing genes that do not exist in *Drosophila* but can modify its lifespan (Humphrey *et al.*, 2009). *Drosophila* has greatly contributed to our knowledge about age-related diseases such as Parkinson's disease. For example, the genetic association between *Pink1* and *parkin* was first described in fruit flies (Park *et al.*, 2006). *Pink1* and *parkin* mutants display reduced lifespan, male sterility and abnormal flight and climbing abilities (Guo, 2012). These phenotypes can be quantified and studied to discover specific therapies that can rescue the phenotypes (Tufi *et al.*, 2014). The former is true for other diseases such as cancer (Dar *et al.*, 2012) and ageing (Brandt and Vilcinskas, 2013), where the ability of the flies to display disease phenotypes provides us with the tools to investigate and identify new therapeutic agents.

1.4.5 Studying mitochondrial function in *Drosophila*

Over the years, experiments using *Drosophila* have contributed a vast amount to the field of mitochondrial disease and studying the role of mitochondria in ageing. In parallel to humans, flies accumulate defective mitochondria during ageing and in models of neurodegeneration (Cho *et al.*, 2011a). One advantage of using *Drosophila* for mitochondrial studies is that mitochondrial proteins are highly conserved between humans and flies. In addition, the nuclear-encoded mitochondrial proteins are also highly conserved, allowing for the genetic manipulation of these genes to study specific mitochondrial diseases. Detailed information about these nuclear-encoded mitochondrial proteins, such as their functions, ontology and respective human homologues, can be easily found in the Mitodrome database (Fernandez-Moreno *et al.*, 2007). Due to the variety of different genetic tools that flies have to offer, there have been many mitochondrial mutation models reported in the literature. For example, mutations that affect the OXPHOS subunits (Walker *et al.*, 2006) (Frolov *et al.*, 2000) (Kemppainen *et al.*, 2014) (Da-Re *et al.*, 2014) (Chen *et al.*, 2015) or other mitochondrial proteins (Vos *et al.*, 2010) (Dorn *et al.*, 2011) (Phillips *et al.*, 1989). These allow us to observe the phenotypes associated with individual mutations. An example is the fly mutant technical knockout (tko), which

carried a point mutation in the mitoribosomal protein S12 gene. This tko fly mutant mimics the phenotype seen in the corresponding human mitochondrial disease, such as ETC deficiency, developmental delay, seizures and hearing loss (Jacobs *et al.*, 2004). Another example is the Leigh Syndrome (LS) fly model caused by mutations in the CI subunit ND2. In this model flies experience CI deficit, abnormal flight, mechanically induced paralysis, metabolic defects, neurodegeneration and decreased lifespan (Burman *et al.*, 2014). An important advantage of being able to observe phenotypes in these *Drosophila* mitochondrial disease models is the ability to find therapeutics, which can reverse the disease pathologies in the flies (Foriel *et al.*, 2015). For example, in the previously discussed LS mitochondrial disease model, a study reported that the administration of rapamycin was able to extend lifespan by rescuing metabolic defects. *Drosophila* are also highly important for the study of mitochondrial dysfunction during ageing. During ageing, *Drosophila* mitochondria exhibit alterations in morphology and functionality (Cho *et al.*, 2011a). Using flies we can examine, *in vivo*, the effect of ageing on the activity of the individual ETC components and ROS production, as well as observing the global effect of mitochondrial dysfunction. Fruit flies, therefore, provide us with the potential to analyse the link between mitochondria and ageing. Finally, age-related disease can be studied in flies, including the Parkinson's model discussed earlier, which exhibits similar phenotypes observed in humans (Tufi *et al.*, 2014).

1.5 Aims

Over the past decade, it has been widely established that ROS possess two distinct behaviours, within cells. Firstly, they are described as toxic by-products that trigger oxidative stress and drive the progression of ageing (Barja, 2014). Conversely, ROS are also recognised as signalling molecules, which are instrumental in maintaining cellular homeostasis (Ray *et al.*, 2012). At present, it is not clear how these contrasting identities are determined. However, it has been speculated that signalling ROS messengers are characterised by site- and time-specific production, under controlled conditions, involving ROS with low reactivity, such as H₂O₂ and superoxide. On the other hand, harmful ROS involved in oxidative damage is generated at non-specific sites, in uncontrolled circumstances and involves highly reactive ROS, such as the hydroxyl radical (Sanz, 2016). The most acknowledged example of site-specific ROS production, which takes into account all of the previous criteria, is ROS-RET, occurring at CI. This process occurs under specific conditions, as a result of redox changes in the ETC, including a highly reduced CoQ pool and a sustained increase in the pmf. In addition, RET triggers a significant increase in ROS production, specifically at CI, which can subsequently be neutralised (Chance and Hollunger, 1961) (Chouchani *et al.*, 2014a). Recent studies have reported the occurrence of RET in specific cell signalling pathways, reviewed in (Scialo *et al.*, 2017). However, despite all the evidence surrounding the occurrence of ROS-RET *in vivo* and its physiological importance, it is still unclear how the conditions required for RET initiation are reached. Therefore, the aims for my thesis were to investigate the mechanisms responsible for triggering ROS-RET, to establish (i) how it can be stimulated *in vivo*, (ii) how altering electron flow through the ETC can effect ROS-RET and (iii) which cellular components are involved in the regulation of ROS-RET. The specific aims of each Chapter were;

- 1) To identify if and how ROS-RET can be stimulated, physiologically in the fly brain (Chapter 3).
- 2) To study the effects of blocking electron entry into the ETC on ROS-RET, through CI and CII inhibition (Chapter 4).
- 3) To study the effects of blocking electrons from exiting the ETC on ROS-RET, through CIII, CIV and CV inhibition (Chapter 5)

- 4) To identify novel genes involved in the regulation of ROS-RET, by performing a Genome-Wide RNAi screen using AOX expression to prevent ROS-RET (Chapter 6).

Chapter 2 Materials and Methods

2.1 Reagents

All of the reagents used during the experiments included in this thesis are listed in Table 2.1, along with their providers and catalogue numbers.

Table 2.1 List of chemical reagents.

Reagent	Company	Catalogue number
Active Dried Yeast	Dutscher Scientific	789093
Adenosine 5'-diphosphate	Sigma	A2754-5X1G
Antimycin A	Santa Cruz Biotechnology	Sc-202467A
Bovine Serum Albumin (BSA)	Sigma	A7906-100G
Bradford Reagent	Sigma	B6916-500ML
Chloroform	Sigma	288306
Nuclease free dH₂O	Qiagen	129112
Dichlorofluorescein (H₂DCF)	Sigma	D6883-50MG
Dimethylsulfoxide (DMSO), sterile filtered	Santa Cruz Biotechnology	Sc-359032
DNase I	Fisher Scientific	10649890
DNase I 10x Buffer	Fisher Scientific	10202730
Drosophila agar Type II	Dutscher Scientific	789150
Ethanol (EtOH)	Fisher Scientific UK	E/0650DF/17
Ethyleneglycol-bis(2-amino-ethylether)-N,N,N',N'-tetracetic acid (EGTA)	Sigma	03777-10G

D-(+)-Glucose	Sigma	16325-1KG
Sn-Glycerol-3-phosphate bis(cyclohexylammonium) salt	Sigma	G7886-5G
HEPES	Sigma	50046-1KG
High-Capacity cDNA Reverse Transcription Kit	Applied Biosystems	4368814
Isopropanol	Sigma	190764
Magnesium Chloride, Hexahydrate	Santa Cruz Biotechnology	Sc-203126A
Maize meal	TRS	/
MitoSOX	Life Technologies	M36008
Nipagin (Methyl 4-hydroxybenzoate)	Sigma	H5501-100G
Sodium Acetate (NaAc pH 5.2 3M)	Life Technologies	AM9740
Phosphate Buffered Saline (PBS) tablets	Cambio	MC-09-9400-100
Potassium Chloride (KCl)	Sigma	P9333-500G
Potassium cyanide (KCN)	Sigma	60178-25G
Potassium Hydroxide (KOH)	Sigma	484016-1KG
Potassium Phosphate, Monobasic (KH₂PO₄)	Santa Cruz Biotechnology	Sc-203211A
L-Proline	Sigma	P5607-25G
Propionic acid	VWR	8.00605.2500
Pyruvic acid monopotassium salt	Sigma	860077-1G
Random Hexamer Primer	Thermo Fisher Scientific	48190011

Rotenone	Santa Cruz Biotechnology	Sc-203242
Saccharose (sucrose)	Sigma	27480.294
SensiFAST SYBR Hi-ROX Kit	Bioline	BIO-92020
(+)-Sodium L-ascorbate	Sigma	A4034-100G
Sodium pyruvate	Sigma	P2256-25G
Sodium succinate dibasic hexahydrate	Sigma	S9637-500G
Soybean flour	Santa Cruz Biotechnology	Sc-215897A
TMPD (N,N,N',N'-Tetramethyl-p-phenylenediamine dihydrochloride)	Sigma	87890-25G
Treacle	Bidvest	90028S
Tris-HCl	Promega	H5121
Trizol/TRIreagent	Fisher Scientific	11312940
Wheat germ	MP biomedicals	0290328805 - 5 lb

2.2 Fly Husbandry

All flies were maintained on standard media, (1% agar, 1.5% sucrose, 3% glucose, 3.5% dried yeast, 1.5% maize, 1% wheat, 1% soya, 3% treacle, 0.5% propionic acid, 0.1% nipagin), prepared as described below and kept in 12 hours light:dark cycle incubators. Incubators were set to different temperatures depending on the experiment. Due to the fact that flies are poikilothermic they adapt to environmental temperature (Dillon *et al.*, 2009), therefore in higher temperatures they develop faster than in lower temperatures. In normal conditions, flies were kept at 25°C whereas stocks were maintained at 18°C. For heat stress experiments flies were exposed to 32°C for 3-4 hours, unless otherwise indicated. All experimental flies were female flies unless otherwise stated.

For collection, flies were anaesthetised using CO₂ and placed in vials containing 2 ml of standard fly food with 20 flies per vial. Vials were changed every 2-3 days. Two different strains were used as controls; *white Dahomey* strain (*w_{DAH}*) and *w¹¹¹⁸*. All lines were backcrossed, for at least 6 generations, into *w_{DAH}* or *w¹¹¹⁸*, or they were used in the original *w¹¹¹⁸* background in the case of RNA interference (RNAi) lines from the Vienna Drosophila Resource Centre (VDRC) used in the screen. Two different drivers were used to express UAS-transgenes: *daughterless-Gal4* (*daGAL4*) and *tubulin-Gene-Switch* (*tubGS*). For experiments using RNAi lines of the ETC subunits the following strategy was used. First of all the *daGAL4* driver was used to achieve expression throughout development. However, if this driver caused lethality or a weak phenotype resulting in mortality soon after eclosion, the *tubGS* driver was used, restricting expression during adulthood only. These particular drivers were picked due to the level of expression induced. For example, tubulin drivers are considered to induce stronger levels of expression, where as *daughterless* are considered to have milder effects. Therefore, the *daGAL4* driver was used instead of the stronger *tubGAL4* driver, to lower the possibility of lethality when expressed during development however, the stronger *tubGS* driver was used instead of the *daGS* to maximise expression of the RNAi during adulthood. The control lines, driver lines and UAS-lines used in this thesis are summarised in Table 2.2. Expression of UAS-transgenes was achieved by crossing virgin females, carrying one of the two drivers, with males carrying the UAS-transgene. Appropriate controls were generated by crossing female virgins carrying the driver, (*daGAL4* or *tubGS*), with male control flies, of the same background, (i.e. *w_{DAH}* or *w¹¹¹⁸*). Fly crosses were made in bottles

with 30 ml of fly food or 5 ml vials and flipped every 2-3 days for a maximum of 4 flips to avoid contamination and whilst virgins were still young. Each bottle reached a density of approximately 100 – 300 flies depending on the genotype. For example, less flies eclosed from bottles containing KD of the ETC complexes, which were overall weaker than control flies.

Table 2.2 List of fly stocks.

Fly Strain	Source	Details
<i>WDAH</i>	Prof Linda Partridge/University College London	<i>White Dahomey</i> , white-eye control type background
<i>w1118</i>	VDRC	<i>w1118</i> , white-eye control type background
<i>WDAH; UAS-Sod2</i>	Bloomington Drosophila Stock Centre (BDSC)	Superoxide dismutase 2 (Mn) under UAS control on the 2 nd chromosome (24494)
<i>WDAH; UAS-mtCat 8M</i>	Prof William Orr / Southern Methodist University Dallas	Catalase targeted to the mitochondrion under UAS control on the 2 nd chromosome.
<i>WDAH; daGAL4</i>	BDSC	GAL4 under the control of the <i>daughterless</i> promoter on the 3 rd chromosome.
<i>w1118; UAS-ND-75</i>	VDRC	RNAi against NADH dehydrogenase (ubiquinone) 75 kDa subunit (CI subunit) on 2 nd chromosome. (CG2286, 100733/KK)
<i>w1118; UAS-ND-42</i>	VDRC	RNAi against NADH dehydrogenase (ubiquinone) 42 kDa subunit (CI subunit) on 2 nd chromosome. (CG6343, 110787/KK)
<i>WDAH; tubGS</i>	Prof Scott Pletcher/University of Michigan	Gene-Switch GAL4 under control of the tubulin promoter, <i>White Dahomey</i> background, 3 rd chromosome.

w1118; tubGS	Prof Scott Pletcher/University of Michigan	GeneSwitch GAL4 under control of the tubulin promoter, w1118 background, 3 rd chromosome.
wDAH; UAS-SdhD	VDRC	RNAi against Succinate dehydrogenase, subunit D (CII subunit) on 2 nd chromosome. (CG10219, 101739/KK)
w1118;UAS-UQCR-Q	VDRC	RNAi against UQCR-Q on the 2 nd chromosome. (CG7580, 101371/KK)
wDAH; UAS-AOX F6	Prof Howy Jacobs/ University of Tampere	AOX from <i>C.intestinalis</i> under UAS control (allele F6) on the 2 nd chromosome.
wDAH; UAS-AOX F6; tubGS		AOX from <i>C.intestinalis</i> under UAS control (allele F6),Gene-Switch GAL4 under control of the tubulin promoter,
wDAH; UAS-Ndi1B20	Prof Howy Jacobs/University of Tampere	Ndi1 from <i>S.cerevisiae</i> under UAS control (allele B20) on the 2 nd chromosome.
w1118; UAS-empty	VDRC	Landing site VIE-260B, insertion on the 2 nd chromosome at position 22019296 (5' to CR33987)
w1118;UAS-VhaPPA1-1	VDRC	RNAi against Vacuolar H+ ATPase PPA1 subunit 1on the 2 nd chromosome. (CG7007, 47188/GD)
w1118; UAS-CG30373	VDRC	RNAi against CG30373 on the 2 nd chromosome. (CG30373, 104802/KK)
w1118; UAS-ABCB7	VDRC	RNAi against ATP binding cassette subfamily B member 7 on the 2 nd chromosome. (CG7955, 106039/KK)
w1118; UAS-Mitofilin	VDRC	RNAi against Mitofilin on the 2 nd chromosome. (CG6455, 106757/KK)
w1118; UAS-Cchl	VDRC	RNAi against Cytochrome c heme lyase on the 2 nd chromosome. (CG6022, 101382/KK)

<i>w1118; UAS-mRpS25</i>	VDRC	RNAi against mitochondrial ribosomal protein S25 on the 2 nd chromosome. (<i>CG14413</i> , 101443/KK)
<i>w1118; UAS-CG11200</i>	VDRC	RNAi against Carbonyl reductase on the 2 nd chromosome. (<i>CG11200</i> , 101697/KK)
<i>w1118; UAS-CG7071</i>	VDRC	RNAi against <i>CG7071</i> on the 2 nd chromosome. (<i>CG7071</i> , 110726/KK)
<i>w1118; UAS-Cul3</i>	VDRC	RNAi against Cullin 3 on the 2 nd chromosome. (<i>CG42616</i> , 109415/KK)
<i>w1118; UAS-Ppn</i>	VDRC	RNAi against Papilin on the 2 nd chromosome. (<i>CG33103</i> , 108005/KK)
<i>w1118; UAS-CG9853</i>	VDRC	RNAi against <i>CG9853</i> on the 2 nd chromosome. (<i>CG9853</i> , 107346/KK)
<i>w1118; UAS-crb</i>	VDRC	RNAi against crumbs on the 2 nd chromosome. (<i>CG6384</i> , 39177/GD)
<i>w^{DAH}; UAS-levy</i>	VDRC	RNAi against levy on the 2 nd chromosome. (<i>CG17280</i> , 101523)
<i>w1118; UAS-ATPsynδ</i>	VDRC	RNAi against ATP Synthase, δ subunit on the 2 nd chromosome. (<i>CG2968</i> , 100621)

2.2.1 Preparation of the fly food

The fly food was prepared using the ingredients described in Table 2.3. The ingredients were weighed into a glass beaker, according to the required volume and mixed. To prepare a litre, approximately 750 ml of deionized water was added to the mixture and heated to 37°C, on a hot plate, under continuous agitation with a magnetic stirrer. Once the mixture had reached 37°C, the yeast undergoes fermentation for 10 minutes, after which the temperature was further increased to 80°C and left to boil for 25 minutes. The remaining deionized water was added, to reach the total desired volume. The food was then allowed to cool to 70°C before the addition of propionic acid and nipagin (diluted in EtOH to a 10% (w/v) stock solution).

Table 2.3 List of fly food ingredients.

Standard medium for 1000ml

% in food	Quantities	Component
1% (w/v)	10g	Drosophila agar Type II
1.5% (w/v)	15g	Saccharose (sucrose)
3% (w/v)	30g	D-(+)-Glucose
3.5% (w/v)	35g	Active Dried Yeast
1.5% (w/v)	15g	Maize meal
1% (w/v)	10g	Wheat germ
1% (w/v)	10g	Soybean flour
3% (w/v)	30g	Treacle
0.5% (v/v)	10ml	Propionic acid
0.1% (w/v)	5ml	Nipagin M

The cooled mixture was then dispensed into vials (2 ml or 5 ml) or bottles (30 ml) and left at room temperature to set, for approximately 60 minutes. Food was stored at 4°C and used within 14 days. Before use, food was left at room temperature to warm up, for approximately 60 minutes. Activation of the modified GAL4 protein GS was achieved by adding mifepristone (RU-486) into the standard fly food mixture. A 100 mM stock solution of RU-486 was prepared in EtOH and diluted to the final concentration to which 200 µL was added to molten food (1 µM during development and 500 µM during adulthood). Adult flies were fed the drug (500 µM) from eclosion for up to 10 days before being used for experiments unless otherwise stated. A fresh

stock of RU-486 was prepared every 2 weeks and the appropriate volume was added to the standard food, to reach desired concentration.

2.2.2 Addition of ETC inhibitors to the fly food

I prepared stock solutions for the different ETC inhibitors in EtOH, except for cyanide, which was dissolved in water. After diluting the stock solution, to reach the desired final concentration of inhibitor, I added 100 µl onto the surface of the set pre-made fly food. The inhibitors were added on top of the 2 ml vials of food and left on a shaker at 4°C overnight, to allow even distribution and absorption into the food. Vials were covered in aluminium foil to prevent contamination. Control vials were prepared concurrently, where the vehicle without drug was added on top of the food. Table 2.4 lists the different ETC inhibitors and concentrations used in this thesis. The flies fed inhibitors were starved before being transferred onto the food with the ETC inhibitors. Starvation was achieved by transferring the flies into empty vials for 1 hour.

Table 2.4 List of ETC inhibitors and their concentrations			
Inhibitor (Complex)	Solvent	Stock concentration	Final concentrations
Rotenone (CI)	EtOH	1 mM	600 µM, 900 µM or 1 mM
Dimethyl Malonate (CII)	EtOH	8.750 M	600 µM
Myxothiazol (CIII)	EtOH	1 mM	10 µM, 50 µM, 100 µM, 500 µM or 1 mM
Cyanide (CIV)	H ₂ O	1 M	12 mM or 18 mM
Oligomycin (CV)	EtOH	1 mM	10 µM or 50 µM
FCCP (uncoupler)	EtOH	1 mM	600 µM, 900 µM or 1 mM

2.2.3 Heat Stress model

Female flies of approximately 3 days old were transferred from a 25°C incubator, (non-stressed conditions), to a 32°C incubator, (heat stress, HS), for 3-4 hours, unless otherwise stated. Flies were used immediately for experiments, (e.g. ROS measurements in the fly brain), after HS. This model is outlined in Figure 3.4. During the HS signalling experiment, studying the effect of HS during 1-6 hours, flies were exposed to HS and measured after every hour. In experiments where flies subjected

to HS were also fed inhibitors, the flies were starved for 1 hour before being transferred onto drug food and placed in 32°C incubators. This included the control flies fed the vehicle, which were also starved for 1 hour. The implementation of the HS model during the lifespan experiments is detailed below.

2.2.4 Lifespan Experiments

For the lifespan experiments, female *w^{DAH}* flies were used. 20 flies were collected one day after eclosion and transferred to 2 ml vials of standard fly food. Each experimental condition had 5 independent replicates of 1 vial, (100 flies in total *per* condition) and each experiment was repeated twice. All vials were maintained at 25°C in a 12 hours light:dark cycle controlled incubator with the exception of the period of time during which experimental flies received their treatments. Flies were changed into fresh food vials every 2-3 days and the number of dead flies was scored. The goal of the lifespan experiments used in this thesis was to test whether induction of ROS-RET using HS could extend lifespan. HS was induced as described above to the experimental group and one control group, fed with 600 µM of rotenone as described in Section 2.2.3. HS was repeated three times a week. The other two control groups were kept at 25°C, where one was fed with 600 µM of rotenone. Three different experimental designs were used; (1) HS 3 times per week during the first 25 days of life, (2) HS 3 times per week from day 25 to day 50 and (3) HS 3 times per week constantly throughout the lifespan of the flies. Figure 3.15-3.16 contains a summary of the experimental plan.

2.2.5 Genome-Wide RNAi Screen

For the screen, 12,719 RNAi lines were acquired from VDRC (Dietzl *et al.*, 2007) (<https://stockcenter.vdrc.at/control/main>). The laboratory acquired all the lines from the KK library (~9,646 lines) and then lines from the GD library for those genes that were not covered in the KK library. Integration of the transgenes in the GD lines is achieved via P-element transposition, which results in random integration, unlike the KK RNAi lines which use PhiC31 site-specific integration (Dietzl *et al.*, 2007) (Bischof *et al.*, 2007). The specific integration site of the KK RNAi library, where the hairpin constructs are targeted to is the 30B landing site. However, recently it has been demonstrated that in fact there are two possible integration sites (Green *et al.*, 2014). Studies have revealed that 75% of KK lines possess the 30B insertion site and the remaining 25% possess both the intended 30B site as well as the 40D landing site

(Vissers *et al.*, 2016). This produces the potential for off target and non-specific phenotypes for the approximate 25% of KK RNAi lines that possess both integration sites, which is documented for on the VDRC website. A total of 12,372 different fly genes covering >91% of protein-coding genes in the *Drosophila melanogaster* genome were studied. The screen was initiated in Tampere (Finland) and finished in Newcastle (United Kingdom) and took over 5 years to be completed. The selected dose of RU-486 (1 μ M), added to the fly food to induce the expression of the RNAi construct and/or AOX, was chosen based on preliminary experiments performed by Essi Kiviranta and Alberto Sanz in Tampere (Finland). In these experiments, it was established that 1 μ M of RU-486 in the fly food was the optimal dose to rescue the lethal phenotype, caused by the knock-down of 4 different genes encoding subunits of CIV (COX4, COX5A, COX5B, COX7A). Dr Rhoda Stefanatos and I completed the screen in Newcastle where all lines were screened at least once.

The 12,719 RNAi lines were analysed in batches of 100-300 lines per week. In most cases, males carrying the UAS-RNAi transgene were selected directly from the vials received from VDRC. Males were crossed with virgin females carrying the *tubGS* driver, (control group), or females carrying both the driver and UAS-AOX construct (AOX group). Crosses were performed in vials of food containing 1 μ M of RU-486 at 25°C. Flies mated and laid eggs for 5 days, after which adult flies were discarded from the vials. After 10 days, vials were scored for the presence of larvae, pupae or adult flies, during 3 consecutive days. I defined lethality as the absence of flies 3 days after the expected eclosion time, (10 days), in the control group. Then, I established three different lethal phenotypes; (1) lethal at embryo stage, where no larvae was observed in the vial, (2) lethal at larval stage, where larvae were observed but no pupae and (3) lethal at pupal stage, where pupae were observed but no adult flies. Within the list of scored lethal genes, I identified a gene as an AOX rescue gene when larvae, pupae or adults were observed in the AOX group but not in the control group. Negative and positive controls were included in each batch of screened flies, to identify potential problems with either the quality of food or the concentration of RU-486. These controls were used to select which lines needed to be rescreened. The negative and positive controls were virgin *tubGS* crossed with *WDAH* males and virgin *tubGS>AOX* crossed with *UAS-COX4-KD* flies, respectively. I rescreened a total of 189 RNAi lines that were originally scored as rescue AOX genes, as described above. The rescreen was performed in the same conditions as the original

screen, (including reordering of the flies from VDRC), with the exception that vials were scored for 5 days instead of 3 days after eclosion. AOX rescue was confirmed only when the knock-down caused a lethal phenotype in the control group that was rescued, (i.e. flies eclosed), or alleviated, (e.g. no larvae or pupae in the control but larvae or pupae in the AOX group), by the presence of AOX. I performed data analysis of the results of the screen in collaboration with Dr Alberto Sanz. First of all, I used data from the original screen. For this analysis, I selected the list of genes that were scored as lethal, as described before. Secondly, I used data from the rescreen of 189 RNAi lines. For this analysis, I used only the list of confirmed AOX rescue genes as indicated before. The analysis was performed using Gene Ontology (GO) analysis with the Database for Annotation, Visualization and Integrated Discovery (DAVID) (Huang da *et al.*, 2009) (<https://david.ncifcrf.gov/summary.jsp>). I also performed network analysis of protein-protein associations among the AOX rescue genes using STRING (Szklarczyk *et al.*, 2017) (<http://string-db.org/>). For DAVID, the Function Annotation Clustering Analysis tool was selected with default settings. STRING analysis was performed using default setting followed by kmeans clustering analysis using 3 clusters.

2.3 Quantitative real-time PCR (qPCR)

2.3.1 RNA Extraction

For each sample, a total of 10 whole flies were anaesthetised on ice and stored immediately at -80°C in 1.5 ml tubes. Once frozen, flies were mechanically homogenized in 50 μl of cold TRIreagent, and a further 250 μl of TRIreagent were added, which was mixed by inversion. The homogenized samples were then incubated at room temperature for 5 minutes. Following incubation, 50 μl of chloroform were added to the samples and mixed thoroughly, before being incubated again for 3 minutes, at room temperature. Samples were then centrifuged for 15 minutes at 12,000 g at 4°C . The upper aqueous phase was then transferred to a new tube, where a 1:1 volume of isopropanol was added and mixed vigorously. Then samples were incubated at room temperature for 10 minutes, to allow the RNA to precipitate out of solution and centrifuged again for 10 minutes. The residual supernatant was removed by pipetting and the pellet was washed by adding 500 μl of 75% EtOH in DEPC and centrifuged for 5 minutes at 7,500 g at 4°C . The EtOH was removed and the pellet was left to air dry for 5 minutes, at room temperature. To remove any DNA contamination, the RNA pellet was first re-suspended in 89 μl of DNase/RNase free H_2O . Then 1 μl of DNase1 and 10 μl of DNase1 buffer were added to each sample. Tubes were mixed gently by pipetting and incubated in a water bath for 60 minutes at 37°C , to allow the reaction to take place. After incubation 10 μl of 3 M sodium acetate (pH 5.2) were added, followed by 275 μl of 95% EtOH in DEPC water and mixed thoroughly. Samples were then stored at -20°C overnight to allow the RNA to precipitate. Following precipitation, the samples were centrifuged at 16,000 g for 20 minutes at 4°C and the remaining supernatant was then removed. The pellet was then washed using 1 ml of 75% EtOH in DEPC and centrifuged again. EtOH was removed and one final wash step took place before drying the pellet at room temperature for 5 minutes. Depending on the size of the pellet, 10-20 μl of DEPC water were added to resuspend the pellet, and then the RNA concentration was measured using a Nano-Drop 2000C, (Thermo Scientific, Wilmington, USA). The concentrations of RNA were then adjusted to no more than 2 $\mu\text{g}/\mu\text{l}$ with DEPC water and stored at -80°C for cDNA synthesis.

2.3.2 cDNA Synthesis

To ensure there was enough cDNA for multiple qPCR measurements, cDNA synthesis was performed in triplicate for each sample. Finally, the cDNA from the

triplicates was pooled in one single tube. Each cDNA synthesis had a final volume of 20 µl, consisting of 10 µl master mix and 10 µl of the sample. All samples and reagents were defrosted on ice and samples were diluted with Nuclease-free H₂O to achieve an RNA maximum concentration of 2 µg. The master mix was prepared using the reagent in Table 2.5.

Table 2.5 List of reagents used during cDNA synthesis.	
Reagents	MM 1x (10 µl)
10x RT Buffer	2.0 µl
25x dNTP Mix (100mM)	0.8 µl
10x Random Primers	2.0 µl
MultiScribe Reverse Transcriptase	1.0 µl
Nuclease-free H₂O	4.2 µl

PCR tubes were used to carry out cDNA synthesis. 10 µl of the sample were added first to the PCR tube, followed by 10 µl of the master mix. The tubes were spun down and placed in the PCR Thermocycler, (Applied Biosystems, California). The following programme was used: 25°C for 10 minutes, 32°C for 120 minutes, 85°C for 5 minutes and finished at 4°C.

2.3.3 q-PCR using the Standard Curve Method

Primers were designed using the Primer 3 web designing software (Untergasser *et al.*, 2012) (<http://primer3.ut.ee/>), for each gene. For the SYBR green reagent used the recommended amplicon length is <200 base pairs. In addition, the T_m was set at 60°C and GC content was set at 50%.

To create the standard curve a serial dilution was made using four points. The cDNA samples were thawed on ice and 5 µl of every sample were added to a new tube to make a stock solution. This stock was then diluted 1:1, using nucleic acid-free water, making the first point of the standard curve. Serial dilutions were then prepared by taking 20 µl of the solution and diluting with 80 µl of nucleic acid-free water, this was repeated three times to obtain four standard dilutions in total. The four points of this standard curve were 1, 1:10, 1:100 and 1:1000. cDNA samples were diluted 1:20 to ensure they would sit in the linear part of the standard curve.

All plates were prepared with a standard curve for each set of primers, (each target genes and the housekeeping gene), as well as the samples for each set of primers.

The house-keeping gene acted as a control and gave a baseline to which the target gene expression was compared to. Standards and samples were run in triplicates in fast optical 96 well plates, (Applied Biosystems, San Francisco, USA), for qPCR. A master mix containing nuclease-free H₂O, SYBR green and the forward and reverse primers was prepared for each primer set, using the amounts shown in Table 2.6.

Table 2.6 List of reagents used for qPCR.	
Reagents	MM 1x (16 ul)
Nuclease-free H₂O	5.2 µl
2x SYBR Green SensiFast Hi-Rox buffer	10 µl
20µM Forward Primer	0.4 µl
20µM Reverse Primer	0.4 µl

The plate was prepared by pipetting 4 µl of standards and samples and then 16 µl of the master mix, containing primers specific to either target gene or house-keeping gene, to obtain 20 µl of reaction mix in each well in total. The plate was then sealed using a clear cover and inserted in the StepOne, qPCR machine (Applied Biosystems, San Francisco, USA). The programme used followed a cycle of 95°C for 2 minutes, then 95°C for 5 seconds, 60°C for 10 seconds and 72°C for 10 seconds. The last three steps were repeated for 40 cycles. Measurements were taken during the 72°C extension stage. The obtained values were quantified using the StepOne v2.1 software. Raw values obtained from the quantification of target genes were normalised against the raw values from the quantification of the house-keeping gene. All primers used in this thesis are outlined in the Table 2.7.

Table 2.7 List of Primers.

Gene/Primer Name	Primer Sequence
<i>SdhD</i> Forward	5'- CTCTGGACTGTGGAGCGAATT-3'
<i>SdhD</i> Reverse	5'- GGATGACGACAGAGATGGCC-3'
<i>VhaPPA1-1</i> Forward	5'- AACGTTCTGTGGCTCTTCC-3'
<i>VhaPPA1-1</i> Reverse	5'- GTTTGAGGAGGCCAGGAACC-3'
<i>Ppn</i> Forward	5'- ATTTAGGACCTTGGACGCCG-3'
<i>Ppn</i> Reverse	5'- GCTTCTCCTCCACGCAATCT-3'
<i>Cchl</i> Forward	5' GCAATACAGCCATCACCCGA-3'
<i>Cchl</i> Reverse	5'- AGGCCGATTTTGCATCTCCA-3'
<i>Rpl32</i> Forward	5'- AGCATACAGGCCCAAGATCGTGAAGAA-3'
<i>Rpl32</i> Reverse	5'- CACGTTGTGCACCAGGAAGTTCTTGAA-3'
<i>Act88f</i> Forward	5'- AGGGTGTGATGGTGGGTATG-3'
<i>Act88f</i> Reverse	5'- CTTCTCCATGTCGTCCCAGT-3'

2.4 High-Resolution Respirometry measurements

Measurements of mitochondrial oxygen consumption were performed by high-resolution respirometry in homogenates from whole flies or fly heads (Sperl *et al.*, 1997). 10-20 female flies, (whole flies), or 20-30, (fly heads), were immobilised on ice and transferred to a mortar at 4°C to which 500 µl of ice-cold isolation buffer without BSA, (250 mM sucrose, 5 mM tris-HCl, 2 mM EGTA, pH 7.4), were added. Flies were then gently homogenised with a pestle to minimise mitochondria damage, caused by rupture of the mitochondrial external membrane. Fly homogenates were collected in a beaker, after being filtered through a polyamide net to remove debris. An additional 500 µl, (for whole flies), or 300 µl, (for fly heads), of isolation buffer without BSA was added and the homogenate was collected into a tube. Samples were prepared every time just before making oxygen consumption measurements.

The Oxygraph 2-K, (Oroboros Instruments, Innsbruck, Austria), was used to measure mitochondrial oxygen consumption of fly homogenates. The Oxygraph 2-K is specially designed to perform high-resolution respirometry measurements with small amounts of sample (Hutter *et al.*, 2006). Before adding the samples, the chambers of the oxygraph machine were cleaned thoroughly, with 70% EtOH and distilled water, to ensure any residual inhibitors or substrates from previous runs were removed. In between runs, the chambers were washed thoroughly 3 times with EtOH and water. A total of 1.9 ml of assay buffer with BSA, (120 mM KCl, 5 mM KH₂PO₄, 3 mM HEPES, 1 mM EGTA, 0.5 mM MgCl₂, 0.2% (w.v) BSA, pH 7.2), were added to the chambers, followed by 100 µl of the homogenate. For each run, one chamber would contain the control group whilst the other would contain the experimental group. To reduce variability between the chambers, the groups were alternated between every run. The chambers were closed after adding the samples and the run was initiated. Substrates and ETC inhibitors were added only after the O₂ flux signal was stable. Hamilton Gastight syringes, (Hamilton Bonaduz AG, Bonaduz, Switzerland), were used to add the substrates and inhibitors. To initiate CI+CIII+CIV respiration the following substrates were added to the chambers: 5 µl of 2 M pyruvate, 5 µl of 2 M L-proline and 4 µl of 0.5 M ADP. Once a stable reading was obtained, CI-linked respiration, (i.e. CI+CIII+CIV), was inhibited using 1 µl of 1 mM rotenone stock. Then 60µl of 0.65M sn-glycerol-3-phosphate (G3P) were added to stimulate CIII+CIV respiration and after a stable reading was obtained, 1 µl of 5 mM antimycin A was added to inhibit CIII. Finally, 5 µl of 0.8 M ascorbate and 4 µl of 0.25 M TMPD were

added to the chambers to initiate CIV respiration, through the donation of electrons to Cyt C. Once the O₂ flux signal was stable, 1 µl of 1 M cyanide was added to inhibit CIV respiration. A minimum of 3 independent biological samples, *per group* were used in each experiment.

Quantification of oxygen consumption was performed using the Oroboros DataLab 5.0 software. Raw values were measured by recording the stabilised rate of O₂ flux after the addition of appropriate substrates. For CI-linked respiration, (also referred to as CI+CIII+CIV respiration), the rate after the addition of pyruvate+proline+ADP was taken. CIII-linked, (also known as CIII+CIV respiration), was quantified by recording the stabilised rate after addition of G3P. Finally, CIV-linked respiration, (also known as CIV respiration), was measured by taking the stabilised rate of respiration after addition of ascorbate+TMPD and subtracting the residual respiration after cyanide was added. When head homogenates were used, only CI+III+IV respiration was measured. This was due to the fact that preparing head homogenates is very time consuming and these homogenates have fewer mitochondria, therefore it is difficult to get good estimations for CIII+CIV linked respiration. Oxygen flux raw values were normalised to the amount of fly protein added to the chamber. The protein concentration measurements were carried out using the Bradford assay. Final values were expressed as picomoles of oxygen per min⁻¹ per mg⁻¹ unless otherwise stated.

2.5 ROS Measurements in the *Drosophila* Brain

Approximately 5-10 female flies were used for each genotype/condition. 10-20 flies were transferred to an ice-cold vial and anaesthetised then kept on chilled aluminium foil to maintain immobilisation. A minimum of 5 brains were imaged per experimental condition but additional brains were dissected, in case of any damage occurring to the brains during dissection. Using forceps the immobilised flies were placed one by one in 70% EtOH for 30 seconds to remove the hydrophobic layer surrounding the flies, which may have caused them to float, making dissection difficult. Once cleaned, flies were then dried and transferred to a glass dissecting dish well, containing chilled 1X PBS. Under a light microscope the brains of flies were carefully dissected, using dissection forceps, ensuring that the brain was fully intact without damage, which could lead to the presence of outliers in the measurements. Each experimental group was dissected in less than 10 minutes to minimise damage to the brain. All trachea and tissue surrounding the brain was removed, to allow clean staining and imaging. A minimum of 5 brains was used for each group. After dissection, the brains were gently transferred to fresh PBS to be cleaned and then relocated to a small glass dish well. A Pasteur pipette coated in silicon was used, to avoid any brains attaching to the inside wall of the pipette during transfer. The excess PBS was removed, and 100 µl of PBS solution containing the appropriate fluorophore were added at the concentrations indicated in Table 2.8.

Table 2.8 List of fluorophores used to measure ROS.

Fluorophore	Stock in DMSO	Working Concentration	Wavelength
MitoSOX	2.5 mM	30 µM	510/580 nm
H ₂ DCF	10 µM	30 µM	495/529 nm

The working concentration of the fluorophore was prepared at the desired concentration in 1X PBS, prior to dissection. The same preparation was used for all of the different groups within the experiment to reduce variability. MitoSOX was used to measure mitochondrial superoxide levels whilst H₂DCF was used to measure total cellular peroxide levels. Experiments using MitoSOX were carried out in collaboration with Filippo Scialo. Once the chosen fluorophore was added, forceps were used to

carefully attach the brains to the bottom of the dish well facing upwards. The dish well was then placed onto a shaker at speed 50 rpm at room temperature and incubated for 10 minutes in the dark, due to light sensitivity of the probes. After incubation, the fluorogenic dye was removed, and the brains were washed with 300 μ l of 1X PBS using a pipette to gently mobilise the brains. Once washed the fly brains were transferred to a poly-lysine coated 35 mm glass-bottom culture dish containing 1X PBS. The fly brains were mounted to the bottom of the dish well, using the forceps, with the antennal lobe facing towards the glass in a line. The dish well was then transferred onto the microscope stage of the SP8 confocal microscope, (Leica Microsystems, Wetzlar, Germany). The microscope was set with a 10x 0.3 NA objective and an argon laser with the required wavelength needed to excite the respective dyes was used, (noted in the table above). To acquire Z stack images, LasX software was used. The same number of stacks was used for each sample to minimize variability. The average total intensity was quantified for each individual brain using FIJI/ImageJ software (<https://imagej.net/Fiji>).

2.6 Statistical Analysis

All data were analysed with GraphPad Prism 8, (GraphPad Software, California), using one-way ANOVA or the unpaired Student's T-test as appropriate. Lifespan survival curves were analysed using the log-rank Mantel Cox Test. Values shown represent means \pm SEM unless otherwise indicated. $p < 0.05$ was taken as statistically significant and represented by *, $p < 0.01$ was represented by ** and $p < 0.001$ was represented by ***.

Chapter 3 Heat Stress Induces ROS-RET physiologically in *Drosophila Melanogaster*

3.1 Reverse Electron Transport

RET is the flow of electrons from the CoQH₂ to CI, reducing NAD⁺ to NADH (Scialo *et al.*, 2016a). For RET to occur, two conditions are required, including a highly reduced CoQ pool and a high pmf (Robb *et al.*, 2018). Once triggered, studies have shown that a dramatic increase in ROS production from CI occurs, as a result of RET (Robb *et al.*, 2018).

The dual nature of ROS has been extensively explored in the past decade, where studies have shown that ROS possess roles in both oxidative stress and redox signalling (Sanz, 2016). Results from previous experiments using the alternative respiratory enzyme, Ndi1, showed that RET produces a ROS-dependent beneficial effect on lifespan in *Drosophila*. Ndi1 mediated ROS production has also been shown to protect mitochondrial function in both *SOD2-KD* and *PINK1-KD* models, which under normal circumstances cause mitochondrial dysfunction (Scialo *et al.*, 2016a). This suggests that ROS produced specifically via RET may possess signalling properties, capable of initiating downstream protective pathways in order to promote healthy ageing. Thus leading to the increase in lifespan, observed in the Ndi1 flies. Understanding the mechanisms behind RET will allow us to induce beneficial ROS-RET that in theory can extend lifespan and protect mitochondrial function.

The Ndi1 model provides us with stimulation of RET, *in vivo*, however Ndi1 isn't endogenously expressed in either humans or flies. Therefore in this Chapter, I attempt to determine if RET can occur physiologically, in *Drosophila*.

3.1.1 RET Under Physiological Conditions

RET was first discovered in the 1960's in isolated mitochondria but was considered to be an *in vitro* artefact lacking physiological relevance (Chance and Hollunger, 1961). However, recently, RET has been recognised in a number of cell signalling processes as well as having a significant role within ageing (Scialo *et al.*, 2017).

The most frequently documented occurrence of RET is during ischemia-reperfusion (IR). IR occurs when tissue is re-oxygenated after a period of oxygen starvation.

During ischemia, succinate levels rise rapidly causing RET to be stimulated when oxygen is re-introduced. This leads to a dramatic increase in ROS production and causes injury to the surrounding tissue (Chouchani *et al.*, 2014a). This example of RET, in physiological conditions, shows that when ROS is produced in a disorderly and uncontrolled manner it can be detrimental. Other cases that require a ROS-RET signal include the differentiation of myoblast into myotubes (Lee *et al.*, 2011), hypoxia response in carotid bodies (Fernandez-Aguera *et al.*, 2015) and during bacterial infection, where macrophages stimulate ROS-RET in order to produce an inflammatory response against the infection (Mills *et al.*, 2016a). At present, it is uncertain how the highly reduced CoQ pool and high pmf, needed for RET to occur, can be generated and sustained physiologically.

To achieve physiological stimulation of RET; I subjected *Drosophila melanogaster* to a stress condition. Here I hypothesised that under stress, mitochondria would need to adapt and produce a beneficial ROS signal, via RET, to protect mitochondrial function during the stress condition. Therefore the stress would need to create both a highly reduced CoQ and high pmf to promote CI to switch ROS production from a forward direction, in non-stressed conditions, to a reverse direction in order to initiate RET. For these reasons I selected heat stress (HS). HS triggers a rise in energy demands and causes mitochondria to consume more O₂. This increases the flow of electrons, into the ETC, to allow mitochondria to respire more. This boost of electrons could lead to the production of a high CoQH₂:CoQ ratio, thereby stimulating RET and the corresponding ROS signal, to counteract the HS (Figure 3.1). Therefore the characteristic increase in ROS production, seen in all RET models, would be the first indication if RET was being achieved.

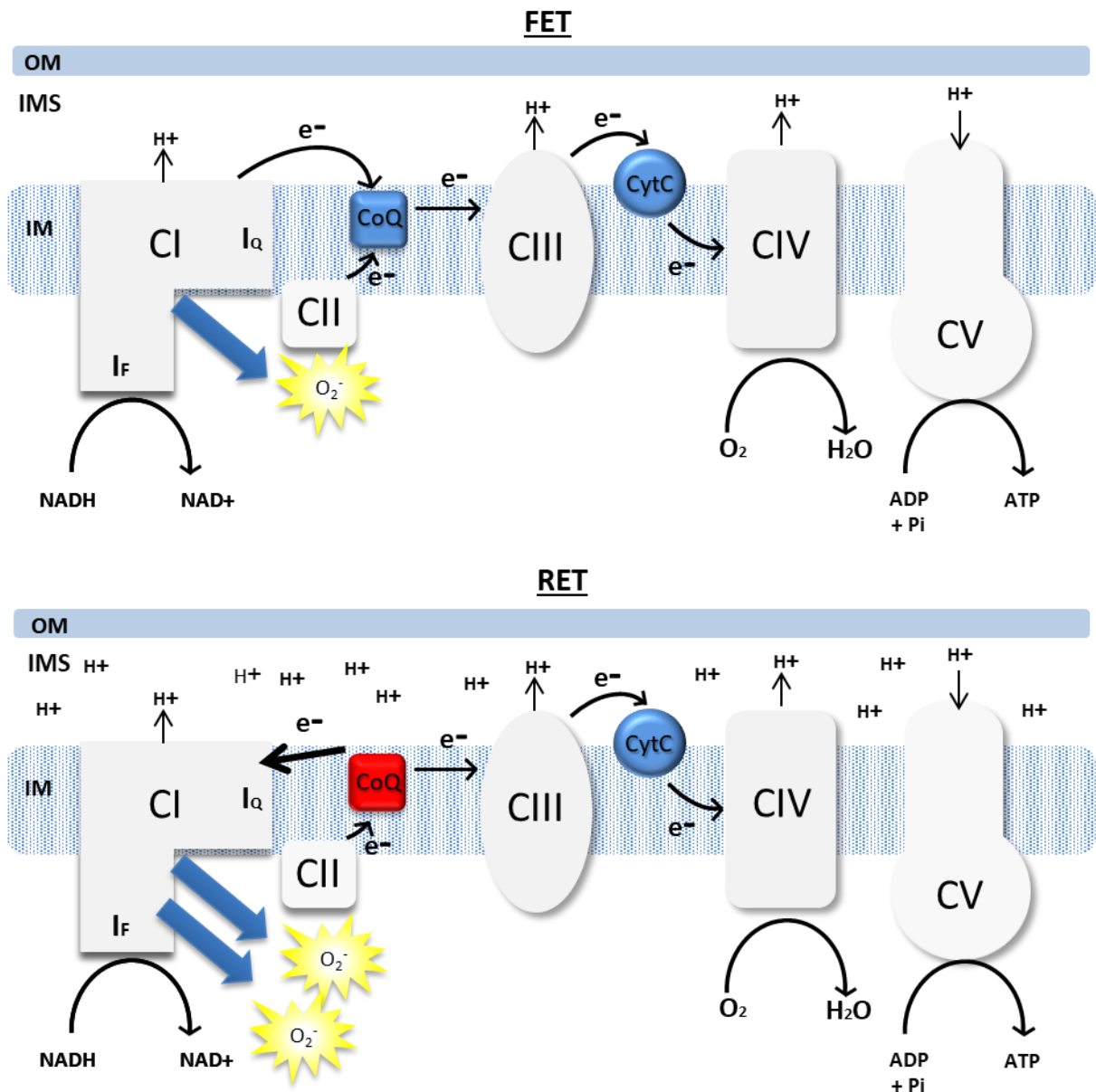


Figure 3.1 Schematic diagram illustrating the differences in ROS production at CI during forward (FET) and reverse (RET) electron transport.

During FET, in non-stressed conditions (top panel), electrons move from complex I to ubiquinone down the electron transport chain. ROS production occurs at CI when electrons escape and react with nearby O_2 molecules. However when the ubiquinone pool becomes highly reduced and a high-membrane potential is established, RET is initiated (bottom panel). Thus electron transport shifts to the reverse direction, from ubiquinol back to CI, leading to a large increase in ROS production at CI.

3.1.2 Validating RET at Complex I

To validate the induction of a physiological RET-ROS signal; two inhibitors, rotenone and FCCP were used.

The well-established CI inhibitor, rotenone, works by binding to the CoQ-binding site of CI, therefore, preventing the transfer of electrons to CoQ (Murphy, 2009). In non-stressed conditions, during forward electron transport, interrupting the flow of electrons down the chain would lead to increased ROS production at CI due to electron leakage (Figure 3.2A). However, during RET, rotenone binding blocks the flow of electrons back to CI, leading to the prevention of RET. For this reason it was anticipated that ROS would decrease following the addition of rotenone, if RET was occurring (Figure 3.2B).

FCCP uncouples the electron transport chain from OXPHOS by forming pores in the IMM, thereby releasing protons and subsequently dissipating membrane potential (Brennan *et al.*, 2006). RET is dependent on achieving a high pmf, therefore administration of FCCP would prevent the stimulation of RET. Similarly to rotenone it was also expected that feeding FCCP during RET would lead to a decrease in ROS production (Figure 3.3).

Previous experiments using the Ndi1 fly model confirmed the prevention of RET, with both rotenone and FCCP (Scialo *et al.*, 2016a). Therefore in this chapter, I took advantage of these inhibitors to help determine if a RET-ROS signal could be achieved physiologically in the fly.

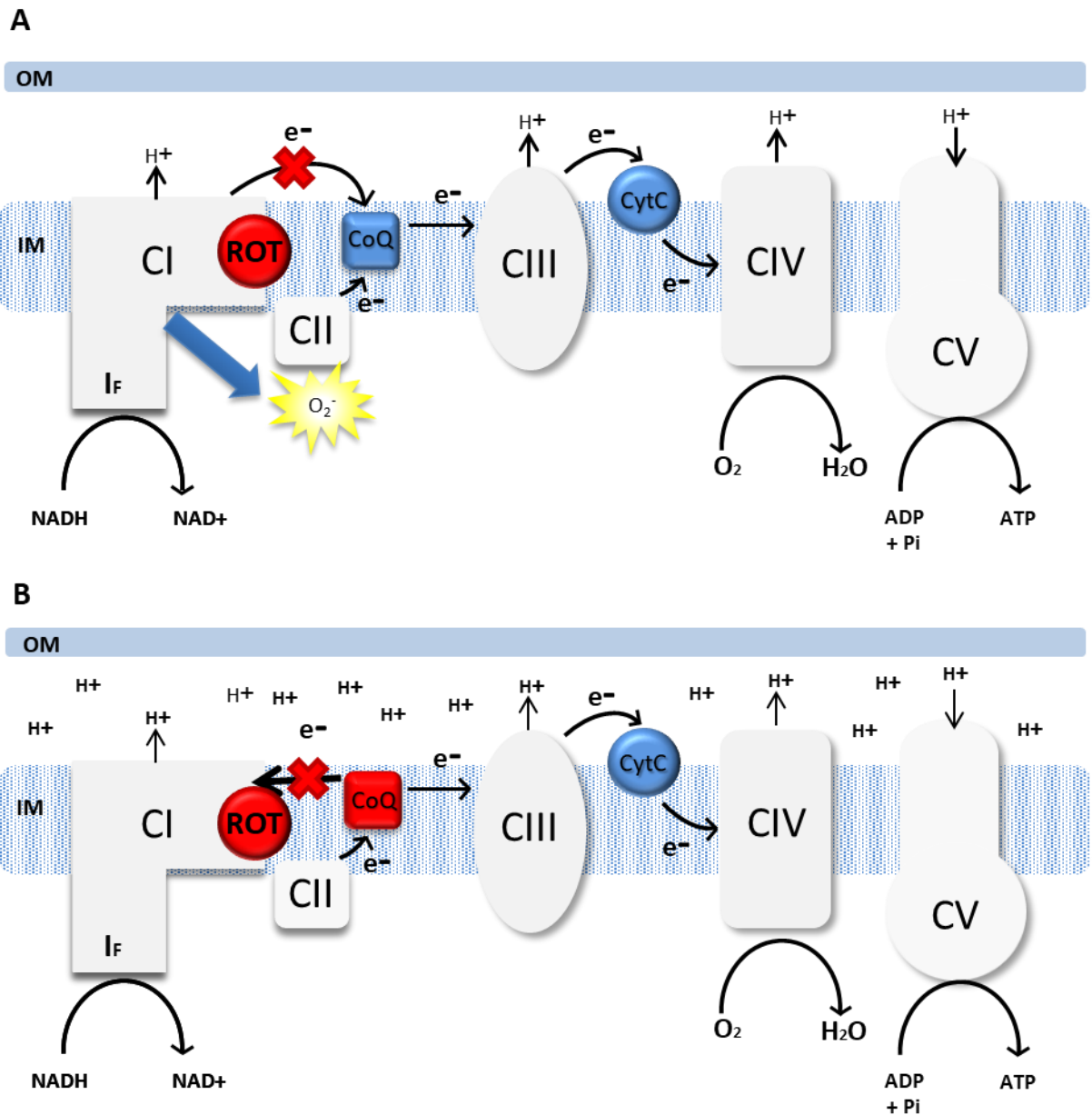


Figure 3.2 The effects of rotenone during FET and RET.

(A) In non-stressed conditions rotenone binds to CI preventing the transfer of electrons to ubiquinone, therefore leading to an increase in ROS production at CI. **(B)** During RET, electrons move backwards from ubiquinol to CI therefore in the presence of rotenone a decrease in ROS is observed, due to rotenone preventing the flow of electrons and subsequent electron leak at CI

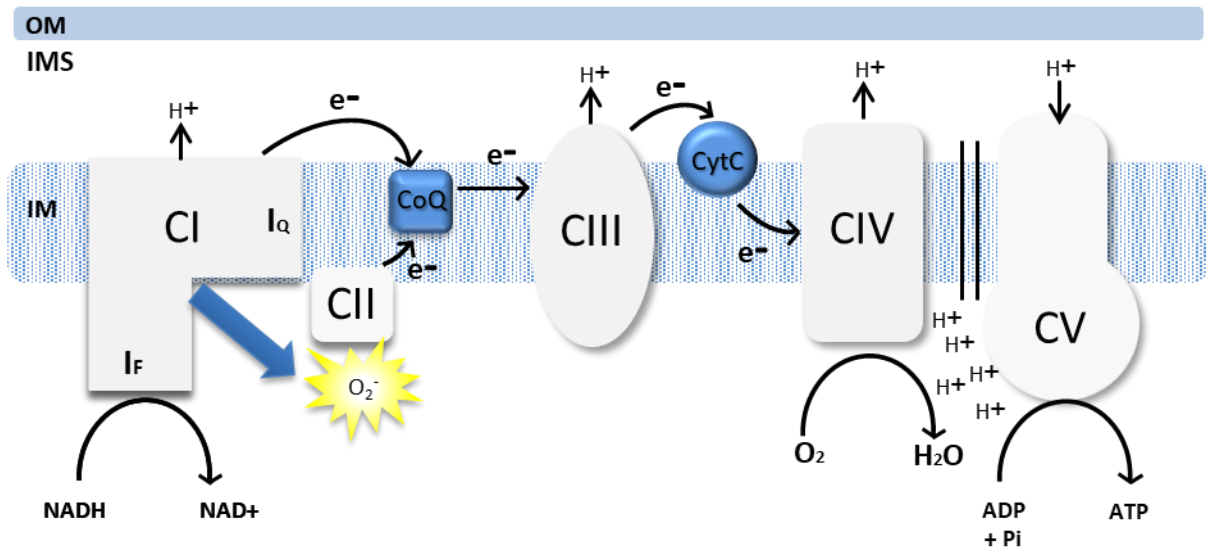


Figure 3.3 The effect of FCCP in normal conditions.

The uncoupler FCCP works by forming pores in the inner mitochondrial membrane, leading to the escape of protons and dissipation of membrane potential.

3.2 Results

3.2.1 Heat stress increases ROS production

I wanted to study the effect of exposing flies to 32°C for several hours. To do this I transferred flies from 25°C (non-stressed conditions) to 32°C (HS) for 6 hours and then measured ROS levels in dissected fly brains, after every hour, using two different fluorescent probes, H₂DCF and MitoSOX. H₂DCF was used to measure total cellular ROS in the form of peroxides, as it emits fluorescence when oxidised by H₂O₂ and other peroxides. To then further confirm a change in ROS, I used MitoSOX, which fluoresces when oxidised by superoxide. Due to MitoSOX possessing a positive charge, it is able to detect superoxide produced specifically in the mitochondrial matrix (Pavelescu, 2015). Experiments using MitoSOX were performed in collaboration with Dr Filippo Scialo. During the experiments I found that H₂DCF gave a strong signal throughout the brain, which also localised at the antennal lobe. The MitoSOX signal was weaker in comparison to H₂DCF, however also appeared to localise at the antennal lobe, therefore supporting that both dyes are successfully absorbed into the fly brain. As *Drosophila* are ectothermic animals they rely on the temperature of their immediate surroundings to adjust their metabolic rate, making them ideal for carrying out HS experiments (Figure 3.4).

HS had no effect on ROS production after 1 and 2 hours, where no change was observed in comparison to the control at 25°C. After 3 hours of HS, ROS levels significantly increased, which was detected using both dyes. ROS levels stayed elevated at 4 hours; however, after 5 hours ROS decreased back down to those seen at 1-2 hours (Figure 3.5). This indicates the presence of a dynamic ROS signal induced by HS, which is switched on at 3 hours and terminated at 5 hours.

Once I had established a specific time point, in which HS was able to increase ROS production, I repeated HS for 4 hours to confirm an increase when compared to control flies at 25°C. As expected, after 4 hours ROS production was increased (Figure 3.6). Between the two experiments shown in Figure 3.5B and 3.6D there was shown to be a larger response to HS in the latter. This could be due to the fact that these experiments were performed on separate occasions, which could affect the magnitude of ROS response between experiments. For example, using different aliquots of fluorescent dye, a different pool of flies, different controls and variations

with the microscope on different days, therefore it is difficult to compare results from different experiments.

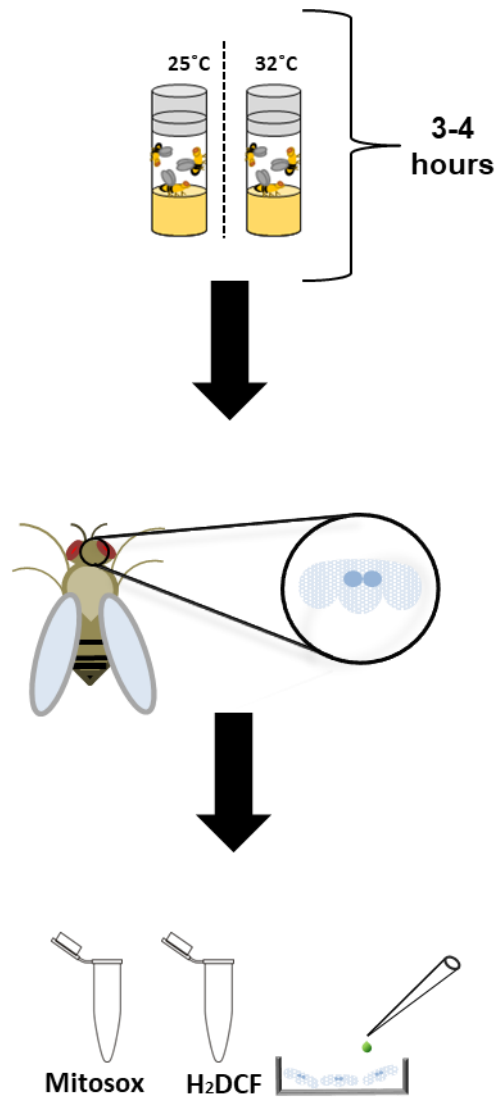


Figure 3.4 Diagram demonstrating the ROS measurement protocol.

Flies are transferred to 32°C for 4 hours. Fly brains are then dissected and incubated in either MitoSOX or H₂DCF for 10 minutes. ROS levels are measured using confocal microscopy and the images are quantified.

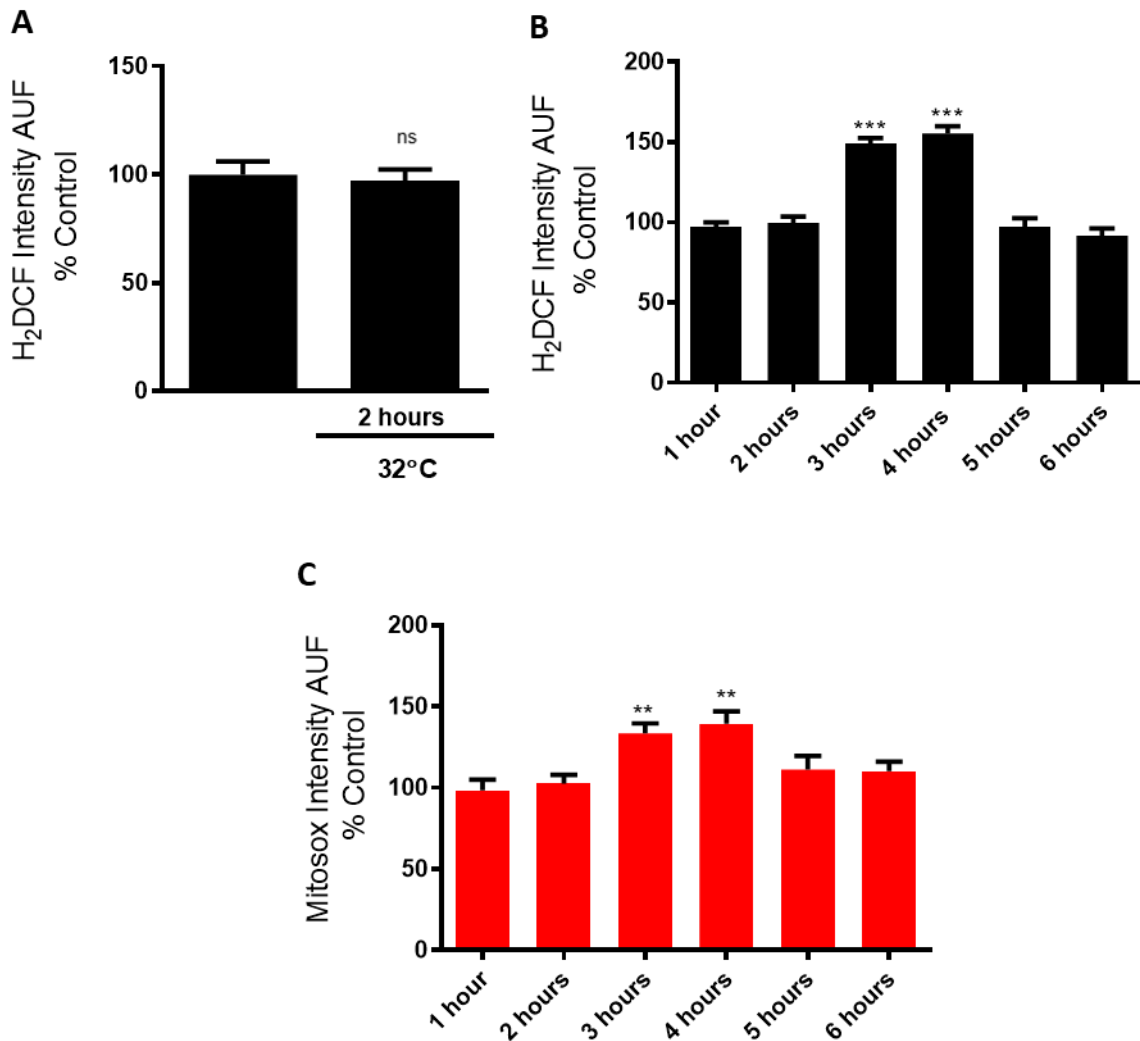


Figure 3.5 ROS measurements of flies subjected to heat stress over a 6 hour time course.

(A) ROS measurements in the brain using H₂DCF after 2 hours of heat stress compared to normal conditions, demonstrating that there is no change in ROS occurring (N = >8) **(B)** H₂DCF (N = >8) and **(C)** MitoSOX time course over 6 hours of HS (N = >8). Flies were approximately 3 days old. P Values were calculated using One-Way ANOVA. Data are shown as mean ± SEM. p < 0.05 was taken as statistically significant and represented by *, p < 0.01 was represented by ** and p < 0.001 was represented by ***. MitoSOX data was carried out in collaboration with Dr Filippo Scialo.

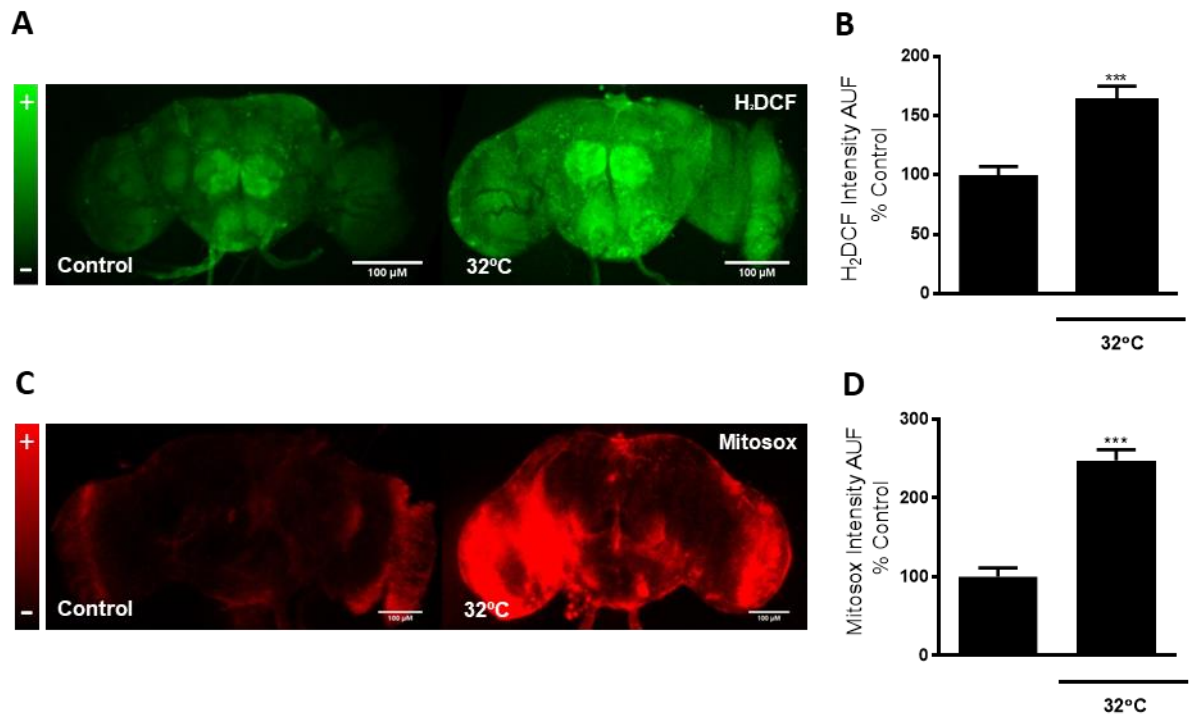


Figure 3.6 ROS measurements of flies subjected to 4 hours of heat stress.

Representative images of dissected fly brains stained with **(A)** H₂DCF (N = >6) and **(C)** MitoSOX (N = >9) from control flies (25°C) and flies subjected to thermal stress (32°C for 4 hours). Quantifications of **(A)** and **(C)** are shown in **(B)** and **(D)**, respectively. Flies were approximately 3 days old. P Values were calculated using unpaired Student's T-test. Data are shown as mean ± SEM. p < 0.05 was taken as statistically significant and represented by *, p < 0.01 was represented by ** and p < 0.001 was represented by ***. MitoSOX data was carried out in collaboration with Dr Filippo Scialo.

3.2.2 Heat Stress changes the way CI produces ROS

I tested that rotenone was able to reach the brain and inhibit mitochondrial respiration in the fly brain after 4 hours of feeding. Lower doses, (600 μM), did not show any major alteration in respiration but high doses, (900 μM and 1 mM), significantly reduced respiration rate, by approximately 50% (Figure 3.7A). Following confirmation of CI inhibition with rotenone after 4 hours, ROS measurements were conducted. As expected, rotenone increased ROS production during forward electron transport when flies were in non-stressed conditions (25°C). This increase was detected even using lower doses (600 μM) where no inhibition in respiration was observed, using an *in vitro* approach (Figure 3.7B – E).

I then measured the effect of rotenone on the ROS levels during HS. As shown previously, an increase in ROS was observed after 4 hours of HS. However, upon addition of rotenone, this increase was abolished and ROS levels were similar to those seen in non-stressed conditions (Figure 3.8). These results support the initiation of a RET during HS, which can be prevented by inhibiting CI with rotenone.

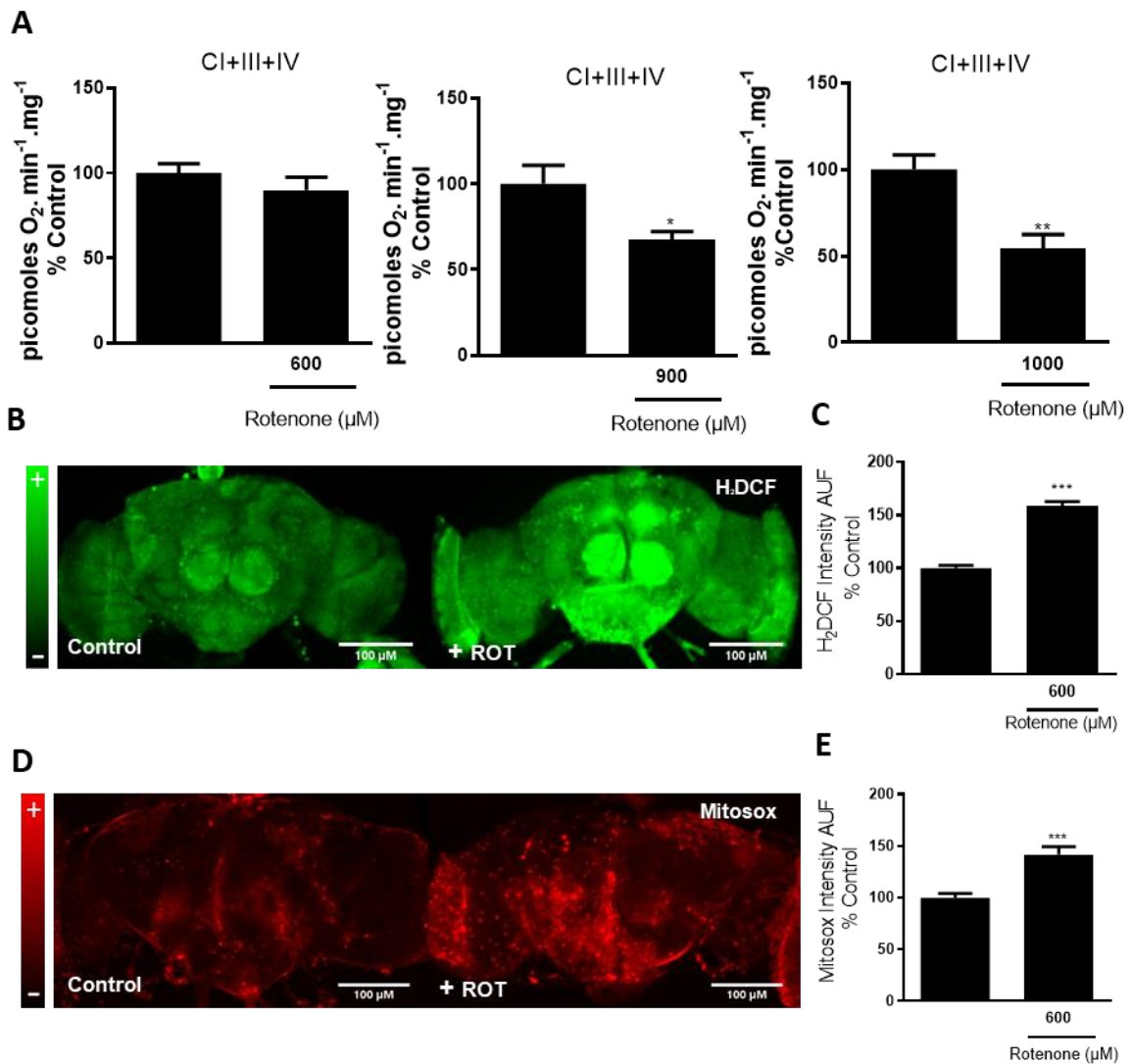
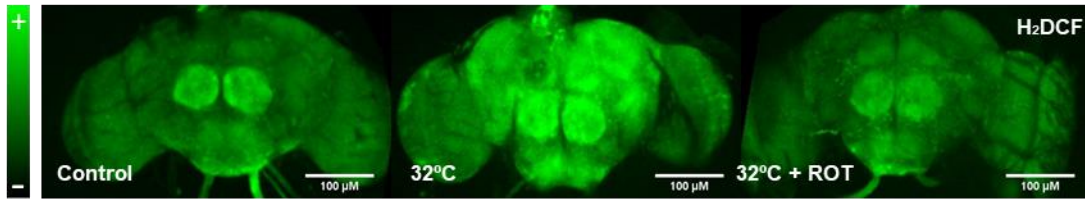


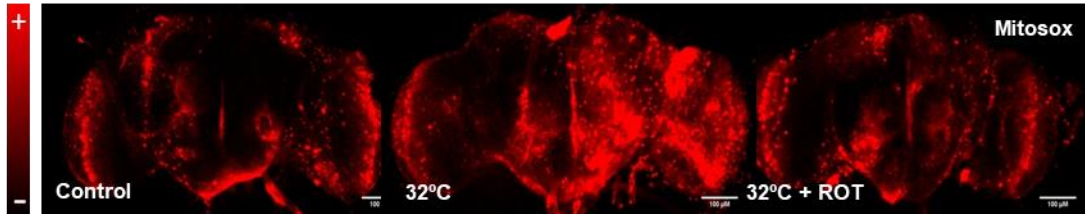
Figure 3.7 The effect of rotenone on ROS production in normal conditions.

(A) Mitochondrial respiration of fly head mitochondria after feeding flies with differing concentrations of rotenone (600 μM, 900 μM and 1 mM) (N = >9). Images of dissected fly brains stained with (B) H₂DCF (N = >7) and (D) MitoSOX (N = >7), showing control flies fed the vehicle (EtOH) (left panel) and CI inhibitor rotenone (right panel) for 4 hours. (C) Quantification of B. (E) Quantification of D. Flies were approximately 3 days old. P Values were calculated using unpaired Student's T-test. Data are shown as mean ± SEM. p < 0.05 was taken as statistically significant and represented by *, p < 0.01 was represent by ** and p < 0.001 was represented by ***. MitoSOX data was carried out in collaboration with Dr Filippo Scialo.

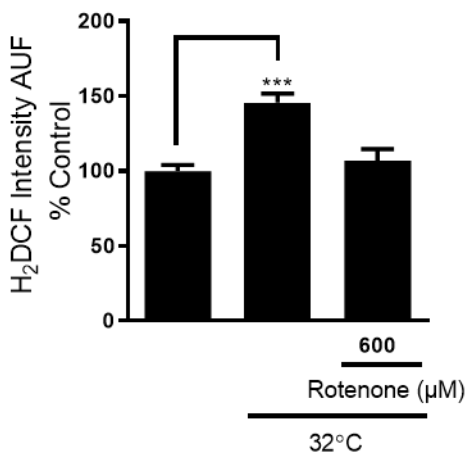
A



B



C



D

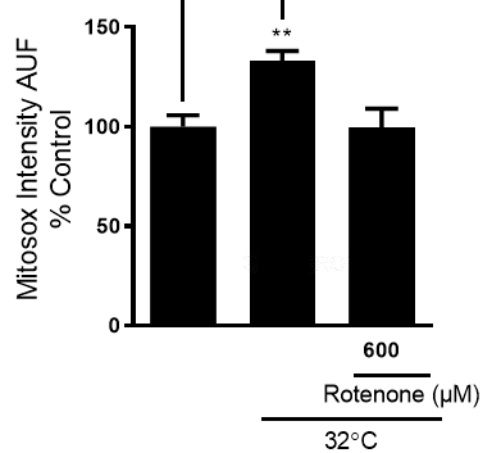


Figure 3.8 The effect of rotenone on ROS production during heat stress.

Images of dissected fly brains stained with **(A)** H₂DCF (N = 8) and **(B)** MitoSOX (N = >9) showing the effect on ROS production after feeding flies rotenone under HS (32°C). Quantifications of **(A)** and **(B)** are shown in **(C)** and **(D)**, respectively. Flies were approximately 3 days old. P Values were calculated using One-Way ANOVA. Data are shown as mean ± SEM. p < 0.05 was taken as statistically significant and represented by *, p < 0.01 was represented by ** and p < 0.001 was represented by ***. MitoSOX data was carried out in collaboration with Dr Filippo Scialo.

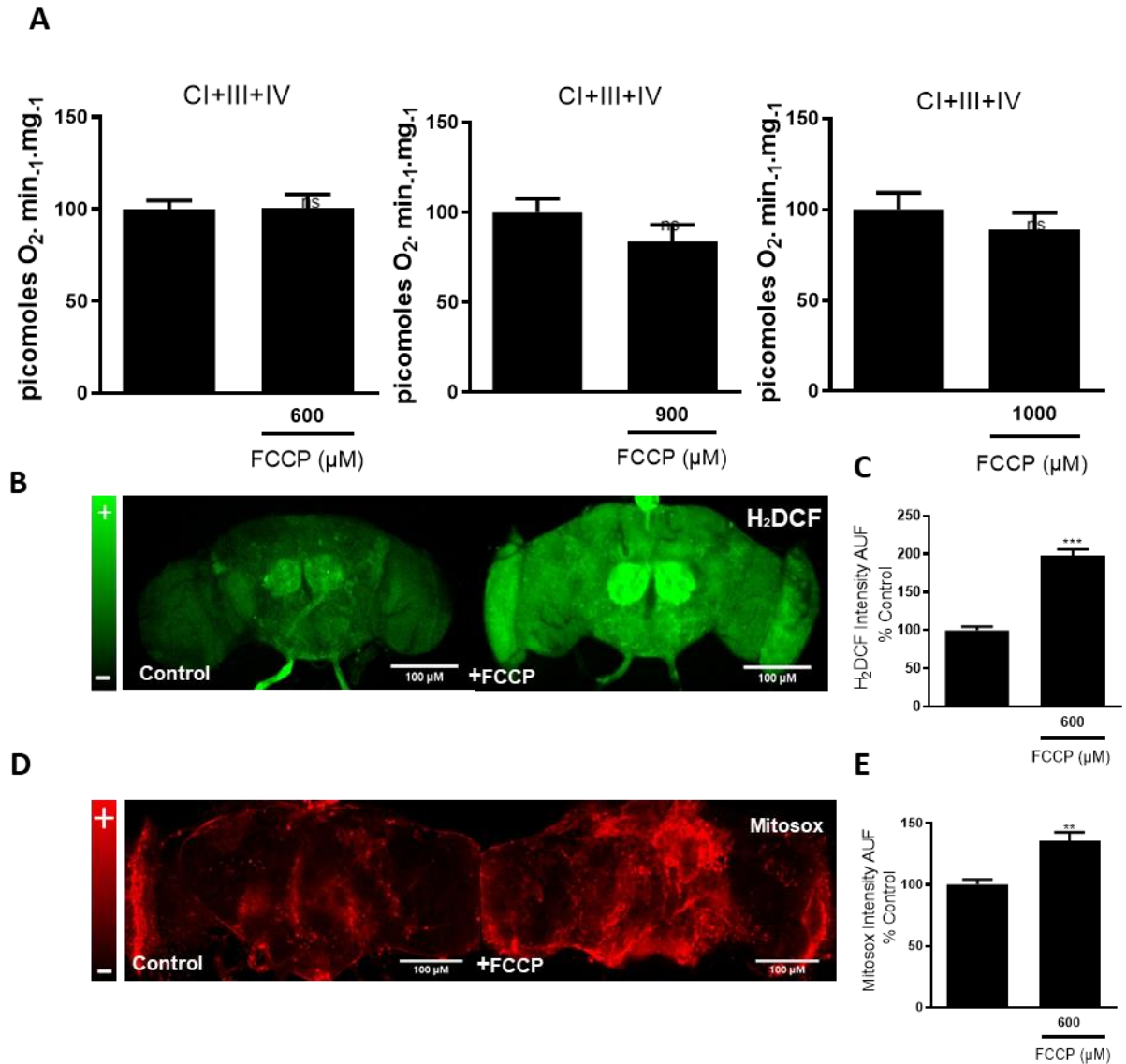
3.2.3 Dissipating proton motive force with FCCP prevents RET during heat stress.

After using rotenone to confirm RET, I then used FCCP to prevent a high membrane potential from being achieved. Feeding flies with FCCP did not alter mitochondrial respiration in fly brain mitochondria (Figure 3.9A). However, in normal conditions, FCCP was capable of increasing ROS production using both H₂DCF and MitoSOX (Figure 3.9 C-F).

When transferred to HS, an increase in ROS could be seen, which was then abolished in the presence of FCCP (Figure 3.10). Therefore by dissipating the RET stimuli; membrane potential during HS, RET was prevented.

It has been previously shown that dissipating the mitochondrial potential can lead to the relocation of MitoSOX from the mitochondria and into the cytosol, resulting in an increased ^{ns} ROS signal (Roelofs *et al.*, ^{ns} 2015). However, due to the fact that we observe an increase in ROS in normal conditions in the presence of FCCP and a contrasting decrease in ROS during HS, which correspond to the H₂DCF results, these data suggest this is not occurring during these experiments.

Figure 3.9 The effect of FCCP on ROS production in non-stressed conditions.



(A) Oxygen consumption of fly head mitochondria after feeding flies with varying concentrations of FCCP (600 μM, 900 μM and 1 mM) (N = 5). Representative images of dissected fly brains stained with **(B)** H₂DCF (N = >7) and **(C)** MitoSOX (N = >6) after feeding the flies with FCCP in non-stressed conditions (25°C). Quantifications of **(B)** and **(D)** are shown in **(C)** and **(E)**, respectively. Flies were approximately 3 days old. P Values were calculated using unpaired Student's T. Data are shown as mean ± SEM. p < 0.05 was taken as statistically significant and represented by *, p < 0.01 was represented by ** and p < 0.001 was represented by ***. Same control used for Figure 3.7D as 3.9D, due to these 3 groups being measured in the same experiment. MitoSOX data was carried out in collaboration with Dr Filippo Scialo.

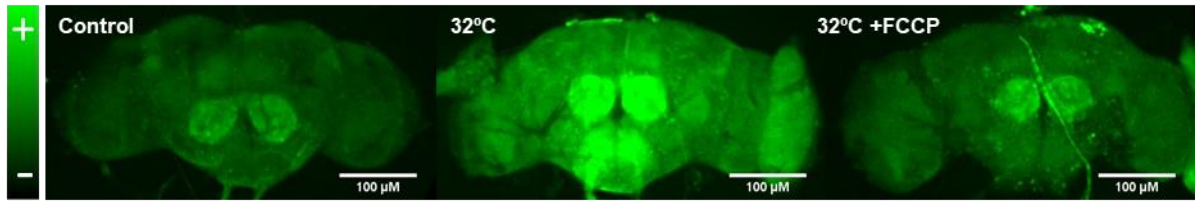
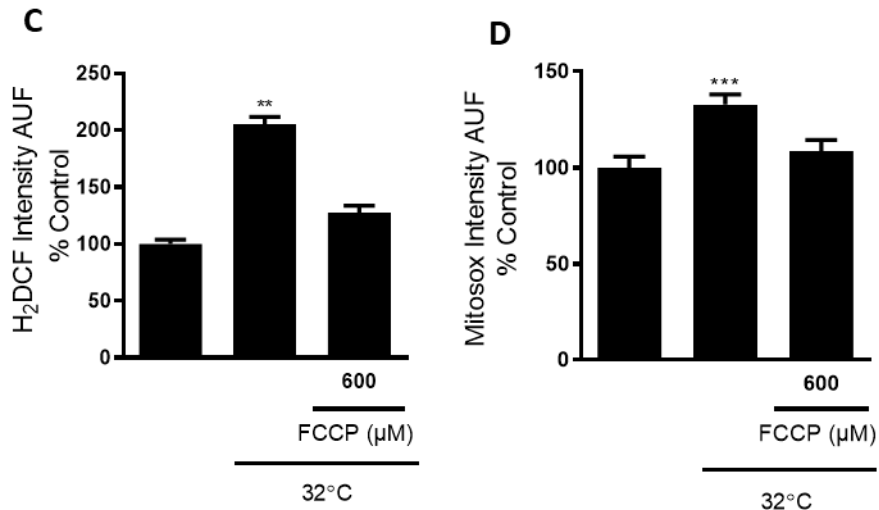
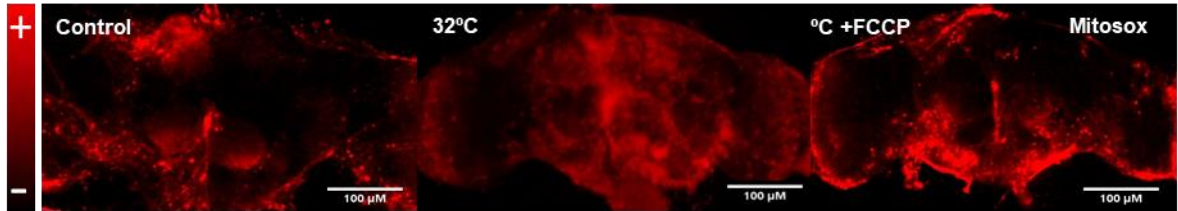
A**B**

Figure 3.10 The effect of FCCP on ROS production during heat stress.

Representative images of dissected fly brains stained with **(A)** H₂DCF (N = >6) and **(B)** MitoSOX (N = 9) after feeding flies with FCCP in non-stressed conditions (25°C). Quantifications of **(A)** and **(B)** shown in **(C)** and **(D)** respectively. Flies were approximately 3 days old. P Values were calculated using One-Way ANOVA. Data are shown as mean ± SEM. p < 0.05 was taken as statistically significant and represented by *, p < 0.01 was represented by ** and p < 0.001 was represented by ***. MitoSOX data was carried out in collaboration with Dr Filippo Scialo.

3.2.4 ROS produced during heat stress originates from mitochondria

To confirm the location of ROS being produced during HS, I took advantage of the antioxidants SOD2 and Catalase, by overexpressing them in the fly. SOD2 resides in the mitochondrial matrix and converts superoxide into the less reactive ROS, H₂O₂. Catalase is then able to completely detoxify H₂O₂, to produce inert water and O₂. For these experiments, I over-expressed a mitochondrial-targeted catalase (Kwong *et al.*, 2000) (Figure 3.11). I predicted that by overexpressing both these mitochondrial antioxidants I would be able to manipulate the levels of ROS produced during HS, to determine whether or not it originates from mitochondria. These experiments were done in collaboration with Dr Filippo Scialo.

When measuring ROS using MitoSOX, SOD2 overexpression revealed a decrease in mitochondrial superoxide during HS. These results support the ability of SOD2 to convert superoxide into H₂O₂, which was further confirmed by an increase in H₂DCF signal, indicating more peroxides (Figure 3.12).

Overexpression of the mitochondrial-targeted catalase enzyme showed a significant decrease in total cellular H₂O₂ levels, after 4 hours in 32°C. However, no change in mitochondrial superoxide levels were observed when measured with MitoSOX. These data are consistent with the fact that Catalase converts H₂O₂ into water, thereby leading to the decrease in ROS but without altering superoxide levels (Figure 3.13).

The results obtained using the expression of antioxidants, SOD2 and catalase, demonstrated that MitoSOX and H₂DCF successfully detect mitochondrial superoxide and cytosolic peroxides, respectively. Therefore, due to the ROS fluctuating specifically in the mitochondria, these results identified mitochondrial ROS production during HS, providing further evidence that RET is being stimulated.

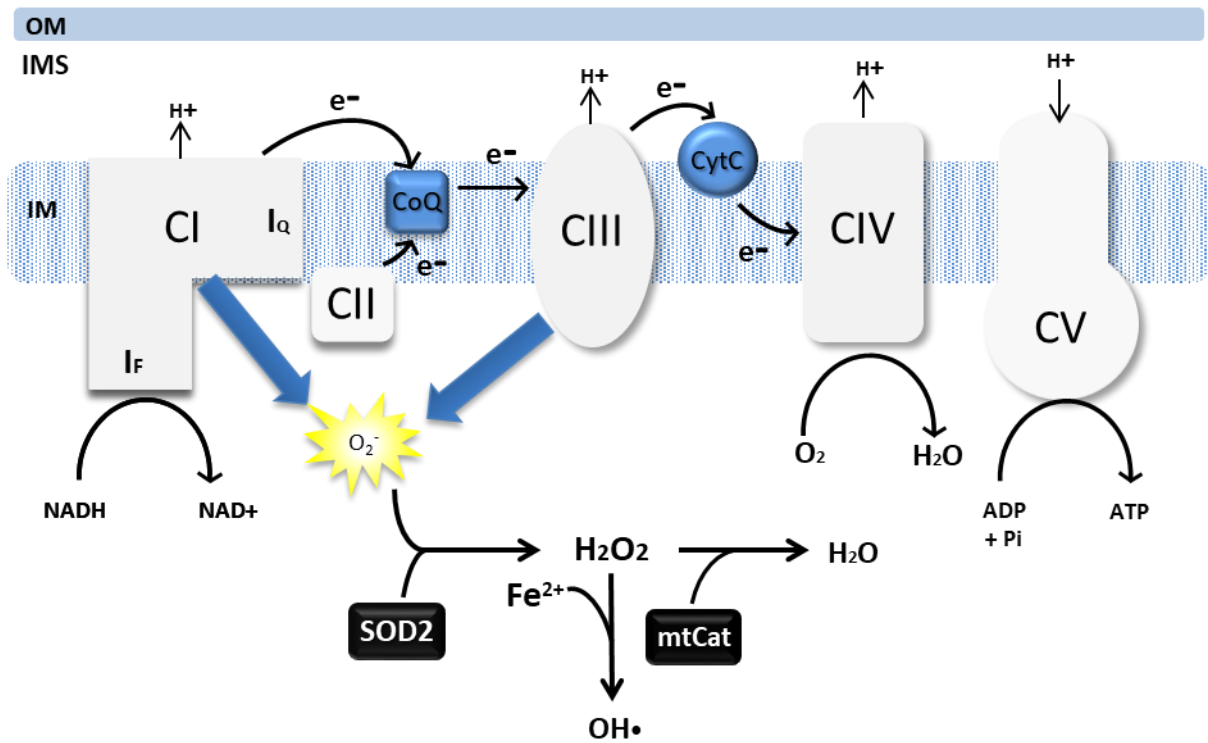


Figure 3.11 Diagram depicting the role of antioxidants inside the mitochondria.

SOD2 catalyses the dismutation of superoxide into H_2O_2 . Whereas mitochondrial targeted catalase detoxifies H_2O_2 into water.

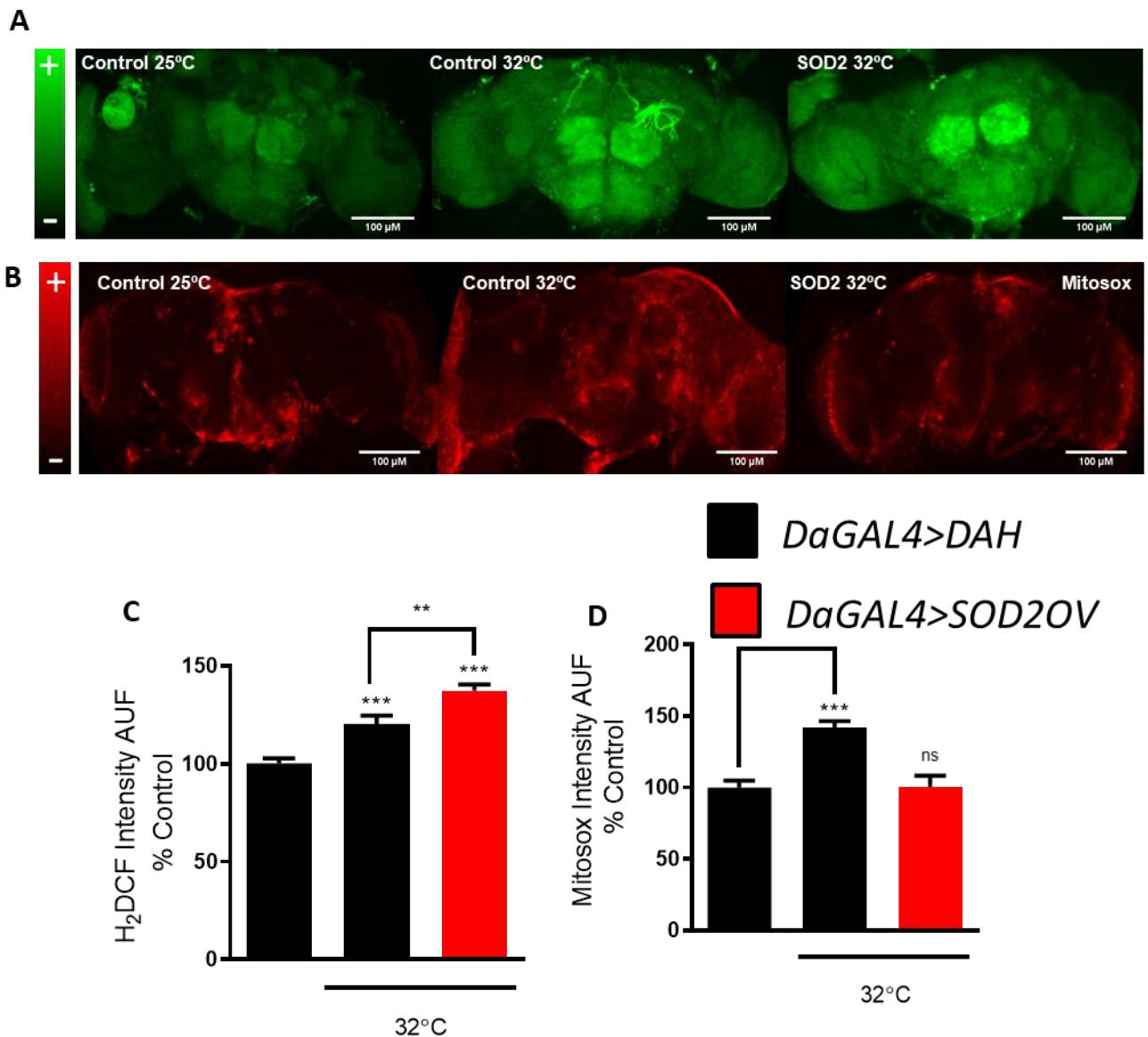


Figure 3.12 The effect of SOD2 overexpression on ROS production during heat stress.

(A) ROS measurements using H₂DCF to measure H₂O₂ levels in flies overexpressing SOD2 (N = >8). **(B)** ROS measurements using MitoSOX to measure superoxide levels in flies overexpressing SOD2 (N = >9). Quantifications of **(A)** and **(B)** shown in **(C)** and **(D)** respectively. Flies were approximately 3 days old. P Values were calculated using One-Way ANOVA. Data are shown as mean ± SEM. p < 0.05 was taken as statistically significant and represented by *, p < 0.01 was represented by ** and p < 0.001 was represented by ***. MitoSOX data was carried out in collaboration with Dr Filippo Scialo.

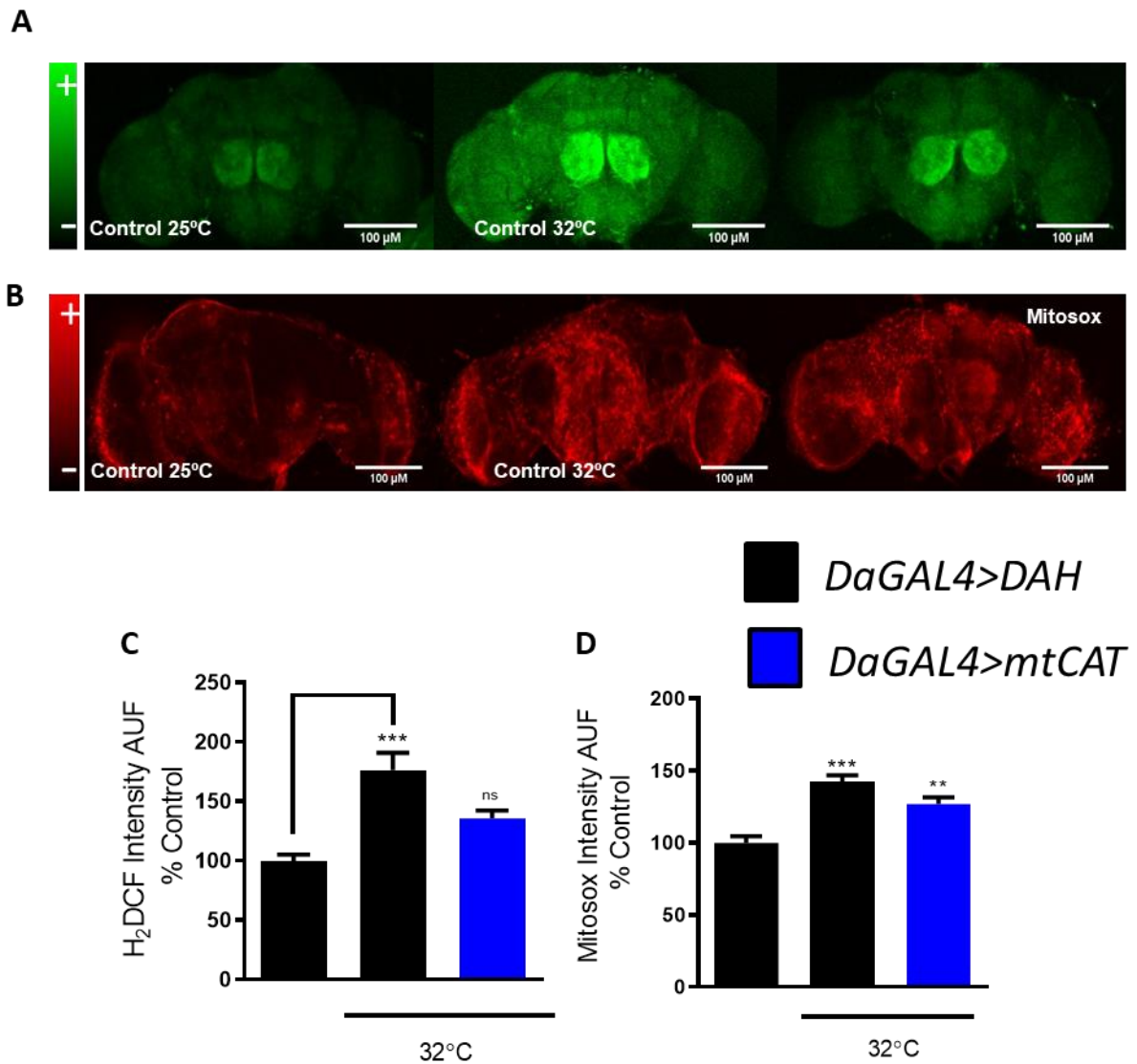


Figure 3.13 The effect of mitochondrial-catalase expression on ROS production during heat stress.

(A) ROS measurements using H₂DCF to measure H₂O₂ levels in flies overexpressing Catalase (N = >10). **(B)** ROS measurements using MitoSOX to measure superoxide levels in flies overexpressing Catalase (N = >8). Quantifications of **(A)** and **(B)** shown in **(C)** and **(D)** respectively. Flies were approximately 3 days old. P Values were calculated using One-Way ANOVA. Data are shown as mean ± SEM. p < 0.05 was taken as statistically significant and represented by *, p < 0.01 was represent by ** and p < 0.001 was represented by ***. This antioxidant data was carried out in collaboration with Dr Filippo Scialo.

3.2.5 Heat stress cannot stimulate RET in old flies

It has been previously shown that CI activity decreases with age. In *Drosophila*, mitochondrial respiration at day 50 is strongly decreased, particularly CI-respiration (Scialo *et al.*, 2016a). Since I have confirmed in this chapter that the CI inhibitor, rotenone, is able to prevent RET from occurring I wanted to test if this age-related loss of CI activity, would affect the stimulation of RET.

Consistent with prior studies (Scialo *et al.*, 2016a), which show that ROS increases with age, *ex vivo* ROS measurements using H₂DCF increased significantly at 25 and 50 days in non-stressed conditions (25°C) (Figure 3.14A). In support of results reported previously in this chapter, when 25-day-old flies were subjected to HS for 4 hours there was an increase in ROS, which was restored to control levels upon the addition of rotenone (Figure 3.14B). Therefore indicating the stimulation of ROS-RET in the 25-day-old flies. However, when conducting the same experiment with 50-day-old flies no increase was observed in the flies exposed to HS. These results suggest that due to a decrease in activity at 50 days, CI loses the ability to switch to RET (Figure 3.14C).

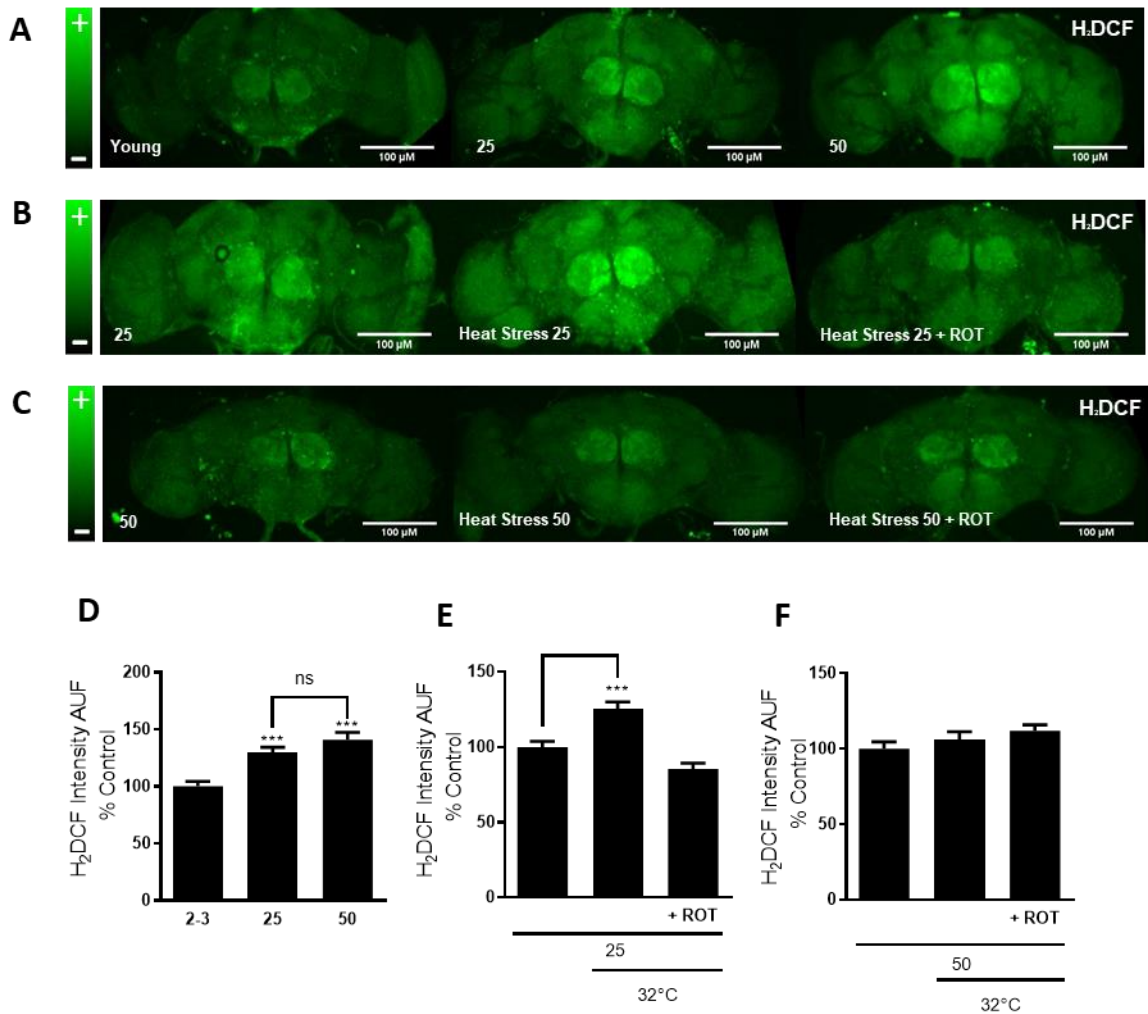


Figure 3.14 The effect of heat stress on ROS production in young and old flies.

(A) Representative images of brains stained with H₂DCF comparing ROS levels in young flies (2 – 3 days old), 25 day old flies and 50 day old flies (N = >8). **(B)** ROS measurements from 25 day old flies subjected to HS and rotenone (600 μM) (N = >8). **(C)** ROS measurements from 50 day old flies subjected to HS and rotenone (600 μM) (N = >7). **(D)** Quantification of A **(E)** Quantification of B **(F)** Quantification of C. Due to these three experiments being performed on separate occasions it is difficult to interpret the different intensities between the different images. P Values were calculated using One-Way ANOVA. Data are shown as mean ± SEM. p < 0.05 was taken as statistically significant and represented by *, p<0.01 was represented by ** and p<0.001 was represented by ***.

ns ns ns

3.2.6 Intermittent induction of ROS-RET and its effect on lifespan

I developed the HS model to test whether RET could be physiologically stimulated in flies and if this RET-ROS would provide the same lifespan extension, as the Ndi1 model. After confirming the stimulation of RET, I wanted to see if the beneficial effect on longevity could be repeated using HS.

To conduct these lifespan experiments, I designed three different groups. In each group, the flies were exposed to HS at different stages, to determine an optimal period of time that could promote lifespan extension. The groups were as follows; HS throughout the entire lifespan (hereafter referred to as intermittent HS), HS from the 1st day of eclosion to the 25th day (hereafter referred to as 1-25) and HS from the 25th day to the 50th day (hereafter referred to as 25-50) (Figure 3.15). All three groups were kept at 32°C for 4 hours, 3 times per week.

Intermittent HS was chosen to see if consistent stimulation of ROS-RET, for 4 hours 3 times per week, could extend lifespan. 1-25 was selected due to previous studies showing that manipulation involving mitochondria or metabolism, such as fasting, or induction of mitochondrial fission, extend lifespan only when implemented during a brief period of time in early adulthood of the fly (Rana *et al.*, 2017) (Catterson *et al.*, 2018). The last group, 25-50, was chosen to see the effect of HS on longevity, in older flies. However, due to previous results showing that CI eventually loses the capacity to create ROS-RET, HS was stopped at 50 days.

Within each group, I had 4 different conditions to help resolve any changes in lifespan that might occur. The first condition was 25°C (non-stressed conditions) which acted as the primary control. These flies were kept in the same incubator and transferred to normal fresh food every 2 days. The second condition was 32°C (heat stress), where flies were kept in 32°C incubators 3 days a week for 4 hours and transferred to normal food every 2 days. The third condition was 32°C + ROT. Here flies were flipped onto food containing rotenone and transferred to 32°C for 4 hours, 3 times a week, before being flipped back onto normal food and placed in 25°C. This condition acted as a control for the HS condition, as the addition of rotenone would prevent RET, therefore in theory, if HS were successful in increasing lifespan, we would expect this to be abolished in the presence of rotenone. The fourth group was 25°C + ROT, where flies were constantly kept in 25°C. However they were also fed

rotenone for 4 hours, 3 times per week. This condition acted as a control for the 32°C + ROT to observe the effect of repeatedly feeding flies rotenone (Figure 3.16).

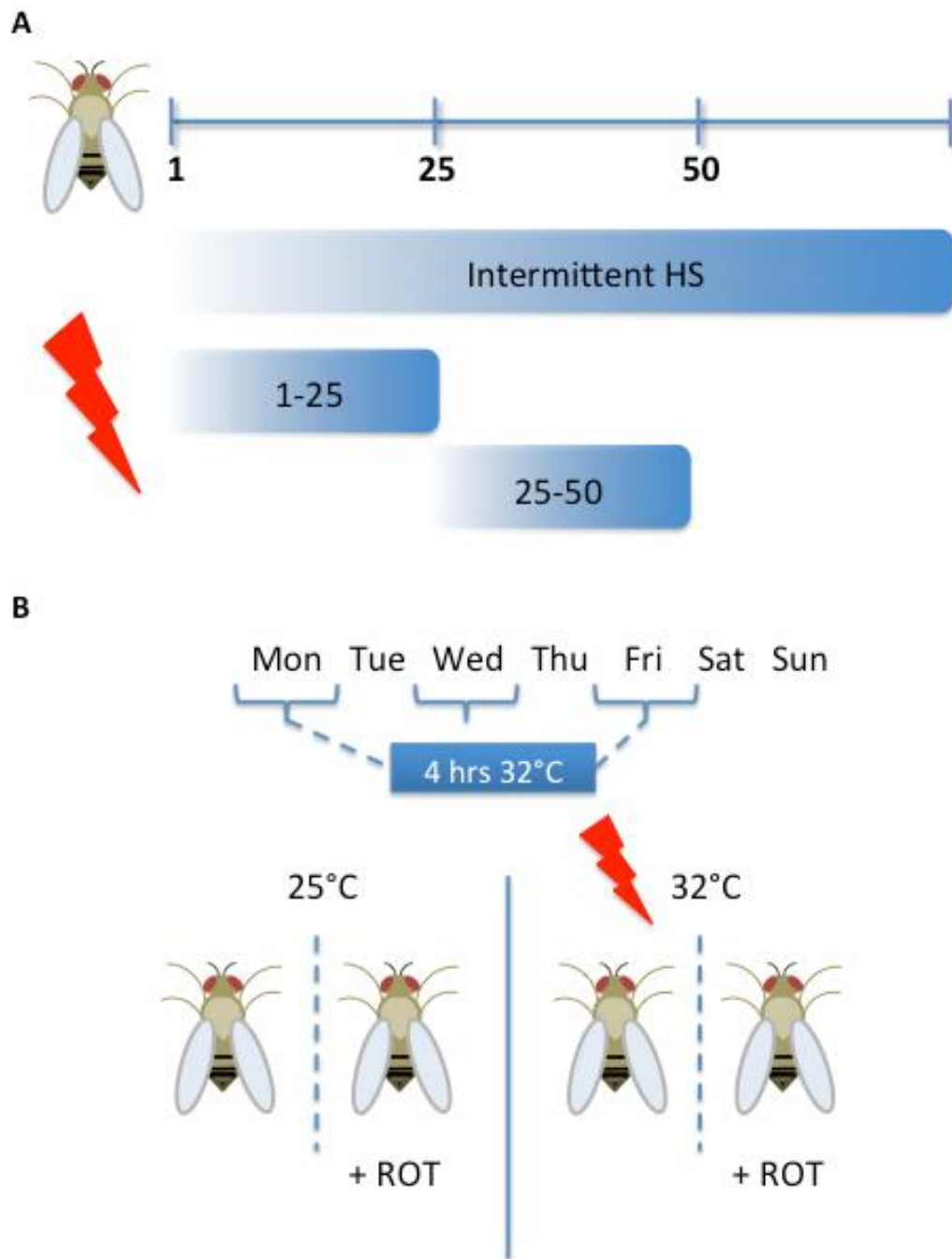


Figure 3.15 Diagram outlining the 3 different groups of the lifespan experiments as well as the 4 conditions used during the lifespan experiments and how this was applied on a weekly basis.

(A) As shown, intermittent HS occurs throughout the *Drosophila*'s lifespan. The 1-25 group is subjected to HS from eclosion to 25th day, whilst the 25-50 groups is subjected to HS from the 25th to the 50th day. **(B)** The flies were subjected to the different conditions three times per week, namely Monday, Wednesday and Friday. The four different conditions included (i) 25°C, (ii) 25°C + ROT, (iii) 32°C and (iv) 32°C + ROT.

3.2.7 Heat stress does not extend lifespan in *Drosophila melanogaster*

Exposing W_{DAH} flies to 32°C for 4 hours 3 times per week throughout adulthood did not extend *Drosophila* lifespan. In comparison to the control (25°C), both treatments (32°C and 25°C + ROT) decreased lifespan. However, flies showed greater sensitivity when both treatments were delivered together (32°C + ROT group), which decreased lifespan even further by approximately 20 days (Figure 3.16A). This decrease may be explained by the changes in ROS production we see in later life of the flies (Figure 3.16B). Therefore, once CI can no longer produce RET-ROS, the stress of 32°C and rotenone has detrimental effects on lifespan.

During the first 25 days of adulthood, neither rotenone feeding nor HS had an effect on the lifespan (Figure 3.16C). This indicates that throughout early adulthood the flies can adapt to overcome stress conditions, more sufficiently than in later life.

HS was not able to extend lifespan when flies were exposed during the 25th to the 50th day of adulthood either. No significant difference was observed between the control, 32°C and 25°C + ROT. However, similarly to intermittent HS, exposing flies to both HS and rotenone during later adulthood led to a significant decrease in lifespan (Figure 3.17A). Since this sensitivity towards 32°C +ROT was specific to the groups exposed in late adulthood and was not seen in the early adulthood group, it further confirms an age-specific inhibition of RET. Thus, indicating that mitochondria can no longer adapt to counteract both HS and rotenone, ultimately leading to the significant decrease in lifespan.

Analysis of the different experimental groups, exposed to conditions at different time periods, revealed clear correlations. Figure 3.17A shows all of the control groups (25°C) together, where as expected, no change in lifespan was observed between the 3 different conditions. The 25°C + ROT group lifespans were not affected when exposed to rotenone during only 1-25 and 25-50 days (Figure 3.17B). However there was a slight decrease detected in longevity, when exposed to rotenone 3 days per week, throughout the whole lifespan. A similar trend was observed in the 32°C group, where flies exposed to HS from 1-25 and 25-50 days, showed no difference in lifespan, whilst flies exposed to intermittent HS, observed a decrease in lifespan (Figure 3.17C). These data clearly show that flies can adapt to a stress condition, i.e. rotenone feeding or HS, in early adulthood more effectively than in later life.

Interestingly, the 32°C + ROT group lifespans were significantly reduced when flies

were exposed constantly and during 25-50 days to HS (Figure 3.17D), in comparison to 1-25 days which were not affected (Figure 3.17B).

Supporting previous observations, this indicates that the flies subjected to stress in later life, i.e. intermittent HS and 25-50 were not able to adapt and overcome stress conditions as well as the flies subjected to stress in early life i.e. 1-25. It is possible that this lack of adaptation is caused by a depletion of CI activity, in older adult flies. As previously shown in *Drosophila*, CI levels are dramatically decreased at day 50. Additionally when 50-day-old flies were subjected to HS, no ROS-RET response was observed. These data together suggest that the loss of CI activity, as the flies age, leads to the inability of CI to switch to RET, from forward electron transport. In doing so it prevents the stimulation of downstream adaptation pathways that can counteract the stress condition, thereby leading to a decrease in longevity. This is in contrast to the 1-25 lifespan studies, in which a fully functioning CI can switch to RET, leading to the generation of ROS and protection against stress-induced damage.

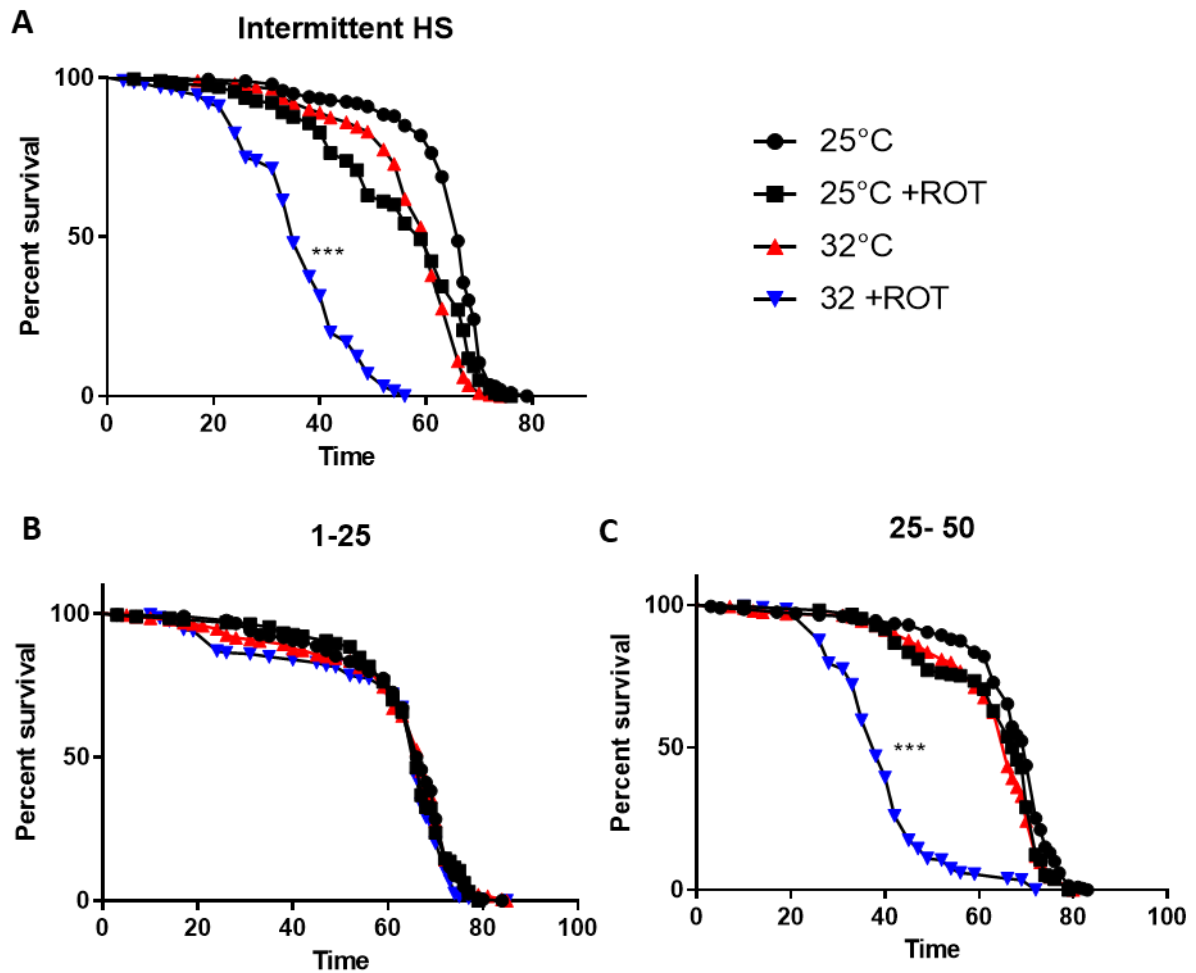


Figure 3.16 The effect of heat stress throughout the *Drosophila* lifespan.

(A) Survival curve data displaying the effect of intermittent HS throughout lifespan. (B) Survival curve data displaying the effect of subjecting flies to HS from 1-25. (C) Survival curve data displaying the effect of subjecting the flies to HS from 25-50 days. HS (32°C) is indicated in red and HS + rotenone (32°C + ROT) is indicated in blue. (N = 200). Lifespan survival curves were analysed using the log-rank Mantel Cox Test. $p < 0.05$ was taken as statistically significant and represented by *, $p < 0.01$ was represented by ** and $p < 0.001$ was represented by ***.

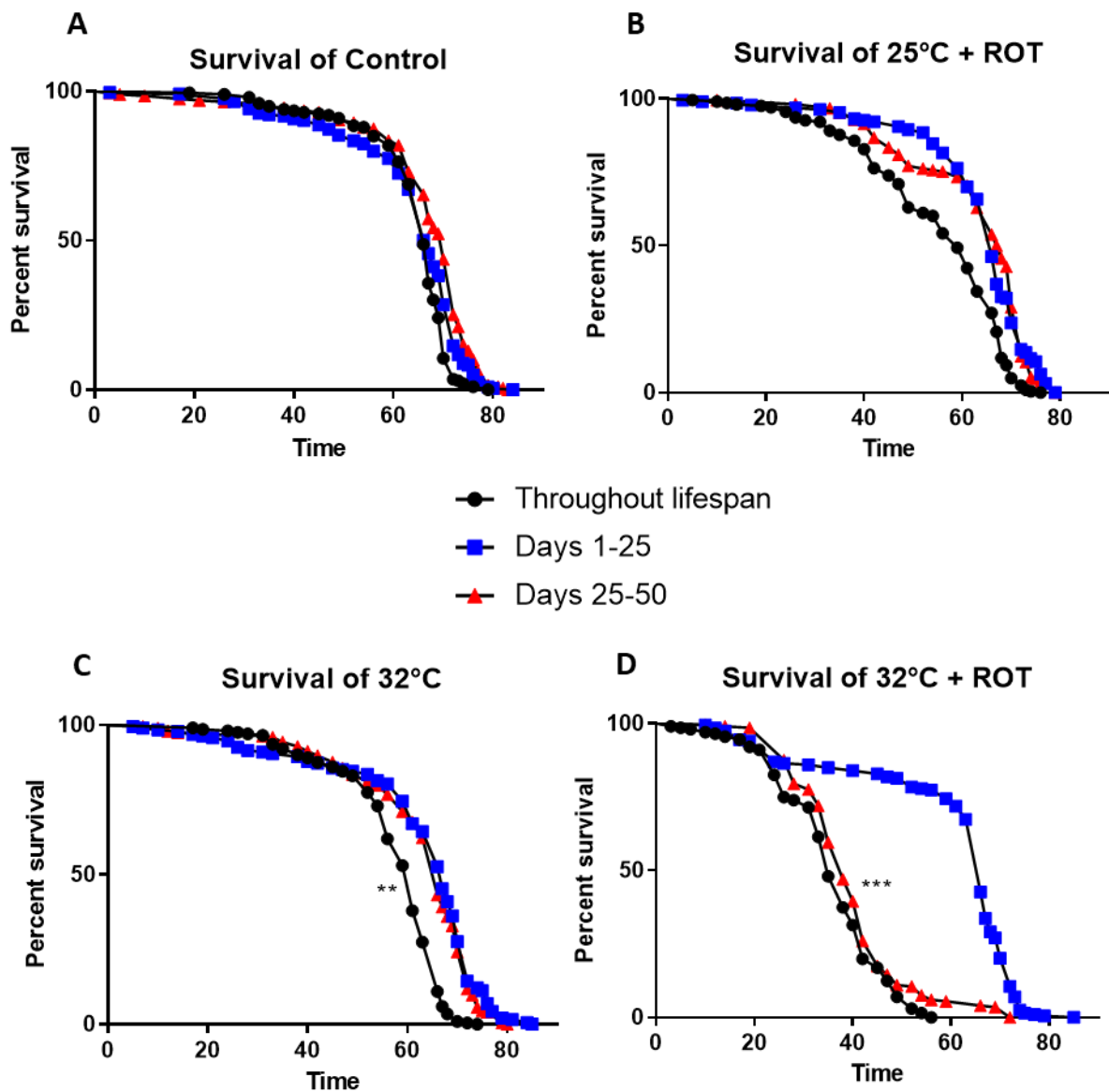


Figure 3.17 Comparison of the different groups from Drosophila lifespans.

(A) Survival curves displaying data of the control (25°C) conditions from each group. Group 25-50 are indicated in red. (B) Survival curves displaying data of the 25°C+ROT conditions from each group. (C) Survival curves displaying data of the 32°C conditions from each group. (D) Survival curve data of the 32°C +ROT conditions from each group. Group 1-25 are indicated in blue and group 25-50 are indicated in red. (N = 200). Lifespan survival curves were analysed using the log-rank Mantel Cox Test. $p < 0.05$ was taken as statistically significant and represented by *, $p < 0.01$ was represented by ** and $p < 0.001$ was represented by ***.

3.3 Discussion

In summary, I have been able to demonstrate that RET can be stimulated physiologically in the brain of the fly, using HS. Results displayed an increase in ROS production after 3 hours of HS, which was detected using both H₂DCF for cellular ROS and MitoSOX for mitochondrial superoxide. I confirmed ROS were produced via RET using rotenone and FCCP, established inhibitors of RET stimuli, which were both able to terminate RET. Additionally, the over-expression of antioxidants SOD2 and a mitochondrially-targeted Catalase indicated that ROS produced during HS originates from the mitochondria, in agreement with MitoSOX, providing further evidence of RET *in vivo*.

I observed that under HS, ROS production is dynamic and behaves as a transient signal, which is initiated at 3 hours and terminated after 5 hours. To characterise the site of ROS production, occurring during 3 and 4 hours of HS, I used rotenone and FCCP, which were both able to abolish the ROS signal, indicating ROS-RET. The use of rotenone as an inhibitor of RET has previously been shown in numerous studies. For example, during Ndi1 expression in *Drosophila*, both rotenone and FCCP were able to reduce the levels of ROS-RET (Scialo *et al.*, 2016a). Additionally, CI inhibition using rotenone was also able to decrease ROS-RET-induced injury during IR (Chouchani *et al.*, 2014a). Thus further supporting the elevated ROS levels observed during HS, as being RET-induced. Interestingly, rotenone and FCCP both resulted in opposing effects when introduced in non-stressed conditions compared to HS. At 25°C, rotenone and FCCP both caused an increase in ROS, in contrast to the decrease in ROS under HS. The contrasting effects on ROS production, using rotenone and FCCP, dependent on the direction of CI activity, i.e. forward or reverse electron transport, provided a reliable and reproducible method of identifying the presence of ROS-RET.

The characteristic features of this ROS signal make it distinctive from other sources of ROS production. The data showed that HS-induced-ROS, is site-specific at CI, resulting from the process of reverse electron transport, which is triggered under specific circumstances i.e. highly reduced CoQ and high membrane potential. In addition, the signal was shown to be transient, as ROS production was terminated 2 hours after initiation. This evidence suggests that under stress, such as HS, mitochondria respond by altering metabolic activity to establish both a high

CoQH₂:CoQ ratio and a pmf, promoting CI to switch to a reverse direction and stimulate a ROS-RET signal. This ROS can then diffuse through the cell, interacting with target proteins and stimulating downstream survival pathways, to counteract the stress condition. After 2 hours of ROS-RET the signal is switched off causing ROS to return back to basal levels. The restoration of ROS levels after this period of time under HS could be caused by the reestablishment of cellular homeostasis, therefore leading to the ROS-RET signal being switched off. Here, ROS-RET may stimulate beneficial processes such as proteostasis and autophagy, which would ultimately remove any damage caused by HS, allowing the return of normal cellular function. Under such circumstances the ROS-RET signal would no longer be required and therefore would be switched off, leading to the reduction of ROS back down to basal levels. This process describes a highly controlled system, where site-specific ROS is produced through a distinct process and removed after a certain period of time, in order to prevent over-oxidation of cellular components, which would lead to damage.

The age-dependent decline in CI activity has been reported in multiple animal models (Tatarkova *et al.*, 2016), more specifically in *Drosophila* (Scialo *et al.*, 2016a). Given that RET is dependent on the uninterrupted activity of CI, which my results demonstrate in the following chapter, I wanted to confirm whether CI depletion in older adult flies, would affect the stimulation of ROS-RET. My data indicated that between 25 and 50 days CI levels are altered, leading to a change in how ROS are produced. In early adulthood of flies, HS triggered a ROS-RET response, which was abolished upon the addition of rotenone. However, under the same experimental techniques, the 50-day-old flies showed no significant changes in ROS levels, under HS or in the presence of rotenone. These results clearly showed that RET was not being stimulated by HS in the 50-day-old flies, as no increase in ROS was observed in 32°C and rotenone was not able to decrease ROS production. Due to similar ROS levels being observed in non-stressed conditions and HS, this indicated that ROS was being produced either in the forward direction or unspecifically elsewhere. Interestingly, rotenone had no effect on ROS production either. In previous results of this chapter, I was able to show that rotenone has contrasting effects on ROS production, depending on the activity of either forward or reverse electron transport. In early life during forward electron transport rotenone was able to elevate ROS levels, therefore, based on these results an increase in ROS would have been expected, upon the addition of rotenone if forward electron

transport was occurring. This indicates that ROS levels are already elevated due to CI depletion in later life, which causes an increase in ROS through the same mechanisms as CI inhibition, via rotenone. The elevated ROS levels in the 50-day-old flies, compared to early adulthood flies, support this suggestion.

To study the downstream consequences of a physiological ROS-RET signal triggered during HS, I designed a lifespan experiment to observe the effects of intermittent HS-derived-RET and if it could elicit beneficial effects on lifespan, reflecting the Ndi1-RET model (Scialo *et al.*, 2016a). The results from the lifespan experiments established that HS could not extend longevity, using the selected periods of time. Firstly, this could be due to the fact that the Ndi1 model is stimulating RET constantly within the fly, leading to a dramatic increase in ROS. Therefore in the HS lifespan study, the stimulation of RET for 4 hours, 3 times a week may not have been enough to produce the beneficial effect on longevity, observed in the Ndi1 expressing flies. Alternatively, previous lifespan studies carried out in *Drosophila* have described a small window of opportunity in early adulthood, in which manipulating mitochondrial function, can lead to lifespan extension (Rana *et al.*, 2017). Therefore, it is possible that different time points may be more effective at achieving an increase in lifespan through HS-derived-RET e.g. development (when Ndi1 is active). The lifespan results obtained, suggest that after 25 days there is an age-related decline in CI activity, which prevents the stimulation of ROS-RET. In which case, future studies should take this into consideration when selecting alternative time periods. Despite not observing an increase in lifespan, the results from these experiments supported the age-dependent change in ROS production. Here, the flies subjected to HS in early life (1-25), showed no change in lifespan, compared to controls in non-stressed conditions. Whereas both groups in later life (intermittent HS and 25-50), exhibited decreased longevity, when subjected to both HS and rotenone feeding. Previous results of this chapter revealed a change in the ability of CI to switch from a forward to a reverse direction between 25 and 50 days in *Drosophila*. This suggests that the two later-life groups exposed simultaneously to both rotenone and HS, were unable to trigger ROS-RET to counteract the stress conditions, thereby leading to an accumulation of damage, detrimental to the flies. In contrast to the early life group (1-25), which could stimulate adaption responses through ROS-RET, to protect mitochondrial function and maintain longevity. In regards to the lifespan results it is also important to consider differences that occur to

feeding rates during ageing. As flies age they tend to eat less food, which could therefore impact how much drug the flies are consuming for the two groups fed rotenone. However due to the fact that in both groups (intermittent HS and 25-50) where rotenone is fed to the flies in later life a decrease in lifespan is observed when flies are subjected to both HS and rotenone, this suggests that the flies are eating the drug food in later life. Age related changes to mitochondrial density and function would also likely cause a change to ROS production. Here, the increase in dysfunctional mitochondria and mutations could have an effect on the ability of CI to produce ROS-RET, as previously discussed.

Finally, I have shown that the ROS changes occurring during HS can be measured using both H₂DCF and MitoSOX. Due to previous studies suggesting H₂O₂ as the primary source of ROS produced during RET, I chose to use H₂DCF to study ROS in the following chapters.

In conclusion, the results from this chapter have provided me with a method of stimulating ROS-RET physiologically in the fly brain, using HS. I can now take advantage of this system to gain a deeper understanding of the mechanisms behind RET i.e. factors essential for its stimulation or modulation. Additionally, I was able to show that the progressive age-related loss of CI can prevent ROS-RET from occurring, which can affect stress adaptations in later life.

Chapter 4 Effect of limiting the entry of electrons into the mitochondrial ETC on ROS-RET.

4.1 Manipulating the Redox State of CoQ

A highly reduced CoQ pool is essential for triggering RET (Robb *et al.*, 2018). The discovery of RET occurred when *Chance* and *Hollunger* observed that feeding the ETC with succinate, (a CII substrate), lead to the production of NADH from NAD⁺ and a rise in ROS generation (Chance and Hollunger, 1961). We now know that RET was achieved as a result of high concentrations of succinate feeding the mitochondrial ETC, causing the CoQ pool to become extremely reduced.

There are multiple different routes in which electrons can enter the ETC and contribute to the reduction of CoQ. One of the major sources being via CI, where soluble NADH, produced through the oxidation of sugars, proteins and fats, is oxidised to NAD⁺. This process donates two electrons that are transferred down the ETC to generate energy (Zhao *et al.*, 2019). Equally important is CII, which oxidises succinate into fumarate via a prosthetic FAD and transfers the electrons directly to CoQ (Sousa *et al.*, 2018). In fact, increased oxidation of succinate, by CII, is responsible for triggering ROS-RET during IR (Chouchani *et al.*, 2014a). Although CI and CII are considered the main entry points for electrons, there are other dehydrogenases that also introduce electrons downstream of CI and CII. For example, G3PDH, which oxidises G3P, through the reduction of FAD into FADH₂ and then carries the electrons to ubiquinone (Mracek *et al.*, 2013). The ETF-QO also contributes to the reduction of the ubiquinone pool, by directly passing electrons to Co-Q from another mitochondrial matrix flavoprotein (Chokchaiwong *et al.*, 2019). Lastly, the enzyme DHODH transfers electrons to the CoQ pool, acquired from catalysing the mitochondrial oxidation step in pyrimidine biosynthesis (Singh *et al.*, 2017).

All electrons entering the ETC, via these different pathways, pass through CoQ, thus making CoQ a central component of the ETC. For this reason the redox state of CoQ allows the rest of the cell to sense the metabolic activity of the mitochondria. For example, if the flow of electrons has been interrupted, the CoQ will be over-reduced, or if there are not enough electrons in the ETC, CoQ will be highly oxidised. Therefore it is possible that the CoQ is part of a system, which allows the sensing of

mitochondrial state to be coupled with the generation of a signal that can activate changes to fine-tune mitochondrial respiration and metabolism. When mutations arise in any of the 10 genes encoding the synthesis and assembly of CoQ, it causes chronic dysfunction that phenocopies mitochondrial disease (Bentinger *et al.*, 2010). Additionally, mitochondrial diseases caused by mutations in genes not involved in the assembly or structure of CoQ can also cause depletion in CoQ levels (Yubero *et al.*, 2016). This highlights the importance of CoQ and its potential role in promoting RET.

In Chapter 3, I was able to confirm that RET occurs under physiological conditions after exposing flies to HS. This provided a physiological model, in which I could take advantage of, to further understand the mechanisms that trigger RET. Using a hypothesis-driven approach to identify components involved in the generation of RET, I decided to manipulate the five respiratory complexes of the mitochondrial ETC. First of all, I decided to study how preventing the entry of electrons into the ETC and therefore the reduction of CoQ, would affect the generation of a ROS-RET signal. To achieve this, I used both chemical and genetic inhibition of CI and CII in order to test the effects of short term and long term inhibition, respectively. It was important to use both short and long term to provide two models of inhibition. Firstly, short term inhibition, allows me to observe the acute effects after 4 hours of blocking the respiratory complexes. Secondly, long term genetic inhibition, allows the observation of adaptations including changes in the expression of transcripts and proteins occurring over long periods of inhibition.

Here I predicted that blocking the entry of electrons into the ETC, via inhibition of CI and CII, would prevent the occurrence of a highly reduced CoQ pool and therefore inhibit the stimulation of RET.

In order to achieve a more comprehensive vision of how manipulation of CI and CII activity affects ROS signalling, I decided to perform experiments under conditions where electrons flow through CI in the forward direction, (25°C), and conditions where electrons also flow in a reverse direction, (after exposure to 32°C for 4 hours, see Chapter 3 for details).

4.2 Reduction of CI activity

CI, the largest of the respiratory chain complexes, occupies an L-shaped structure, which consists of a long hydrophobic arm embedded into the IMM and a hydrophilic arm that protrudes into the mitochondrial matrix (Zhu *et al.*, 2016). As previously shown in Chapter 3, the CI inhibitor, rotenone, was able to increase ROS production in non-stressed conditions. However under a stress condition (HS), rotenone decreased ROS production. This indicated that during HS, CI can switch to produce ROS via RET, which was validated using the membrane potential dissipater, FCCP. After testing chemical inhibition using rotenone, I wanted to genetically inhibit CI to observe the effect of reducing the levels of CI, the primary site of ROS-RET generation. Therefore, I tested two genetic knockdown models of the CI subunits, *ND-75* and *ND-42*.

The core subunit *ND-75* (*NDUFS1*) resides in the hydrophilic region of CI. Here it participates in electron transfer between the flavin, where NADH is oxidised, to the CoQ pool (Brandt, 2006) (Figure 4.1). Thus I anticipated that silencing *ND-75* would stop the movement of electrons through CI and decrease the amount of electrons contributing to the reduction of CoQ. Previous papers using the same CI subunit had reported a clear KD (Garcia *et al.*, 2017a).

In addition, I studied an accessory subunit of CI; *ND-42* (*NDUFA10*) found in the hydrophobic region of CI (Stroud *et al.*, 2016) (Figure 4.1). Although its role within CI is unclear, *ND-42* seems instrumental for the reduction of ubiquinone. The KD of *ND-42* has previously been shown to phenocopy mutations in *Pink1*. Conversely, when overexpressed, *ND-42* was able to partially rescue *Pink1* mutants, corresponding to results from the *Ndi1* fly model (Pogson *et al.*, 2014). These data suggest that alterations in mitochondrial morphology associated with *Pink1* and *ND-42* depletion, could be related to a defect in ROS signalling, caused by a loss of ROS-RET.

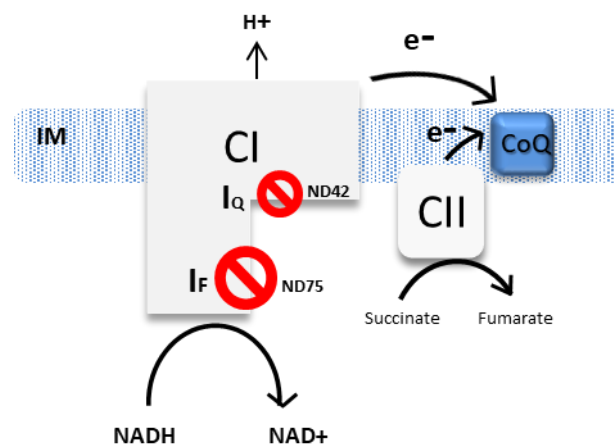


Figure 4.1 Schematic diagram indicating the RNAi constructs used to target CI subunits.

ND-75 is found in the hydrophilic arm, where transfer of electrons to CoQ occurs, therefore its knockdown prevents the entry of electrons into CI. ND-42 resides in the hydrophobic region, near to the CoQ binding site where electrons are passed to CoQ. Knockdown of both genes blocks the transfer of electrons to the CoQ pool, therefore inhibiting the formation of a high $\text{CoQH}_2:\text{CoQ}$ ratio.

4.3 A fully functional CI is required for ROS-RET.

I checked that the KD of *ND-75* effectively decreased CI function by measuring mitochondrial respiration in whole fly lysates. As expected, a significant decrease, specific to CI-linked respiration alone, was observed in *ND-75-KD* flies, (*DaGAL4>ND-75-KD*), when compared to wild type control flies, (*DAH>ND-75-KD*) (Figure 4.2A). This is in agreement with the phenotype observed after knocking down two different CI subunits, *ND-39* and *ND-19* (Sanz *et al.*, 2010b) (Scialo *et al.*, 2016b). Additionally, I performed qPCR to quantify the RNAi line (Figure 4.2B), which also confirmed the presence of CI KD. After confirming, that CI-linked respiration was specifically decreased, I then measured ROS levels in non-stressed conditions (25°C), where electrons flow through CI in the forward direction. At 25°C, no significant difference was observed between the KD flies and their respective control flies (Figure 4.2B). I then transferred the flies into HS to test whether reduction in CI-linked respiration altered the stimulation of ROS-RET. As shown previously, a clear increase in ROS levels was observed in control flies exposed at 32°C, when compared to the control flies at 25°C. Interestingly, this increase was not observed in *ND-75-KD* flies at 32°C, indicating that a fully functioning CI is required for ROS produced via RET (Figure 4.2C).

The efficiency of the RNAi against *ND-42* to deplete CI was again confirmed by measuring mitochondrial respiration. As observed when *ND-75* subunit was KD, there was a significant decrease in CI-linked respiration in the *ND-42-KD* flies, (*DaGAL4>ND-42-KD*), compared to the control flies, (*DAH>ND-42-KD*) (Figure 4.3A). The decrease in respiration observed was similar in both CI subunits. As in the case of *ND-75-KD*, no effect in CIII-linked or CIV-linked respiration backflow in the mutant flies. However due to the experiments being performed separately it cannot be determined how strong the decrease in CI activity is when comparing the two subunits. The health of the flies does suggest that the expression of the *ND-75-KD* flies was stronger than the *ND-42-KD* flies, as they were weaker than the latter.

Ex-vivo ROS measurements at 25°C showed no difference in ROS production associated with the KD of *ND-42* (Figure 4.3B). However, under HS, we observed that mutant flies were not able to up-regulate ROS levels, as observed in the controls (Figure 4.3C). In summary, I have shown that genetic depletion of two CI subunits, which reduce mitochondrial respiration, prevent the triggering of ROS-RET in

physiological, together with the results obtained using rotenone to chemically block CI, demonstrates that CI is required for ROS-RET.

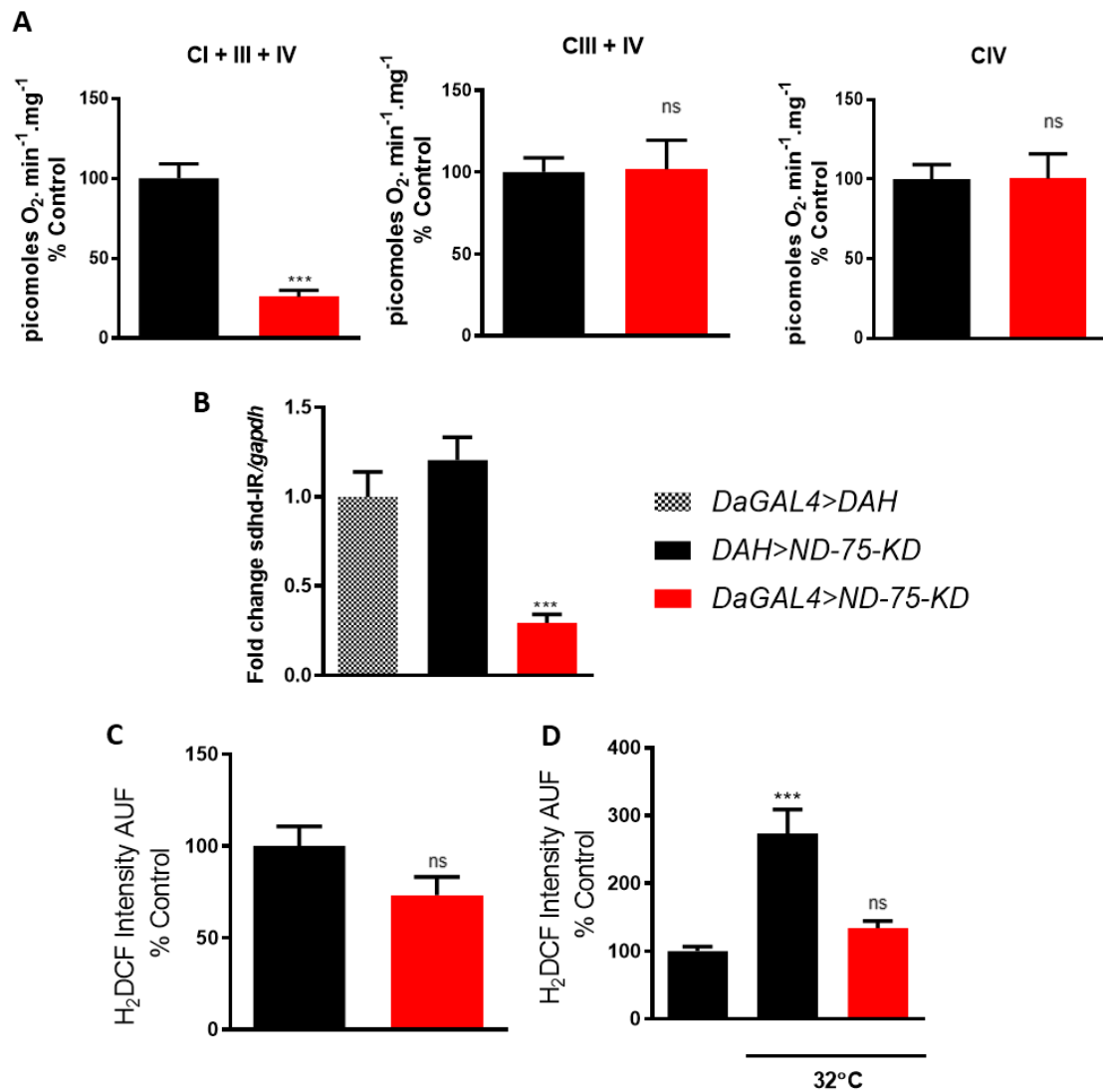


Figure 4.2 Effect of *ND-75-KD* on ROS production in non-stressed conditions and during heat stress.

(A) Mitochondrial respiration using CI-linked, CIII-linked and CIV-linked substrates in *ND-75-KD* whole fly homogenates, (*DaGAL4>ND-75-KD*), compared to the respective controls, (*DAH>ND-75-KD*) (N = 7). **(B)** Quantification of mRNA levels in *ND-75-KD* flies by qPCR. Control flies (*DaGAL4>DAH* and *DAH>ND-75-KD*) and KD flies (*DaGAL4>ND-75-KD*) were used (N = 3). **(C)** Quantification of ROS levels in fly brains in controls and *ND-75-KD* fly brains in non-stressed conditions (25°C) (N = >6). **(D)** Quantification of ROS levels in fly brains in controls and *ND-75-KD* fly brains subjected to HS (32°C) (N = 7). Flies were approximately 3 days old. P Values were calculated using unpaired Student's T-test and One-Way ANOVA, where appropriate. Data are shown as mean ± SEM. p < 0.05 was taken as statistically significant and represented by *, p<0.01 was represented by ** and p<0.001 was represented by ***.

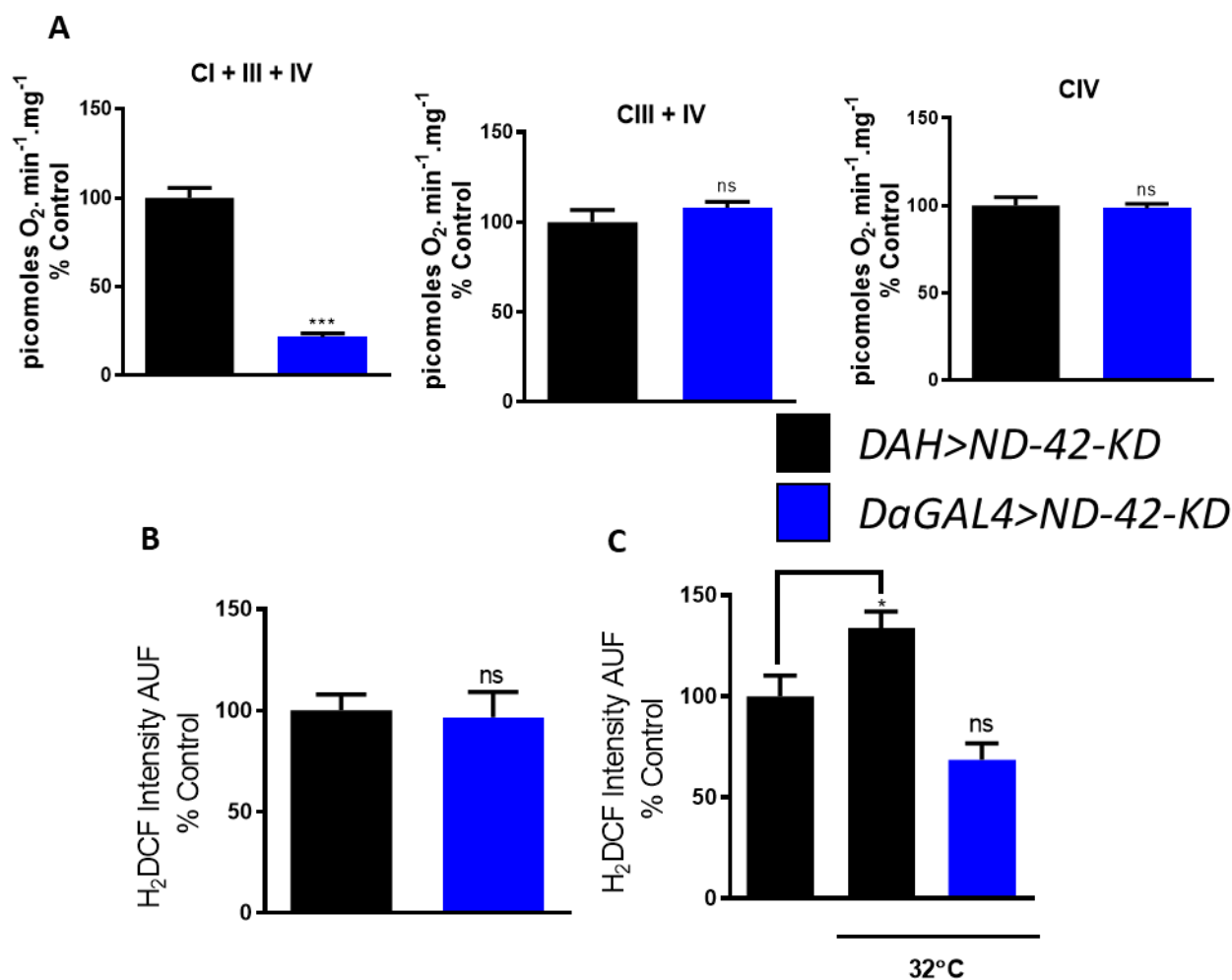


Figure 4.3 Effect of *ND-42-KD* on ROS production in non-stressed conditions and during heat stress.

(A) Mitochondrial respiration using CI-linked, CIII-linked and CIV-linked substrates in *ND-42-KD* flies whole fly homogenates, (*DaGAL4>ND-42-KD*), compared to the respective controls, (*DAH>ND-42-KD*) (N = 7). **(B)** Quantification of ROS levels in fly brains in controls and *ND-42-KD* fly brains in non-stressed conditions (25°C) (N = >7). **(C)** Quantification of ROS levels in fly brains in controls and *ND-42-KD* fly brains subjected to HS (32°C) (N = 7). Flies were approximately 10 days old. P Values were calculated using unpaired Student's T-test and One-Way ANOVA, where appropriate. Data are shown as mean \pm SEM. $p < 0.05$ was taken as statistically significant and represented by *, $p < 0.01$ was represented by ** and $p < 0.001$ was represented by ***.

4.4 Reduction of CII activity

CII is by far the simplest component of the ETC and is anchored into the IMM by the two smaller subunits. It consists of only 4 assembled subunits including SdhA and SdhB found in the soluble domain, which catalyses succinate oxidation, as well as SdhC and SdhD, which constitute the membrane-bound domain, responsible for transferring electrons to the ubiquinone pool (Rutter *et al.*, 2010). To study how decreasing entry of electrons through CII affects ROS signalling, I inhibited CII using malonate, to block the entry of electrons into the complex and expressed an RNAi construct against the SdhD subunit, to prevent the binding of CoQ.

Malonate is a well-established competitive inhibitor of CII. It reversibly binds to the active site, which resides in the SdhA subunit of the complex, therefore competing with the CII substrate, succinate (Kim, 2002) (Figure 4.4). Here it was predicted that by using malonate to inhibit the oxidation of succinate, the transfer of electrons to the CoQ pool would be decreased, avoiding the reduction of CoQ and therefore preventing ROS-RET. Dimethyl-malonate was used instead of malonate to facilitate the entry of the inhibitor into the cells and subsequently into the mitochondria.

Since malonate achieves inhibition of the SdhA subunit, found in the hydrophilic region of CII, I wanted to genetically target the membrane-bound region. For this reason, I chose to use an RNAi to knock down the *SdhD* subunit (Figure 4.4). This subunit participates in the direct reduction of the CoQ pool (Hagerhall, 1997). Therefore I anticipated that the disruption of electron transfer to ubiquinone, through knocking down *SdhD*, would prevent the stimulation of RET.

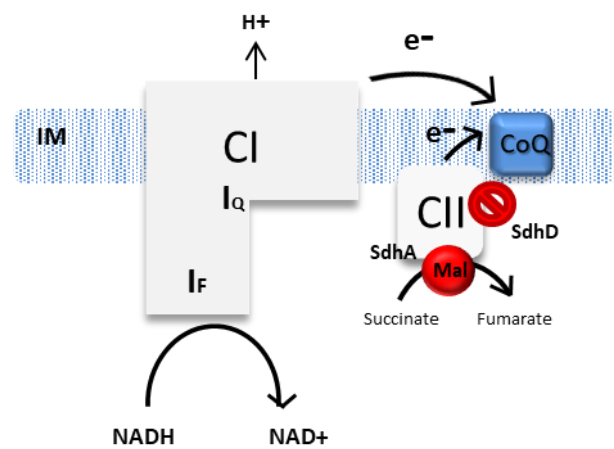


Figure 4.4 Schematic diagram showing the methods of CII inhibition used.

Malonate targets the catalytic region of CII found in the SdhA subunit, therefore preventing the entry of electrons into CII. RNAi construct of *SdhD* was used, which is normally involved in the direct transfer of electrons to the CoQ pool.

4.5 CII is required for triggering ROS-RET.

Mitochondrial respiration was measured to test whether malonate is able to reach the brain and inhibit CI-linked respiration, after 4 hours of feeding. Succinate, a CII substrate and citric acid cycle intermediate, has a very low permeability across the mitochondrial inner membrane in *Drosophila melanogaster* and other insects (Miwa *et al.*, 2003) (Sanz *et al.*, 2010c). For this reason, CII-linked respiration was not measured using this technique. Mitochondrial respiration showed no significant change in CI-linked respiration. Mitochondrial CI-linked respiration was not altered after feeding flies with dimethyl-malonate for 4 hours (Figure 4.5A). These results show that any effect on ROS production is not caused by the interruption of electron flow through CI, however, it is not known whether CII is inhibited in the experimental condition assayed.

Under non-stressed conditions (25°C), dimethyl-malonate feeding had no effect on the ROS levels in the fly brain (Figure 4.5B). However, feeding with dimethyl-malonate prevented the increase in ROS that occurs after 4 hours of HS. These results suggest that CII is also required for the production of RET (Figure 4.5C).

To further confirm the requirement of CII for initiation of RET; I used an alternative approach depleting CII levels by expressing an RNAi construct against *SdhD*. Due to the lack of a reliable respirometry method to evaluate the efficiency of the KD, I validated the KD by qPCR. This experiment was done in collaboration with Dr Filippo Scialo. Figure 4.6A shows a significant decrease in the mRNA levels of *SdhD*. In addition, I measured mitochondrial respiration to check that CI-linked respiration was not affected by CII disruption. However, in contrast to the results gained using malonate, there was a decrease in CI-linked respiration in *SdhD-KD* flies, (*TubGS>SdhD-KD*), compared to control flies, (*TubGS>DAH*), whereas CIII and CIV linked respiration did not change (Figure 4.6B). This effect on CI activity could be due to the fact that CII is part of the Krebs cycle therefore inhibiting CII genetically may also inhibit CI indirectly by preventing the donation of electrons from NADH and other electron carriers.

I then measured ROS levels in the *SdhD-KD* flies to see their effect on the stimulation of RET during HS. In non-stressed conditions (25°C) there was no change in ROS levels (Figure 4.6C), reflecting the results obtained from

pharmacological inhibition using dimethyl-malonate or when CI-subunits were knocked-down. However, when *SdhD-KD* flies were subjected to HS for 4 hours, a significant decrease in ROS levels was observed compared to the control flies at 32°C (Figure 4.6D). The fact that CI-linked respiration was affected by depleting CII complicates the interpretation of the ROS data. Therefore is it not possible to discard the fact that suppression of ROS-RET is potentially caused by alterations in CI.

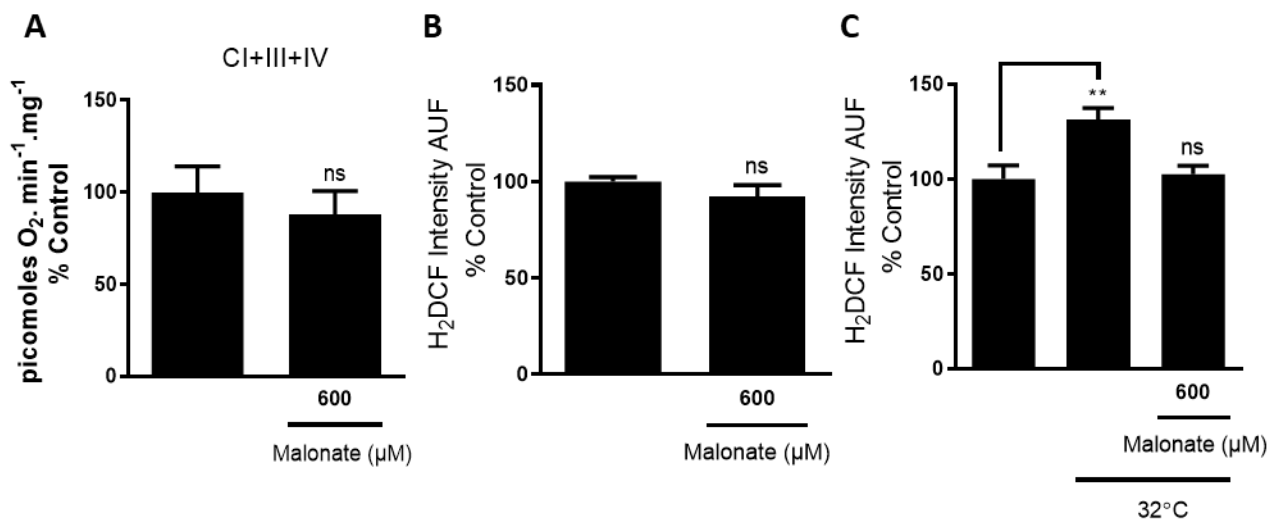


Figure 4.5 Effect of malonate on ROS production in non-stressed conditions and during heat stress.

(A) Mitochondrial respiration of fly head mitochondria fed 600 μM of dimethylmalonate (N = 5). **(B)** ROS measurements of brains in flies fed 600 μM of dimethyl-malonate, in non-stressed conditions (25°C) (N = 7). **(C)** ROS measurements of brains in flies fed 600 μM of dimethyl-malonate subjected to HS (32°C) (N = 8). Flies were approximately 3 days old. P Values were calculated using unpaired Student's T-test and One-Way ANOVA, where appropriate. Data are shown as mean \pm SEM. $p < 0.05$ was taken as statistically significant and represented by *, $p < 0.01$ was represented by ** and $p < 0.001$ was represented by ***.

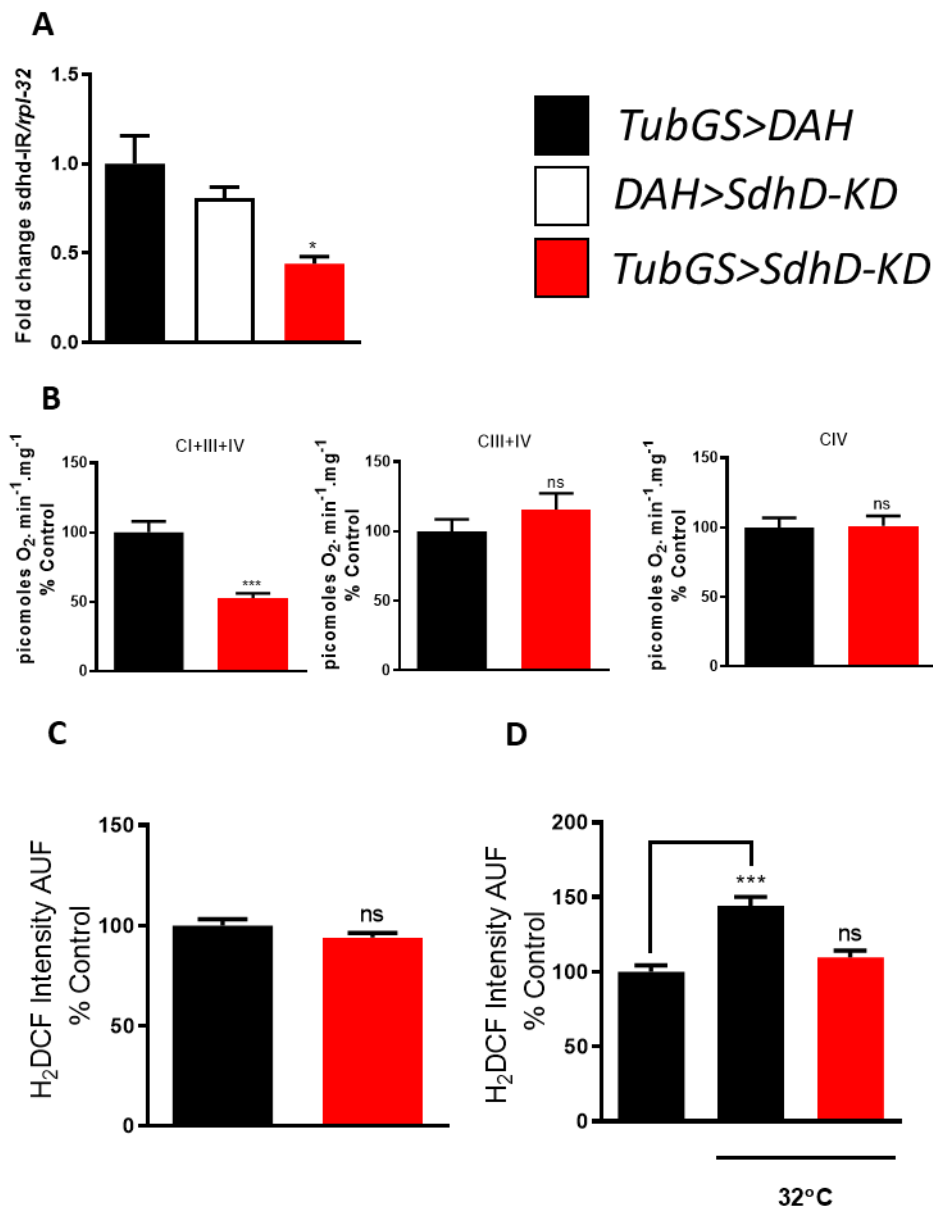


Figure 4.6 Effect of *SdhD-KD* on ROS production in non-stressed conditions and during heat stress.

(A) Quantification of mRNA levels in *SdhD-KD* flies by qPCR. Control flies (*TubGS>DAH* and *DAH>SdhD-KD*) and KD flies (*TubGS>SdhD-KD*) were used (N = 3). **(B)** Mitochondrial respiration of *SdhD-KD* fly whole fly homogenates showing CI-linked, CIII-linked and CIV-linked respiration as indicated (N = 7). **(C)** ROS measurements of *SdhD-KD* in non-stressed conditions (25 °C) (N = >7). **(D)** ROS measurements of *SdhD-KD* flies in heat stress (32°C) (N = >7). Flies were approximately 10 days old. P Values were calculated using unpaired Student's T-test and One-Way ANOVA, where appropriate. Data are shown as mean ± SEM. p < 0.05 was taken as statistically significant and represented by *, p<0.01 was represent by ** and p<0.001 was represented by ***.

4.6 Discussion

The results from this chapter show that limiting the entry of electrons into the ETC, via CI and CII inhibition, prevents the occurrence of RET. Thus confirming that CI and CII activity are both essential for the stimulation of physiological ROS-RET. Additionally, I was able to demonstrate that both short term and long term inhibition of CI and CII, using chemical inhibition and genetic silencing respectively, were sufficiently able to prevent the initiation of RET, during HS.

As previously established in Chapter 3, short term chemical inhibition of CI using rotenone was able to inhibit RET from occurring, by preventing the backflow of electrons from the CoQ pool to CI. To further confirm this, I manipulated the expression of two CI subunits, *ND-75* and *ND-42*, by genetically silencing them to achieve long term CI inhibition. Both models exhibited the same effect on ROS-RET as rotenone, where the burst in ROS production during HS-induced-RET was abolished. This provides strong evidence that active CI is necessary for RET. An interesting observation occurred when *ND-42-KD* flies in HS revealed an even further decrease in ROS levels, compared to the control flies in non-stressed conditions. This could be due to a reduction of CI assembly, which would lead to an overall decrease in ROS being generated at CI. The same decrease may not have been observed in the *ND-75-KD* flies due to a difference in the levels of RNAi expression between the two subunits. However, this would have to be tested using Blue Native Electrophoresis (BNE) to study the levels of CI in each model. In this case we would expect to observe even lower levels of CI in *ND-42-KD* flies in comparison to *ND-75-KD* flies, resulting in the decrease in ROS.

When CII was inhibited, using either chemical inhibition with dimethyl-malonate or genetic reduction using an *SdhD-KD* fly model, the stimulation of RET during HS was prevented. Mitochondrial respiration of *SdhD-KD* flies revealed a decrease in oxygen consumption specific to CI-linked respiration, which was not reflected in the dimethyl-malonate fed flies. This is possibly due to the fact that CII, otherwise known as SDH, also plays a role in the CAC, which delivers electrons to the ETC. Hence, the long-term and stronger inhibition of SDH by genetic depletion would most likely lead to a reduction in electron supply at CI, thus responsible for the decrease in respiration. This decrease was not observed in CIII respiration due to the substrate G3P being used, which introduces electrons directly to the CoQ pool via the enzyme G3PDH.

Electrons are then transferred directly to CIII, from CoQ, therefore bypassing CI. This effect was not observed when using chemical inhibition. This may be due to that fact that malonate feeding provided us with short-term inhibition of CII. Therefore, the effect after 4 hours may not have been enough to disrupt electron supply, from the Krebs cycle to CI. Unlike the long-term inhibition represented by the *SdhD-KD* flies, therefore resulting in decreased CI-linked respiration. An alternative explanation is that an increase in CII levels can affect the assembly of CI into supercomplexes, which has been shown in *C.elegans* and human cells (Guaras *et al.*, 2016). Under these circumstances, degradation of CI from the supercomplexes would occur through long term chronic inhibition. Therefore allowing adaptations and changes to expression of transcripts and proteins, including posttranslational modification, which would not be possible under short-term inhibition, using malonate. Despite the fact that I was not able to confirm the inhibition of CII in the mitochondria of fly heads after 4 hours of malonate feeding, I was able to show that malonate elicits the same effect on ROS production as the *SdhD-KD* flies, indicating CII inhibition. Additionally, although there is the possibility that RET was prevented via CI inhibition in the *SdhD-KD* flies, malonate prevented RET without altering activity of CI respiration, suggesting that the genetic depletion of CII reduces RET through the same mechanism as malonate.

In conclusion, these results show that CI and CII inhibition suppresses RET. This has been supported previously by numerous studies. For example, in flies expressing *Ndi1*, depletion of CI activity was shown to prevent the occurrence of ROS-RET (Scialo *et al.*, 2016a). Another study showed that in *Ndufs2-null* mice the arterial chemoreceptors lost their ability to sense oxygen levels and stimulate a hypoxia response due to the suppression of RET (Fernandez-Aguera *et al.*, 2015). In addition, the inhibition of CI has been shown to prevent succinate driven RET during IR, providing protection against IR injury (Chouchani *et al.*, 2014a). Collectively, my results and those of previous studies show the necessity of both CI and CII activity to supply electrons to the CoQ pool, thus forming a high CoQH₂:CoQ ratio and the subsequent stimulation of RET.

Chapter 5 Effect of limiting the exit of electrons from the mitochondrial ETC on ROS-RET

5.1 Halting the exit of electrons

The stimulation of RET relies primarily on the flow of electrons, determining the redox state of the CoQ pool and the transport of protons across the inner mitochondrial membrane, to achieve a highly reduced CoQ pool and establish a high proton motive force, respectively (Scialo *et al.*, 2017). At present, it is unknown how CoQ becomes highly reduced or how a high pmf is accomplished and sustained to trigger RET, in physiological conditions. Since the individual complexes, that constitute the ETC, orchestrate the movement of electrons and protons, it is reasonable to postulate that the manipulation of these complexes may produce the conditions favourable for RET.

In Chapter 4, I demonstrated that RET requires free circulation of electrons through CI and CII to occur and that inhibiting these complexes prevents RET. Blocking the exit of electrons through the inhibition of either CIII or CIV should increase the reduction state of CoQ. However, it is unclear how the pmf will be affected under these conditions *in vivo*, as both CIII and CIV are involved in the translocation of protons across the IMM. Thus, inhibition of the complexes would block proton pumping. If upon CIII and CIV inhibition, CV starts to work in a reverse direction, by transporting protons from the matrix to the IMS, the pmf will be maintained and ROS-RET may be triggered. However, if CV does not work in reverse or the binding of ATP Inhibitory Factor 1 (ATPIF1) to CV occurs, preventing CV from working in the reverse direction, then a high pmf will not be established and ROS-RET will not be stimulated.

Different studies in isolated mitochondria and cells show that blocking respiratory CIII and CIV boosts mitochondrial ROS levels (Taylor and Moncada, 2010) (Rajendran *et al.*, 2019). However, it is unclear whether this increase in ROS is produced at CI via RET, or by other sites within the ETC, such as CIII. The effect of inhibiting CIV on ROS production is particularly relevant since three different signalling molecules have been reported to inhibit CIV in physiological conditions, namely CO (Zuckerbraun *et al.*, 2007), NO (Beltran *et al.*, 2002) and H₂S (Sun *et al.*, 2012). In addition, mutations in several CIV subunits, that affect the assembly and function of the complex, have been described in mitochondrial patients (DiMauro *et al.*, 2012).

Therefore is it essential to understand whether blocking CIII and CIV increases ROS *in vivo* and if so where and how these ROS are generated.

5.2 Maintaining a High Proton Motive Force

RET is extremely sensitive to decreases in membrane potential, which constitutes one component needed to generate a pmf (Robb *et al.*, 2018). Therefore it was important to address the question of how a high pmf is maintained during RET. *In vitro*, inhibiting CV with oligomycin slows down electron transfer, resulting in the reduction of CoQ. Oligomycin also maintains a high pmf by preventing the re-entry of protons from the matrix, therefore establishing the two conditions that are needed to trigger ROS-RET. Additionally, several publications have reported an increase in ROS production upon the addition of oligomycin in isolated mitochondria or cells in culture, including *Drosophila S2* cells (Liu and Schubert, 2009) (Fukuoh *et al.*, 2014) (Zhou *et al.*, 2018).

Furthermore, physiological inhibition of CV activity has also been reported to increase ROS levels. For example, in macrophages exposed to LPS, glycolysis is increased to compensate for the reduction in mitochondrial ATP production. Under these circumstances, mitochondria produced ROS via RET, resulting from an increase in succinate oxidation and inhibition of ATP synthase (CV), that increased membrane potential (Mills *et al.*, 2016b). Similarly, blocking CV with oligomycin, or knocking-down CV subunits, in *Drosophila S2* cells increased ROS production (Fukuoh *et al.*, 2014). Thus these data suggest that the inhibition of CV can achieve a high CoQH₂:CoQ ratio, by slowing down respiration and also establish a high pmf to potentially stimulate ROS-RET. There are two prospective examples of how CV inhibition could be accomplished physiologically. The first is through a protein called ATP inhibitory factor 1 (ATPIF1). ATPIF1 has been shown to bind to CV during mitochondrial dysfunction, stopping CV from working in the reverse direction and therefore preventing ATP depletion (Chen *et al.*, 2014). It has also been reported that ATPIF1 is capable of binding to CV in normal conditions when overexpressed, therefore preventing the movement of protons into the matrix, leading to a high proton motive force (Garcia-Bermudez and Cuezva, 2016). Experimental data has shown that during binding of ATPIF1 to CV in normal conditions, there is an increase in ROS production, suggesting the stimulation of RET (Esparza-Molto *et al.*, 2017). The second mechanism proposed to inhibit CV physiologically is through alpha-ketoglutarate (2-oxoglutaric acid). A recent study showed that supplementation of

alpha-ketoglutarate was able to inhibit CV and extend lifespan by approximately 50% in *C.elegans*. In parallel with alpha-ketoglutarate administration was an increase in ROS production (Chin *et al.*, 2014a). Therefore it is possible that alpha-ketoglutarate is able to produce the conditions needed for the stimulation of RET resulting in the lifespan extension, also observed in the Ndi1 RET model (Scialo *et al.*, 2016a). In addition, the Alzheimer's candidate drug J147 has also been reported to inhibit CV. Alongside CV inhibition, J147 has also been shown to increase membrane potential and superoxide levels in human cells and extend lifespan in *Drosophila* (Goldberg *et al.*, 2018). This beneficial effect on longevity, seen in *Drosophila*, could be related to the mechanism by which Ndi1 extends lifespan.

Therefore, in this Chapter, I wanted to study the effect of manipulating the exit of electrons, from the ETC, in order to initiate RET. To do this, I inhibited CIII and CIV, to block the exit of electrons and CV, to slow-down electron exit and maintain a high pmf. In all three models, I used both chemical inhibition and genetic reduction of the complexes. I studied the effect of such experimental manipulations in non-stressed conditions to determine if RET could be initiated. ROS measurements were used to identify any increase in ROS production, characteristic of RET. Subsequently, rotenone was used to confirm if RET was the source of increased ROS, as in previous chapters I have shown that CI inhibition prevents RET from occurring. Additionally, I also checked the effect of CIII, CIV and CV inhibition under HS, which as I have demonstrated in Chapters 3 and 4 causes the stimulation of RET and the production of ROS, in physiological conditions.

5.3 Decreasing Complex III activity

Coenzyme Q: cytochrome c oxidoreductase, otherwise known as cytochrome bc₁ or Complex III (CIII), is the third respiratory enzyme in the ETC. It is responsible for transporting electrons from the CoQ pool to Cyt C, as well as pumping protons to the IMS, to contribute to the generation of the electrochemical proton gradient, required for ADP phosphorylation (Berry and Huang, 2011). CIII consists of two Q sites, which both possess roles in the Q cycle needed for the transportation of electrons and protons. The first is the Q_o site that resides near the outer face of the IM. The Q_o site oxidises ubiquinol and transfers half of the electrons to Cyt C as well as transporting four protons to the IMS. The second is the Q_i site, which is situated near the matrix side of the IM and is involved in reducing CoQ and taking protons from the matrix (Xia *et al.*, 2013). To inhibit CIII, I used myxothiazol to block the Q_o site and prevent the entry of electrons into CIII and I knocked-down *UQCR-Q*, (fly orthologue of the ubiquinol-cytochrome c reductase complex III subunit VII), to prevent the binding of CoQ to CIII.

The antibiotic, myxothiazol, produced by *Myxococcus fulvus* can bind to the Q_o site of CIII and therefore inhibit electron transfer from ubiquinol to the Rieske iron-sulfur protein (Thierbach and Reichenbach, 1981) (Figure 5.1). This specific inhibitor was chosen to stop the movement of electrons downstream of the CoQ pool. I hypothesised that by preventing the exit of electrons from the ETC, caused by the presence of myxothiazol, the CoQ pool will become highly reduced, allowing the stimulation of RET. The alternative CIII Q_i site inhibitor, antimycin A, was not chosen as I wanted to prevent the entry of electrons into CIII, which occurs at the Q_o site. Additionally, it has been reported that antimycin A dramatically increases ROS production at the Q_o site of CIII. Therefore this inhibitor would not have been suitable, considering I was initially interested in studying the production of ROS from CI, when CIII is inhibited.

UQRC-Q is a 9.5kDa core subunit within CIII responsible for the binding of ubiquinone (Barel *et al.*, 2008) (Figure 5.1). Therefore silencing of this gene allowed me to inhibit CIII, by preventing the transfer of electrons from CoQ. I anticipated that knocking down this gene would lead to the accumulation of a high CoQH₂:CoQ ratio, one of the conditions needed to trigger RET.

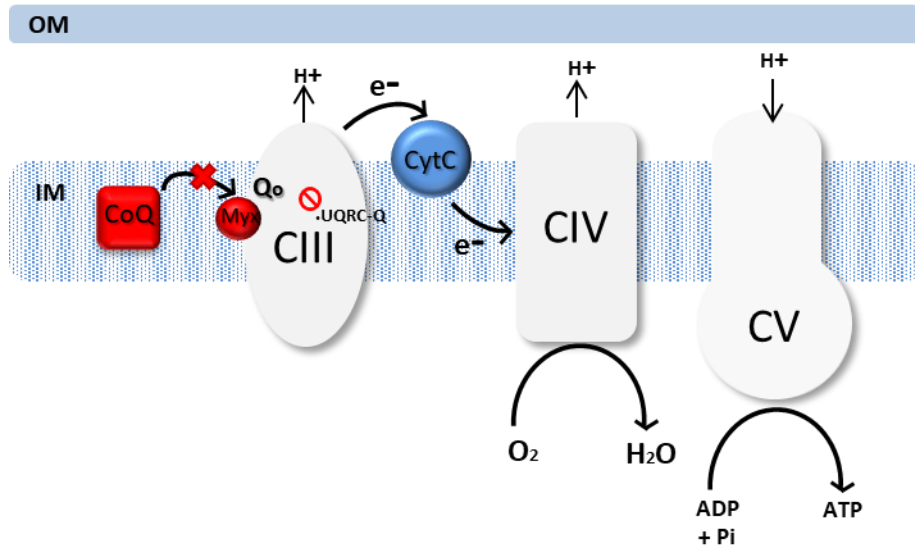


Figure 5.1 Schematic diagram indicating the binding site of myxothiazol and the RNAi construct used to target the CIII UQRC-Q subunit.

Myxothiazol binds to the Q_0 site of CIII, preventing the binding of ubiquinol and subsequently the transfer of electrons. UQRC-Q resides near the Q_0 site, and participates in CoQ binding. Both types of inhibition will inhibit the entry of electrons into CIII, therefore causing the accumulation of electrons upstream the ETC, resulting in a highly reduced CoQ pool.

5.4 The effect of decreasing CIII activity on ROS-RET signalling

5.4.1 The CIII inhibitor, myxothiazol, does not trigger ROS-RET in the brain of *Drosophila melanogaster*.

The first experiments I carried out were to confirm that myxothiazol can reach the brain of the flies and inhibit CIII, after 4 hours of feeding. To determine a suitable concentration of myxothiazol, I measured mitochondrial respiration using a range of different drug concentrations. I wanted to find a high enough concentration, with the potential to trigger ROS-RET by reducing the CoQ pool but minimising any potential damage. I tested 5 different concentrations spanning from 10 μM to 1 mM (Figure 5.2). Although reduced mitochondrial respiration was observed with all doses, statistical significance was only reached with doses $\geq 100 \mu\text{M}$. The highest doses reduced respiration between 62 to 92% (Figure 5.2C-E).

Next, I measured ROS in all 5 different concentrations of myxothiazol. No significant change in ROS was observed using 10 μM of myxothiazol; however flies fed with 50 μM displayed a decrease in ROS (Figure 5.3A). When exposed to HS, the control flies showed an increase in ROS levels in the brain, as expected. Flies fed with 10 or 50 μM of myxothiazol, under HS, also displayed increased ROS levels, however 50 μM was significantly lower than the control at 32°C (Figure 5.3B). The effect of 100 μM myxothiazol on ROS production led to a decrease, similarly to the lower dose of 50 μM at 25°C (Figure 5.3C). However, at 32°C, the same dose completely abolished the increase in ROS, with levels reflecting those of the control in non-stressed conditions (Figure 5.3D). This was an interesting observation since the dose that suppresses ROS-RET, does not induce ROS at 25°C, discarding the possibility that CI is inhibited and suggesting that the effect was caused by dissipating the pmf. Surprisingly, higher doses of myxothiazol $\geq 500 \mu\text{M}$, increased ROS both at 25 and 32°C (Figure 5.4A-B). If this increase in ROS levels was due to the stimulation of RET, I would have expected this to be attenuated with the addition of rotenone. However, ROS levels increased even further, when 1 mM myxothiazol and rotenone were added together in the fly food (Figure 5.4C). It is also important to discuss the fact that 100 μM and 500 μM of myxothiazol both display similar degrees of inhibition, when comparing the respiration data, despite their opposing effects on ROS production. Although this is observed it is difficult to interpret the levels of inhibition from these experiments alone, due to the fact that they were performed on separate occasions and using a different pool of flies. It would be interesting to explore this

further in the future and test both concentrations of myxothiazol in the same experiment to compare the respiration rates. Here, it is possible that we would observe even higher levels of inhibition using the higher dose of 500 μM compared to 100 μM , which could explain the opposing effects on ROS production.

With the present data, it is clear that CI is not producing ROS via RET, during CIII inhibition with myxothiazol. It is possible, however, that CI could be producing ROS in a forward direction encouraged by a high NADH/NAD⁺ ratio, occurring as a result of strongly inhibited respiration, achieved in presented circumstances. In addition, it is also possible that ROS are being produced at other sites of the ETC, for example CII (Quinlan *et al.*, 2012), alpha-ketoglutarate dehydrogenase (Mailloux *et al.*, 2016) or even non-mitochondrial sites such as cytosolic NADPH oxidases (Wong *et al.*, 2019).

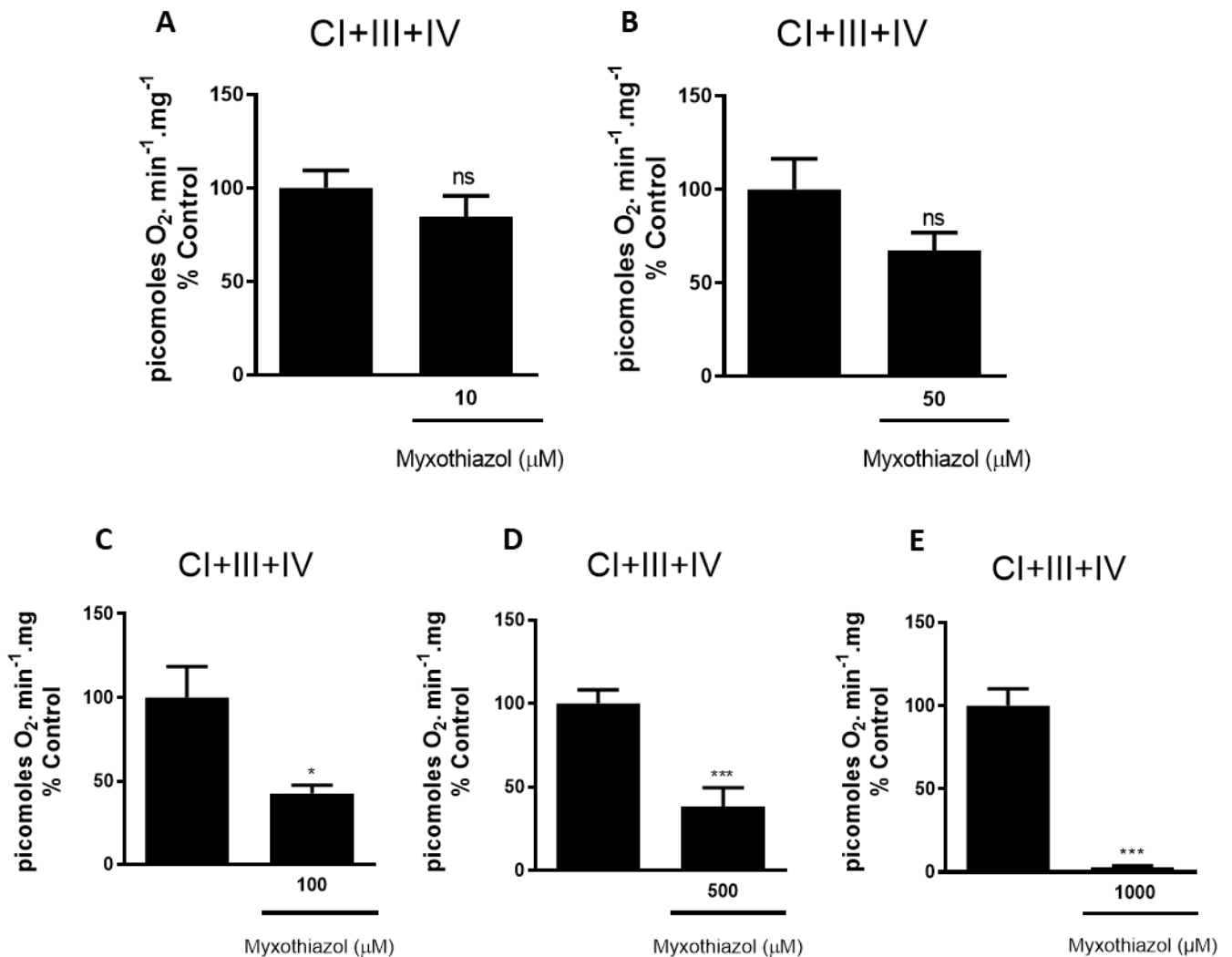


Figure 5.2 The effect of myxothiazol on respiration.

Mitochondrial respiration of fly head mitochondria after feeding flies with varied concentrations of myxothiazol using **(A)** 10 μM (N = 5), **(B)** 50 μM (N = 6), **(C)** 100 μM (N = 5), **(D)** 500 μM (N = 7) and **(E)** 1 mM (N = 5). Flies were approximately 3 days old. P Values were calculated using unpaired Student's T-test. Data are shown as mean \pm SEM. $p < 0.05$ was taken as statistically significant and represented by *, $p < 0.01$ was represent by ** and $p < 0.001$ was represented by ***.

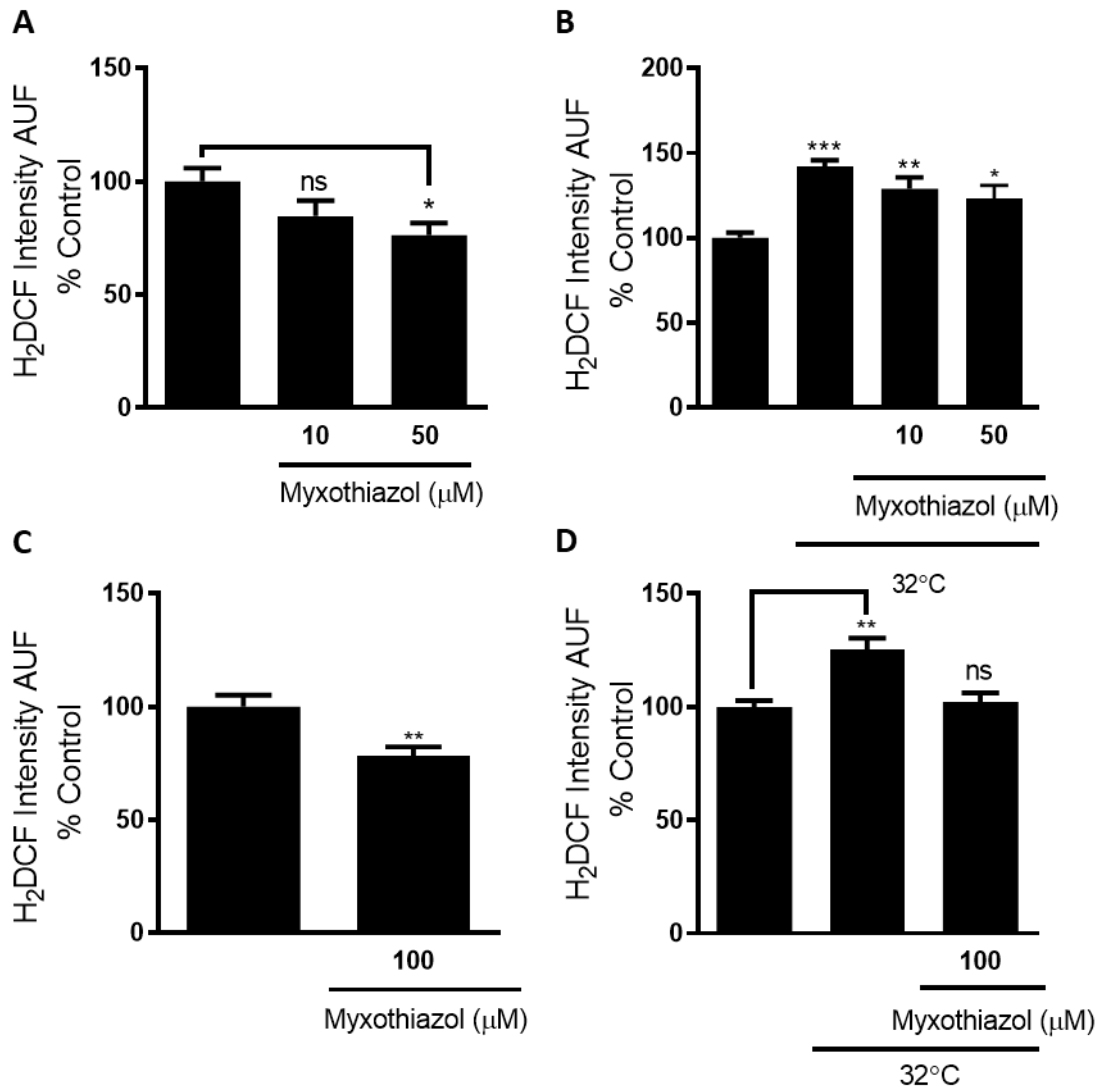


Figure 5.3 The effect of myxothiazol (10, 50, 100 μM) on ROS production in non-stressed conditions and during heat stress.

Quantification of *ex vivo* ROS measurements in fly brains fed 10-100 μM myxothiazol **(A)** 10 and 50 μM in non-stressed conditions (25°C) (N = >6), **(B)** 10 and 50 μM under HS (32°C) (N = 8), **(C)** 100 μM in non-stressed conditions (25°C) (N = >8) and **(D)** 100 μM under HS (32°C) (N = >5). Flies were approximately 3 days old. P Values were calculated using unpaired Student's T test and One-Way ANOVA, where appropriate. Data are shown as mean ± SEM. p < 0.05 was taken as statistically significant and represented by *, p < 0.01 was represented by ** and p < 0.001 was represented by ***.

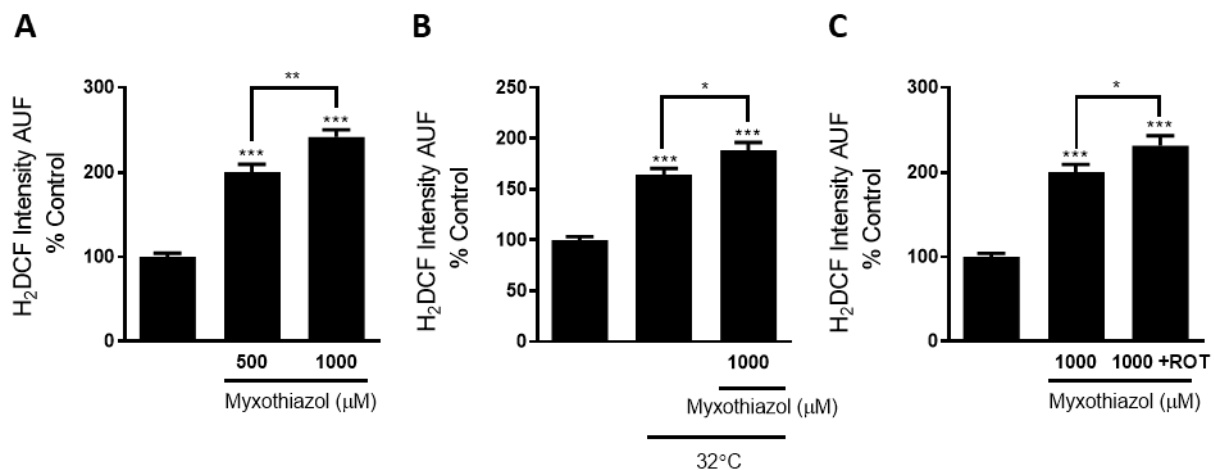


Figure 5.4 The effect of myxothiazol (500 μM, 1 mM) on ROS production in non-stressed conditions and during heat stress.

Quantification of *ex vivo* ROS measurements in fly brains of flies fed 500 μM – 1 mM of myxothiazol **(A)** 500 μM and 1 mM in non-stressed conditions (25°C) (N = >7), **(B)** 1 mM in HS (32°C) (N = >8) and **(C)** 1 mM in non-stressed conditions (25°C) also fed rotenone (600 μM) (N = >7). Flies were approximately 3 days old. P Values were calculated using One-Way ANOVA. Data are shown as mean ± SEM. p < 0.05 was taken as statistically significant and represented by *, p < 0.01 was represented by ** and p < 0.001 was represented by ***.

5.4.2 Genetic depletion of CIII does not stimulate ROS-RET

To understand whether the increase in ROS, observed by reducing electron transfer through CIII, was an acute effect or could also be observed during long-term CIII inhibition, I knocked-down the gene encoding for the CIII subunit, *UQRC-Q*. First, I confirmed the reduction in CIII-linked respiration by using high-resolution respirometry. As anticipated, CI and CIII linked respiration were reduced in the *UQRC-Q-KD* flies, (*TubGS>UQCRQ IR*), compared to the control group, (*TubGS>w1118*), whereas CIV-linked respiration was not affected (Figure 5.5A). This is in contrast with the results obtained when CI subunits were targeted (Figure 4.3A and 4.4A), where CIII linked and CIV linked respiration were not altered. However this is expected as blocking electron flow downstream of CI, leading to a decrease in CIII and CIV-linked respiration, will prevent the electrons reaching O₂ and will subsequently lead to a decrease in CI-linked respiration. This correlates with previous studies, which show that CIII dysfunction can reduce CI levels *in vitro*.

After validating the reduction of CIII activity, I carried out ROS measurements. In non-stressed conditions, there was a significant increase in the levels of ROS in the brain of *UQCR-Q-KD* flies, compared to the controls (Figure 5.5B). When flies were exposed to HS, both the control and *UQCR-Q-KD* flies at 32°C had increased ROS levels, compared to the control at 25°C. However, the ROS levels in the *UQCR-Q-KD* flies subjected to HS were slightly lower than those of the HS controls (Figure 5.5C). To determine if this increase in ROS in the *UQCR-Q-KD* flies was as a result of RET being stimulated, I fed the KD flies rotenone. However, ROS levels did not change in the presence of rotenone, indicating that ROS-RET was not occurring (Figure 5.5D). These results are in agreement with the results observed using doses of myxothiazol that inhibit mitochondrial respiration more than 60% (Figure 5.2C-E) and indicate that acute or chronic inhibition of CIII does not trigger ROS-RET.

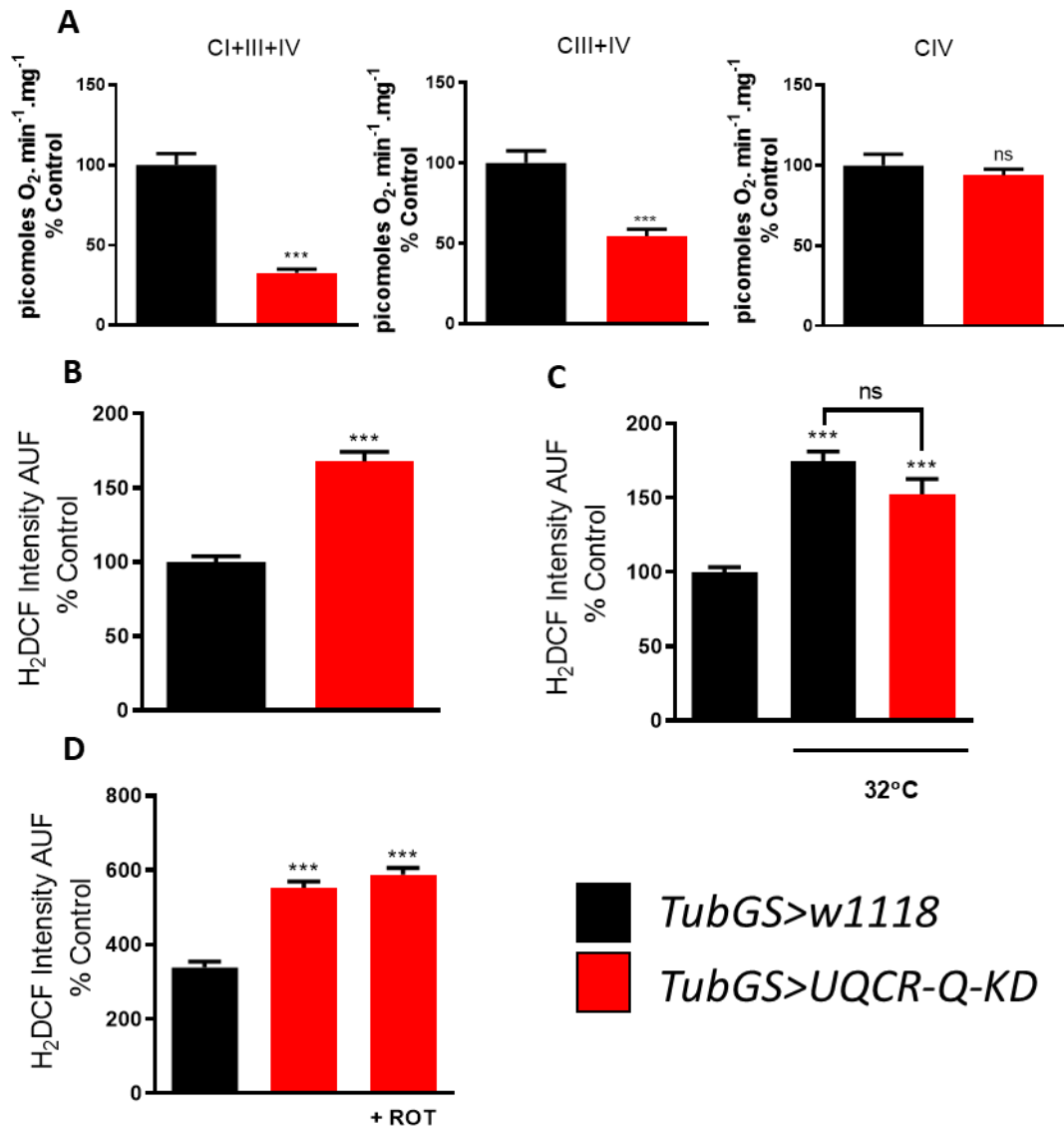


Figure 5.5 The effect of *UQCR-Q-KD* on ROS production in non-stressed conditions and during heat stress.

(A) Mitochondrial respiration in *UQCR-Q-KD* whole fly homogenates, (*TubGS>UQCR-Q-KD*), compared to the respective controls, (*TubGS>w1118*) (N = 6). **(B)** ROS measurements of *UQCR-Q-KD* fly brains in non-stressed conditions (25°C) (N = >7). **(C)** ROS measurements of *UQCR-Q-KD* fly brains subjected to heat stress (32°C) (N = 8). **(D)** ROS measurements of *UQCR-Q-KD* fly brains at 25°C fed rotenone (600 μM) (N = >7). Flies were approximately 10 days old after being fed RU-486 to induce expression. P Values were calculated using unpaired Student's T-test and One-Way AVOVA, where appropriate. p < 0.05 was taken as statistically significant and represented by *, p < 0.01 was represent by ** and p < 0.001 was represented by ***.

5.5 Decreasing Complex IV activity

Cytochrome c oxidase or Complex IV (CIV) is the final respiratory complex, in the ETC, involved in electron transport. Its role is to accept four electrons from Cyt C and then carry out the reduction of O₂, the final electron acceptor, into water (Timon-Gomez *et al.*, 2018). During this process, CIV also pumps four protons to the IMS contributing to the generation of the proton gradient, necessary for ATP synthesis (Lu and Gunner, 2014). The structure of mammalian CIV consists of 13 subunits where 3 larger subunits form the catalytic core. Subunits I and II control the movement of electrons and protons, whereas subunit III confers structural integrity of CIV. Subunit I is home to 2 haem centres, haem a and haem a₃. Additionally, haem a₃ forms a binuclear centre with the copper centre, CuB, which is involved in the reduction of O₂. Subunit II contains the copper centre CuA and binds directly to Cyt C to accept electrons (Srinivasan and Avadhani, 2012). To achieve CIV inhibition I used cyanide (CN) that prevents reduction of O₂ to water and I knocked-down *levy*, which is required to assemble a fully functioning CIV.

CN is a well-established competitive inhibitor of CIV and binds to the haem a₃-CuB binuclear centre of subunit I (Jensen *et al.*, 1984) (Figure 5.6). Binding of CN prevents electrons being transferred to molecular O₂ and therefore blocks the exit of electrons from the ETC.

The gene *levy* encodes the orthologue of the human subunit VIa (COX6A) in CIV and possesses a regulatory role, responsible for dimerisation of CIV (Kemppainen *et al.*, 2014) (Figure 5.6). In models where *levy* is mutated, it has been shown to reduce the activity of CIV (Liu *et al.*, 2007) (Kemppainen *et al.*, 2014). I predicted that by using both of these methods of CIV inhibition, I would be able to prevent electrons from leaving the ETC, increasing the reduction state of the CoQ upstream of CIV, therefore allowing the generation of at least one condition required for the initiation of RET.

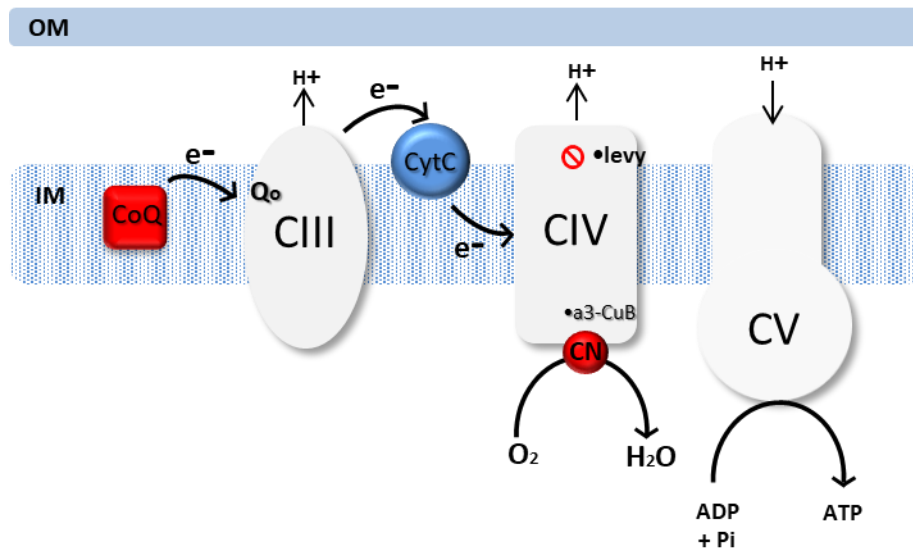


Figure 5.6 Schematic diagram indicating the binding site of CN and the RNAi construct used to target the CIV *levy* subunit.

CN binds to the binuclear centre, (haem $a3-CuB$) of CIV and inhibits the transfer of electrons to molecular oxygen. *levy* is responsible for the correct assembly and therefore activity of CIV. Both types of inhibition will inhibit the exit of electrons from the ETC, therefore causing the accumulation of electrons upstream the ETC, resulting in a highly reduced CoQ.

5.6 Inhibition of CIV increases ROS production but does not trigger ROS-RET

5.6.1 Pharmacological inhibition of CIV increases ROS production.

To ensure that CN was able to reach the brain and inhibit CIV within the 4 hours of feeding, I measured mitochondrial respiration in the heads of the flies, using high-resolution respirometry. I used two different doses of CN, 12 and 18 mM, that inhibit respiration less and more than 50%, respectively, to see if different effects were observed, depending on the inhibition of the complex (Figure 5.7A-B). An important rise in ROS production, which correlated with the amount of inhibition of CIV, was observed in non-stressed conditions (25°C) (Figure 5.7C). When subjected to HS, to initiate physiological RET, milder inhibition of CIV did not affect ROS levels, whereas stronger inhibition increased ROS levels even more (Figure 5.7D). Rotenone was then used in conjunction with the higher dose of CN, to determine if RET stimulation was occurring as a result of CIV inhibition. However, ROS levels did not change in the presence of rotenone, indicating that ROS-RET was not the cause of the increase in ROS observed (Figure 5.7E).

Since inhibition of CIV activity is an important physiological mechanism to modulate mitochondrial respiration, I decided to dissect where the ROS were originating from using a combination of different ETC inhibitors. I focused on CI and CIII since it has been widely established that these two respiratory complexes are the two major sites of *in vivo* ROS production, within the mitochondria. First, I decided to use FCCP to dissipate the pmf and study whether this manipulation would affect ROS levels after CIV inhibition. Interestingly FCCP (600 μ M) significantly reduced ROS levels when combined with CN in the fly food (Figure 5.8A). Although the FCCP results could support ROS-RET as the mechanism triggered by CIV inhibition, the results using rotenone clearly demonstrated that RET was not responsible for the elevated ROS levels, as no decrease in ROS after blocking the quinone binding site, was observed. Therefore, I decided to test whether CIII was implicated, since production by the Q_o site of CIII also requires a high membrane potential (Larosa and Remacle, 2018). To test the former hypothesis, I fed flies with both CN and myxothiazol (100 μ M), to block the Q_o site of CIII and measured ROS levels. Interestingly, myxothiazol completely abolished the increase in ROS (Figure 5.8B), supporting CIII as the site of ROS production, not CI, when CIV is inhibited.

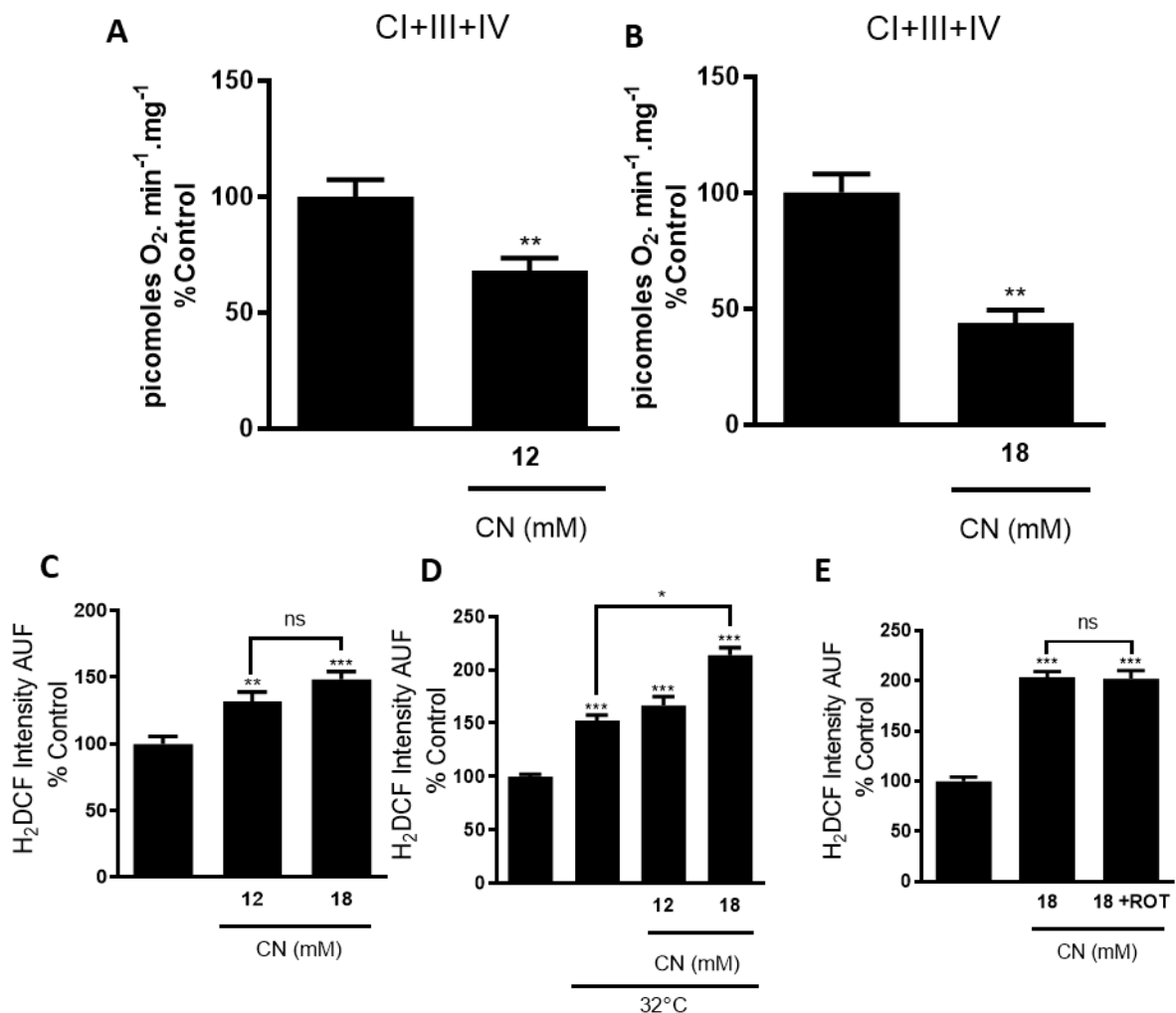


Figure 5.7 The effect of CN on ROS production in non-stressed conditions and during heat stress

(A) Mitochondrial respiration of fly head mitochondria after feeding flies with 12 mM of CN for 4 hours (N = 6). (B) Mitochondrial respiration after feeding flies with 18 mM of CN for 4 hours (N = 3). (C) Quantification of ROS measurements in fly brains fed 12 and 18 mM of CN at 25°C (N = >8). (D) ROS measurements in fly brains fed 12 and 18 mM of CN under HS (32°C) (N = 9). (E) ROS measurements in fly brain fed 18mM of CN and rotenone (600 µM) at 25°C (N = >8). Flies were approximately 3 days old. P Values were calculated using unpaired Student's T-test and One-Way ANOVA, where appropriate. p < 0.05 was taken as statistically significant and represented by *, p<0.01 was represented by ** and p<0.001 was represented by ***.

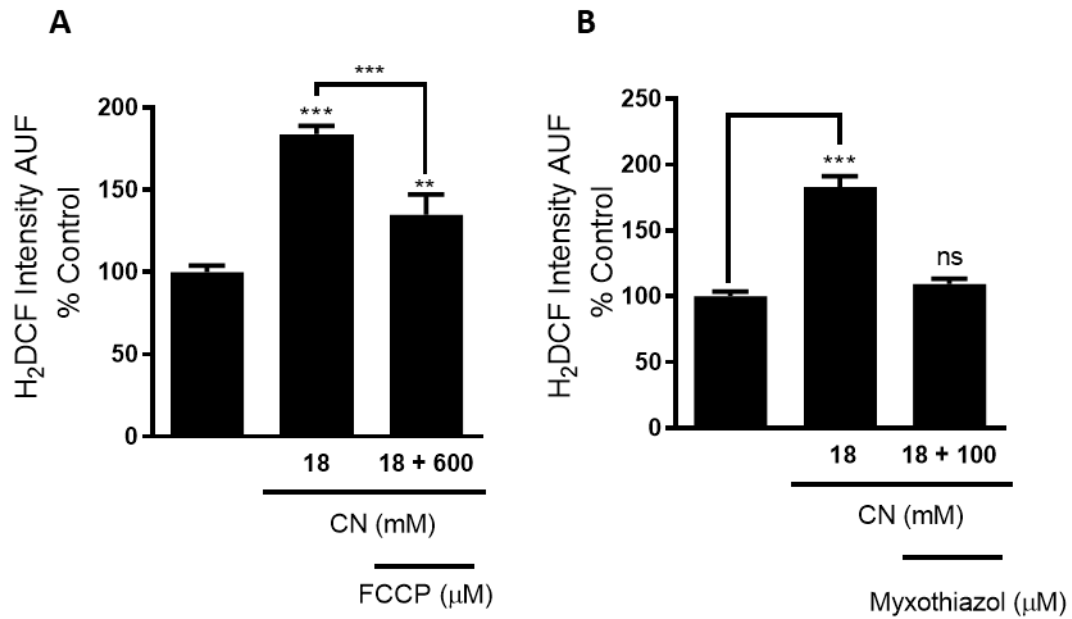


Figure 5.8 The effect of CN on ROS production in combination with the uncoupler, FCCP and the CIII inhibitor, myxothiazol.

(A) ROS measurements in fly brains of flies fed 18 mM of CN and 600 μ M of FCCP at 25°C (N = >7). **(B)** ROS measurements in fly brains of flies fed 18 mM of CN and 100 μ M of myxothiazol at 25°C (N = 10). Flies were approximately 3 days old. P Values were calculated using One-Way ANOVA. $p < 0.05$ was taken as statistically significant and represented by *, $p < 0.01$ was represented by ** and $p < 0.001$ was represented by ***.

5.6.2 Genetic depletion of CIV elevates ROS production but does not trigger ROS-RET

As in the case of CIII, I was interested in identifying differences in blocking CIV, acutely (chemical inhibition) or chronically (genetic depletion), on ROS levels. I used an RNAi line expressing a transgene against *levy* to decrease CIV levels and used high-resolution respirometry to test the effect on mitochondrial respiration. I confirmed a significant decrease in CIV-linked respiration in the *levy-KD* flies, (*DaGAL4>levy-KD*), compared to the two controls used in this experiment, (*DaGAL4>DAH* and *DAH>levy-KD*) (Figure 5.9A). Inhibition of CI+CIII+CIV respiration was also observed in the *levy-KD* flies, whereas CIII+CIV respiration was significantly decreased only with respect to one of the controls, (*DaGAL4>DAH*). This could be due to background differences between the experimental groups since flies were not backcrossed for this experiment and two different backgrounds were used (our White *Dahomey* flies and *w1118* flies from Vienna). My results confirm previous observations reporting that *levy* is required for the assembly of CIV and its knock-down severely compromises the activity of the complex. Furthermore, *levy* is also involved in the assembly of respiratory supercomplexes containing CI (Kemppainen *et al.*, 2014). Additionally, as discussed previously, the inhibition of electron flow downstream of CI, would lead to the reduction in CI linked respiration, which is observed in the both the *UQRC-Q-KD* and *levy-KD* fly models.

Silencing the CIV subunit, *levy*, induced a large increase in ROS production compared to both of the controls (Figure 5.9B). When *levy-KD* flies were subjected to 4 hours of HS this increase in ROS was also present compared to the control at 25°C. However, compared to the control at 32°C there was a slight but non-significant decrease in ROS levels (Figure 5.9C). To establish the site of ROS production and whether the increase in ROS was caused by the stimulation of RET, rotenone was fed to the *levy-KD* flies. Rotenone feeding caused a further increase in ROS production, therefore discarding ROS-RET as the source of ROS (Figure 5.9D). These results reflected those previously described using CN to inhibit CIV, therefore to establish where ROS was being produced during CIV inhibition, I employed the same strategy carried out for CN experiments and measured ROS levels in conjunction with other inhibitors of the ETC. Feeding FCCP to *levy-KD* flies significantly increased ROS levels, compared to the controls flies (Figure 5.10A). Feeding 100 µM of myxothiazol to *levy-KD* flies also supported the previous

conclusion of the CN experiments, where a decrease in ROS back down to control levels, was observed (Figure 5.10).

Overall the results from both chemical and genetic inhibition of CIV indicate that when the exit of electrons is blocked, through CIV inhibition, electrons accumulate at the Q_o site of CIII and consequently cause a dramatic increase in ROS production. These data confirm that inhibition of CIV, using two complementary approaches, did not stimulate ROS-RET and elevated ROS production, from respiratory CIII.

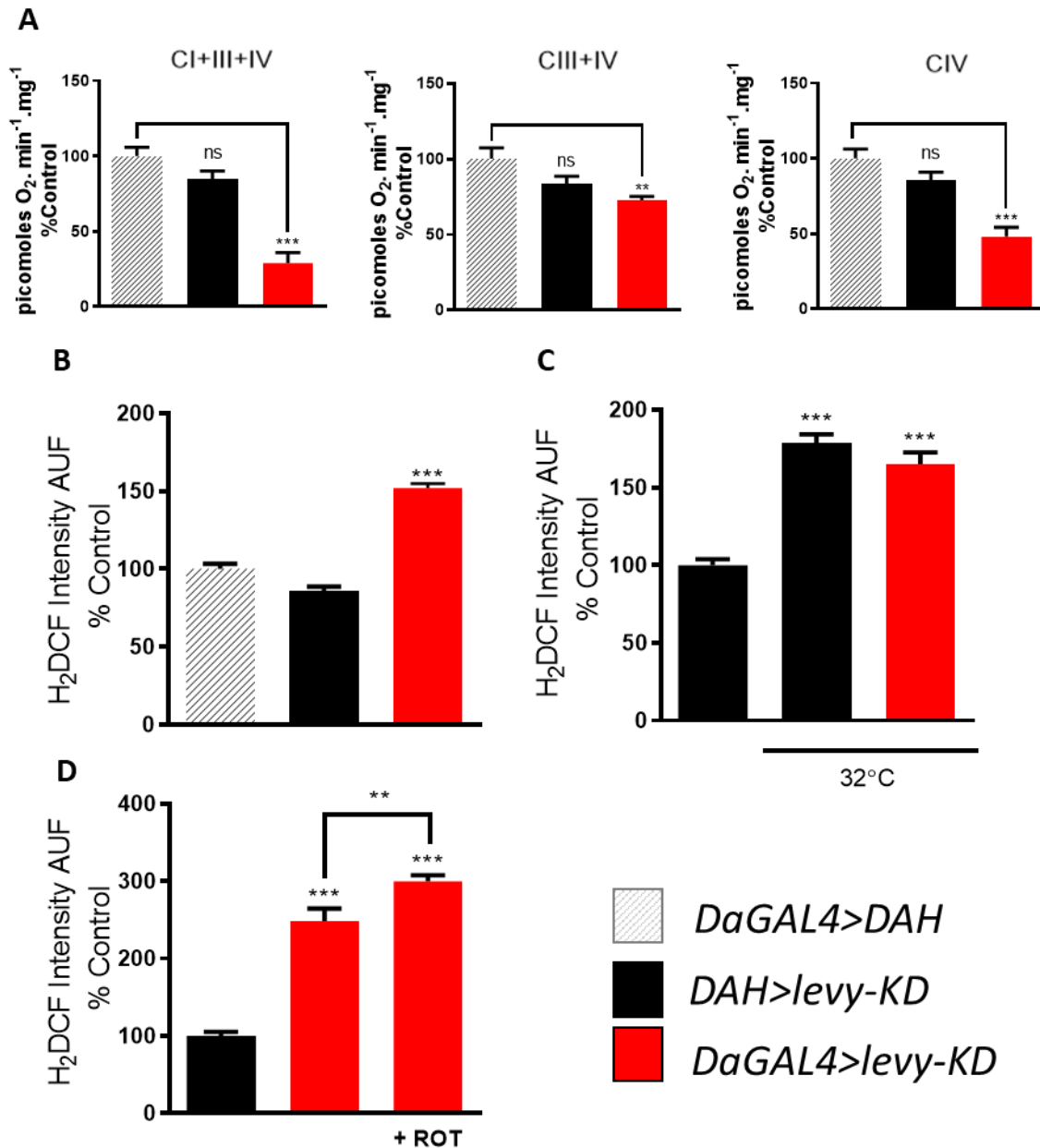


Figure 5.9 The effect of *levy-KD* on ROS production in non-stressed conditions and during heat stress.

(A) Mitochondrial respiration in *levy-KD* whole fly homogenates (*DaGAL4>levy-KD*) compared to the respective controls (*DaGAL4>DAH* and *DAH>levy-KD*) (N = >5). **(B)** Quantification of *ex vivo* ROS measurements of *levy-KD* fly brains in non-stressed conditions (25°C) (N = >7). **(C)** ROS measurements of *levy-KD* flies subjected to HS (32°C) (N = 9). **(D)** ROS measurements of *levy-KD* flies at 25°C fed rotenone (600 μM) (N = >8). Flies were approximately 10 days old. P Values were calculated using One-Way ANOVA. p < 0.05 was taken as statistically significant and represented by *, p < 0.01 was represented by ** and p < 0.001 was represented by ***.

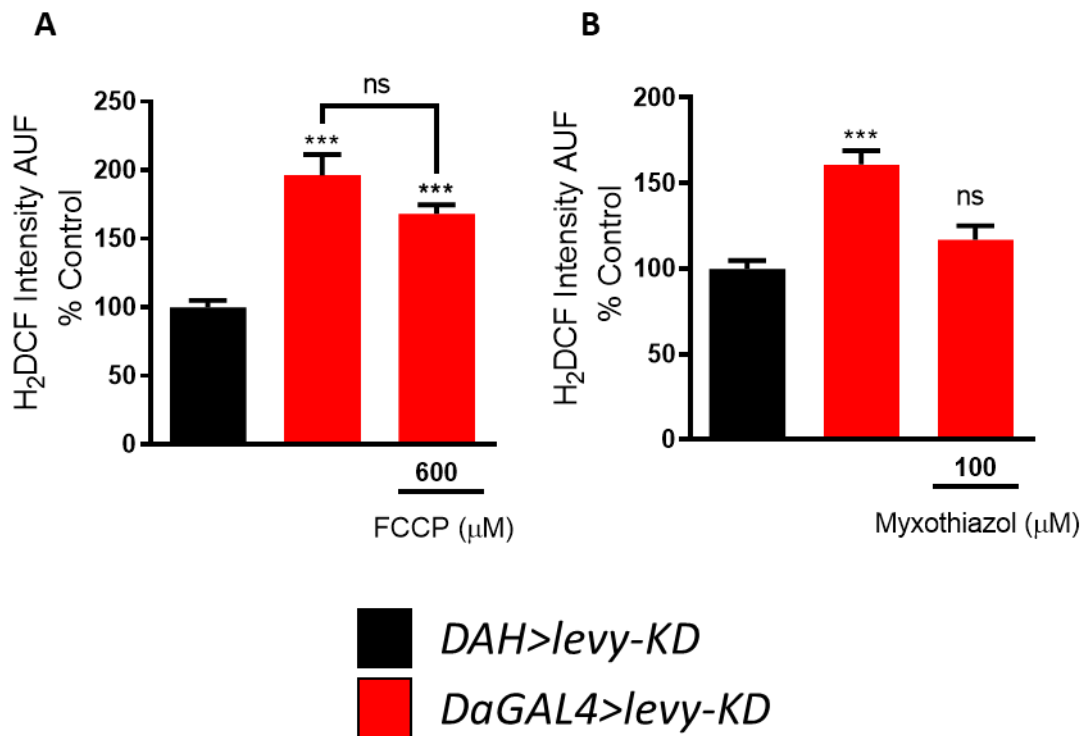


Figure 5.10 The effect of *levy-KD* on ROS production in combination with the uncoupler, FCCP and the CIII inhibitor, myxothiazol.

(A) ROS measurements in the brain of *levy-KD* flies fed 600 μM of FCCP at 25°C (N = >6). **(B)** ROS measurements in the brain of *levy-KD* flies fed 100 μM of myxothiazol at 25°C (N = >8). Flies were approximately 3 days old. P Values were calculated using One-Way ANOVA. p < 0.05 was taken as statistically significant and represented by *, p<0.01 was represent by ** and p<0.001 was represented by ***.

5.7 Reduction of CV activity

ATP Synthase or Complex V (CV) is the enzyme responsible for the production of energy in the form of ATP. It achieves this via the movement of protons down the electrochemical proton gradient, which drives ATP synthesis, from ADP and P_i . The structure of CV comprises of two key subcomplexes, F_0 and F_1 . The integral membrane-bound F_0 subcomplex facilitates translocation of protons through CV, triggering a rotary motion. The soluble F_1 resides in the mitochondrial matrix and catalyses ATP synthesis. Connecting these two components is the stalk, which spans the length of the complex (Xu *et al.*, 2015). In an attempt to inhibit CV, I used the established chemical inhibitor oligomycin and the proposed novel inhibitors alpha-ketoglutarate and J147. Additionally, I used an RNAi line targeting the ATPase synthase δ subunit to genetically inhibit CV.

The macrolide antibiotic, oligomycin, is a highly specific inhibitor of CV. It binds to the c ring of CV, in the F_0 subcomplex (Symersky *et al.*, 2012) (Figure 5.11). Therefore its binding blocks the passage of protons through CV to the mitochondrial matrix. This should lead to the accumulation of protons in the IMS and subsequently, the generation of a high pmf. Another consequence of oligomycin binding is the interruption of proton pumping when the membrane becomes too hyperpolarised. Due to the electron transfer within the ETC being reliant on the movement of protons to drive the redox reactions, oligomycin causes the ETC to come to a halt, forcing mitochondria to remain in respiratory State 4. Electrons from within the ETC may then gather at CoQ to cause an increase in the $CoQH_2:CoQ$ ratio. From these observations, it is reasonable to speculate that oligomycin is capable of producing the two conditions needed to initiate a ROS-RET signal. Accordingly multiple publications have reported an increase in ROS levels in response to blocking CV with oligomycin, overexpression of ATPIF1 or the genetic depletion of CV (Liu and Schubert, 2009) (Fukuoh *et al.*, 2014) (Formentini *et al.*, 2012). One publication showed that the addition of rotenone suppressed the increase in ROS, suggesting that ROS-RET is stimulated during CV inhibition (Chouchani *et al.*, 2014a). However, to the best of my knowledge, there has not been a consistent attempt to investigate how and where ROS are generated in response to CV inhibition *in vivo*.

As discussed previously, AKG has recently been characterised as a novel uncompetitive inhibitor of CV (Chin *et al.*, 2014b). This study identified the catalytic β subunit of the F_1 subcomplex, ATP5B, as the binding site for AKG (Figure 5.11). AKG

is a CAC cycle intermediate, produced by the enzyme isocitrate dehydrogenase, which catalyses the oxidative decarboxylation of isocitrate. Due to the fact that AKG is an endogenous metabolite, it has the potential to be a physiological stimulator of RET through the inhibition of CV. Therefore, I hypothesised that physiological changes that cause the accumulation of AKG could trigger ROS-RET as a physiological response to stress.

ATP synthase, δ subunit (ATPsyn δ) is situated at the top of the stalk that connects F_0 and F_1 and is essential for the regulation of both proton translocation and ATP synthesis (Olahova *et al.*, 2018) (Figure 5.11). RNA interference was used to silence the gene encoding *ATPsyn δ* and achieve CV depletion.

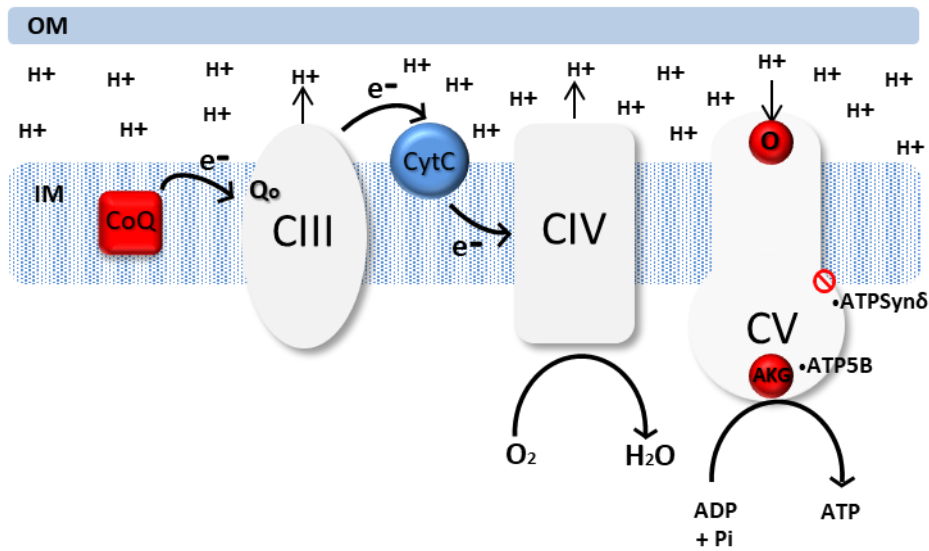


Figure 5.11 Schematic diagram indicating the binding sites of oligomycin and AKG and the RNAi construct used to target the CV ATPsyn δ subunit.

Oligomycin binds to the c subunit of CV, which is responsible for the translocation of protons. AKG binds to the ATP5B subunit found in the β subunit of the catalytic head. *ATPsyn δ* resides at the top of the connective stalk. All types of inhibition will prevent the passage of protons and the synthesis of ATP, therefore allowing the ETC to slow down, producing a high $\text{CoQH}_2:\text{CoQ}$ ratio and also a high proton motive force.

5.8 Genetic inhibition of CV triggers ROS-RET

5.8.1 Oligomycin specifically inhibits CV without initiation of a ROS-RET signal.

First, I performed experiments in fly homogenates, where oligomycin was directly added to the oxygraph chamber, to obtain a respiratory profile, showing the consequences of specific CV inhibition on respiration. This profile was necessary to test the abilities of AKG and J147 as CV inhibitors in *Drosophila*, by comparing the effects of the novel inhibitors with the effects of a validated inhibitor, oligomycin.

Initially, I stimulated State 3, adding ADP and a combination of pyruvate and proline to feed CI+CIII+CIV respiration, which caused a significant increase in oxygen consumption. Adding oligomycin prevents the transit of protons through CV, raising the pmf and initiating State 4 (where oxygen is consumed but ADP is not phosphorylated to ATP). As expected, I observed a dramatic inhibition (>95%) in mitochondrial respiration, after the addition of oligomycin (Figure 5.12A). To confirm that the decrease in respiration was caused by specific inhibition of CV, I added the uncoupler FCCP that generates pores in the IMM, allowing protons to return to the mitochondrial matrix independently of CV, thus uncoupling mitochondrial respiration from ATP synthesis. As anticipated, FCCP restored respiration (Figure 5.12A). Since a real State 4 cannot be observed using pyruvate and proline in fruit flies (Miwa *et al.*, 2003), I repeated the experiments using G3P that feeds electrons directly to the CoQ pool, using the G3PDH located in the outer face of the IMM (Miwa *et al.*, 2003). Once again, if oligomycin (or any other CV inhibitor) specifically inhibits CV then I expected to see a decrease in respiration back down to the levels observed in State 4. First, I initiated State 2, adding only G3P to the oxygraph chamber. State 2 is similar to State 4, however, during State 2 small amounts of endogenous ADP can be present, promoting minimal ATP synthesis. In contrast to State 4, where no ADP is present. Addition of ADP triggered State 3, which was once again inhibited by adding oligomycin, returning mitochondria into State 4 (Figure 5.12B). As anticipated no significant differences were observed between State 2 and State 4 and both were significantly lower than State 3. Finally, adding FCCP once again restored the respiration, by uncoupling electron transport from OXPHOS, as described in the previous experiment (Figure 5.12B). As one final experiment to validate the specificity of oligomycin, I initiated State 3 respiration and added FCCP, a slight but not statistically significant increase was observed (Figure 5.12C). However, on this

occasion oligomycin did not decrease respiration, due to the fact that electron transport was no longer dependent on CV to move protons into the matrix.

In addition to the *in vitro* experiments, as I did with the previous inhibitors, I wanted to also confirm that oligomycin can reach the brain and inhibit CV, after 4 hours of feeding. I used two different doses of oligomycin and measured respiration using pyruvate and proline as CI substrates. After feeding flies for 4 hours with oligomycin, respiration decreased similarly using two doses, 50 μM and 100 μM (Figure 5.13A & B).

To test the effect of oligomycin on the production of ROS, I used two different doses of 50 and 100 μM . Unexpectedly, oligomycin did not increase ROS in the brain of wild type flies (Figure 5.13C). Moreover, the highest concentration (100 μM) decreased ROS levels. Interestingly, oligomycin (50 μM) suppressed ROS-RET in wild type flies exposed to HS (Figure 5.13D). In a separate experiment, I tested the effect of 100 μM of oligomycin in flies expressing Ndi1. Reflecting the HS data, oligomycin decreased ROS, indicating that high doses of oligomycin can suppress ROS-RET (Figure 5.13E). Since oligomycin has been described before to increase ROS in isolated mitochondria and different cell types (Liu and Schubert, 2009), although not in fly brain to the best of my knowledge, I performed a few additional experiments. Firstly, I used a much higher concentration of oligomycin (400 μM) that decreased ROS levels in the brain, even further than 50 μM (Figure 5.14A). Secondly, I fed the flies with two doses of oligomycin 50 μM and 100 μM during a 3 day period rather than 4 hours (Figure 5.14B). Surprisingly, I did not observe a reduction in ROS levels with the lowest dose but the higher dose clearly reduced ROS levels in the fly brain. My results show that none of the concentrations or experimental conditions assayed, induced ROS-RET. Moreover, oligomycin suppressed or reduced ROS-RET in two different models; Ndi1 and HS, discarding the theory that oligomycin can induce ROS in the fly brain.

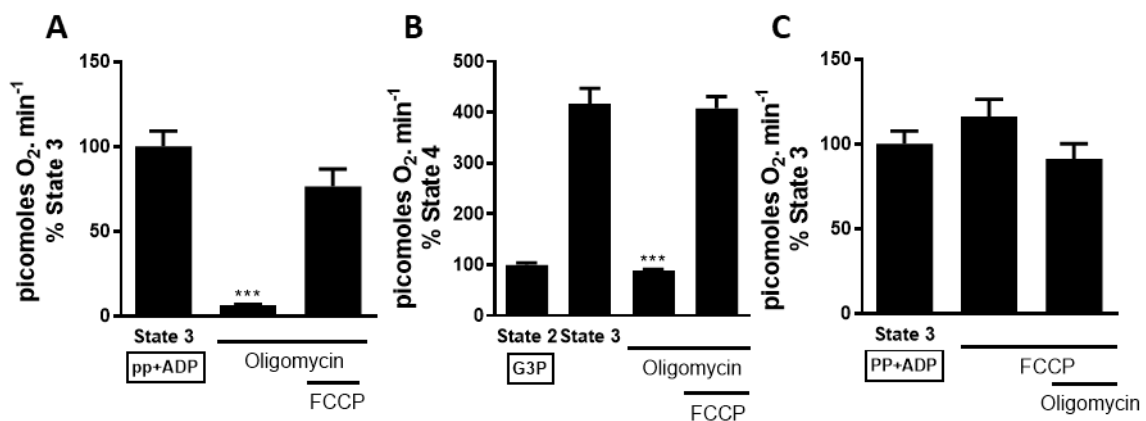


Figure 5.12 High-resolution respirometry measurements showing the inhibitory effect of oligomycin.

(A) State 3 respiration using whole fly homogenates was initiated and Oligomycin was added, followed by FCCP to uncouple ETC from OXPHOS (N = 6). (B) State 2 for respiration was stimulated, followed by the addition of ADP to initiated State 3 (N = 6). Oligomycin was subsequently added followed by FCCP (N = 4). (C) State 3 respiration was initiated followed by FCCP and oligomycin. Flies were approximately 3 days old. P Values were calculated using One-Way AVOVA. Data are shown as mean ± SEM. p < 0.05 was taken as statistically significant and represented by *, p<0.01 was represented by ** and p<0.001 was represented by ***.

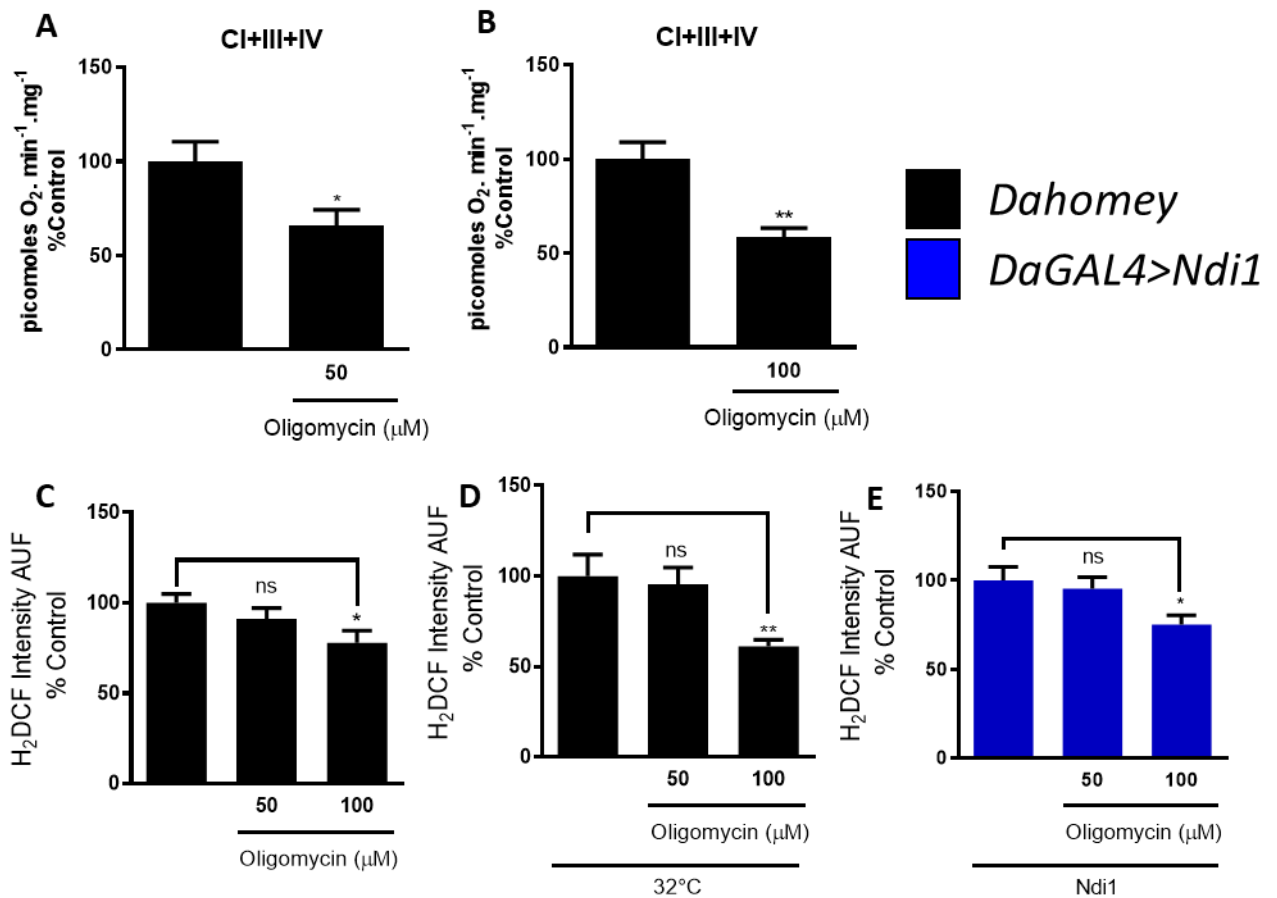


Figure 5.13 The effect of oligomycin on ROS production in non-stressed conditions.

(A) Mitochondrial respiration using whole fly homogenates in flies fed 50 μM of oligomycin for 4 hours (N = 6). (B) Mitochondrial respiration in flies fed 100 μM of oligomycin for 4 hours (N = 6). (C) ROS measurements in brains of flies fed with 50 and 100 μM oligomycin at 25°C (N = >7). (D) ROS measurements in brains of flies fed with 50 and 100 μM oligomycin under HS (32°C) (N = >5). (E) ROS measurements in brain of flies expressing Ndi1 fed 50 and 100 μM of oligomycin (N = >6). Flies were approximately 3 days old. Ndi1 flies were approximately 10 days old. P Values were calculated using unpaired Student's T-test and One-Way ANOVA, where appropriate. $p < 0.05$ was taken as statistically significant and represented by *, $p < 0.01$ was represented by ** and $p < 0.001$ was represented by ***.

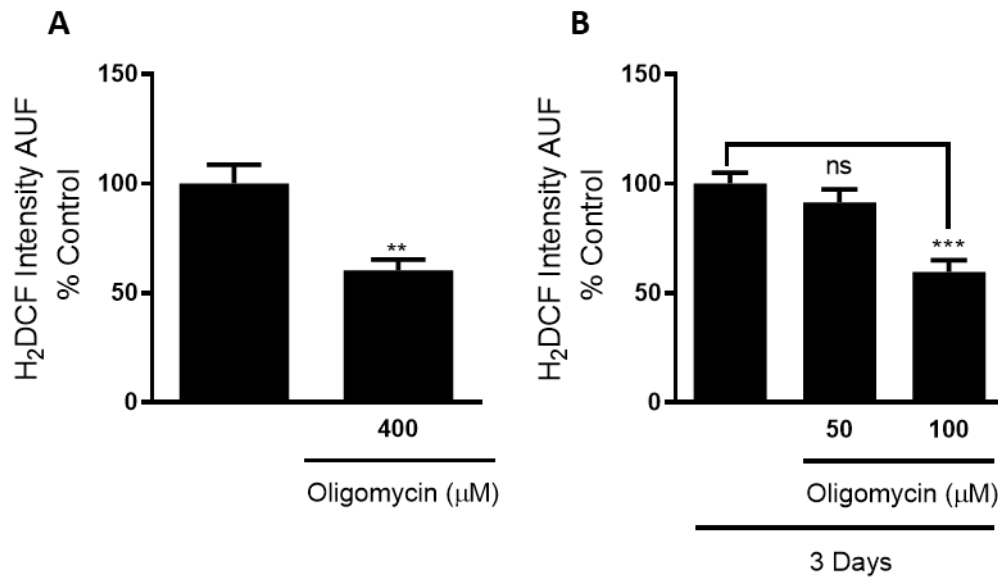


Figure 5.14 The effect of oligomycin in high concentrations and after 3 days in non-stressed conditions.

(A) ROS measurements in brains of flies fed 400 μM of oligomycin ($N = >7$). **(B)** ROS measurements in brains of flies fed 50 and 100 μM of oligomycin for 3 days ($N = 7$). Flies were approximately 3 days old. P Values were calculated using unpaired Student's T-test and One-Way ANOVA, where appropriate. $p < 0.05$ was taken as statistically significant and represented by *, $p < 0.01$ was represented by ** and $p < 0.001$ was represented by ***.

5.8.2 Genetic depletion of CV, using *ATPSynthase-δ-KD* line increases ROS via RET

Since the results obtained with oligomycin were in contradiction with other reports, including measurements in fly cells, showing a clear increase in mitochondrial ROS (Fukuoh *et al.*, 2014), I decided to measure ROS levels in the brain of flies with depleted levels of CV. To deplete CV, I knocked-down *ATPsynδ*. To confirm the knock-down, I measured mitochondrial respiration. As anticipated, oxygen consumption was dramatically decreased using substrates that introduce electrons via CI (i.e. CI+CIII+CIV) or downstream (CIII+CIV) in the KD flies, (*TubGS>ATPsynδ-KD*), compared to control flies, (*TubGS>DAH*) (Figure 5.15A). I found that CIV-linked respiration was also reduced, which is surprising since CIV-linked respiration is not dependent on the membrane potential and should not be directly affected by reducing CV activity. This indicates a possible reduction in mitochondrial mass, which coincidentally, has been previously described when *ATPsynδ* and other CV subunits are depleted in *Drosophila* S2 cells (Fukuoh *et al.*, 2014).

Next, I tested whether the knock-down of *ATPsynδ* subunit could stimulate ROS production. In contrast to CV inhibition with oligomycin, the genetic depletion of CV increased ROS in the fly brain (Figure 5.15B). To establish whether or not this increase in ROS was as a result of RET, I fed the KD flies rotenone. In the presence of rotenone, ROS levels were decreased significantly, even further than those seen in the controls (Figure 5.15C). Under HS, KD and control flies exhibited similar levels of ROS (Figure 5.15D). These results were also in contrast to the results of oligomycin, which prevented the increase in ROS induced by HS.

The results obtained by knocking-down *ATPsynδ* seem to support that genetically inhibiting CV, triggers ROS-RET. However, this conclusion should be approached with caution. Firstly, these results are in conflict with the results obtained using oligomycin, including experiments where higher concentrations (400 μM) or long term administration of the drug was used. Secondly, although it is possible that feeding flies with oligomycin does not establish a high enough membrane potential to trigger RET, it is also possible that the ROS observed in *ATPsynδ-KD* flies are not mitochondrial or are produced non-specifically in the mitochondria (i.e not via RET), due to the high levels of damage these flies seem to support. Under this model, the decrease in ROS observed after feeding flies with rotenone, would be the result of the collapsed pmf that would cause the mitochondria to stop generating ROS. It is worth mentioning that the knock-down of *ATPsynδ* causes an extremely debilitating

phenotype with the flies dying just a few days after eclosion. Therefore the flies used for these experiments were only 2-3 days old and fed RU-486 for the duration of this time after eclosion. Additionally, these flies were weak from eclosion however I did not perform analysis of their lifespan with and without RU-486 feeding. This phenotype was not observed in the CI, CII, CIII or CIV subunit knock-down models and is probably the consequence of extremely low levels of mitochondrial respiration. Furthermore, the low CIV-linked respiration observed indicated a reduction in mitochondrial mass, which has been shown in *S2* cells, upon depletion of CV, by knocking down *ATPsyn δ* and other CV subunits (Fukuoh *et al.*, 2014). To determine if genetic inhibition of CV can stimulate a RET-ROS response other subunits should be explored especially those, which do not display the weak phenotype observed when using the *ATPsyn δ -KD*. This may explain the contrasting results displayed between the oligomycin and the genetic model, even after feeding oligomycin over long periods of time. In the future, it will also be interesting to investigate if CV depletion stimulates mitophagy *in vivo*. Additionally, if this stimulation of mitophagy is ROS-dependent and more importantly if this ROS is RET-derived.

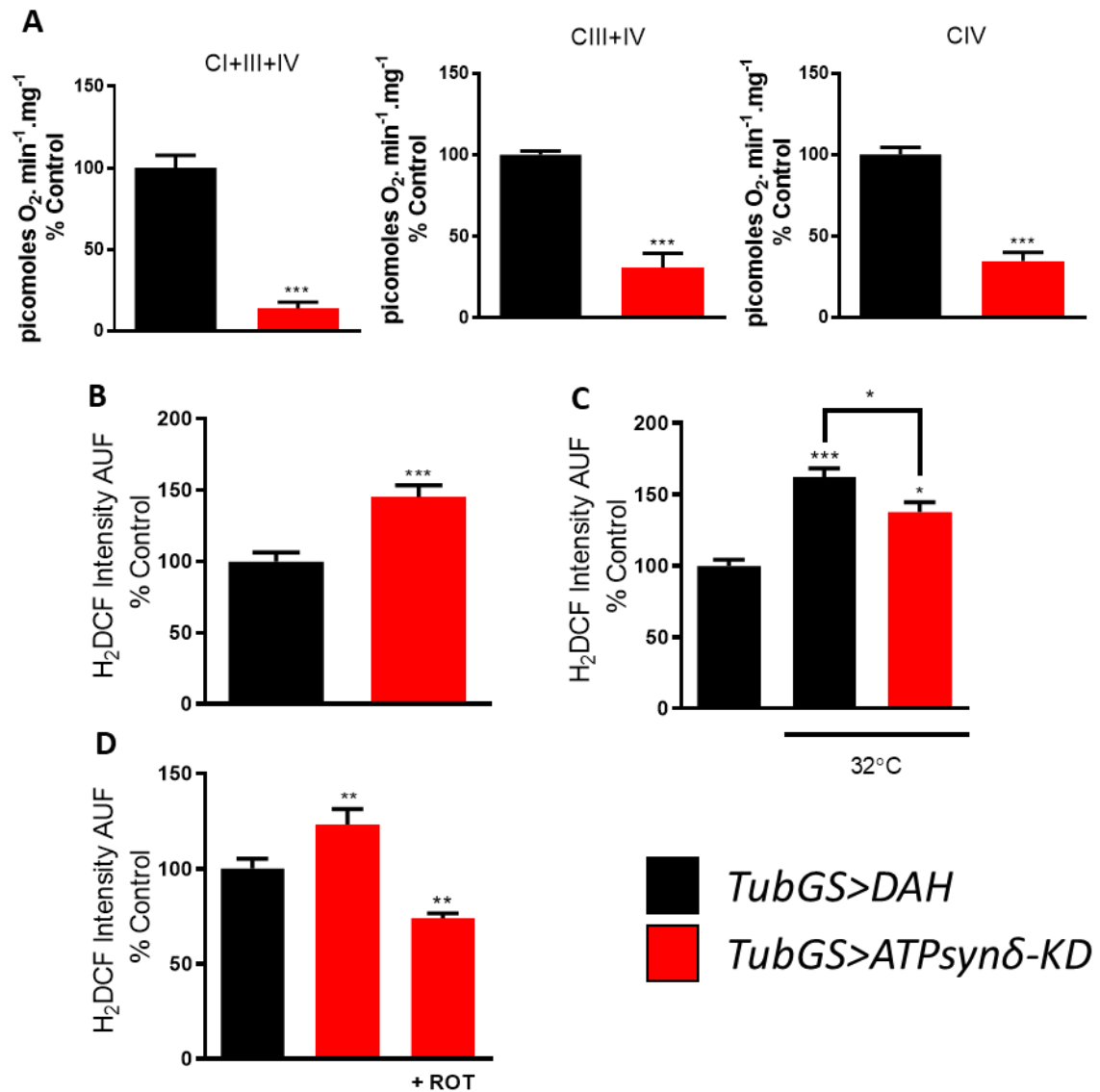


Figure 5.15 The effect of *ATPsynδ-KD* on ROS production in non-stressed conditions and during heat stress.

(A) Mitochondrial respiration in *ATPsynδ-KD* whole fly homogenates, (*TubGS>ATPsynδ-KD*), compared to the respective controls, (*TubGS>DAH*) (N = 5). (B) Quantification of *ex vivo* ROS measurements using H₂DCF of *ATPsynδ-KD* fly brains in non-stressed conditions (25°C) (N= 9). (C) ROS measurements of *ATPsynδ-KD* flies subjected to heat stress (32°C) (N = >7). (D) ROS measurements of *ATPsynδ-KD* flies at 25°C fed rotenone (600 μM) (N = >7). The *ATPsynδ-KD* flies used in these experiments were approximately 2-3 days old and fed RU-486 from eclosion. P Values were calculated using unpaired Student T-test and One-Way ANOVA, where appropriate. p < 0.05 was taken as statistically significant and represented by *, p<0.01 was represented by ** and p<0.001 was represented by ***.

5.8.3 Alpha-ketoglutarate (AKG) is not a CV inhibitor in *Drosophila melanogaster*

In an attempt to conciliate the opposite effects on ROS levels observed with the other models, oligomycin and knocking-down of *ATPsyn δ* , I decided to test, whether AKG inhibited *Drosophila* CV as an alternative way to block the complex. To validate AKG as a specific inhibitor of CV, I carried out similar experiments to the ones shown in Figure 5.12, to allow the comparison with oligomycin.

When using pyruvate+proline as substrates to feed CI with electrons, I observed that AKG (0.25 μ M) had a potent inhibitory effect (Figure 5.16A). However, the addition of the uncoupler FCCP did not restore mitochondrial respiration, indicating that the effect of AKG was not caused by CV inhibition. I then used a different substrate, G3P, to feed respiration downstream of CI but no inhibition was observed with 0.25 μ M of AKG (Figure 5.16B). With doses of AKG 3-4 times higher, I observed inhibition in respiration but once again it was not restored by FCCP (Figure 5.16B). This provides further support that the target of AKG in fly mitochondria is not CV. Finally, I performed the last experiment adding AKG + ADP and observed a modest but significant increase in respiration (Figure 5.16B). This was not unexpected since AKG is a CAC intermediate that can be oxidized producing NADH. My results disprove AKG as an inhibitor of *Drosophila melanogaster* CV, as it has been suggested in worms, bovine heart mitochondria and in mammalian cells (Chin *et al.*, 2014b). The experiments from this particular paper showed that AKG could inhibit CV activity by measuring the levels of ATP production, which were shown to decrease upon addition of AKG. Additionally, Chin *et al* demonstrated that in mammalian cells and worms AKG lowered oxygen consumption, similarly to my initial experiments. Interestingly, when using isolated mitochondria from mouse liver they found that AKG lowered respiration in State 3 however not in the presence of oligomycin (State 4). Therefore these data are in contrast to my results as I was not able to show that FCCP could restore respiration, as it does in presence of the CV inhibitor oligomycin. The decrease in respiration upon addition of AKG may be due to the fact that AKG is an intermediate belonging to the CAC. It is possible that a build-up of AKG could lead to disruption of the CAC. This in turn would affect respiration by hindering electron supply via NADH, a co-factor of the CAC. The lack of effect of low doses of AKG on respiration by CIII+CIV supports this hypothesis. Since AKG does not inhibit *in vitro* CV, I did not study its effect on ROS levels in the fly brain.

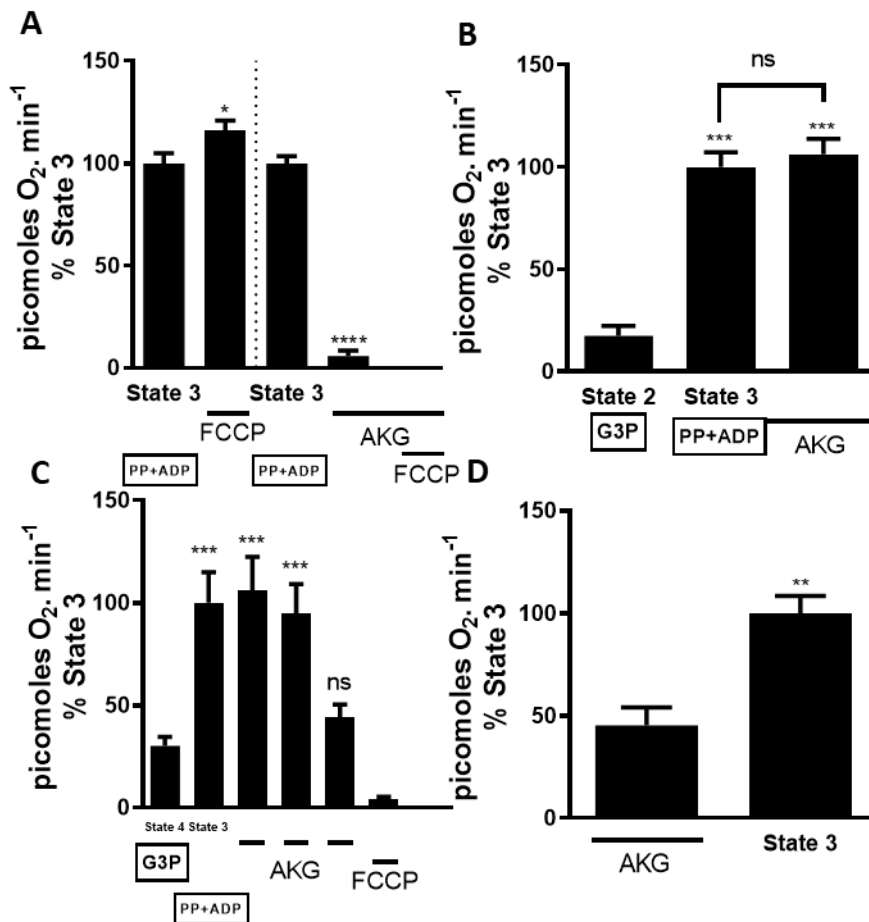


Figure 5.16 High-resolution respirometry demonstrating the effect of AKG on State 3 and 4 respiration.

(A) In the left panel State 3 respiration was initiated using whole fly homogenates and the uncoupler FCCP was subsequently added. In the right panel, AKG was added, after the initiation of State 3 respiration, followed by FCCP (N = 5). (B) State 4 respiration was initiated followed by the addition of ADP to stimulate State 3, to which AKG was added (N = 3). (C) State 3 respiration was initiated followed by State 4. AKG was sequentially added until a decrease in respiration is observed, followed by the addition of uncoupler FCCP (N = 6). (D) AKG was added as a substrate to initiate respiration followed by ADP (N = 4). Flies were approximately 3 days old. P Values were calculated using One-Way ANOVA. Data are shown as mean ± SEM. * = p < 0.05 signifying statistical significance.

5.8.4 J147 does not significantly alter mitochondrial respiration in *Drosophila melanogaster*

J147 has been reported to cause inhibition of CV activity, from isolated bovine heart mitochondria (Goldberg *et al.*, 2018). Using fly homogenates, I tried a range of concentrations of J147 from 2 μ M to 4 mM without observing any significant inhibition in respiration, using either pyruvate+proline to feed CI+CIII+CIV or G3P to feed CIII+CIV (data not shown). In an experiment comparing the effects of oligomycin and J147 run in parallel, I showed how different their effects are on respiration (Figure 5.17). Using double the concentration of J147 shown to inhibit CV in isolated bovine mitochondria (i.e. 2 μ M) and a combination of pyruvate+proline+G3P to feed the ETC, I did not find any inhibition in respiration, compared with oligomycin that strongly decreased State 3 respiration in the same experimental conditions (Figure 5.17 compare panels A and B). Therefore, demonstrating contrasting results to previous studies showing that J147 could specifically inhibit CV. As expected, FCCP restored or prevented inhibition of respiration when added after or before oligomycin.

In the previously mentioned *Goldberg et al* experiments they measured the enzymatic activity of CV in isolated bovine heart instead of oxygen consumption. Upon the addition of J147 they saw that there was partial inhibition (approximately 30%) of CV activity, however even under saturating concentrations this inhibition did not increase further. During these experiments they used oligomycin as a positive control but the results using oligomycin were not shown. These results are in contrast with the results I obtained, which showed that J147 and oligomycin possessed different effects on respiration in isolated fly mitochondria.

In summary, I did not find any evidence that J147 is a CV inhibitor in fruit flies, and therefore I did not proceed to analyse its effects on ROS levels.

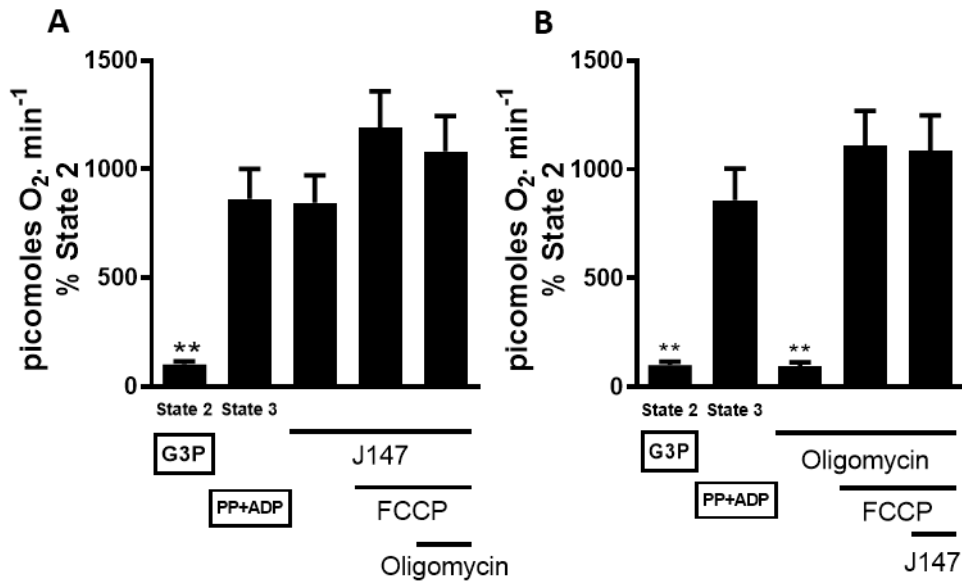


Figure 5.17 High-resolution respirometry demonstrating the effect of AKG on State 3 and 4 respiration, in comparison to oligomycin.

(A) State 2 was initiated followed by the addition of ADP to stimulate State 3. J147 was added, followed by the uncoupler FCCP and finally the CV inhibitor oligomycin (N = 4). **(B)** State 2 was initiated, followed by State 3. Oligomycin was added to inhibit CV, followed by the uncoupler FCCP and lastly J147 (N = 4). Flies were approximately 3 days old. P Values were calculated using One-Way AVOVA. Data are shown as mean \pm SEM. * = $p < 0.05$ signifying statistical significance. These experiment were done in collaboration with Angeline Yek.

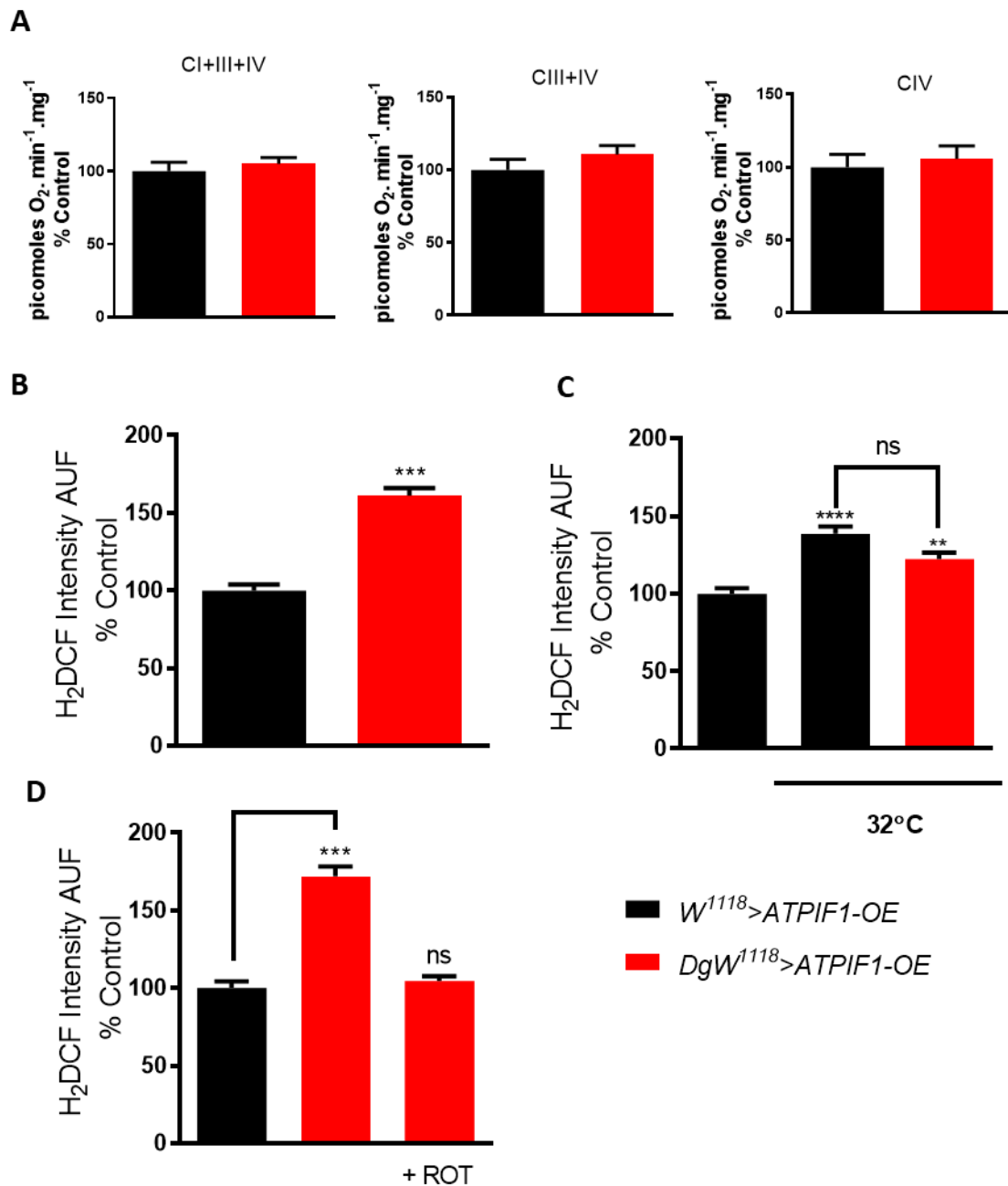


Figure 5.18 The effect of *ATPIF1-OE* on ROS production in non-stressed conditions and during heat stress.

(A) Mitochondrial respiration in *ATPIF1-OE* whole fly homogenates, (*DaGAL4W1118>ATPIF1-OE*), compared to the respective control, (*W1118>ATPIF1-OE*) (N = 5). **(B)** Quantification of *ex vivo* ROS measurements using H₂DCF of *ATPIF1-OE* fly brains in non-stressed conditions (25°C) (N= >8). **(C)** ROS measurements of *ATPIF1-OE* flies subjected to heat stress (32°C) (N = >8). **(D)** ROS measurements of *ATPIF1-OE* flies at 25°C fed rotenone (600 μM) (N = >8). Flies were approximately 10 days old. P Values were calculated using unpaired Student T-test and One-Way AVOVA, where appropriate. p < 0.05 was taken as statistically significant and represented by *, p<0.01 was represent by ** and p<0.001 was represented by ***.

5.9 Discussion

The aim for this chapter was to test the effects of inhibiting or reducing the activity of CIII, CIV and CV on ROS levels and whether blocking or slowing down the exit of electrons from the ETC triggers ROS-RET. To do this, I used both chemical inhibition and genetic depletion of the three respiratory complexes mentioned, to achieve both short- and long-term inhibition, respectively. ROS measurements were taken in order to detect changes in the levels of mitochondrial ROS in the fly brain and different inhibitors were used to dissect where and how ROS were being generated. Although an increase in ROS was identified during both CIII and CIV inhibition, rotenone, an established RET inhibitor, did not decrease ROS levels. Thus showing that RET was not the mechanism responsible for ROS production, when CIII and CIV were inhibited. These results collectively show that in order to stimulate RET via manipulation of the ETC; preventing the exit of electrons to increase the reduction of CoQ pool is not sufficient. This could be due to the fact that pmf is reduced, resulting from a decrease in proton pumping by blocking CIII and CIV, which would prevent RET.

When using long-term genetic inhibition of CV, by silencing *ATPsyn δ* , an increase in ROS production, which was abolished by rotenone, was detected. This could be indicative that a reduction in CV activity, triggers RET. However, experiments blocking CV with oligomycin did not show the same result, so the effect of blocking/depleting CV on ROS-RET remains inconclusive. I tried to use two new proposed inhibitors of CV, AKG and J147 that have been reported to increase lifespan in worms and flies, respectively (Goldberg *et al.*, 2018) (Chin *et al.*, 2014b). However, in contrast to previous reports, I did not find any evidence of CV inhibition in fly homogenates. To the best of my knowledge, there is no published report showing direct inhibition of *Drosophila* CV for any of them and this is the first report testing their efficiency in fly mitochondria.

Chemical inhibition of CIII, using myxothiazol, showed varying results according to the concentration used. The lowest dose, 10 μ M, did not achieve inhibition of respiration and additionally had no effect on ROS production, therefore deeming this concentration of myxothiazol redundant for these experiments. Although no statistically significant inhibition of respiration was observed using 50 μ M of myxothiazol, it did elicit a response when measuring ROS levels. This is similar to

results shown in Chapter 3, where smaller doses of rotenone were not shown to significantly inhibit respiration but increased ROS production to the same extent as higher doses, which did significantly reduce respiration. However, in the case of myxothiazol, a concentration of 50 or 100 μM , decreased ROS both at 25 and 32°C, whereas rotenone had the opposite effect at both temperatures. This indicates flexibility in the way CI produces ROS that changes from a forward to a reverse direction depending on the temperature, which CIII does not seem to demonstrate.

Data from other studies have also shown that low doses of myxothiazol decrease ROS production at the Q_o site. This is due to myxothiazol preventing the binding of CoQ to the Q_o site and the subsequent transfer of electrons. My data suggests that in normal conditions, (25°C), the Q_o site of CIII is an important generator of ROS, although further experiments are required to confirm this. Under HS, flies treated with low doses of myxothiazol were still able to trigger ROS-RET but at a lower intensity than non-treated controls. I speculate that this is caused by a slight but significant reduction in proton pumping and therefore the pmf, as a result of decreasing the transfer of electrons through CIII. This has been shown in mammalian mitochondrial where a progressive reduction in the pmf, reduces ROS-RET (Robb *et al.*, 2018). However, to confirm the former point, the pmf would need to be measured, which is not an easy task in whole fly brains.

High doses of myxothiazol $\geq 500 \mu\text{M}$, increased ROS production independently of the temperature, or the presence of rotenone. These results clearly show that ROS are not produced via RET, under these circumstances. However, it is not possible to discard CI as the source of ROS completely, given that higher concentrations myxothiazol also inhibits CI (Bacsi *et al.*, 2006). Similarly, the genetic inhibition of CIII, via knocking-down *UQCR-Q*, led to a significant increase in ROS production. Corresponding to the results using high doses of myxothiazol, the increase in ROS was not reversed by the presence of rotenone. Collectively, the results from CIII inhibition show that RET cannot be induced using both chemical and genetic inhibition. Despite the possibility of a highly-reduced CoQ pool being established through CIII inhibition, the loss of two complexes involved in proton translocation (CIII-CIV), would prevent the generation of the pmf, required for RET. Accordingly previous studies have shown a decrease in membrane potential upon addition of myxothiazol. In conclusion, short-term chemical inhibition using 5 doses of

myxothiazol or knock-down of a CIII subunit, was not able to stimulate a ROS-RET response.

Both forms of CIV inhibition, using CN and *levy*-KD flies, for chemical and genetic depletion respectively, elicited the same response in ROS production. In each case, there was a significant increase in ROS, which was maintained when flies were fed with rotenone. These data demonstrated that RET was not occurring, as rotenone should have prevented this increase in ROS production, if CIV inhibition had successfully initiated RET. To understand where this increase in ROS was originating from, other inhibitors of the ETC were used. Myxothiazol (100 μ M) reversed the increase in brain ROS levels when CIV was inhibited or depleted, indicating the Q_o site within CIII as the source of ROS production. The results show that ROS-RET cannot be initiated through short-term (chemical) or long-term (genetic) inhibition of CIV. Although a highly reduced CoQ pool could be achieved through CIV inhibition, it is unlikely that the second condition of RET, a high membrane potential, would be established. In fact, CIV inhibition would lead to reduced proton translocation to the IMS, therefore lowering the pmf. This may provide an explanation as to why RET cannot be stimulated. The former has been observed in a mouse model where the CIV subunit COX15 is knocked out, specifically in skeletal muscle. The mutant mice have a highly reduced CoQH₂:CoQ ratio and elevated ROS levels compared to the controls but the membrane potential is decreased (Dogan *et al.*, 2018). Suggesting that ROS are not being produced by RET, therefore supporting the data I obtained. The authors claim that mitochondria from the *COX15 KD* mice, produce ROS through the stimulation of RET, due to the fact that AOX abolished the excessive ROS production. However, as previously demonstrated AOX can reduce ROS induced by antimycin, at the Q_o site of CIII (Sanz *et al.* 2010), as well as ROS produced via RET. Paradoxically, decreasing ROS levels in the *COX15 KD* mice, using the co-expression of AOX and antioxidants, did not ameliorate the phenotype but in fact caused the mice to die faster than the *COX15 KD* mice alone. This was due to impaired mitochondrial myopathy caused by the decreased ROS production. In contrast, AOX extends the lifespan of another mutant mouse model; *Bcs1l^{p.S78G}* knock-down mice. This mouse model displays defective CIII, which induces elevated ROS production (Rajendran *et al.*, 2019). Interestingly, results indicate that AOX does not alleviate the phenotype through the reduction of ROS levels but rather by partially restoring respiration, proton pumping through CI and recycling reduced

CoQH₂. Thus, leading to the partial restoration of numerous metabolic routes such as CAC, pyrimidine synthesis and glycolysis. Overall, these results suggest that inhibition CIII and CIV can result in the production of ROS at different sites of the mitochondrial respiratory chain. Additionally, depending on the specific sites of ROS production they can promote different downstream physiological effects. Based on the results of the studies discussed above, in these mutant models the reduction of ROS can elicit positive or negative outcomes, which is dependent on the location of generation. These data support the results I obtained in my thesis, using the CIII/CIV inhibition models, by displaying increased ROS production by blocking the flow of electrons through CIII and CIV, which are not ROS-RET dependent. In addition these models allow the possibility of studying the downstream physiological effects of ROS produced as a result of blocking CIII and CIV.

Contrasting results were obtained when CV was chemically inhibited with oligomycin or depleted using an RNAi construct against *ATPsynδ*. Several experiments exposing flies to different concentrations of oligomycin, for different periods of time (hours or days), failed to show any increase in ROS levels in the fly brain. Furthermore, oligomycin attenuated ROS-RET in two different models, HS and Ndi1 flies. The latter has been shown before both in mammalian cells and in isolated fly mitochondria, where oligomycin reduces ROS in conditions where RET is active, such as exposition to LPS, staurosporine or blocking of CV (Mills *et al.*, 2016a) (Sanz *et al.*, 2010c) (Santamaria *et al.*, 2006) (Mills *et al.*, 2016a). These results therefore support my results obtained from feeding oligomycin to HS and Ndi1 fly models, which both displayed a decrease in ROS. This indicates that blocking CV, in situations where RET is occurring, can abolish the increase in ROS.

Oligomycin has been reported to increase ROS in isolated mitochondria and several cell types (including *Drosophila* S2 cells) (Liu and Schubert, 2009). However, to the best of my knowledge, there have been no studies about mitochondrial ROS levels in the *Drosophila* brain. AKG and J147 have been reported to extend lifespan in worms and flies by inhibiting CV and triggering a ROS signal that attenuates TOR signalling (Goldberg *et al.*, 2018) (Chin *et al.*, 2014b). I hypothesized that the ROS could be generated by RET, leading to a similar lifespan extension observed in Ndi1. However, I did not find any evidence that either of the two inhibitors target CV *in vitro*. Although the results from depleting *ATPsynδ* support that long-term inhibition of CV triggers ROS-RET, these results must be approached with caution since the flies

were extremely weak and the decrease observed with rotenone administration, could be caused by a collapse of the membrane potential, rather than blocking RET. I observed a similar result when I overexpressed ATP1F1 (Figure 5.18). The overexpression of ATP1F1 lead to a dramatic increase in ROS that was attenuated with rotenone, indicative of RET stimulation, without altering O₂ levels. However, I could not confirm the overexpression of the gene and did not observe any decrease in oxygen consumption, therefore the definitive conclusion about the role of CV in ROS-RET requires to be addressed in the future. The laboratory which created the OE flies did not carry out qPCR or any other method of confirmation therefore it is possible that the flies do not overexpress ATP1F1. In the future it would be of interest to try and confirm the OE of ATP1F1 so that the results gained in Figure 5.18 could be validated, supporting the hypothesis that CV inhibition can induce ROS-RET.

In summary, my results indicated that CIII and CIV inhibition increased ROS production through an alternative mechanism to RET in the fly brain, whereas the effect of CV inhibition on ROS-RET requires further investigation.

Chapter 6 A Genome-Wide RNA Interference screen to identify genes involved in the regulation of ROS-RET

6.1 The importance of genome-wide RNA interference screens

RNA interference (RNAi) is a powerful genetic tool in which the introduction of double-stranded RNA molecules can promote degradation of a targeted sequence, thereby allowing the genetic silencing of a single gene product (Ni and Lee, 2010). This technology enables the reverse genetic approach in revealing a gene's function within a cell, through its inhibition (Mohr and Perrimon, 2012). The potential of reverse genetics has been harnessed, to carry out large scale genome-wide RNAi screens (Mohr *et al.*, 2010). This systematic and unbiased approach allows the individual knockdown of genes, within an entire genome, to reveal those that produce a specific phenotype when inhibited, giving rise to the identification of novel genes involved in several biological pathways (Perrimon *et al.*, 2010). At present, genetic screening has commonly been performed in models such as *C.elegans*, mammalian cells and *Drosophila melanogaster*, amongst others. Since the first genome-wide RNAi screen, using *Drosophila* cells; they have provided a vast amount of insight into a wide range of important processes. *Drosophila* screens alone have been able to discover genes involved in circadian rhythm (Sathyanarayanan *et al.*, 2008), signalling (Kategaya *et al.*, 2009), cell cycle (Bjorklund *et al.*, 2006), infectious diseases (Foley and O'Farrell, 2004) and mitochondrial function (Chen *et al.*, 2008). Due to the complete sequencing of the *Drosophila* genome, this makes flies an extremely useful model for carrying out *in vivo* high-throughput genetic screens. In addition, the availability of RNAi lines for the majority of fly genes provides the opportunity for genome-wide screening. The aim of this chapter was to take advantage of this technique to identify genes with a role in the regulation of mitochondrial ROS.

6.2 The use of the alternative oxidase; AOX

Present in the mitochondria of plants and fungi are alternative oxidases, which can bypass specific components of the ETC, namely respiratory complexes I, III and IV. Alternative respiratory enzymes are divided into two groups: those that give electrons to the CoQ pool, called NADH dehydrogenases, and those that extract electrons from the CoQ pool, called alternative oxidases (McDonald and Gospodaryov, 2019).

NADH dehydrogenases, such as Ndi1, oxidise NADH to NAD⁺ and transfer electrons to CoQ, by-passing CI. On the other hand, alternative oxidases, such as AOX, use electrons from ubiquinol to reduce O₂ to water, by-passing complexes III and IV. Neither of these systems partake in the direct translocation of protons across the IMM. For my screen, I took advantage of the alternative oxidase, AOX, from *Ciona intestinalis*. AOX was cloned and introduced into the fly genome in the laboratory of Professor Howy Jacobs in Tampere (Finland) (Fernandez-Ayala *et al.*, 2009). AOX resides in the IMM of the mitochondria and can reduce O₂ to water directly with electrons from CoQH₂, thereby supporting electron transport without the need for a functional CIII or CIV (Figure 6.1). Previous studies have shown that the expression of AOX confers resistance to chemical inhibitors of CIII and CIV, as well as reversing lethality caused by genetic modifications to the subunits of CIV (Kemppainen *et al.*, 2014) (Dogan *et al.*, 2018) (Rajendran *et al.*, 2019). These studies have also demonstrated that the phenotypic rescue conferred by AOX during CIII or CIV inhibition, occurs in parallel to a decrease in ROS levels (Rajendran *et al.*, 2019) (Dogan *et al.*, 2018) (Sanz *et al.*, 2010a).

It has been established that AOX is able to reduce ROS-RET elicited by ectopic expression of Ndi1 (Scialo *et al.*, 2016a), or physiological exposure of flies to HS (Scialo, unpublished). Similarly, AOX is able to decrease ROS-RET in mice when RET is induced by injecting mice with LPS (Mills *et al.*, 2016a). In addition to ROS-RET, AOX is able to attenuate the increase in ROS produced by CIII, when inhibited by antimycin in mouse cells (El-Khoury *et al.*, 2013) (Cannino *et al.*, 2012) and fly mitochondria (Sanz *et al.*, 2010a). Given that AOX is capable of neutralising both CIII-derived ROS and ROS-RET, I undertook a genome-wide RNAi screen, using co-expression of AOX with RNA interference constructs, targeted against specific *Drosophila melanogaster* genes, to identify novel genes involved in the regulation of ROS production. In the previous results chapters, I attempted to identify approaches which could initiate RET, physiologically in the fly. Therefore my aim for this chapter was to then further identify other genes that controlled the levels of ROS, focusing on those that participate in ROS-RET.

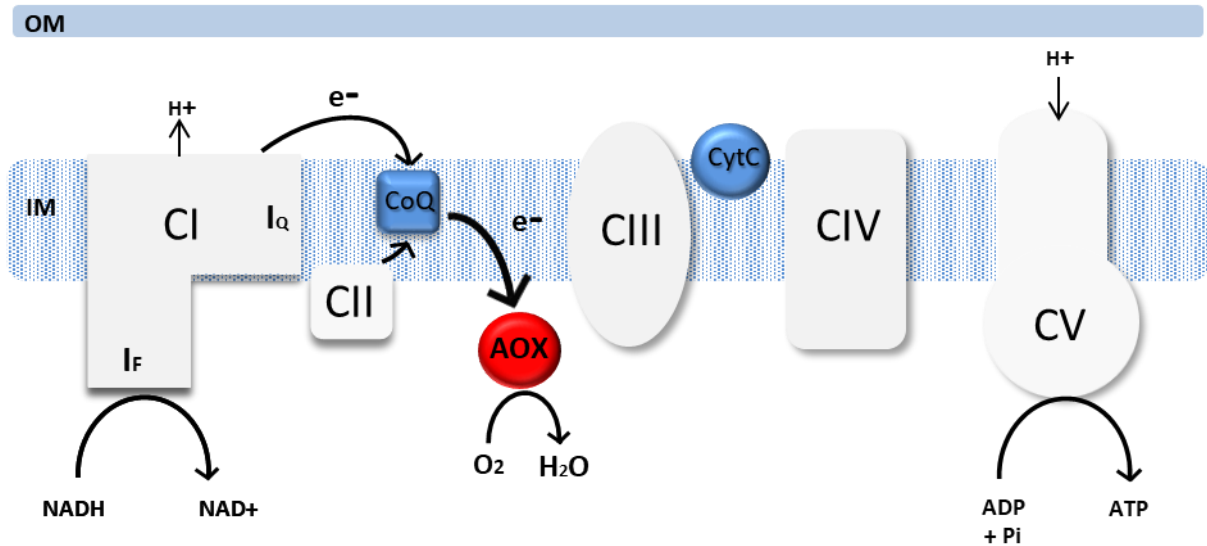


Figure 6.1 Schematic diagram showing how the expression of AOX by-passes CIII and CIV.

AOX resides on the matrix side of the IMM where it takes electrons directly from the ubiquinol pool, reducing O₂ into water, therefore bypassing respiratory CIII and CIV.

6.3 Hypothesis behind the screen

It has been well established that mitochondrial ROS signalling is required for maintaining cellular homeostasis (Shadel and Horvath, 2015). However, any imbalances in the redox signalling system can trigger oxidative stress. For example, ROS-RET seems to regulate many physiological processes, such as triggering appropriate cardiorespiratory responses to hypoxia (Fernandez-Aguera *et al.*, 2015) or activation of macrophages in the presence of pathogens (Mills *et al.*, 2016a). Nevertheless, in all redox-regulated processes, exquisite control of ROS levels is critical to prevent oxidative damage. In the case of IR, a pathological example of ROS-RET, ROS production is unregulated and produced under dysfunctional circumstances, resulting in tissue injury caused by excess ROS levels (Chouchani *et al.*, 2014b). Due to AOX's ability to decrease ROS production at CIII and prevent ROS-RET from occurring, I used the expression of AOX to identify genes involved in regulating ROS levels, during development. I hypothesised that the downregulation of genes involved in the maintenance of basal ROS levels, or switching off ROS-RET signal, would lead to dysfunctional ROS production and ultimately generate a lethal phenotype. Under these circumstances, expression of AOX would lead to the reduction of ROS levels and rescue or palliate any lethal phenotype, therefore allowing me to identify novel genes responsible for the regulation of mitochondrial ROS production, *in vivo* (Figure 6.2).

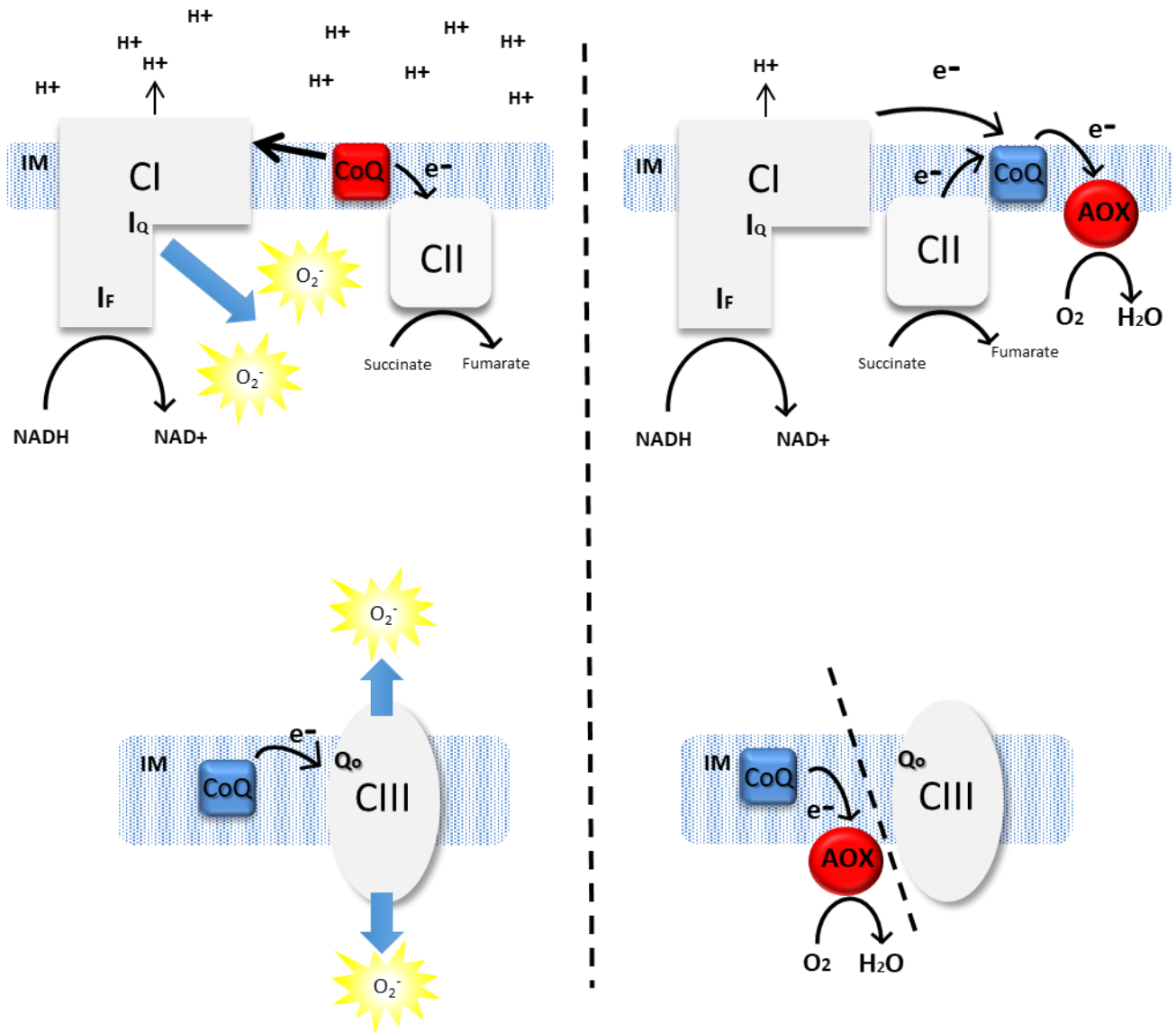


Figure 6.2 Schematic diagram showing how the expression of AOX can manipulate ROS production from the ETC and rescue lethal phenotypes in KD lines.

In the left panel (without AOX expression) the KD of genes involved in regulating RET and CIII ROS production will cause excessive generation of ROS leading to a lethal phenotype. However, the expression of AOX, which prevents ROS-RET (through the oxidation of ubiquinol) and decreases CIII ROS production (through the reduction of electrons entering CIII) will rescue the lethal phenotype.

6.4 Screening strategy

The screening strategy employed was based on the use of RNAi constructs targeted against specific fly genes, in combination with the Gene Switch GAL4 (GS) system, to allow spatial and temporal control of gene expression, previously explained in Chapter 2. The synthetic progesterone analogue mifepristone (RU-486) was used to drive RNA interference (and AOX) expression, during development. Figure 6.3 summarises the overall strategy of the screen. UAS-RNA interference (RNAi) male flies were selected and crossed with virgin female flies carrying the *Tubulin-GS* driver alone (control group) or in combination with the *UAS-AOX* construct (AOX group). These crosses were then placed in vials of food containing 1 μ M RU-486 and left to mate and lay eggs for 5 days, after which adults flies were discarded from the vials and eggs were left to develop. After 10 days the vials were scored for the presence of larvae, pupae or adult flies, which was then repeated for 2 consecutive days. Selection of candidate genes depended on the rescue of any developmental delay or lethal phenotype by AOX expression. The rescue was identified as the absence of larvae, pupae or adults in the control group and their presence in the AOX group.

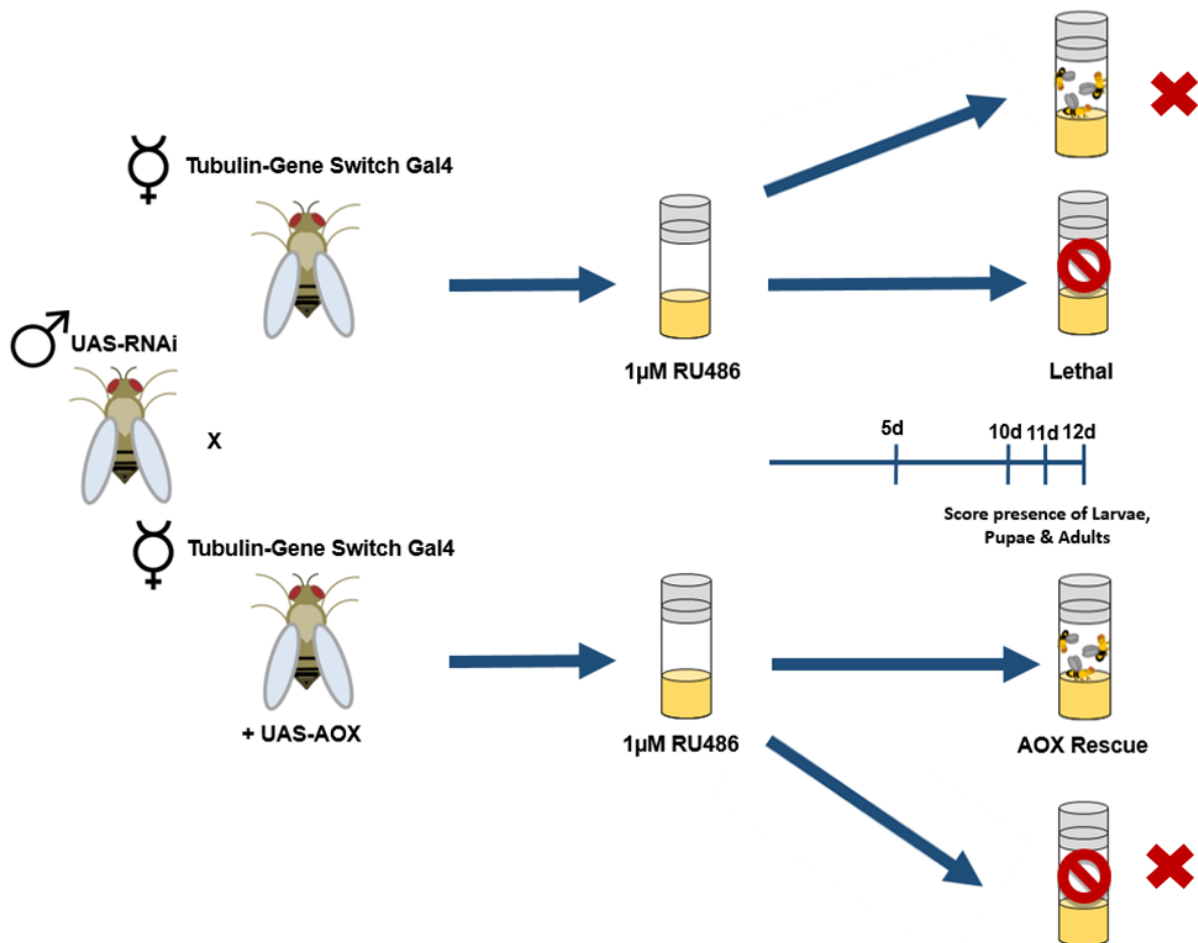


Figure 6.3 Diagram displaying the strategy of the genome-wide RNAi screen.

UAS-RNAi male flies were crossed with control virgin females and UAS-AOX virgin females. The flies were placed in vial of food containing 1 μM drug (RU-486) and after 10 days the vials were scored for the presence of larvae, pupae or adult flies. Selection of candidate genes depended on rescue of any developmental delay or lethality phenotype by AOX expression. Therefore lines, which had normally developed flies in the control or those showing a lethal phenotype in the presence of AOX were discarded.

6.5 Analysis of the identified hits

I screened 12,719 different RNAi lines from the VDRC RNAi Library (Dietzl *et al.*, 2007), covering 12,372 genes (>90% of the fly genome). From the first list of screened hits, I discarded any lines that were screened more than once, which did not produce the same result, in the different trials. Then, I started my analysis with 12,575 unique RNAi lines targeting 12,234 genes. The knockdown of 1,448 genes (12% of the total screened) caused a lethal phenotype (Table 6.1). Most lethal genes caused interruption of development at the pupal stage (61%), whereas only 8% of genes did not produce larvae when knocked down (Table 6.1). AOX rescued the lethal phenotype of 322 genes, (22% of total lethal genes), with most of the rescues occurring when development was arrested at the pupal stage (57%), versus embryonic and larval stages (18% and 25%, respectively) (Table 6.1).

Next, I performed Gene Ontology (GO) term enrichment analysis, using those genes that caused a lethal phenotype. I used the Functional Annotation Clustering Analysis tool from DAVID (Huang *et al.*, 2009) to select clusters of genes containing specific enriched terms. According to GO analysis (Table 6.2) most genes that were identified as lethal were related to “splicing” (Annotation Cluster 1), “cytosolic and mitochondrial translation of proteins” (Annotation Cluster 2), “nucleotide-binding” (Annotation Cluster 3), “transcription” (Annotation Cluster 4) and “cell cycle/division” (Annotation Cluster 5). These results are unsurprising since interrupting any of the former processes is expected to disrupt development. I found the term “mitochondrion” in Annotation Cluster 6, and “mitochondrial electron transport” term in Annotation Cluster 20 (data not shown). Based on the former results, I manually inspected genes encoding OXPHOS components and found that 36 out of 87 genes screened, caused a lethal phenotype (41%) (Table 6.3). Between 40-60% of the genes encoding for CIII, CIV and CV subunits were lethal, whereas the same was true for fewer than 40% of the genes encoding for subunits of the other respiratory complexes (Table 6.3). AOX rescued 100% of lethal genes encoding CIV subunits and 67% of those encoding CIII subunits, whereas for the other respiratory complexes only 1 gene was rescued for each. Furthermore, a rescreen of the positive hits confirmed 100% of the genes encoding complexes III and IV subunits but none of those encoding for subunits of the other respiratory complexes (Table 6.4). Interestingly, none of the genes encoding antioxidants caused lethality when knocked down (data not shown). The latter was not completely unexpected since, in

different animal species, it has been shown that antioxidant levels can be drastically abolished without interrupting development (Martin *et al.*, 2009) (Van Remmen *et al.*, 2003) (Elchuri *et al.*, 2005) (Van Raamsdonk and Hekimi, 2012) (Doonan *et al.*, 2008).

Given that *Drosophila* RNAi lethality screens are prone to both false positives and negatives (Dietzl *et al.*, 2007), I rescreened 189 RNAi lines. I selected 156 (78%), 42 (21%) and 6 (3%) lines where AOX rescued pupal, larval and embryonic lethality, respectively. The different number of lines rescreened was intended to reflect the different % of genes rescued by AOX at the three different stages. However, I chose to screen more lines rescued at the pupal stage rather than embryonic stage because the latter is more prone to suffer from false positives, caused by bacterial growth on food. I confirmed 41 hits (20%) as AOX rescue (Table 6.5), indicating that my screen strategy was prone to false positives. This was not unexpected and has been reported before in other RNAi fly screens (Fukuoh *et al.*, 2014). In the rescreen list, 11 OXPHOS genes were included. Interestingly, the 11 genes were lethal again in the rescreen but only the 8 genes encoding subunits of CIII-CIV were rescued by AOX this time. This indicates that rescreening is required, to confirm AOX rescue hits. Accordingly, positive hits that were not rescreened this time should be rescreened in the future.

The motivation behind the screen was to identify novel genes involved in the regulation of mitochondrial ROS. A large proportion of the 41 confirmed genes rescued by AOX (68% vs 32%), did not contain any reference to mitochondria, according to the GO information contained in Flybase (<https://flybase.org/>). This notable difference could be due to the overall abundance of mitochondrial proteins in a cell being significantly lower than non-mitochondrial. However, further characterisation of these non-mitochondrial genes may reveal a novel relationship involving the mitochondria, which has not been previously established. It is possible that some of the genes identified, encoded protein isoforms that can be targeted to the mitochondrion, however these mitochondrial isoforms have not yet been identified. For example, it has been recently described that mitochondrial isoforms can be produced by non-canonical translation in yeast (Monteuuis *et al.*, 2019). It would be interesting to check whether this phenomenon also occurs in *Drosophila* and whether this applies to any confirmed hits, in my list.

GO analysis of the confirmed rescued candidates showed two clusters of genes

(Table 6.6) containing terms related with “oxidative phosphorylation”, “mitochondrial respiratory chain complex IV” and “mitochondrial respiratory chain complex III”. I also performed network analysis for protein interactions using STRING (von Mering *et al.*, 2005) with default settings. This analysis revealed a clear network connecting all mitochondrial proteins (with the exception of ABCB7). Apart from the mitochondrial genes, only 2 other pair of genes were connected: *CG7071* and *VhPPA1-1* and *Cul3* and *CSN3* (Figure 6.4). Kmeans clustering analysis revealed 3 different clusters with genes encoding ETC proteins, other mitochondrial genes (*mRpS25*, *mRpS26* and *Cchl*) and the rest of genes confirmed as hits.

Using FlyAtlas2 and Flybase to analyse tissue distribution of the AOX rescue hits I found that most genes had ubiquitous expression throughout the whole fly body, with moderate expression within the brain. A few of the hits had high expression on in specific tissues of the fly for example *CG31882*, *CG9853*, *CG42616* and *CG5585*, where expression was mainly localised to the testis. Furthermore, hits such as *CG2079* and *CG16885* had high expression in the gut and trachea, with low expression elsewhere. As expected, those with the high tissue expression throughout the whole body included *CG106604*, *CG9603*, *CG7181*, *CG8784* and *CG4168*, which all encode mitochondrial ETC subunits. From these hits *CG33103*, *CG16885* and *CG7007* had especially high expression in the head, eye and trachea and gut, respectively. Hits with very low tissue expression throughout the body included hits *CG7760*, *CG14230* and *CG7071*.

Table 6.1 Number of genes screened indicating lethal genes and lethal genes rescued by AOX.

Phenotype	Number of Genes	Hits	%	Embryonic Stage	%	Larval Stage	%	Pupal Stage	%
Lethal	12234	1448	12	111	8	450	31	887	61
Rescued	1448	322	22	57	18	81	25	184	57

Table 6.2 Functional Annotation Clustering Analysis of lethal genes.

Annotation Cluster 1		Enrichment Score: 18.1	
Category	Term	Fold Enrichment	Benjamini
GOTERM_BP_DIRECT	GO:0000398~mRNA splicing, via spliceosome	3.2	0.000
GOTERM_CC_DIRECT	GO:0071011~precatalytic spliceosome	3.7	0.000
GOTERM_CC_DIRECT	GO:0071013~catalytic step 2 spliceosome	3.5	0.000
KEGG_PATHWAY	dme03040:Spliceosome	2.2	0.000

Annotation Cluster 2		Enrichment Score: 17.6	
Category	Term	Fold Enrichment	Benjamini
UP_KEYWORDS	Ribonucleoprotein	5.3	0.000
UP_KEYWORDS	Ribosomal protein	5.2	0.000
GOTERM_BP_DIRECT	GO:0032543~mitochondrial translation	4.7	0.000
GOTERM_BP_DIRECT	GO:0002181~cytoplasmic translation	4.1	0.000
GOTERM_CC_DIRECT	GO:0005840~ribosome	4.0	0.000
GOTERM_CC_DIRECT	GO:0005762~mitochondrial large ribosomal subunit	5.3	0.000
GOTERM_MF_DIRECT	GO:0003735~structural constituent of ribosome	2.5	0.000
GOTERM_CC_DIRECT	GO:0022625~cytosolic large ribosomal subunit	4.0	0.000
GOTERM_CC_DIRECT	GO:0022627~cytosolic small ribosomal subunit	4.3	0.000
KEGG_PATHWAY	dme03010:Ribosome	1.4	0.006

Annotation Cluster 3		Enrichment Score: 14.4	
Category	Term	Fold Enrichment	Benjamini
UP_KEYWORDS	Nucleotide-binding	2.0	0.000
UP_KEYWORDS	ATP-binding	2.1	0.000
GOTERM_MF_DIRECT	GO:0005524~ATP binding	1.7	0.000

Annotation Cluster 4 Enrichment Score: 11.8			
Category	Term	Fold Enrichment	Benjamini
UP_KEYWORDS	Transcription	2.4	0.000
UP_KEYWORDS	Transcription regulation	2.2	0.000
UP_KEYWORDS	Activator	3.2	0.000
GOTERM_BP_DIRECT	GO:0006351~transcription, DNA-templated	1.9	0.000

Annotation Cluster 5 Enrichment Score: 6.6			
Category	Term	Fold Enrichment	Benjamini
UP_KEYWORDS	Cell cycle	3.2	0.000
UP_KEYWORDS	Cell division	3.1	0.000
UP_KEYWORDS	Mitosis	3.1	0.000
GOTERM_BP_DIRECT	GO:0051301~cell division	2.4	0.000

Annotation Cluster 6 Enrichment Score: 5.7			
Category	Term	Fold Enrichment	Benjamini
UP_KEYWORDS	Mitochondrion	2.1	0.000
UP_KEYWORDS	Transit peptide	2.5	0.000

Annotation Cluster 7 Enrichment Score: 5.4			
Category	Term	Fold Enrichment	Benjamini
GOTERM_BP_DIRECT	GO:0000470~maturation of LSU-rRNA	6.6	0.000
GOTERM_CC_DIRECT	GO:0030687~preribosome, large subunit precursor	4.1	0.000
GOTERM_BP_DIRECT	GO:0000460~maturation of 5.8S rRNA	6.7	0.006

Annotation Cluster 8 Enrichment Score: 5.2			
Category	Term	Fold Enrichment	Benjamini

GOTERM_MF_DIRECT	GO:0003899~DNA-directed RNA polymerase activity	5.4	0.000
GOTERM_CC_DIRECT	GO:0005666~DNA-directed RNA polymerase III complex	6.4	0.000
UP_KEYWORDS	Nucleotidyltransferase	3.3	0.000
GOTERM_BP_DIRECT	GO:0006383~transcription from RNA polymerase III promoter	6.9	0.000
KEGG_PATHWAY	dme03020:RNA polymerase	3.1	0.000
UP_KEYWORDS	DNA-directed RNA polymerase	6.0	0.000
GOTERM_BP_DIRECT	GO:0006360~transcription from RNA polymerase I promoter	6.0	0.001
GOTERM_CC_DIRECT	GO:0005736~DNA-directed RNA polymerase I complex	5.1	0.006

Annotation Cluster 9		Enrichment Score: 5.1	
Category	Term	Fold Enrichment	Benjamini
UP_KEYWORDS	DNA replication	4.1	0.000
GOTERM_BP_DIRECT	GO:0006260~DNA replication	3.4	0.000
KEGG_PATHWAY	dme03030:DNA replication	2.3	0.014

Annotation Cluster 10		Enrichment Score: 3.9	
Category	Term	Fold Enrichment	Benjamini
UP_KEYWORDS	Aminoacyl-tRNA synthetase	5.9	0.000
UP_KEYWORDS	Ligase	2.2	0.000

Table 6.3 OXPHOS genes screened indicating the number of lethal genes (when knocked-down) and rescued by AOX.

	Genes	Genes Screened	Lethal	%	Rescued	%
CI	48	38	14	37	1	7
CII	6	5	1	20	1	100
CIII	12	10	6	60	4	67
CIV	17	14	6	43	6	100
CV	21	18	9	50	1	11

Table 6.4 OXPHOS genes rescreened indicating the number of lethal genes (when knocked-down) and rescued by AOX.

	Genes	Genes Screened	Lethal	%	Rescued	%
CI	48	1	1	100	0	0
CII	6	1	1	100	0	0
CIII	12	4	4	100	4	100
CIV	17	4	4	100	4	100
CV	21	1	1	100	0	0

Table 6.5 Confirmed candidate genes rescued by AOX

FlyBase Id	Annotation Symbol	Symbol	VDRC ID	Description in STRING
FBgn0035244	CG7955	ABCB7	106039	"ATP binding cassette subfamily B member 7 (ABCB7) is a transporter that likely dimerizes to form a functional transporter. ABCB7 may act in the mitochondria to transport substrates necessary for the maturation of ICS proteins, which are involved in iron homeostasis (743 aa)".
FBgn0265598	CG44425	Bx	109933	"Beadex, isoform B; Beadex (384 aa)".
FBgn0037788	CG3940	CAH7	108233	"CG3940, isoform A; Carbonate dehydratase activity; zinc ion binding. It is involved in the biological process described with- one-carbon metabolic process (304 aa)".
FBgn0024249	CG7760	cato	101564	"Cousin of atonal; Sequence-specific DNA binding transcription factor activity; protein dimerization activity. It is involved in the biological process described with- regulation of transcription, DNA-templated; sensory organ development (189 aa)".
FBgn0038925	CG6022	Cchl	101382	"Cytochrome c heme lyase; Links covalently the heme group to the apoprotein of cytochrome c (281 aa)".
FBgn0032811	CG10268	CG10268	110640	"Phosphomevalonate kinase activity. It is involved in the biological process described with- isoprenoid biosynthetic process; cholesterol biosynthetic process (189 aa)".
FBgn0037543	CG10903	CG10903	109610	"Uncharacterized protein, isoform A; S-adenosylmethionine-dependent methyltransferase activity. It is involved in the biological process described with- neurogenesis; metabolic process (276 aa)".
FBgn0034500	CG11200	CG11200	101697	"Carbonyl reductase (NADPH) activity. It is involved in the biological process described with- metabolic process; Belongs to the short-chain dehydrogenases/reductases (SDR) family (355 aa)".
FBgn0040588	CG13841	CG13841	100876	"annotation not available (120 aa)".
FBgn0031062	CG14230	CG14230	104096	"Probable RNA-binding protein CG14230; mRNA binding; nucleotide binding; nucleic acid binding. It is involved in the biological process described with- neurogenesis (580 aa)".
FBgn0029525	CG18273	CG18273	107818	"LD21943p; It is involved in the biological process described with- neurogenesis (1377 aa)".

FBgn0050373	CG30373	CG30373	104802	"annotation not available (158 aa)".
FBgn0051882	CG31882	CG31882	100160	"annotation not available (121 aa)".
FBgn0260467	CG7071	CG7071	110726	"annotation not available (302 aa)".
FBgn0036173	CG7394	CG7394	101490	"Mitochondrial import inner membrane translocase subunit TIM14; Probable component of the PAM complex, a complex required for the translocation of transit peptide-containing proteins from the inner membrane into the mitochondrial matrix in an ATP-dependent manner. May act as a co-chaperone that stimulate the ATP-dependent activity (By similarity) (128 aa)".
FBgn0086605	CG9853	CG9853	107346	"Golgi to ER traffic protein 4 homolog; May play a role in insertion of tail-anchored proteins into the endoplasmic reticulum membrane (339 aa)".
FBgn0044324	CG10712	Chro	101663	"Chromator, isoform A; Histone binding. It is involved in the biological process described with- metaphase plate congression; chromosome organization; mitotic spindle organization; mitotic anaphase; metamorphosis; chromosome segregation; chromatin organization; mitotic spindle assembly checkpoint (926 aa)".
FBgn0032833	CG10664	COX4	109338	"Cytochrome-c oxidase activity. It is involved in the biological process described with- negative regulation of neuroblast proliferation; cell proliferation; mitochondrial electron transport, cytochrome c to oxygen; mitotic cell cycle; Golgi organization (182 aa)".
FBgn0040529	CG9603	COX7A	106661	"Cytochrome c oxidase subunit 7A, mitochondrial; This protein is one of the nuclear-coded polypeptide chains of cytochrome c oxidase, the terminal oxidase in mitochondrial electron transport (98 aa)".
FBgn0263911	CG7181	COX8	104047	"Cytochrome-c oxidase activity. It is involved in the biological process described with- mitochondrial electron transport, cytochrome c to oxygen (68 aa)".
FBgn0259685	CG6383	crb	39177	"Crumbs, isoform C; Crumbs is a transmembrane protein that binds to multiple proteins such as sdt, par-6, AP-2alpha, yrt, ex and Moe. It contributes to organization of zonula adherens, epithelial morphogenesis, apico-basal cell polarity, and is a negative regulator of Notch activity and growth control via the Hippo pathway. In photoreceptor cells it is involved in morphogenesis, ninaE trafficking and prevention of light-dependent photoreceptor degeneration (2253 aa)".

FBgn0027055	CG18332	CSN3	101516	"COP9 signalosome complex subunit 3; Component of the COP9 signalosome complex (CSN), a complex involved in various cellular and developmental processes. The CSN complex is an essential regulator of the ubiquitin (Ubl) conjugation pathway by mediating the deneddylation of the cullin subunits of the SCF-type E3 ligase complexes, leading to decrease the Ubl ligase activity of SCF. The CSN complex plays an essential role in oogenesis and embryogenesis and is required for proper photoreceptor R cell differentiation and promote lamina glial cell migration or axon targeting. It also promotes [...] (445 aa)".
FBgn0261268	CG42616	Cul3	109415	"Cullin 3, isoform F; Ubiquitin-protein transferase activity; ubiquitin protein ligase binding; Belongs to the cullin family (934 aa)".
FBgn0015031	CG14028	cype	102336	"Cyclope (Cype) is a cytochrome c oxidase subunit VIc homolog acting as an enhancer of dpp pathway phenotypes. Cype is involved in hair and cell growth and in ommatidia development (77 aa)".
FBgn0035600	CG4769	Cyt-c1	109809	"Cytochrome c1, isoform A; Electron transporter, transferring electrons within CoQH2-cytochrome c reductase complex activity; iron ion binding; heme binding. It is involved in the biological process described with- oxidative phosphorylation; mitochondrial electron transport, ubiquinol to cytochrome c (307 aa)".
FBgn0029944	CG2079	Dok	108544	"Downstream of kinase (Dok) is a membrane-associated protein that functions upstream of Shark to activate Jun kinase signaling during embryonic dorsal closure (622 aa)".
FBgn0053810	CG33810	His1:CG33810	109034	"His1-CG33810; DNA binding. It is involved in the biological process described with- chromatin assembly or disassembly; nucleosome assembly (256 aa)".
FBgn0037657	CG11990	hyx	103555	"Hyrax, isoform A; Hyrax is recruited by signaling pathway specific transcriptional regulators such as arm and ci and is important for the output of Wingless and Hedgehog pathways, respectively (538 aa)".
FBgn0019960	CG6455	Mitofilin	106757	"MICOS complex subunit Mic60; Component of the MICOS complex, a large protein complex of the mitochondrial inner membrane that plays crucial roles in the maintenance of crista junctions, inner membrane architecture, and formation of contact sites to the outer membrane (By similarity) (739 aa)".
FBgn0030572	CG14413	mRpS25	101443	"Probable 28S ribosomal protein S25, mitochondrial; Structural constituent of ribosome. It is involved in the biological process described with- translation (167 aa)".

FBgn0036774	CG7354	mRpS26	100067	"Probable 28S ribosomal protein S26, mitochondrial; Structural constituent of ribosome. It is involved in the biological process described with- translation; Belongs to the mitochondrion-specific ribosomal protein mS26 family (225 aa)".
FBgn0011227	CG8764	ox	35829	"Cytochrome b-c1 complex subunit 9; This is a component of the ubiquinol-cytochrome c reductase complex (complex III or cytochrome b-c1 complex), which is part of the mitochondrial respiratory chain. This subunit interacts with cytochrome c1 (By similarity)".
FBgn0003137	CG33103	Ppn	108005	"Papilin; Essential extracellular matrix (ECM) protein that influences cell rearrangements. May act by modulating metalloproteinases action during organogenesis. Able to non- competitively inhibit procollagen N-proteinase, an ADAMTS metalloproteinase; Belongs to the papilin family (2898 aa)".
FBgn0036973	CG5585	Rbbp5	106139	"Retinoblastoma-binding protein 5 homolog; Component of the SET1 complex that specifically di- and trimethylates 'Lys-4' of histone H3 and of the MLL3/4 complex which also methylates histone H3 'Lys-4' (489 aa)".
FBgn0261792	CG5454	snRNP-U1-C	108933	"U1 small nuclear ribonucleoprotein C; Component of the spliceosomal U1 snRNP, which is essential for recognition of the pre-mRNA 5' splice-site and the subsequent assembly of the spliceosome. U1-C is directly involved in initial 5' splice-site recognition for both constitutive and regulated alternative splicing. The interaction with the 5' splice-site seems to precede base-pairing between the pre-mRNA and the U1 snRNA. Stimulates commitment or early (E) complex formation by stabilizing the base pairing of the 5' end of the U1 snRNA and the 5' splice-site region (By similarity). Regulat [...] (145 aa)".
FBgn0038320	CG4931	Sra-1	108876	"Cytoplasmic FMR1-interacting protein; Specifically Rac1-associated protein 1 (Sra-1) is an essential protein that is a component of the WAVE actin nucleator complex that controls actin cytoskeleton remodeling and also interacts with Fmr1 and Rac1. Sra-1 controls morphogenesis and synapse organization (1291 aa)".
FBgn0015828	CG10415	TfIIealpha	100572	"Transcription factor IIealpha (TfIIealpha) is the large subunit of the RNA polymerase II general transcription factor TFIIE. TfIIealpha, together with TfIIebeta, is essential for transcription initiation in vitro and acts with RNA polymerase II and the other general transcription factors (429 aa)".
FBgn0250814	CG4169	UQCR-C2	100818	"Ubiquinol-cytochrome-c reductase activity; metal ion binding. It is involved in the biological process described with- mitochondrial electron transport, ubiquinol to cytochrome c (440 aa)".

FBgn0036728	CG7580	UQCR-Q	101371	"Ubiquinone binding; ubiquinol-cytochrome-c reductase activity. It is involved in the biological process described with- mitochondrial electron transport, ubiquinol to cytochrome c (89 aa)".
FBgn0032538	CG16885	Vajk2	102569	"annotation not available (270 aa)".
FBgn0028662	CG7007	VhaPPA1-1	47188	"Vacuolar H ⁺ ATPase PPA1 subunit 1, isoform A; Proton-transporting ATPase activity, rotational mechanism; hydrogen ion transmembrane transporter activity. It is involved in the biological process described with- ATP hydrolysis coupled proton transport; mitotic spindle organization; Belongs to the V-ATPase proteolipid subunit family (212 aa)".

Table 6.6 Functional Annotation Clustering Analysis of lethal genes rescued by AOX.

Annotation Cluster 1		Enrichment Score: 3.8	
Category	Term	Fold Enrichment	Benjamini
KEGG_PATHWAY	dme00190:Oxidative phosphorylation	9.8	0.000
GOTERM_MF_DIRECT	GO:0004129~cytochrome-c oxidase activity	51.6	0.002
GOTERM_BP_DIRECT	GO:0006123~mitochondrial electron transport, cytochrome c to oxygen	80.9	0.040
GOTERM_CC_DIRECT	GO:0005751~mitochondrial respiratory chain complex IV	65.1	0.014
<hr/>			
Annotation Cluster 2		Enrichment Score: 2.4	
Category	Term	Fold Enrichment	Benjamini
KEGG_PATHWAY	dme00190:Oxidative phosphorylation	9.8	0.000
GOTERM_CC_DIRECT	GO:0005750~mitochondrial respiratory chain complex III	110.5	0.000
GOTERM_BP_DIRECT	GO:0006122~mitochondrial electron transport, ubiquinol to cytochrome c	80.9	0.002
GOTERM_MF_DIRECT	GO:0008121~ubiquinol-cytochrome-c reductase activity	77.4	0.013

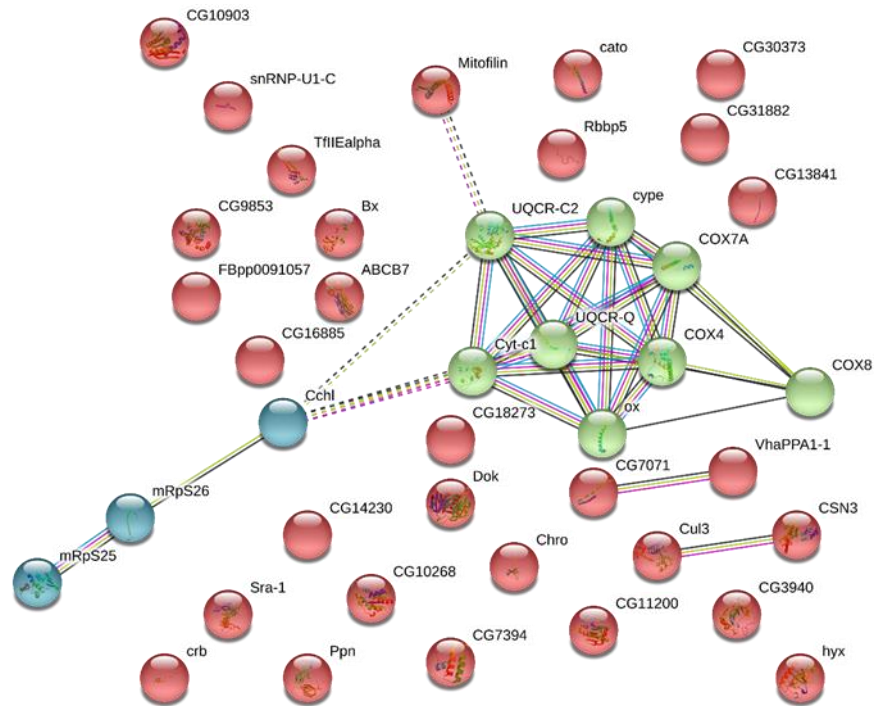


Figure 6.4 Schematic diagram of STRING analysis showing protein interactions between the 41 confirmed hits.

The mitochondrial genes, mostly consisting of subunits of the respiratory complexes III and IV and other mitochondrial proteins, are shown in green and blue. Two other connections also revealed were Cul3 and CSN3, as well as CG7071 and VhaPPA1-1.

6.6 Selection criteria of candidate genes

To further characterise the AOX rescue hits and test whether they were able to alter mitochondrial ROS levels, I measured mitochondrial ROS in the brain of selected RNAi lines. I used a specific selection criterion to comprise a shorter list of 12 confirmed genes rescued by AOX. Selection of candidate genes was firstly dependent on the possession of human orthologues. This was important to identify genes involved in the regulation of RET that are also conserved in humans, giving the potential for future therapeutics involved in targeting ROS signalling. The second criterion was a moderate to high expression of the target gene in the head of the fly during early adulthood, according to data reported in Flybase in the “Expression Data” section. This was important due to the fact that ROS would be measured in the brain of the young fly.

Table 6.5 outlines a brief description of each of the candidate genes including location and function within the cell. The only exception of these criteria was the gene CG30373, an uncharacterised *Drosophila* gene, unknown to possess any human homologues. This gene was chosen to validate the AOX rescue phenotype even further, by testing a gene of unknown function. This approach could also help reveal the different roles of ROS in different species (i.e. insects *versus* mammals) and how ROS levels are regulated, specifically in the fruit fly. From the remaining 11 confirmed genes, 4 hits were well-characterized mitochondrial proteins whereas the rest had not been reported to possess any association with mitochondria, to the best of my knowledge. The genes encoding mitochondrial proteins were *Cchl* (CG6022), *ABCB7* (CG7955), *Mitofilin* (CG6455) and *mRpS25* (CG14413). *ABCB7* and *Cchl* are involved in the processing of heme groups. *ABCB7* (ATP-binding cassette subfamily B member-7) encodes a mitochondrial inner membrane heme transporter, important for delivering iron to proteins containing Fe-S clusters (Sato *et al.*, 2011). *Cchl* (cytochrome c heme lyase) is found in the IMS and functions to aid the assembly of Cyt C, by providing the heme group (Babbitt *et al.*, 2017). This heme is instrumental in the transfer of electrons from CIII to CIV. Another inner mitochondrial membrane protein is Mitofilin, in charge of maintaining mitochondrial cristae structure and contact sites with the ER, organisation of respiratory complexes and regulation of mitochondrial protein import (Xu *et al.*, 2015). The final mitochondrial gene encoding mRpS25 (mitochondrial ribosomal protein subunit 25), is a structural component of the mitochondrial ribosome and is required for the synthesis of mitochondrial

proteins, encoded by genes arranged in the mitochondrial DNA (Bugiardini *et al.*, 2019a).

Another candidate gene included the uncharacterised fly gene, *CG7071*, whose human homologue TMEM199 is a transmembrane protein. In yeast, this protein is responsible for the assembly of the proton pump, Vacuolar H⁺ ATPase (V-ATPase) (Vajro *et al.*, 2018). Interestingly a gene encoding the subunit 1 of the Vacuolar H⁺ ATPase PPA1 (*VhaPPA1-1*) (*CG7007*) was another confirmed AOX rescue hit. As expected STRING network analysis showed that both these genes interact with each other (Figure 6.4), since TMEM199 ensures the correct assembly of the V_o domain embedded in the membrane, where *VhaPPA1-1* resides. The role of this V-ATPase is the translocation of protons into endomembrane organelles and vesicles such as lysosomes and Golgi apparatus, to maintain a low pH required for digestion of damaged protein and organelles (Hirata *et al.*, 1997).

The final 5 hits were *CG11200* (*carbonyl reductase*), *Cul3* (*Cullin3*), *Ppn* (*Papilin*), *GET4* (*CG9853*) and *crb* (*crumb*). *CG11200* is an enzyme from a superfamily of short-chain dehydrogenase/reductase (SDR) (Zhang *et al.*, 2014), specifically with a role as an NADPH-dependent carbonyl reductase involved in the reduction of carbonyl groups, where NADPH serves as the donor (Sgraja *et al.*, 2004). *Cul 3* is an ubiquitin ligase protein, involved in the ubiquitination of damaged proteins targeted for degradation (Tan *et al.*, 2017). *Ppn* is an extracellular matrix protein, required for the arrangement of the extracellular matrix, during development (Fessler *et al.*, 2004). *GET4* is required for the transport of tailor-anchored proteins from the Golgi to the endoplasmic reticulum (Gristick *et al.*, 2014). The final candidate gene is *crb* a transmembrane protein involved in the organisation of the epithelia and establishment of cellular polarity (Guerin *et al.*, 2017).

6.7 Effect of knocking down candidate genes on brain mitochondrial ROS levels

After comprising a list of 12 candidate genes rescued by AOX, I wanted to test whether they participate in regulating mitochondrial ROS levels. To achieve this, I measured ROS levels in the brains of the lines, carrying RNAi constructs against the candidate genes and their respective controls. To overcome the lethality observed as a result of knocking down the genes during development, I fed the flies RU-486 only after eclosion. Thus, limiting the depletion of the protein only during adulthood. I measured ROS in the brains of 10 day old flies. From the list, 10 out of the 12 genes had increased ROS levels when knocked down during adulthood (Figure 6.5).

The two candidate genes that did not show a significant increase in ROS were *mRpS25* and *CG11200*. It was surprising that downregulation of *mRpS25* did not elicit an increase in ROS, due to the fact that it is responsible for the direct translation of the components from the ETC, encoded by mitochondrial DNA. It is known that disruption of the respiratory chain components can lead to dysfunction and increased ROS production, which is commonly observed in mitochondrial diseases (Kirkinetzos and Moraes, 2001). Therefore, it was expected that the reduction of CIII and CIV subunits, resulting from the KD of *mRpS25*, would also lead to an increase in ROS production. Mutations in mitochondrial ribosomal proteins (MRP) subunits have been previously reported in patients clinically diagnosed with mitochondrial disorders (Menezes *et al.*, 2015). A recent study showed that a patient suffering from mitochondrial encephalomyopathy, resulting from mutated MRPS25 (human orthologue of *mRpS25*), had decreased expression of CI, CIII and CIV (Bugiardini *et al.*, 2019b). Although ROS levels in *mRpS25* mutants have not been reported elsewhere, MRPL35, which encodes a protein in the large subunit of the mitochondrial ribosome, leads to elevated ROS levels, when down-regulated *in vitro* (Zhang *et al.*, 2019). Similarly, in Chapter 5, I have shown that knockdown of subunits of CIII, CIV and CV increases mitochondrial ROS levels in the fly brain. However, I did not observe any significant change in ROS, when I knocked down *mRpS25*. It is possible that AOX rescued the lethal phenotype not by reducing ROS production but instead by improving electron transport and therefore overcoming any dysfunction occurring, due to the reduced activity of CIII and CIV. Interestingly, another MRP subunit (*mRpS26*) was also confirmed in my rescreen, which needs to be rescreened in the future (data not shown). Checking ROS levels in these other subunits could help to clarify the effect of interrupting mitochondrial translation on

ROS production. Furthermore, rescreening all the genes encoding mitochondrial ribosomal subunits in different conditions, such as using a different concentration of RU-486 or a different driver, could produce different results. Therefore, the question of whether interruption of mitochondrial translation increases ROS or not, remains unanswered. The second candidate gene which failed to show any rise in mitochondrial ROS levels was, *CG11200*, the predicted fly orthologue of the human dehydrogenase/reductase X-linked (DHRSX). DHRSX is a short-chain dehydrogenase/reductase (SDR). Another member of the SDR superfamily, DHRS2 (dehydrogenase/reductase 2), was found to be down-regulated in tumorous tissue associated with oesophageal cancer. In this cancer model, decreased activity of DHRS2 led to increased mitochondrial ROS production, *in vitro* (Zhou *et al.*, 2018). It is possible that the knockdown of *mRpS25* and/or *CG11200* causes an increase in ROS only during development or in different tissues (or cell types) aside from the brain. Measuring mitochondrial ROS during development or in other tissues may produce a different result and explain why AOX rescued the lethal phenotype, without altering ROS production in the brain. Despite the two hits that did not exhibit an effect on ROS levels, the results from the other 10 candidate genes show that using AOX expression is a promising new strategy to reveal genes that possess a regulatory role in mitochondrial ROS production.

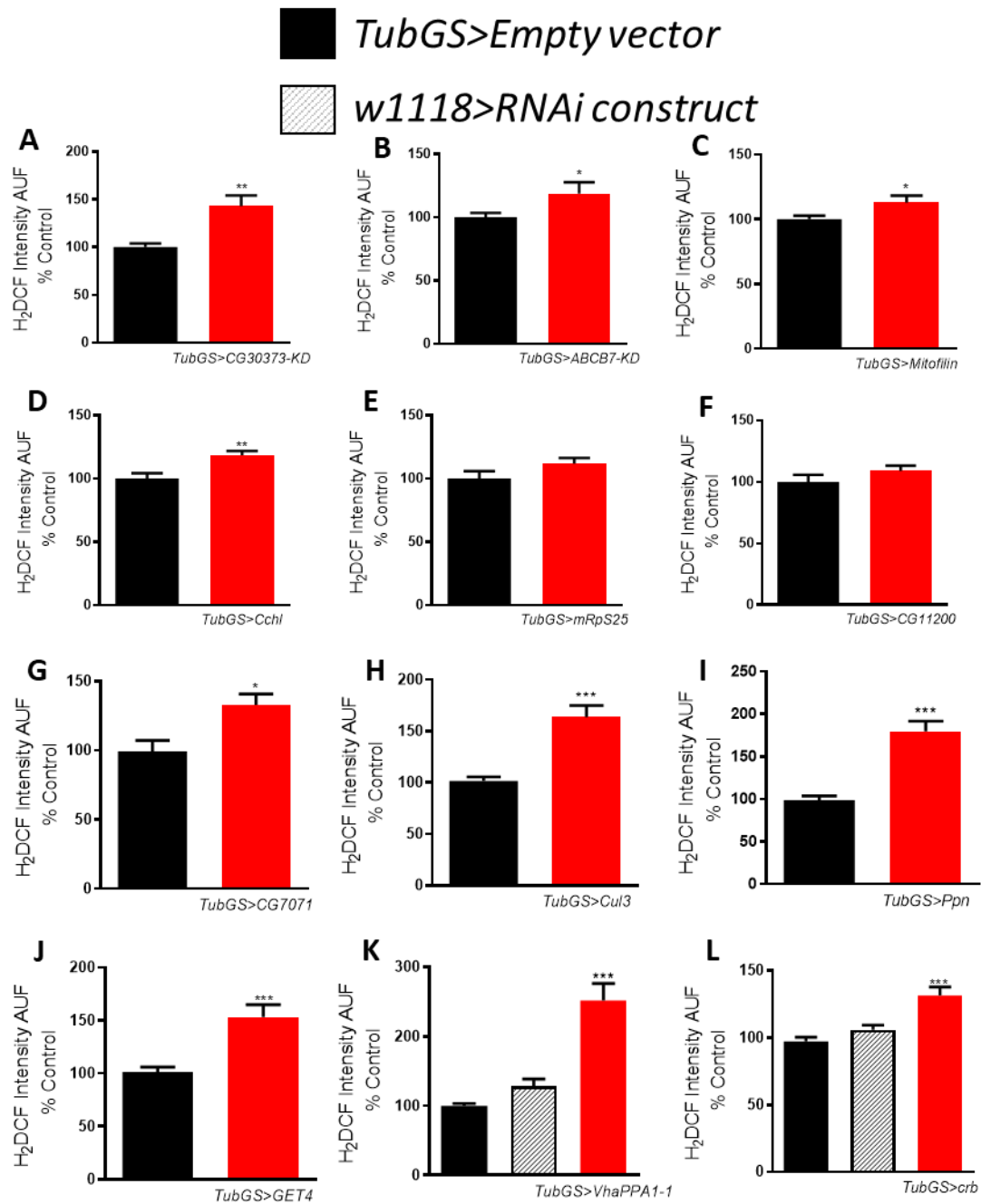


Figure 6.5 ROS measurements of 12 candidate genes in normal conditions (25°C).

(A) *CG30373-KD* (N = 7), (B) *ABCB7-KD* (N = >7), (C) *Mitofilin-KD* (N = >8), (D) *Cchl-KD* (N = >7), (E) *mRpS25-KD* (N = >7), (F) *CG11200-KD* (N = >7), (G) *CG7071-KD* (N = >8), (H) *Cul3-KD* (N = >8), (I) *Ppn-KD* (N = >9), (J) *GET4-KD* (N = >7), (K) *VhaPPA1-1-KD* (N = >7) and (L) *crb-KD* (N = >8). Flies were approximately 10 days old after being fed RU-486 to induce expression. P Values were calculated using unpaired Student's T-test and One-Way ANOVA, where appropriate. P Values were taken as statistically significant and represented by *, p<0.01 was represented by ** and p<0.001 was represented by ***.

6.8 AOX rescues the knockdown of genes that induce RET-dependent and RET-independent ROS

Results from the previous section showed that most of the confirmed hits, rescued by AOX, increased mitochondrial ROS levels when knocked down. Following these data, I wanted to determine how those ROS were being produced. Therefore I chose 3 candidate genes, to characterise their ROS production further and to test whether ROS were being generated via RET, or by another mechanism. The 3 genes I selected were *VhaPPA1-1* (CG7007), *Ppn* (CG33103) and *Cchl* (CG6022). The reasoning for choosing the proton-pump subunit *VhaPPA1-1* was due to the fact that another hit, *CG7071*, encoding an assembly factor of this transmembrane protein, was also a positive AOX rescue hit. Therefore, I wanted to explore this pathway further, to study whether reduction in the acidification of non-mitochondrial organelles, such as lysosomes, could induce ROS-RET. The second gene, *Ppn*, was chosen as previous experimentation had confirmed lethality in *Drosophila* and *C.elegans*, when it was knocked down during development. In these models, severe cellular defects in ECM arrangement were observed without reporting any alterations to mitochondrial phenotype (Kramerova *et al.*, 2000). Therefore I wanted to study how alterations in ECM caused a mitochondrial phenotype that was rescued by AOX. Lastly, I chose to characterise, *Cchl*, a gene encoding a protein needed for the assembly of heme group in mitochondrial Cyt C. This gene was selected to serve, as a positive control since the KD of *Cchl* would prevent Cyt C from accepting or donating electrons from CIII to CIV, respectively. Thus, effecting the electron flow through CIV, which as I described in Chapter 5, increases the leak of electrons at the Q_o site of CIII. Furthermore, the bypassing CIII and CIV, elicited by AOX expression should decrease the ROS production in *Cchl-KD* flies and rescue the lethal phenotype.

The method of characterisation was to measure ROS levels in the brain, in combination with feeding the CI inhibitor rotenone to one of the experimental groups. Given that rotenone inhibits RET, this would allow the distinction between ROS-RET and non-ROS-RET production. Respiration was also measured to infer whether ROS were being increased due to alterations in mitochondrial respiration.

To check the knockdown of *VhaPPA1-1*, I performed qPCR, which confirmed lower expression levels of the gene in the line expressing the RNAi construct (Figure 6.8A). To validate the rise in ROS production observed previously, I repeated ROS

measurements in normal conditions. As expected, the ROS levels increased when *VhaPPA1-1* was genetically silenced, compared to its respective controls (Figure 6.8B). In an attempt to determine the type of ROS responsible for the elevated levels, during inhibition of *VhaPPA1-1*, I fed the knockdown flies rotenone. The effect of rotenone feeding completely abolished the increase in mitochondrial ROS (Figure 6.8C). These results suggest that ROS-RET is activated when *VhaPPA1-1* is down-regulated. The developmental lethality observed in the *VhaPPA1-1* knockdown flies may be caused by a sustained un-regulated ROS-RET signal, which is ultimately rescued by the expression of AOX. When I measured mitochondrial respiration using high-resolution respirometry, I did not observe any difference between the groups, indicating that the knockdown of *VhaPPA1-1* does not significantly impair mitochondrial respiration in adult flies (Figure 6.8D).

qPCR measurements confirmed a significant decrease in the expression of *Ppn* in the knockdown flies, compared to the control, therefore I moved onto ROS measurements (Figure 6.9A). In normal conditions, inhibition of *Ppn* elevated the ROS levels significantly, in comparison to the control, reflecting prior data (Figure 6.9B). To depict where this ROS generation was occurring, within the ETC, I fed the knockdown flies rotenone. Quantification of ROS levels in the brain, revealed that rotenone had no effect on ROS production in the *Ppn* knockdown flies (Figure 6.9C). These results determined that the ROS production occurring, as a result of *Ppn* inhibition, was not through the activation of ROS-RET. Based on the fact that AOX was able to rescue the lethal phenotype of *Ppn-KD* during development, it is therefore reasonable to postulate that this was due to AOX preventing excess ROS production, caused by electrons leaking from the Q_o site of CIII. However, to confirm this hypothesis experiments using myxothiazol will need to be conducted. Finally, no difference was detected in CI, CIII or CIV-linked respiration (Figure 6.9D). Suggesting that *Ppn* does not have a direct effect on the mitochondrial ETC and that ROS elevation, when *Ppn* is down-regulated, is not a direct consequence of interrupting electron flow or proton pumping.

The targeted decrease in *Cchl* expression of the knockdown flies was confirmed by performing qPCR (Figure 6.10A). Repetition of ROS measurements in normal conditions confirmed that the knockdown of *Cchl* increases mitochondrial ROS levels (Figure 6.10B). To further characterise the origin of ROS produced during inhibition of *Cchl*, I fed rotenone to the knockdown flies; however no effect on ROS production

was observed (Figure 6.10C). The lack of effect of rotenone confirmed that the stimulation of RET was not the source of ROS, in this case. These data indicate that excessive ROS production is occurring at CIII, suggesting that AOX is able to alleviate this increase during development. This result was expected since knockdown of *Cchl* will limit the amount of Cyt C that is able to transfer electrons from CIII to CIV. Therefore mimicking the consequences observed during the inhibition of CIV with cyanide or preventing the assembly of the CIV, by knocking down *levy*. Accordingly, I observed a specific decrease in CIV-linked respiration in the knock down flies (Figure 6.10D). This was caused by a decrease in Cyt C activity, which in normal conditions is able to accept electrons from TMPD (Veltri *et al.*, 1978). The fact that inhibition was specific to CIV-linked respiration, indicates that the knockdown only mildly affects the levels of active Cyt C and that the block in electron flow is not as strong as those implemented in Chapter 5. Although, it was enough to increase ROS in the fly brain, indicating that even moderate reduction in electron flow, can increase ROS levels by CIII.

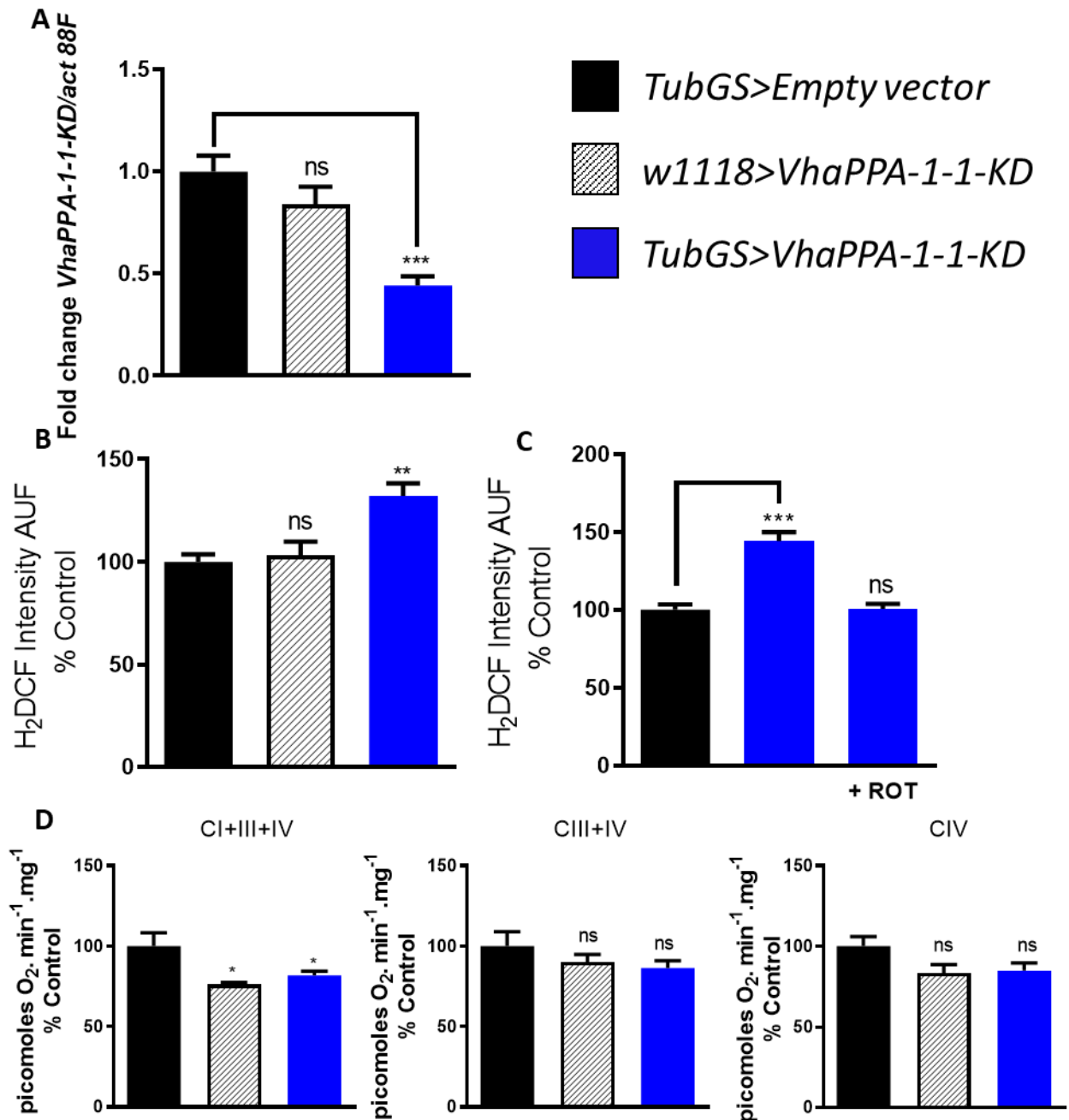


Figure 6.6 Characterisation of VhaPPA-1-1-KD flies.

(A) Quantification of mRNA levels in *VhaPPA1-1-KD* flies by qPCR. Control flies (*TubGS>Empty vector* and *w1118> VhaPPA1-1-KD*) and KD flies (*TubGS>VhaPPA1-1KD*) were used (N = 4). (B) ROS measurements in the brain of *VhaPPA1-1-KD* flies in non-stressed conditions (25 °C) (N = >7). (C) ROS measurements in the brain of *VhaPPA1-1-KD* flies fed rotenone (600 μM) in 25 °C (N = >8). (D) Mitochondrial respiration of *VhaPPA1-1-KD* whole fly homogenates showing CI-linked, CIII-linked and CIV-linked respiration as indicated (N = 4). Flies were approximately 10 days old after being fed RU-486 to induce expression. P Values were calculated using unpaired Student's T-test and One-Way ANOVA, where appropriate. Data are shown as mean ± SEM. p < 0.05 was taken as statistically significant and represented by *, p < 0.01 was represent by ** and p < 0.001 was represented by ***.

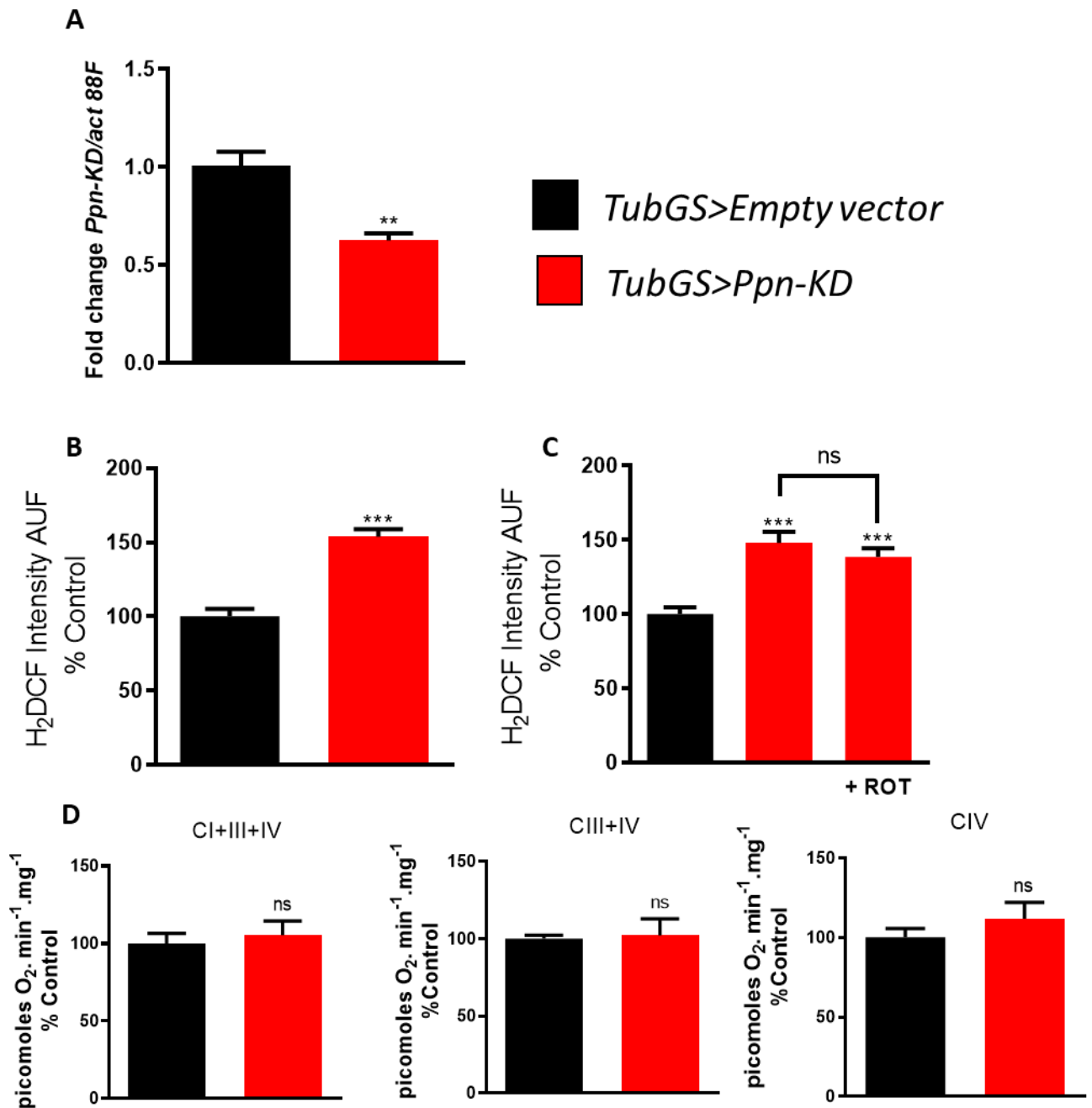


Figure 6.7 Characterisation of *Ppn-KD* flies.

(A) Quantification of mRNA levels in *Ppn-KD* flies by qPCR. Control flies (*TubGS>Empty vector*) and KD flies (*TubGS>Ppn-KD*) were used (N = 4). **(B)** ROS measurements in brains of *Ppn-KD* flies in non-stressed conditions (25 °C) (N = >8). **(C)** ROS measurements in brains of *Ppn-KD* flies fed rotenone (600 μM) at 25 °C (N = >9). **(D)** Mitochondrial respiration of *Ppn-KD* whole fly homogenates showing CI-linked, CIII-linked and CIV-linked respiration as indicated (N = 6). Flies were approximately 10 days old after being fed RU-486 to induce expression. P Values were calculated using unpaired Student's T-test and One-Way ANOVA, where appropriate. Data are shown as mean ± SEM. p < 0.05 was taken as statistically significant and represented by *, p<0.01 was represented by ** and p<0.001 was represented by ***.

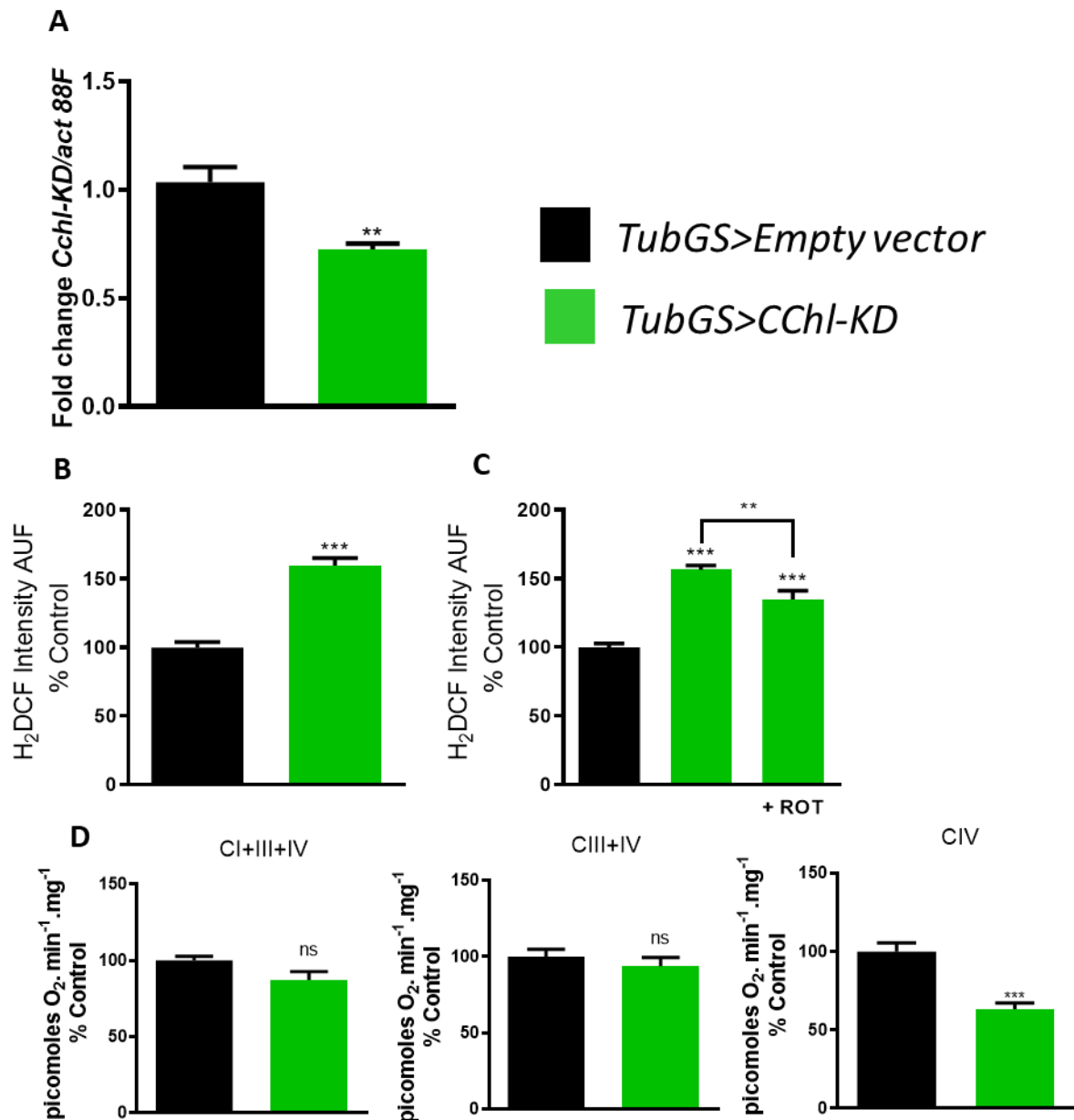


Figure 6.8 Characterisation of Cchl-KD flies.

(A) Quantification of mRNA levels in *Cchl-KD* flies by qPCR. Control flies (*TubGS>Empty vector*) and KD flies (*TubGS> Cchl-KD*) were used (N = 4). (B) ROS measurements in brains of *Cchl-KD* flies in non-stressed conditions (25 °C) (N = >7). (C) ROS measurements in brains of *Cchl-KD* flies fed rotenone (600 μM) at 25 °C (N = 10). (D) Mitochondrial respiration of *Cchl-KD* whole fly homogenates showing CI-linked, CIII-linked and CIV-linked respiration as indicated (N = 6). Flies were approximately 10 days old after being fed RU-486 to induce expression. P Values were calculated using unpaired Student's T-test and One-Way ANOVA, where appropriate. Data are shown as mean ± SEM. p < 0.05 was taken as statistically significant and represented by *, p<0.01 was represent by ** and p<0.001 was represented by ***.

6.9 Discussion

Elucidating the processes behind the generation of mitochondrial ROS, is central to gaining insight into their complex relationship with ageing, in order to ameliorate age-related disease and promote healthy ageing. To confront this challenge, I conducted a genome-wide RNAi screen to identify new genes involved in the regulation of mitochondrial ROS production. This method facilitated an unbiased and systematic approach on a large scale, taking advantage of AOX that reduces excessive ROS production at both CI and CIII. After screening >13,500 RNAi lines (covering >90% of the fly genome), I reported 41 genes, whose knockdown during development caused a lethal phenotype, which is rescued by AOX expression. The former suggests that these genes are involved in the regulation of ROS during development and supports ROS signalling as a vital process needed for normal development, of an adult fly. As expected, many of the genes identified, encoded both CIII and CIV subunits, due to AOX being able to complement mutations or chemical blocks in both CIII and CIV (Rajendran *et al.*, 2019) (Dogan *et al.*, 2018) (Fernandez-Ayala *et al.*, 2009) (Sanz *et al.*, 2010a). Subsequent analysis of 12 confirmed hits showed that the majority of genes, (10 out of 12), increase ROS levels when knocked down, only in adults. My results support the concept of using AOX to screen for genes involved in the generation of mitochondrial ROS. Remarkably 67% of genes encoding CIII subunits and 100% for genes encoding CIV subunits, which caused a lethal phenotype, were rescued by AOX, with 100% confirmation in the rescreen. On the other hand, AOX did not rescue any of the genes encoding subunits of complexes I, II or V. Among the CIII subunit RNAi lines, whose lethality was rescued by AOX, I found *UQCR-Q*. Surprisingly, the knockdown of either *levy* or *ATPsyn δ* did not cause any developmental arrest. However, the knockdown of 9 different genes, encoding CV subunits, were lethal and none of them were rescued by AOX. This indicates that those flies are probably arrested during development for a lack of ATP, rather than excess ROS levels.

Although some new and novel ROS regulators were identified by the screening strategy, used in the present study, I have identified numerous drawbacks that will need to be addressed for future screens or rescreens. (i) The confirmation of targets identified during the initial screen was quite low (~20%), which may be due to several reasons. For example, *Drosophila* lethality screens are prone to false positives and negatives, due to contamination of the vials with bacteria that prevent the

development of viable flies. Here, if the contamination is confined to the controls, a false positive would be detected, whereas, if it occurred in the AOX group, it would produce a false negative, resulting in this gene being discarded. Similarly, if not all female flies are virgins, or there is a male fly among the females, a false negative or positive may occur. For example, if there is one or more non-virgin fly among the controls a false negative is possible, whereas if the same occurs among the AOX flies the outcome would be a false positive. Since hundreds of vials were simultaneously prepared and screened every week, the technical errors described above may have occurred more often than anticipated. Additionally, due to the high numbers of vials needed per week, the quality of the food and concentration of RU-486 could also be variable between repetitions. For future work regarding the screen it may be useful to make note of those hits, which showed signs of bacterial infection and carry out rescreens to identify any false negatives or false positives. (ii) Due to technical reasons the completion of the screen took over four years, which could have led to changes in the food, flies (do to background changes and accumulation of mutations) or even the RU-486, during this time. In addition, the dose of drug used to express the RNAi constructs (and AOX) was set up at the beginning of the screen and was optimal to rescue the lethal phenotype, caused by the knockdown of three different CIV subunits, by AOX. Lower doses did not cause a lethal phenotype, whereas higher doses prevented the rescue by AOX. This explains why only a moderate number of OXPHOS genes were lethal (41%). Higher doses would have increased the number of lethal genes detected but as a side effect the number of genes rescued by AOX would have decreased. Although, internal controls including an RNAi line against *COX4 (CIV-IV-KD)*, was used during the screen, 'recalibration' of the optimal concentration every time would have helped to increase the reproducibility. (iii) The use of duplicates or triplicates in each round would also have helped to increase the reproducibility, although this would have raised both costs and time required to complete the screen. (iv) Using a ubiquitous driver may prevent the detection of genes that are important for ROS regulation in specific tissues. Similarly, genes that are involved in ROS regulation, in a certain tissue, can cause lethality in another tissue by a mechanism that is not ROS dependent. (v) Finally, an alternative to a genome-wide RNAi screen may be to screen only certain families of genes, such as, mitochondrial ribosomal proteins or MAPK proteins, instead of the whole genome. A limited screen would allow using different concentrations of drug, more replicates in each round and the use of several different drivers.

For a small number of the confirmed hits, an increase in ROS can be justified by their function within the cell. For example, the ABCB7 protein is responsible for the transport of iron from the mitochondria, into the cytosol. Therefore, its inhibition would cause a build-up of iron within the mitochondria and lead to an increase in ROS generation. Additionally, the role of Mitofilin involves the organisation of the ETC in supercomplexes; hence any disruption to the activity of Mitofilin would lead to a dysfunctional ETC and elevate ROS levels in the mitochondria. Nevertheless, the majority of hits possess no previous association with the mitochondria, or the production of ROS and therefore they are possible novel ROS regulators.

From the 3 confirmed genes that increased mitochondrial ROS levels and were characterised further, *VhaPP1-1* was identified as a potential novel regulator of ROS-RET. When down-regulated, *VhaPP1-1* displayed an increase in ROS, which was abolished in the presence of the RET inhibitor, rotenone. These data suggested that depletion of *VhaPP1-1* can trigger ROS-RET. Interestingly another gene required for the assembly of the VhaPPA proton pump, *CG7071*, was also identified as an AOX rescue hit, which reinforces the involvement of VhaPPA1-1 as a ROS regulator. In the future, it would be interesting to test whether the increase in ROS, elicited by *CG7071*, is also caused by triggering RET. Vacuolar ATPases are instrumental for the acidification of the lysosome, which is required for the turnover of damaged proteins and organelles. Therefore depletion of *VhaPPA1-1* could cause the accumulation of damaged mitochondria that activates a ROS-RET signal, to stimulate mitochondrial turnover. Mitochondrial ROS levels have been described to activate mitophagy (Pirastu *et al.*, 1990) (Wang *et al.*, 2012) but where and how these ROS are generated remains to be elucidated. The models developed during my thesis could help answer that question.

Although inhibition of VhaPPA1-1 had no effect on the mitochondrial respiration of the knockdown flies, this may have been due to the sample preparation, as samples consisted of whole bodies. Under these conditions, most of the mitochondria are muscle mitochondria from the thorax (Cocheme *et al.*, 2011); therefore it is possible that mitochondrial respiration is altered specifically in the brain where ROS were measured.

Ppn is a component of the ECM. Results from downregulation of this gene revealed an increase in ROS production that was not attenuated when the RET inhibitor rotenone was administered. It is plausible that this ROS is generated at the Q_o site of

CIII. However, to confirm this, it will be necessary to repeat ROS measurements in the presence of myxothiazol. The inhibition of *Ppn* also had no effect on mitochondrial respiration when whole flies were used but a different result could be obtained if only fly heads are used instead. With the present information, it is not possible to depict the mechanism by which *Ppn* increases mitochondrial ROS and how this alteration interrupts fly development. In the future, further experiments including tissue-specific measurements of mitochondrial respiration and knockdown of other proteins that interact with Papilin, such as metalloproteinases, will help to understand how its knockdown affects mitochondrial ROS levels.

Cchl was identified as a novel fly regulator of both CIV activity and ROS production. Downregulation of *Cchl* exhibited a CIV-specific decrease in respiration, explained by lower levels of functional Cyt C, which normally functions to transfer electrons to CIV. The fact that CI and CIII-linked respiration were not affected, indicates that Cyt C is in excess, in the ETC. Interestingly, reducing the amount of functional Cyt C reproduces the effect of chemical inhibition and genetic silencing of CIV subunits. In Chapter 5, it was established that the Q_o site of CIII was the most probable source of ROS, during CIV inhibition and I hypothesize that the same site is producing ROS when *Cchl* is knocked down. The AOX rescue can be explained either because its expression prevents excessive ROS production by CIII, or because it complements the reduction in CIV activity. Experiments overexpressing antioxidants such as SOD2 or mitochondrial-targeted catalase, used in Chapter 3, will help to clarify this point.

In summary, my screen strategy using AOX has been able to identify new regulators of mitochondrial ROS production, in the fly brain. The effectiveness of this strategy requires the rescreen of any candidate gene, confirmation of the knockdown by qPCR or western-blot and measuring ROS levels in independent experiments with and without specific ETC inhibitors. Furthermore, the use of other RNAi fly lines targeting other parts of the gene is highly recommendable, to further confirm the results. The latter will need to be performed in the future for the different genes I have found and described. Finally, the strategy presented here can be adapted to the specific needs of any researcher for example screening deformations of the fly eye (Ma *et al.*, 2009), using tissue-specific drivers to study particular organs or cells, or selecting specific families of genes to be screened.

Chapter 7 General Discussion

7.1 Introduction

It has become apparent over the last decade that the behaviour of Reactive Oxygen Species (ROS), within our cells, represents a double-edged sword. On the one hand, their excessive production is responsible for oxidative stress that drives cellular dysfunction and damage (Barja, 2014). On the other hand, basal levels of ROS are essential for maintaining cellular homeostasis (Ray *et al.*, 2012). From the perspective of the MFRTA, ROS have been well documented. Here, mitochondrial ROS are described as toxic by-products of metabolism that accumulate with age and create a vicious cycle of mitochondrial dysfunction, a universal hallmark of ageing (Lopez-Otin *et al.*, 2013). Studies have been able to confirm an age-dependent increase in the extent of oxidative damage, as well as a negative correlation between ROS levels and lifespan, in multiple animal models and species (Cui *et al.*, 2012). Moreover, chronic mitochondrial ROS production has been recognised in a diverse range of age-related diseases such as Parkinson's disease (Zhang *et al.*, 1999), Alzheimer's disease (Wang *et al.*, 2014), diabetes (Anderson *et al.*, 2009), cardiovascular disease (Puca *et al.*, 2013) and cancer (Kudryavtseva *et al.*, 2016). Despite the vast amount of experimental data supporting the MFRTA, contradictory evidence has challenged the integrity of this theory. For example, it is anticipated that the concentration of mitochondrial ROS influences lifespan, however, administration of antioxidants or manipulation of endogenous antioxidant expression, to moderate ROS levels, has not been shown to extend lifespan (Sanz *et al.*, 2006) (Liu, 2014). Additionally, the direct reduction of ROS, by e.g. the expression of AOX in fruit flies, does not increase longevity (Sanz *et al.*, 2010a). In fact, in many cases an increase in mitochondrial ROS has led to lifespan extension (Yang and Hekimi, 2010) (Scialo *et al.*, 2016a) (Hekimi *et al.*, 2011) (Schmeisser *et al.*, 2011). These contrasting data highlight the complexity of studying the role of ROS, due to their dual identity both as signalling molecules and toxic by-products of metabolism.

In their role as cellular messengers, mitochondrial ROS production has been shown to be necessary for many biological processes. For example, without mitochondrial ROS it is not possible to initiate a pro-inflammatory response required for activating innate immunity or establishing a senescence phenotype to prevent cancer (Mills *et*

et al., 2016a) (Soberanes *et al.*, 2019) (Nelson *et al.*, 2018). Paradoxically, ROS are also required for promoting cell proliferation and differentiation (Diebold and Chandel, 2016). A primary example of this is seen in cancer cells, where ROS are maintained at heightened levels in order to encourage proliferation (Moloney and Cotter, 2018). To achieve this process, ROS target specific pathways including HIF, NF- κ B, MAPKs and PI3K (Galanis *et al.*, 2008) (Huang *et al.*, 2016) (Wang *et al.*, 2017) (Lu *et al.*, 2017). Other studies have also shown that mitochondrial ROS can regulate blood pressure (Dhalla *et al.*, 2000), programmed neuronal cell death (Tan *et al.*, 1998) and even the length and quality of sleep (Kempf *et al.*, 2019). These findings all support the role of mitochondrial ROS as essential regulators in redox signalling. It is now essential to study what defines the behaviour of ROS, for example the mechanisms behind how they are produced.

CI and CIII, of the respiratory chain, are the two major sites of ROS production within the mitochondria and have both been implicated in numerous specific cellular pathways. One of the most characteristic and best-described processes, leading to site- and time-specific ROS production is RET. The process of RET, which results in augmented ROS production at CI, has recently been described to play a central role in distinct physiological and pathological processes. These include the differentiation of myoblasts into myotubes, triggering an immune response to bacterial infection and sensing and reacting to hypoxia by arterial chemoreceptors in the carotid body (Garaude *et al.*, 2016) (Fernandez-Aguera *et al.*, 2015) (Lee *et al.*, 2011). In all of the former situations, ROS are not produced at random but rather as a signal in response to specific stimuli, at specific times and specific sites. Furthermore, there are mechanisms that both stimulate and terminate the ROS-RET signal. Interestingly, it has also been shown that the expression of Ndi1 from *Saccharomyces cerevisiae* promotes a sustained ROS-RET signal, when expressed in the mitochondria of *Drosophila melanogaster* (Scialo *et al.*, 2016a). Continuous activation of ROS-RET signalling leads to lifespan extension in fruit flies (Scialo *et al.*, 2016a) (Sanz *et al.*, 2010b) (Bahadorani *et al.*, 2010). Unfortunately, the downstream pathways responsible for these beneficial effects, elicited by Ndi1 expression, are yet to be determined. Presently, we know that activation of RET requires a highly reduced CoQ pool, along with a high proton motive force but so far only speculation has been provided surrounding how RET can be stimulated, in physiological conditions. Exploring the mechanisms behind ROS-RET and the signalling pathways that drive

its downstream outcomes may be instrumental in understanding the role of ROS in health and disease. Thus, it can provide us with new strategies to stimulate ROS signalling in young individuals or to restore it in later life, to promote healthy ageing.

7.2 Main findings and contributions to the field

Since its discovery in 1961, RET was considered to be an *in vitro* phenomenon (Chance and Hollunger, 1961). This perception began to change when publications reporting the production of ROS-RET in the mitochondria from ischemic tissues started to emerge, thus increasing the interest surrounding RET (Lesnefsky *et al.*, 2004), (Chen *et al.*, 2006). These reports showed that the detrimental effects of IR were palliated when rotenone was administered to animal models (Lesnefsky *et al.*, 2004), (Chen *et al.*, 2006). However, it was a publication from the laboratory of Mike Murphy in Cambridge, which brought RET to the forefront of research. This study confirmed the existence of ROS-RET *in vivo* as well as being the main mechanism responsible for the oxidative damage, occurring as a result of IR (Chouchani *et al.*, 2014a). Since then, ROS-RET has been shown to be instrumental in many biological events, discussed previously in this thesis. It has been well documented that the stimulation of RET requires both a high CoQH₂:CoQ ratio and a high proton motive force, to make RET favourable. Nevertheless, evidence surrounding how these two essential conditions are achieved *in vivo* has not been established (Scialo *et al.*, 2017).

One of the aims of my thesis was to test whether ROS-RET occurs in physiological conditions and to dissect how the redox state of CoQ and the proton motive force contribute to this. In Chapter 3, I showed that heat stress (HS) triggers ROS-RET in the brain of *Drosophila melanogaster*. Under HS, there is an increase in energy demand that enhances oxidative phosphorylation, increasing the entry of electrons into the ETC. According to unpublished data from our laboratory, the increase occurs due to a rise in the activity of not only CI and CII but also of other dehydrogenases, such as G3P, ETF-QO and DHOD, which can also reduce the mitochondrial CoQ pool. This boost of electrons entering the ETC increases the reduction state of CoQ and also drives the transport of protons across the inner membrane, thus establishing a high proton motive force. In summary, HS creates the perfect conditions for inducing RET, allowing CI to switch from a forward to a reverse

direction, thereby altering the mechanism of CI ROS production. This burst in mitochondrial ROS can be modulated in intensity and duration, to produce a signal in response to stress. To confirm that ROS were produced via RET; I used the specific CI inhibitor, rotenone and the mitochondrial uncoupler, FCCP. Both of them have been extensively used to confirm the existence of ROS-RET in the literature (Robb *et al.*, 2018) (Scialo *et al.*, 2016a) (Chouchani *et al.*, 2014a). When rotenone and FCCP were supplemented, to block the quinone binding site of CI and dissipate the proton motive force respectively, ROS-RET was prevented. Interestingly, in non-stressed conditions (25°C), both rotenone and FCCP increased ROS in the fly brain, indicating production of ROS by CI and/or CIII in the forward direction. However, under HS both mitochondrial inhibitors decreased ROS levels, supporting production of ROS by CI in the reverse direction. These results reflected those seen in Ndi1 flies, where rotenone and FCCP decrease ROS (Scialo *et al.*, 2016a).

Lastly, I used the over-expression of two antioxidants SOD2 and a mitochondrial-targeted catalase to confirm the location of the ROS production. Results from these experiments showed that the increased ROS production, in response to HS, was originating exclusively from the mitochondrial matrix, as expected from a ROS-RET signal. My results using the referred specific mitochondrial inhibitors and antioxidants showed that ROS-RET can occur in the fly brain in physiological conditions. Interestingly, mitochondrial ROS levels were increased after only 3 hours at 32°C and returned to the level of unexposed controls, after 5 hours. This supports the idea that ROS-RET is not produced randomly but as a signal to adapt to HS. Accordingly, unpublished data from the Sanz's laboratory showed that preventing ROS-RET under HS, attenuates the expression of genes involved in the anti-stress responses and dramatically shortens the lifespan of the flies.

It is widely accepted that mitochondrial dysfunction is one of the hallmarks of ageing (Lopez-Otin *et al.*, 2013). The two main phenotypes of 'old' mitochondria are a decrease in ATP production and an increase in mitochondrial ROS generation (Gabbita *et al.*, 1997) (Drew *et al.*, 2003) (Sanz *et al.*, 2010a) (Cocheme *et al.*, 2011), (Pollard *et al.*, 2016). Some reports have described that during ageing, CI activity is the first to be altered and to a much greater extent than the other ETC components in flies and humans (Scialo *et al.*, 2016a) (Cooper *et al.*, 1992) (Cabre *et al.*, 2017). Similarly, in Parkinson's patients, CI has been reported to be the most affected

respiratory complex. CI inhibitors elicit a Parkinson's like phenotype in humans and animal models (Tanner *et al.*, 2011). Additionally, CI dysfunction has also been observed in mouse models of ataxia (Pollard *et al.*, 2016), associated with cancer proliferation (Gui *et al.*, 2016) and even in psychiatric conditions such as bipolar disorder (Duong *et al.*, 2016). Our laboratory has shown that CI-linked respiration is specifically reduced from 50 days onwards followed by a decrease in the levels of CI, in 75 days old flies (Scialo *et al.*, 2016a). Interestingly, the decrease in CI-activity occurs in parallel with the increase in mitochondrial ROS levels in the fly brain (Scialo *et al.*, 2016a). Given that ROS-RET is dependent on the activity of CI, I hypothesized that age-related alterations of CI could lead to changes in redox signalling, mediated by ROS-RET. This would explain the protective effect of Ndi1 on mitochondrial function observed both in old flies (Sanz *et al.*, 2010b) and in *pink1* and *Sod2* mutants, since Ndi1 would rescue redox signalling, through the stimulation of ROS-RET (Scialo *et al.*, 2016a), (Vilain *et al.*, 2012).

As I anticipated, at 50 days, mitochondria from old flies were unable to trigger ROS-RET, in response to HS. Similarly, no increase in ROS was observed in response to rotenone, under non-stressed conditions. 50 day old flies had very high levels of mitochondrial ROS in the brain and did not change ROS production in response to stress, in contrast to the younger flies. For example, 25 day old flies, had higher levels of mitochondrial ROS than controls but they were still able to trigger ROS-RET, in response to HS. I proposed a model where HS (and possibly other types of stress) during early life, would encourage a fully functioning CI to switch from producing ROS in a forward direction to RET. Producing a rise in ROS that would act as signalling molecules, to trigger various pro-survival pathways. Once the appropriate pathways are stimulated, and cellular homeostasis is re-established, the ROS-RET signal is terminated, and ROS decreases to basal levels. However, during ageing the decline in CI activity attenuates the ROS-RET response, preventing the stimulation of the required survival pathways. Thus, providing an explanation as to why I did not observe a ROS-RET response, in 50 day old flies, when mitochondrial respiration is significantly decreased. I speculated that the decline of redox signalling contributes to the accumulation of damaged mitochondria, which causes the unregulated production of ROS. In contrast to ROS-RET, the high levels of mitochondrial ROS observed in old individuals, cannot be neutralised, which therefore drives the oxidative stress that is observed in old flies (Jacobson *et al.*,

2010), (Magwere *et al.*, 2006). In addition, the background oxidative stress also interferes with normal redox signalling, altering processes that require ROS signalling (Figure 7.1). For example, autophagy (Scherz-Shouval *et al.*, 2007); a process that is strongly reduced when flies become old (Simonsen *et al.*, 2008).

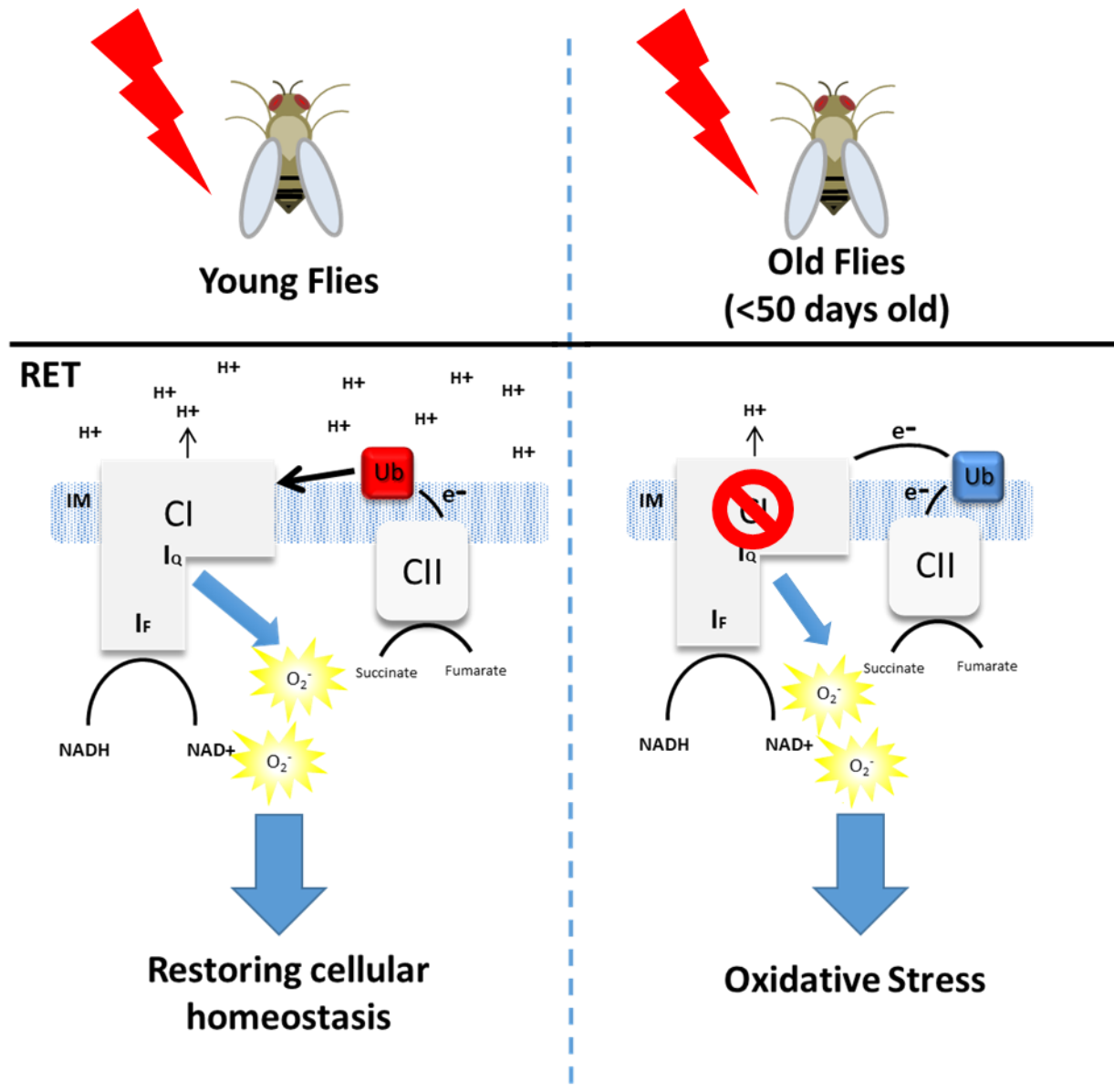


Figure 7.1 The effect of CI ROS production in young versus old flies.

In young flies, when a stress occurs, RET is stimulated to produce ROS signalling messengers which can leave the mitochondria and target cysteine groups of specific proteins to restore cellular homeostasis. Eventually, the ROS signal is terminated. However, in old flies, CI levels progressively decrease during ageing. Thus, RET can no longer be stimulated to overcome the stress condition by promoting cellular survival pathways. Instead, CI dysfunction leads to chronic ROS production, which drives oxidative stress and further damage.

Inducing ROS-RET by subjecting flies, for four hours, 3 times per week to HS, did not extend lifespan. This is in contrast with the results previously shown by Ndi1

expression (Scialo *et al.*, 2016a). This could be due to a number of different reasons, for example, the duration of ROS-RET, the intensity of the signal or the tissues where ROS-RET is induced. In the case of Ndi1, the signal seems to be activated all of the time, whereas, in the HS model, RET only lasts for 2 hours. It would be interesting to test whether exposing flies to HS more often (e.g. every day), would positively affect lifespan. In addition, Ndi1 increases mitochondrial ROS levels higher than HS, so it is possible that the intensity of the signal during HS is not enough to activate the same mechanisms that Ndi1 does. It cannot be discarded either that the effect of Ndi1 on longevity, is due to its expression during development. Alternatively, it is possible that ubiquitous Ndi1 expression, increases ROS-RET in tissues that are not affected by HS. Time- and tissue-specific expression of Ndi1 will help to answer the former questions. Interestingly, exposing flies to HS in combination with rotenone, dramatically shortened lifespan, when the combined treatment was administered after day 25. Thus, when I fed 50-day-old flies with rotenone and exposed them to HS, many of them died within hours. This data indicates that ROS-RET is instrumental for stress adaptation, thus preventing RET, dramatically decreases survival under stress, in an age-dependent manner. The fact that suppressing ROS-RET did not have any effect in young flies, in the conditions assayed, indicates the existence of stress adaptation mechanisms in early life that are lost during ageing.

After establishing that ROS-RET occurs physiologically, I developed different fly models to study in detail how the individual components of the ETC contribute to the formation of ROS-RET, *in vivo*. Starting with CI and CII, I was able to confirm that the entry of electrons into the ETC is essential for the production of ROS-RET. When electron entry was blocked, using both short-term and long-term inhibition of CI and CII during HS, the increase in ROS was abolished. This data indicated that without the activity of CI and CII the CoQ pool could not reach the reduction state required to initiate ROS-RET. Previous studies from our laboratory, have shown that reduction of CI activity (by knocking down *ND-39*) reduces RET, during expression of Ndi1 (Scialo *et al.*, 2016a). Other laboratories have also found that CI inhibition by rotenone was able to prevent ROS-RET during IR (Chouchani *et al.*, 2014a) or to stop the pro-inflammatory response caused by injecting mice with LPS that is also ROS-RET dependent. Additionally, genetic depletion of CI, specifically in cells of the carotid body abolished the increase in ROS in response to hypoxia, as well as the organismal response, of increasing respiratory rate in mice, in the presence of low

oxygen levels (Arias-Mayenco *et al.*, 2018) (Mills *et al.*, 2016a). Collectively, these observations all confirm the necessity of CI and CII activity in the formation of ROS-RET.

I then studied the effect of blocking the exit of electrons from the ETC, via the inhibition of CIII and CIV. In contrast to blocking CI and CII, I hypothesised that inhibiting the flow of electrons would lead to an accumulation of electrons upstream of CIII and CIV, promoting a highly reduced CoQ (Jacobson *et al.*, 2005), (Drew *et al.*, 2003), (Zuckerbraun *et al.*, 2007), (Eghbal *et al.*, 2004). Prior to my own experimentation, it has been documented that the endogenous CIV inhibitors, such as NO, CO and H₂S, could elicit an increase in mitochondrial ROS levels after blocking CIV (Taylor and Moncada, 2010). Therefore I hypothesised that inhibition of either CIII or CIV would trigger ROS-RET. The conclusion from all my experiments was that blocking the exit of electrons elevated ROS production, as previously described but not due to the stimulation of RET.

The results obtained after CIII short-term inhibition were difficult to interpret. I observed a dose-dependent effect, where small doses reduced ROS production and high doses lead to increased ROS levels. The decrease in ROS, caused by low doses of myxothiazol, may be explained by two previous observations. The first is partial inhibition of CI, caused by the inhibition of CIII (Bacsi *et al.*, 2006), which would prevent ROS-RET from occurring. The second and non-exclusive is a decrease in membrane potential caused by the inhibition of CIII. It has been reported in mammalian cells that inhibition of CIII with antimycin A, makes CV work in the reverse direction (i.e. transporting protons from the matrix to the intermembrane space) to maintain the mitochondrial membrane potential (Metzen *et al.*, 2003). Under these circumstances, ATPIF1 is activated to inhibit the reverse motion and prevent ATP hydrolysis. This preserves energy levels, but it decreases membrane potential (Gaude and Frezza, 2014). It is possible that the same depolarisation occurs in fruit flies, since ATPIF1 has two fly orthologues, explaining why ROS-RET does not occur in the fly brain in response to CIII inhibition (Metzen *et al.*, 2003). Obviously to confirm the implication of the membrane potential, its measurement in the fly brain would be required, which is technically challenging.

Higher concentrations of myxothiazol induced a substantial rise in mitochondrial ROS levels. This increase in ROS was insensitive to rotenone feeding, discarding ROS-RET as the source. It is possible that under these conditions, the increase in ROS is the result of chronic damage to the mitochondria and global dysfunction, with electrons leaking from non-specific places, within and outside the ETC. Long-term genetic inhibition of CIII also resulted in a large increase in ROS production that was proven not to be due to RET either. An alternative possibility is that CII is generating the ROS since it has been described that CII ROS production may occur in response to CIII/CI inhibition (Quinlan *et al.*, 2012). To test the latter hypothesis, I fed flies with the CII inhibitor, malonate and observed a significant decrease in ROS production (data not shown), supporting CII as the source of ROS, during inhibition of CIII with high doses of myxothiazol. However, this may require further confirmation, by testing a genetic model of CII depletion, since I was not able to confirm CII inhibition in the fly brain using malonate. In any case, my results clearly show that CIII inhibition, both long and short term, was not able to stimulate ROS-RET *in vivo*.

CIV inhibition using either chemical or genetic approaches, elicited an increase in ROS production. Further characterisation indicated that the increase in ROS was not produced via RET but instead was originating from the Q_o site of CIII. This was confirmed by the use of the Q_o site inhibitor, myxothiazol. Similarly to CIII inhibition, blocking the electron flow through CIV would decrease the proton motive force, due to CIV no longer contributing to the transfer of protons across the inner membrane. Consequently, the decrease in the proton motive force would prevent the occurrence of ROS-RET at CI. However, the first upstream site of CIV able to generate ROS is CIII. Therefore the inhibition of electron flow at CIV would lead to an accumulation of electrons at CIII, increasing the electron leak and ROS generation at the Q_o site of this complex. ROS produced at the Q_o site are released into both the mitochondrial matrix and the intermembrane space (Muller *et al.*, 2004). Superoxide produced in the intermembrane space is usually converted into peroxides by SOD, which enables them to diffuse into the cytoplasm and interact with proteins. This makes CIII an advantageous site for sending ROS signals directly to the cytoplasm (Chandel, 2010). Recently, ROS generated at the Q_o site of CIII have been described as initiators of important signalling events. For example, during hypoxia, CIII acts as an oxygen sensor and releases ROS from the Q_o site, to trigger a survival response. CIII-derived-ROS are required to stabilise HIF-1 α , therefore when the Q_o site inhibitor

stigmatellin, is administered, HIF-1 α is not stabilized and consequently degraded (Chandel *et al.*, 2000). During the last 10 years the laboratory of Navdeep Chandel and associates, have shown that ROS produced at the Q_o site are required for physiological processes, such as proliferation in certain types of cancer, activation of T cells, adipocyte differentiation or production and release of IL-6 (Chandel *et al.*, 2000) (Diebold *et al.*, 2019) (Weinberg *et al.*, 2010) (Tormos *et al.*, 2011). However, it remains unsolved how CIII increases ROS production *in vivo*. In the future, it would be interesting to test whether the inhibition of CIV, is responsible for the processes mentioned before and if this inhibition occurs physiologically. The latter is possible since at least three endogenous messengers (NO, CO, H₂S) have been shown to block CIV as previously discussed (Taylor and Moncada, 2010).

One of the genes identified from the screen, *Cchl*, reduced CIV activity and also increased mitochondrial ROS levels. Knockdown of *Cchl* during development was lethal, despite no significant alterations in mitochondrial respiration, apart from the mild decrease in CIV-linked respiration. The fact that the lethal phenotype was rescued by AOX, indicates that even mild inhibition of CIV can increase ROS and this can have deleterious consequences in the normal development of the fly. Our results do not support the idea that blocking CIV induces ROS-RET (Dogan *et al.*, 2018), although this may not be the case in other organisms or tissues. In summary the results from the inhibition of CIII and CIV showed in both cases, an important increase in ROS as previously reported (Srinivasan and Avadhani, 2012). However, my results demonstrated that ROS are not produced via RET in the mitochondria of the fly brain when electron flow through CIII and CIV is interrupted.

Finally, CV showed contrasting results when inhibited. Results regarding acute CV inhibition, using oligomycin, could not elicit a ROS-RET response. This contradicts what has been previously reported in the literature using different models (Chouchani *et al.*, 2014a; Fukuoh *et al.*, 2014; Mills *et al.*, 2016a), see Chapter 5 for details. Feeding flies with oligomycin resulted in a decrease in mtROS, in the brain, using a wide range of concentrations and varying time periods. During HS, a physiological RET model, oligomycin also attenuated the ROS-RET response. Furthermore, feeding oligomycin to Ndi1 flies also decreased mitochondrial ROS levels. Suppression of ROS-RET by oligomycin, has been independently reported by other studies (Sanz *et al.*, 2010c), (Santamaria *et al.*, 2006), (Mills *et al.*, 2016a). When

long-term genetic inhibition was employed, a rotenone sensitive increase in mitochondrial ROS levels was detected, suggestive of ROS-RET. However, these results should be interpreted with caution. Knockdown of *ATPsyn* δ produces a dramatic decrease in mitochondrial respiration and the flies that eclose are very weak and die within days. Therefore, it is possible that rotenone feeding alongside strong CV inhibition could produce severe mitochondrial dysfunction, resulting in the proton motive force becoming completely collapsed. This could cause massive cell death leading to the observed decrease in mitochondrial ROS levels. Studying cell death in the fly brain, under these experimental conditions, will help to confirm or discard this hypothesis. In summary, my results regarding the role of CV inhibition, in relation to the stimulation of ROS-RET, were inconclusive and further investigation is required to establish how manipulation of CV affects mitochondrial ROS levels.

In an alternative attempt to study the mechanisms behind the regulation of ROS-RET, I used a high-throughput unbiased approach, by performing a genome-Wide RNAi screen that covered over 90% of fly genes. Using the expression of AOX, a RET suppressor (Scialo *et al.*, 2016a); I identified various genes involved in the modulation of mitochondrial ROS levels. Given that AOX is also able to decrease ROS produced by CIII (Sanz *et al.*, 2010a), I used rotenone in my ROS measurements to distinguish between ROS-RET and CIII-derived ROS production. Using this strategy, I identified a new gene whose knockdown stimulates ROS-RET in the fly brain: *VhaPPA1-1*. Interestingly, another gene, *CG7071*, required for the assembly of VhaPPA1 was also identified in my screen, and I confirmed that upon its knockdown, mtROS levels are also increased. However, whether the increase in ROS, after the knockdown of *CG7071*, is ROS-RET dependent requires further confirmation. Two other genes, *Ppn* and *Cchl*, were shown to be involved in the regulation of mitochondrial ROS levels. However, my data does not support ROS-RET, as the mechanisms of production. It is possible that they are produced at the Q_o site of CIII, which would explain why AOX was able to decrease and rescue the lethal phenotype. However, confirmation with CIII inhibitors, such as myxothiazol, is needed. Additionally I showed that knockdown of *Cchl*, limited the entry of electrons to CIV and supported previous results of CIV inhibition, such as depletion of *levy* or cyanide administration, which resulted in an increase in ROS upstream of CIV. Overall, my screen strategy was successful in identifying new genes involved in the regulation of mtROS levels, in the brain. Thus, it shows AOX as a powerful tool for

similar screens, where the strategy could be adapted to the needs of the user, e.g. performing tissue-specific screens or targeting only individual families of genes.

In summary, my work has dissected how ROS-RET occurs in the fly brain. Using *ex vivo* ROS measurements, I provided evidence that ROS-RET can be stimulated physiologically using HS. I have shown that RET depends on the free entry of electrons into ETC and that blocking electron exit increases ROS but not via RET. This is particularly interesting for CIV, which can be blocked by endogenous messengers, such as NO and CO. My experiments using myxothiazol showed that CIII is the place where electrons leak when CIV is blocked. I have also generated a list with more than 40 candidate genes, with the potential to regulate mitochondrial ROS levels *in vivo*. In addition, I have characterised three of the candidate genes, including one that is involved in the generation of ROS-RET. Finally, one of the most important contributions of my thesis is the generation of several new fly models to study ROS. Including, ROS specifically produced via RET (HS and knockdown of *ATPsyn δ*) or ROS produced by CIII (inhibition using cyanide or knocking down *levy* or *Cchl*). Similarly, these fly models will make it possible to study the physiological consequences of being unable to induce ROS-RET under stress (e.g. by knocking down CI/CII subunits or blocking RET with rotenone or FCCP). In addition, they will allow the study of how sporadic or chronic high levels of mitochondrial ROS upstream of CIV (blocking CIII/CIV with myxothiazol/cyanide or knocking down *UQCR-Q*, *levy* or *Cchl*) affects lifespan. Characterising these fly models in detail will provide us with a more comprehensive understanding of how ROS signalling operates *in vivo*, allowing the discovery of new drug targets to combat ageing and age-related diseases.

7.3 Future Work

The on-going challenges regarding the measurement of ROS levels have previously limited the study of ROS. The vast majority of previous studies have been performed *in vitro* using isolated mitochondria or cell culture, which presents a range of drawbacks, reviewed in my introduction. Briefly, the use of isolated mitochondria removes the organelle from its natural environment, leading to a loss of physiological relevance. Although cell culture eliminates this disadvantage, the conditions in which they are grown in, for example, hyperoxic oxygen levels and glucose-rich media again, lead to poor physiological relevance. Furthermore, the use of non-

physiological concentrations for ETC substrates or the use of inhibitors can lead to high rates of ROS production that are not observed *in vivo*. To overcome these limitations observed with *in vitro* techniques, *in vivo* strategies of ROS measurements are starting to be implemented (Cocheme *et al.*, 2011) (Albrecht *et al.*, 2011). The use of *in vivo* or *ex vivo* methods allows for a more accurate representation of ROS dynamics, occurring within an organism.

For my thesis, I have measured mitochondrial ROS levels in the dissected brain of *Drosophila melanogaster*. This approach allows *ex vivo* measurements with a consistent area of tissue (the whole brain) to minimise variation between samples, a disadvantage of using other tissue such as muscle. I initially used two fluorescent dyes to validate the results obtained in Chapter 3. First of all H₂DCF, a well-established cell-permeable and highly sensitive general ROS detector (Kalyanaraman *et al.*, 2012) and secondly MitoSOX, another extended ROS probe that is targeted into the mitochondrion and is preferentially oxidised by superoxide (Zielonka and Kalyanaraman, 2010). I confirmed that the signals detected using H₂DCF and MitoSOX were attenuated in response to the expression of a mitochondrial-targeted catalase and the overexpression of SOD2 in the mitochondrion, respectively. However, both probes present several drawbacks as reviewed in (Sanz, 2016). To confirm the results of my thesis, it may be beneficial to explore other complementary approaches to quantify mitochondrial ROS, *in vivo*. This will help to validate my results and test the physiological relevance of the processes, described in my thesis. I propose several alternative approaches. First of all, the use of the ratiometric probe MitoB/MitoP (Cocheme *et al.*, 2011), which would allow a precise estimation of the levels of mitochondrial H₂O₂ in *Drosophila* homogenates or specific tissues. In addition, I would image cells or fly organs measuring ROS using both *ex vivo* and *in vivo* techniques, by using the genetically encoded mitochondrial H₂O₂ redox reporter mtORP1-roGFP (Albrecht *et al.*, 2011). Furthermore, highly sensitive reporters, using the same principle as the former example, have been engineered by the laboratory of Tobias Dick in Heidelberg that could be expressed in the fly, to replace the old mtORP1-roGFP (Albrecht *et al.*, 2011). It may also be interesting to measure ROS in different fly tissues, such as the flight muscle, gut or fat body, which have been shown to have different proteomic responses to alterations that extend lifespan, such as reduced insulin signalling (Tain *et al.*, 2017). In this study, mitochondrial respiration was altered in fat body but not in

brain, skeletal muscle or gut. It would be interesting to test whether ROS are altered in these alternative tissues and if alterations in ROS are instrumental for extending lifespan. In addition, unpublished results from the Sanz's laboratory, show that genetic depletion of CoQ, by knocking down genes involved in CoQ synthesis, causes an increase in mitochondrial ROS in skeletal muscle but not in the brain.

The next step in this line of research will be to take advantage of the HS model to induce ROS-RET and explore the pathways that are activated in response to this signal. Unpublished data from our laboratory show that preventing ROS-RET, using AOX or mitochondrial-targeted catalase expression to decrease ROS levels, shortens lifespan under HS. This supports a major role of ROS-RET signalling, in stress adaptation. To study this further, a hypothesis-driven approach could be used to test whether pathways that have been shown to be ROS regulated, for example, Nf- κ B, HIFs, PI3K and MAPK, are activated by ROS-RET. A non-hypothesis driven approach to study transcriptomic and metabolomics changes, in response to ROS-RET, has been already carried out in our laboratory. The results from this approach have shown that ROS-RET is required for activating pro-survival pathways in response to HS (Scialo and colleagues, unpublished results). ROS-RET activation diverts glycolytic intermediates to the pentose phosphate pathway, to produce NADPH and precursors for nucleotide biosynthesis. Finally, in the future, it will be interesting to use new proteomics approaches (Bagwan *et al.*, 2018) to detect post-translational modifications in proteins (including changes in redox-sensitive cysteines) (Menger *et al.*, 2015) in response to ROS-RET.

The identification of ROS-RET is based on the administration of rotenone and FCCP, to block the CI quinone-binding site and dissipate the mitochondrial proton motive force, respectively. Although these effects are well characterized *in vitro*, it remains to be determined whether they accomplish the same *in vivo* and specifically in the conditions assayed in the present work, i.e. the *Drosophila* brain. Therefore, another future objective is to assess both parameters in parallel to ROS measurements in the brain. Measuring the redox state of the CoQ pool is relatively simple using LC-UV, which our group has done in the past for Ndi1 flies in collaboration with Prof Placido Navas (Scialo *et al.*, 2016a). However, measuring the proton motive force is more technically challenging. In fact, in most cases, only one of its components, the mitochondrial membrane potential, is assessed. Although measurements of the

mitochondrial membrane potential *per se* are easier to perform, there are still a lot of technical difficulties summarised in (Perry *et al.*, 2011). Therefore, similarly to mitochondrial ROS measurements, most data have been obtained *in vitro* using isolated mitochondria or cells. A new method combining MS and *click chemistry* has been recently published showing promising results in the mouse heart (Logan *et al.*, 2016). Using the same approach in the fly brain will help to determine how mitochondrial membrane potential changes during ROS-RET, as well as allowing us to confirm the role of FCCP in dissipating the membrane potential and how CIII and CIV inhibition affects this parameter.

My experiments involved in the manipulation of CV levels or activity were inconclusive. Unexpectedly, the well-characterized CV inhibitor, oligomycin, decreased ROS under non-stress conditions and prevented ROS-RET under HS as well as in *Ndi1* flies. Future work should explore alternative CV inhibitors and knocking down other CV subunits, including different components of the F₁ and F₀ regions. Alternatively, experiments overexpressing the fly orthologue of ATP1F1 (*CG13551*) must be repeated. Despite the promising data I obtained, I was not able to demonstrate the overexpression of ATP1F1 and neither were the authors that generated the UAS-ATP1F1 flies. Therefore these results have not been included in my thesis. Making new fly models of ATP1F1 with and without e.g. a GFP tagged version to confirm its expression will help to clarify the role of ATP1F1 and CV, in mitochondrial ROS production. Experiments involving ATP1F1 are particularly relevant due to the many functions ATP1F1 seems to play in cancer and non-cancer cells (Garcia-Aguilar and Cuezva, 2018).

Future work regarding the screen should focus on dissecting how *VhaPPA1-1* triggers ROS-RET. First, I would repeat the ROS experiments with *CG7071*, to test whether its knockdown also triggers RET. Following confirmation, I would test other subunits of the V-ATPase, by knocking them down, to observe if they are also involved in regulating ROS-RET to identify if this effect is dependent of the activity of V-ATPase. Secondly, I would try to dissect the mechanisms, by which V-ATPases regulate mitochondrial ROS production. Additionally, I would study the rest of the confirmed genes from the AOX screen to identify new regulators involved in ROS-RET signalling. These experiments must include confirmation that AOX not only rescues the lethal developmental phenotype but also reduces ROS in adult flies. Finally, I would perform alternative screens using AOX, by targeting families of genes

that based on data from the literature affect ROS production. These screens, with fewer lines to be studied, will allow the use of different RU486 concentrations to titrate AOX expression and the expression of the RNAi construct and different drivers to study tissue-specific ROS production.

7.4 Final Conclusions

In conclusion, in my thesis, I described a physiological method of inducing ROS-RET in the fly brain, using HS. To dissect this ROS signal further, I manipulated the levels of individual components of the mitochondrial ETC. Here, my results showed that maintaining electron flow through CI and CII, of the respiratory chain, is instrumental for triggering ROS-RET. Blocking the exit of electrons from the ETC via CIII and CIV inhibition increased ROS through an alternative mechanism, excluding RET. The effect of CV inhibition of ROS-RET was inconclusive with acute and long-term inhibition providing contrasting results. Finally, I performed a genome-wide RNAi screen that was successful in identifying new genes involved in the regulation of ROS. Using AOX I reported 40 candidate genes, one of which, *VhaPP1-1*, I confirmed is involved in regulating ROS-RET in the fly brain (Figure 7.2).

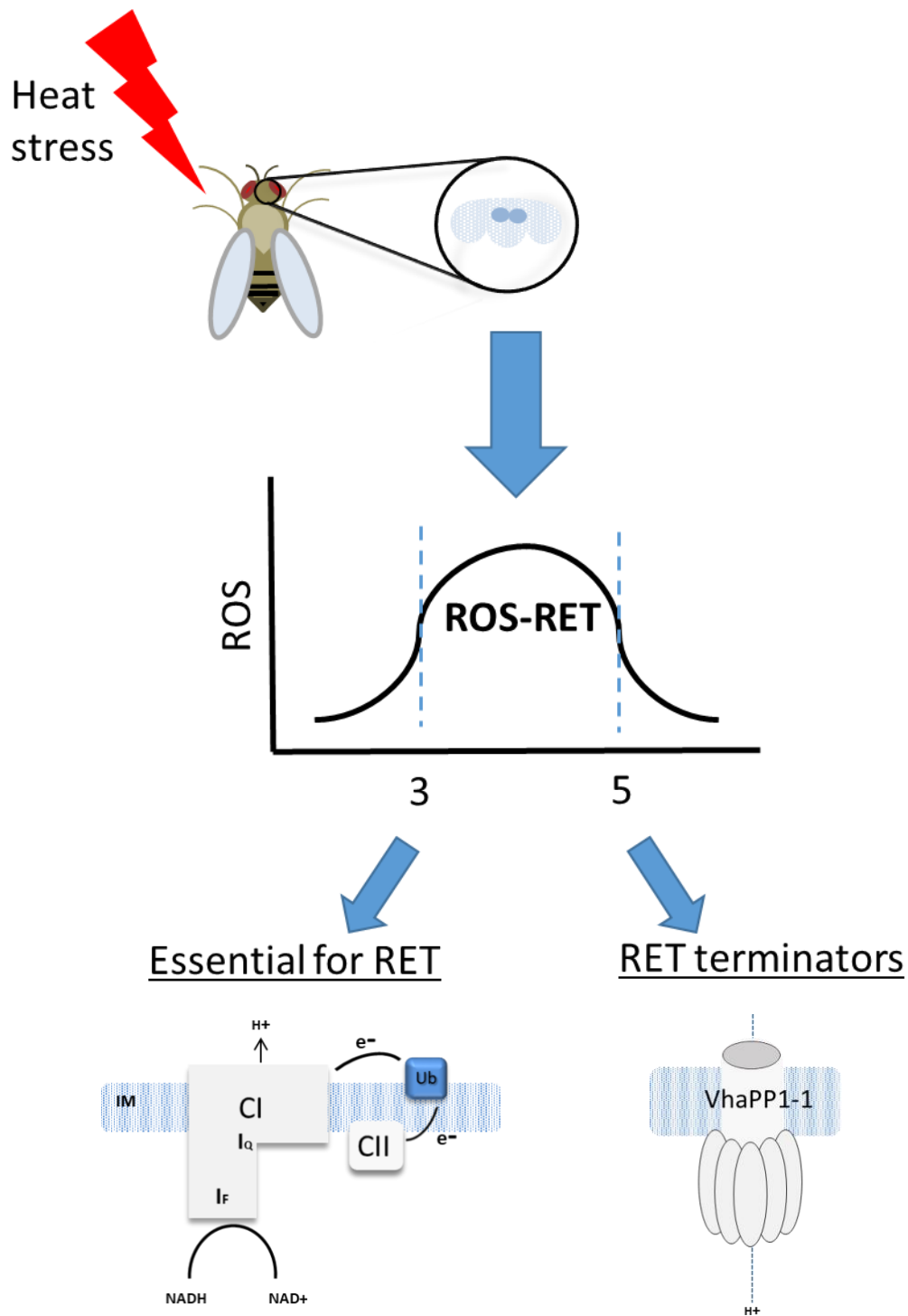


Figure 7.2 Diagram displaying the ROS-RET signal.

The results of this thesis show that subjecting flies to heat stress, provides the conditions needed in order to stimulate ROS-RET physiologically in the fly brain, between 3-5 hours. In addition, I have been able to demonstrate that CI and CII are essential for establishing a ROS-RET signal. Furthermore, results from a genome-wide RNAi screen were able to identify VhaPP1-1, as a potential RET regulator.

References

- Abdul-Ghani, M.A., Jani, R., Chavez, A., Molina-Carrion, M., Tripathy, D. and Defronzo, R.A. (2009) 'Mitochondrial reactive oxygen species generation in obese non-diabetic and type 2 diabetic participants', *Diabetologia*, 52(4), pp. 574-82.
- Ackrell, B.A. (2002) 'Cytopathies involving mitochondrial complex II', *Mol Aspects Med*, 23(5), pp. 369-84.
- Adams, M.D., Celniker, S.E., Holt, R.A., Evans, C.A., Gocayne, J.D., Amanatides, P.G., Scherer, S.E., Li, P.W., Hoskins, R.A., Galle, R.F., George, R.A., Lewis, S.E., Richards, S., Ashburner, M., Henderson, S.N., Sutton, G.G., Wortman, J.R., Yandell, M.D., Zhang, Q., Chen, L.X., Brandon, R.C., Rogers, Y.H., Blazej, R.G., Champe, M., Pfeiffer, B.D., Wan, K.H., Doyle, C., Baxter, E.G., Helt, G., Nelson, C.R., Gabor, G.L., Abril, J.F., Agbayani, A., An, H.J., Andrews-Pfannkoch, C., Baldwin, D., Ballew, R.M., Basu, A., Baxendale, J., Bayraktaroglu, L., Beasley, E.M., Beeson, K.Y., Benos, P.V., Berman, B.P., Bhandari, D., Bolshakov, S., Borkova, D., Botchan, M.R., Bouck, J., Brokstein, P., Brottier, P., Burtis, K.C., Busam, D.A., Butler, H., Cadieu, E., Center, A., Chandra, I., Cherry, J.M., Cawley, S., Dahlke, C., Davenport, L.B., Davies, P., de Pablos, B., Delcher, A., Deng, Z., Mays, A.D., Dew, I., Dietz, S.M., Dodson, K., Doup, L.E., Downes, M., Dugan-Rocha, S., Dunkov, B.C., Dunn, P., Durbin, K.J., Evangelista, C.C., Ferraz, C., Ferriera, S., Fleischmann, W., Fosler, C., Gabrielian, A.E., Garg, N.S., Gelbart, W.M., Glasser, K., Glodek, A., Gong, F., Gorrell, J.H., Gu, Z., Guan, P., Harris, M., Harris, N.L., Harvey, D., Heiman, T.J., Hernandez, J.R., Houck, J., Hostin, D., Houston, K.A., Howland, T.J., Wei, M.H., Ibegwam, C., et al. (2000) 'The genome sequence of *Drosophila melanogaster*', *Science*, 287(5461), pp. 2185-95.
- Akila, V.P., Harishchandra, H., D'Souza, V. and D'Souza, B. (2007) 'Age related changes in lipid peroxidation and antioxidants in elderly people', *Indian J Clin Biochem*, 22(1), pp. 131-4.
- Albrecht, S.C., Barata, A.G., Grosshans, J., Teleman, A.A. and Dick, T.P. (2011) 'In vivo mapping of hydrogen peroxide and oxidized glutathione reveals chemical and regional specificity of redox homeostasis', *Cell Metab*, 14(6), pp. 819-29.
- Anderson, E.J., Lustig, M.E., Boyle, K.E., Woodlief, T.L., Kane, D.A., Lin, C.T., Price, J.W., 3rd, Kang, L., Rabinovitch, P.S., Szeto, H.H., Houmard, J.A., Cortright, R.N., Wasserman, D.H. and Neuffer, P.D. (2009) 'Mitochondrial H₂O₂ emission and cellular redox state link excess fat intake to insulin resistance in both rodents and humans', *J Clin Invest*, 119(3), pp. 573-81.
- Anderson, S., Bankier, A.T., Barrell, B.G., de Bruijn, M.H., Coulson, A.R., Drouin, J., Eperon, I.C., Nierlich, D.P., Roe, B.A., Sanger, F., Schreier, P.H., Smith, A.J., Staden, R. and Young, I.G. (1981) 'Sequence and organization of the human mitochondrial genome', *Nature*, 290(5806), pp. 457-65.
- Andjelkovic, A., Mordas, A., Bruinsma, L., Ketola, A., Cannino, G., Giordano, L., Dhandapani, P.K., Szibor, M., Dufour, E. and Jacobs, H.T. (2018) 'Expression of the Alternative Oxidase Influences Jun N-Terminal Kinase Signaling and Cell Migration', *Mol Cell Biol*, 38(24).

Arias-Mayenco, I., Gonzalez-Rodriguez, P., Torres-Torrelo, H., Gao, L., Fernandez-Aguera, M.C., Bonilla-Henao, V., Ortega-Saenz, P. and Lopez-Barneo, J. (2018) 'Acute O₂ Sensing: Role of Coenzyme QH₂/Q Ratio and Mitochondrial ROS Compartmentalization', *Cell Metab*, 28(1), pp. 145-158 e4.

Babbitt, S.E., Hsu, J., Mendez, D.L. and Kranz, R.G. (2017) 'Biosynthesis of Single Thioether c-Type Cytochromes Provides Insight into Mechanisms Intrinsic to Holocytochrome c Synthase (HCCS)', *Biochemistry*, 56(26), pp. 3337-3346.

Bacsi, A., Woodberry, M., Widger, W., Papaconstantinou, J., Mitra, S., Peterson, J.W. and Boldogh, I. (2006) 'Localization of superoxide anion production to mitochondrial electron transport chain in 3-NPA-treated cells', *Mitochondrion*, 6(5), pp. 235-44.

Bagwan, N., Bonzon-Kulichenko, E., Calvo, E., Lechuga-Vieco, A.V., Michalakopoulos, S., Trevisan-Herraz, M., Ezkurdia, I., Rodriguez, J.M., Magni, R., Latorre-Pellicer, A., Enriquez, J.A. and Vazquez, J. (2018) 'Comprehensive Quantification of the Modified Proteome Reveals Oxidative Heart Damage in Mitochondrial Heteroplasmy', *Cell Rep*, 23(12), pp. 3685-3697 e4.

Bahadorani, S., Cho, J., Lo, T., Contreras, H., Lawal, H.O., Krantz, D.E., Bradley, T.J. and Walker, D.W. (2010) 'Neuronal expression of a single-subunit yeast NADH-ubiquinone oxidoreductase (Ndi1) extends Drosophila lifespan', *Aging Cell*, 9(2), pp. 191-202.

Bai, Y., Hajek, P., Chomyn, A., Chan, E., Seo, B.B., Matsuno-Yagi, A., Yagi, T. and Attardi, G. (2001) 'Lack of complex I activity in human cells carrying a mutation in MtDNA-encoded ND4 subunit is corrected by the *Saccharomyces cerevisiae* NADH-quinone oxidoreductase (NDI1) gene', *J Biol Chem*, 276(42), pp. 38808-13.

Bak, D.W. and Weerapana, E. (2015) 'Cysteine-mediated redox signalling in the mitochondria', *Mol Biosyst*, 11(3), pp. 678-97.

Barber-Singh, J., Seo, B.B., Nakamaru-Ogiso, E., Lau, Y.S., Matsuno-Yagi, A. and Yagi, T. (2009) 'Neuroprotective effect of long-term NDI1 gene expression in a chronic mouse model of Parkinson disorder', *Rejuvenation Res*, 12(4), pp. 259-67.

Barel, O., Shorer, Z., Flusser, H., Ofir, R., Narkis, G., Finer, G., Shalev, H., Nasasra, A., Saada, A. and Birk, O.S. (2008) 'Mitochondrial complex III deficiency associated with a homozygous mutation in UQCRQ', *Am J Hum Genet*, 82(5), pp. 1211-6.

Barja, G. (1999) 'Mitochondrial oxygen radical generation and leak: sites of production in states 4 and 3, organ specificity, and relation to aging and longevity', *J Bioenerg Biomembr*, 31(4), pp. 347-66.

Barja, G. (2007) 'Mitochondrial oxygen consumption and reactive oxygen species production are independently modulated: implications for aging studies', *Rejuvenation Res*, 10(2), pp. 215-24.

Barja, G. (2014) 'The mitochondrial free radical theory of aging', *Prog Mol Biol Transl Sci*, 127, pp. 1-27.

Barja, G. (2019) 'Towards a unified mechanistic theory of aging', *Exp Gerontol*, 124, p. 110627.

- Barja, G., Cadenas, S., Rojas, C., Perez-Campo, R. and Lopez-Torres, M. (1994) 'Low mitochondrial free radical production per unit O₂ consumption can explain the simultaneous presence of high longevity and high aerobic metabolic rate in birds', *Free Radic Res*, 21(5), pp. 317-27.
- Battelli, M.G., Polito, L., Bortolotti, M. and Bolognesi, A. (2016) 'Xanthine Oxidoreductase-Derived Reactive Species: Physiological and Pathological Effects', *Oxid Med Cell Longev*, 2016, p. 3527579.
- Bell, E.L., Klimova, T.A., Eisenbart, J., Moraes, C.T., Murphy, M.P., Budinger, G.R. and Chandel, N.S. (2007) 'The Qo site of the mitochondrial complex III is required for the transduction of hypoxic signaling via reactive oxygen species production', *J Cell Biol*, 177(6), pp. 1029-36.
- Beltran, B., Quintero, M., Garcia-Zaragoza, E., O'Connor, E., Esplugues, J.V. and Moncada, S. (2002) 'Inhibition of mitochondrial respiration by endogenous nitric oxide: a critical step in Fas signaling', *Proc Natl Acad Sci U S A*, 99(13), pp. 8892-7.
- Bentinger, M., Tekle, M. and Dallner, G. (2010) 'Coenzyme Q--biosynthesis and functions', *Biochem Biophys Res Commun*, 396(1), pp. 74-9.
- Berry, B.J., Trewin, A.J., Amitrano, A.M., Kim, M. and Wojtovich, A.P. (2018) 'Use the Protonmotive Force: Mitochondrial Uncoupling and Reactive Oxygen Species', *J Mol Biol*, 430(21), pp. 3873-3891.
- Berry, E.A. and Huang, L.S. (2011) 'Conformationally linked interaction in the cytochrome bc(1) complex between inhibitors of the Q(o) site and the Rieske iron-sulfur protein', *Biochim Biophys Acta*, 1807(10), pp. 1349-63.
- Betarbet, R., Sherer, T.B., MacKenzie, G., Garcia-Osuna, M., Panov, A.V. and Greenamyre, J.T. (2000) 'Chronic systemic pesticide exposure reproduces features of Parkinson's disease', *Nat Neurosci*, 3(12), pp. 1301-6.
- Bielski, B.H., Arudi, R.L. and Sutherland, M.W. (1983) 'A study of the reactivity of HO₂/O₂- with unsaturated fatty acids', *J Biol Chem*, 258(8), pp. 4759-61.
- Bienert, G.P., Schjoerring, J.K. and Jahn, T.P. (2006) 'Membrane transport of hydrogen peroxide', *Biochim Biophys Acta*, 1758(8), pp. 994-1003.
- Bier, E., Harrison, M.M., O'Connor-Giles, K.M. and Wildonger, J. (2018) 'Advances in Engineering the Fly Genome with the CRISPR-Cas System', *Genetics*, 208(1), pp. 1-18.
- Bischof, J., Maeda, R.K., Hediger, M., Karch, F. and Basler, K. (2007) 'An optimized transgenesis system for Drosophila using germ-line-specific phiC31 integrases', *Proc Natl Acad Sci U S A*, 104(9), pp. 3312-7.
- Bjorklund, M., Taipale, M., Varjosalo, M., Saharinen, J., Lahdenpera, J. and Taipale, J. (2006) 'Identification of pathways regulating cell size and cell-cycle progression by RNAi', *Nature*, 439(7079), pp. 1009-13.

Bleier, L. and Drose, S. (2013) 'Superoxide generation by complex III: from mechanistic rationales to functional consequences', *Biochim Biophys Acta*, 1827(11-12), pp. 1320-31.

Bowman, A. and Birch-Machin, M.A. (2016) 'Age-Dependent Decrease of Mitochondrial Complex II Activity in Human Skin Fibroblasts', *J Invest Dermatol*.

Brand, A.H. and Perrimon, N. (1993) 'Targeted gene expression as a means of altering cell fates and generating dominant phenotypes', *Development*, 118(2), pp. 401-15.

Brand, M.D., Goncalves, R.L., Orr, A.L., Vargas, L., Gerencser, A.A., Borch Jensen, M., Wang, Y.T., Melov, S., Turk, C.N., Matzen, J.T., Dardov, V.J., Petrassi, H.M., Meeusen, S.L., Perevoshchikova, I.V., Jasper, H., Brookes, P.S. and Ainscow, E.K. (2016) 'Suppressors of Superoxide-H₂O₂ Production at Site IQ of Mitochondrial Complex I Protect against Stem Cell Hyperplasia and Ischemia-Reperfusion Injury', *Cell Metab*, 24(4), pp. 582-592.

Brand, M.D. and Nicholls, D.G. (2011) 'Assessing mitochondrial dysfunction in cells', *Biochem J*, 435(2), pp. 297-312.

Brandt, A. and Vilcinskas, A. (2013) 'The Fruit Fly *Drosophila melanogaster* as a Model for Aging Research', *Adv Biochem Eng Biotechnol*, 135, pp. 63-77.

Brandt, U. (2006) 'Energy converting NADH:quinone oxidoreductase (complex I)', *Annu Rev Biochem*, 75, pp. 69-92.

Brandt, U., Kerscher, S., Drose, S., Zwicker, K. and Zickermann, V. (2003) 'Proton pumping by NADH:ubiquinone oxidoreductase. A redox driven conformational change mechanism?', *FEBS Lett*, 545(1), pp. 9-17.

Bratic, I. and Trifunovic, A. (2010) 'Mitochondrial energy metabolism and ageing', *Biochim Biophys Acta*, 1797(6-7), pp. 961-7.

Brennan, J.P., Berry, R.G., Baghai, M., Duchon, M.R. and Shattock, M.J. (2006) 'FCCP is cardioprotective at concentrations that cause mitochondrial oxidation without detectable depolarisation', *Cardiovasc Res*, 72(2), pp. 322-30.

Brown, G.C. and Borutaite, V. (2008) 'Regulation of apoptosis by the redox state of cytochrome c', *Biochim Biophys Acta*, 1777(7-8), pp. 877-81.

Brown, G.C. and Borutaite, V. (2012) 'There is no evidence that mitochondria are the main source of reactive oxygen species in mammalian cells', *Mitochondrion*, 12(1), pp. 1-4.

Brunelle, J.K., Bell, E.L., Quesada, N.M., Vercauteren, K., Tiranti, V., Zeviani, M., Scarpulla, R.C. and Chandel, N.S. (2005) 'Oxygen sensing requires mitochondrial ROS but not oxidative phosphorylation', *Cell Metab*, 1(6), pp. 409-14.

Bugiardini, E., Mitchell, A.L., Rosa, I.D., Horning-Do, H.T., Pitmann, A., Poole, O.V., Holton, J.L., Shah, S., Woodward, C., Hargreaves, I., Quinlivan, R., Amunts, A., Wiesner, R.J., Houlden, H., Holt, I.J., Hanna, M.G., Pitceathly, R.D.S. and

- Spinazzola, A. (2019a) 'MRPS25 mutations impair mitochondrial translation and cause encephalomyopathy', *Hum Mol Genet*.
- Bugiardini, E., Mitchell, A.L., Rosa, I.D., Horning-Do, H.T., Pitmann, A.M., Poole, O.V., Holton, J.L., Shah, S., Woodward, C., Hargreaves, I., Quinlivan, R., Amunts, A., Wiesner, R.J., Houlden, H., Holt, I.J., Hanna, M.G., Pitceathly, R.D.S. and Spinazzola, A. (2019b) 'MRPS25 mutations impair mitochondrial translation and cause encephalomyopathy', *Hum Mol Genet*, 28(16), pp. 2711-2719.
- Burman, J.L., Itsara, L.S., Kayser, E.B., Suthammarak, W., Wang, A.M., Kaeberlein, M., Sedensky, M.M., Morgan, P.G. and Pallanck, L.J. (2014) 'A Drosophila model of mitochondrial disease caused by a complex I mutation that uncouples proton pumping from electron transfer', *Dis Model Mech*, 7(10), pp. 1165-74.
- Busuttil, R.A., Rubio, M., Dolle, M.E., Campisi, J. and Vijg, J. (2003) 'Oxygen accelerates the accumulation of mutations during the senescence and immortalization of murine cells in culture', *Aging Cell*, 2(6), pp. 287-94.
- Cabre, R., Naudi, A., Dominguez-Gonzalez, M., Ayala, V., Jove, M., Mota-Martorell, N., Pinol-Ripoll, G., Gil-Villar, M.P., Rue, M., Portero-Otin, M., Ferrer, I. and Pamplona, R. (2017) 'Sixty years old is the breakpoint of human frontal cortex aging', *Free Radic Biol Med*, 103, pp. 14-22.
- Cai, Z. and Yan, L.J. (2013) 'Protein Oxidative Modifications: Beneficial Roles in Disease and Health', *J Biochem Pharmacol Res*, 1(1), pp. 15-26.
- Cannino, G., El-Khoury, R., Pirinen, M., Hutz, B., Rustin, P., Jacobs, H.T. and Dufour, E. (2012) 'Glucose modulates respiratory complex I activity in response to acute mitochondrial dysfunction', *J Biol Chem*, 287(46), pp. 38729-40.
- Carroll, J., Fearnley, I.M., Skehel, J.M., Shannon, R.J., Hirst, J. and Walker, J.E. (2006) 'Bovine complex I is a complex of 45 different subunits', *J Biol Chem*, 281(43), pp. 32724-7.
- Catterson, J.H., Khericha, M., Dyson, M.C., Vincent, A.J., Callard, R., Haveron, S.M., Rajasingam, A., Ahmad, M. and Partridge, L. (2018) 'Short-Term, Intermittent Fasting Induces Long-Lasting Gut Health and TOR-Independent Lifespan Extension', *Curr Biol*, 28(11), pp. 1714-1724 e4.
- Cecchini, G. (2003) 'Function and structure of complex II of the respiratory chain', *Annu Rev Biochem*, 72, pp. 77-109.
- Cedikova, M., Pitule, P., Kripnerova, M., Markova, M. and Kuncova, J. (2016) 'Multiple roles of mitochondria in aging processes', *Physiol Res*, 65(Supplementum 5), pp. S519-S531.
- Chance, B. and Hollunger, G. (1961) 'The interaction of energy and electron transfer reactions in mitochondria. I. General properties and nature of the products of succinate-linked reduction of pyridine nucleotide', *J Biol Chem*, 236, pp. 1534-43.
- Chandel, N.S. (2010) 'Mitochondrial complex III: an essential component of universal oxygen sensing machinery?', *Respir Physiol Neurobiol*, 174(3), pp. 175-81.

Chandel, N.S. (2014) 'Mitochondria as signaling organelles', *BMC Biol*, 12, p. 34.

Chandel, N.S., McClintock, D.S., Feliciano, C.E., Wood, T.M., Melendez, J.A., Rodriguez, A.M. and Schumacker, P.T. (2000) 'Reactive oxygen species generated at mitochondrial complex III stabilize hypoxia-inducible factor-1alpha during hypoxia: a mechanism of O₂ sensing', *J Biol Chem*, 275(33), pp. 25130-8.

Chen, J., Shi, X., Padmanabhan, R., Wang, Q., Wu, Z., Stevenson, S.C., Hild, M., Garza, D. and Li, H. (2008) 'Identification of novel modulators of mitochondrial function by a genome-wide RNAi screen in *Drosophila melanogaster*', *Genome Res*, 18(1), pp. 123-36.

Chen, Q., Moghaddas, S., Hoppel, C.L. and Lesnefsky, E.J. (2006) 'Reversible blockade of electron transport during ischemia protects mitochondria and decreases myocardial injury following reperfusion', *J Pharmacol Exp Ther*, 319(3), pp. 1405-12.

Chen, W.W., Birsoy, K., Mihaylova, M.M., Snitkin, H., Stasinski, I., Yucel, B., Bayraktar, E.C., Carette, J.E., Clish, C.B., Brummelkamp, T.R., Sabatini, D.D. and Sabatini, D.M. (2014) 'Inhibition of ATRIF1 ameliorates severe mitochondrial respiratory chain dysfunction in mammalian cells', *Cell Rep*, 7(1), pp. 27-34.

Chen, Y.N., Wu, C.H., Zheng, Y., Li, J.J., Wang, J.L. and Wang, Y.F. (2015) 'Knockdown of ATPsyn-b caused larval growth defect and male infertility in *Drosophila*', *Arch Insect Biochem Physiol*, 88(2), pp. 144-54.

Chin, R.M., Fu, X., Pai, M.Y., Vergnes, L., Hwang, H., Deng, G., Diep, S., Lomenick, B., Meli, V.S., Monsalve, G.C., Hu, E., Whelan, S.A., Wang, J.X., Jung, G., Solis, G.M., Fazlollahi, F., Kaweeteerawat, C., Quach, A., Nili, M., Krall, A.S., Godwin, H.A., Chang, H.R., Faull, K.F., Guo, F., Jiang, M., Trauger, S.A., Saghatelian, A., Braas, D., Christofk, H.R., Clarke, C.F., Teitell, M.A., Petrascheck, M., Reue, K., Jung, M.E., Frand, A.R. and Huang, J. (2014a) 'The metabolite [agr]-ketoglutarate extends lifespan by inhibiting ATP synthase and TOR', *Nature*, 510(7505), pp. 397-401.

Chin, R.M., Fu, X., Pai, M.Y., Vergnes, L., Hwang, H., Deng, G., Diep, S., Lomenick, B., Meli, V.S., Monsalve, G.C., Hu, E., Whelan, S.A., Wang, J.X., Jung, G., Solis, G.M., Fazlollahi, F., Kaweeteerawat, C., Quach, A., Nili, M., Krall, A.S., Godwin, H.A., Chang, H.R., Faull, K.F., Guo, F., Jiang, M., Trauger, S.A., Saghatelian, A., Braas, D., Christofk, H.R., Clarke, C.F., Teitell, M.A., Petrascheck, M., Reue, K., Jung, M.E., Frand, A.R. and Huang, J. (2014b) 'The metabolite alpha-ketoglutarate extends lifespan by inhibiting ATP synthase and TOR', *Nature*, 510(7505), pp. 397-401.

Chistiakov, D.A., Sobenin, I.A., Revin, V.V., Orekhov, A.N. and Bobryshev, Y.V. (2014) 'Mitochondrial aging and age-related dysfunction of mitochondria', *Biomed Res Int*, 2014, p. 238463.

Cho, J., Hur, J.H., Graniel, J., Benzer, S. and Walker, D.W. (2012) 'Expression of yeast ND11 rescues a *Drosophila* complex I assembly defect', *PLoS One*, 7(11), p. e50644.

Cho, J., Hur, J.H. and Walker, D.W. (2011a) 'The role of mitochondria in *Drosophila* aging', *Exp Gerontol*, 46(5), pp. 331-4.

Cho, K.J., Seo, J.M. and Kim, J.H. (2011b) 'Bioactive lipoxygenase metabolites stimulation of NADPH oxidases and reactive oxygen species', *Mol Cells*, 32(1), pp. 1-5.

Choi, H., Kim, S., Mukhopadhyay, P., Cho, S., Woo, J., Storz, G. and Ryu, S.E. (2001) 'Structural basis of the redox switch in the OxyR transcription factor', *Cell*, 105(1), pp. 103-13.

Chokchaiwong, S., Kuo, Y.T., Hsu, S.P., Hsu, Y.C., Lin, S.H., Zhong, W.B., Lin, Y.F. and Kao, S.H. (2019) 'ETF-QO Mutants Uncoupled Fatty Acid beta-Oxidation and Mitochondrial Bioenergetics Leading to Lipid Pathology', *Cells*, 8(2).

Chouchani, E.T., Pell, V.R., Gaude, E., Akseptijevic, D., Sundier, S.Y., Robb, E.L., Logan, A., Nadtochiy, S.M., Ord, E.N., Smith, A.C., Eyassu, F., Shirley, R., Hu, C.H., Dare, A.J., James, A.M., Rogatti, S., Hartley, R.C., Eaton, S., Costa, A.S., Brookes, P.S., Davidson, S.M., Duchon, M.R., Saeb-Parsy, K., Shattock, M.J., Robinson, A.J., Work, L.M., Frezza, C., Krieg, T. and Murphy, M.P. (2014a) 'Ischaemic accumulation of succinate controls reperfusion injury through mitochondrial ROS', *Nature*, 515(7527), pp. 431-5.

Chouchani, E.T., Pell, V.R., Gaude, E., Akseptijevic, D., Sundier, S.Y., Robb, E.L., Logan, A., Nadtochiy, S.M., Ord, E.N.J., Smith, A.C., Eyassu, F., Shirley, R., Hu, C.H., Dare, A.J., James, A.M., Rogatti, S., Hartley, R.C., Eaton, S., Costa, A.S.H., Brookes, P.S., Davidson, S.M., Duchon, M.R., Saeb-Parsy, K., Shattock, M.J., Robinson, A.J., Work, L.M., Frezza, C., Krieg, T. and Murphy, M.P. (2014b) 'Ischaemic accumulation of succinate controls reperfusion injury through mitochondrial ROS', *Nature*, 515(7527), pp. 431-435.

Chouchani, E.T., Pell, V.R., James, A.M., Work, L.M., Saeb-Parsy, K., Frezza, C., Krieg, T. and Murphy, M.P. (2016) 'A Unifying Mechanism for Mitochondrial Superoxide Production during Ischemia-Reperfusion Injury', *Cell Metab*, 23(2), pp. 254-63.

Claiborne, A., Yeh, J.I., Mallett, T.C., Luba, J., Crane, E.J., 3rd, Charrier, V. and Parsonage, D. (1999) 'Protein-sulfenic acids: diverse roles for an unlikely player in enzyme catalysis and redox regulation', *Biochemistry*, 38(47), pp. 15407-16.

Clancy, D.J., Gems, D., Harshman, L.G., Oldham, S., Stocker, H., Hafen, E., Leevers, S.J. and Partridge, L. (2001) 'Extension of life-span by loss of CHICO, a *Drosophila* insulin receptor substrate protein', *Science*, 292(5514), pp. 104-6.

Cocheme, H.M., Quin, C., McQuaker, S.J., Cabreiro, F., Logan, A., Prime, T.A., Abakumova, I., Patel, J.V., Fearnley, I.M., James, A.M., Porteous, C.M., Smith, R.A., Saeed, S., Carre, J.E., Singer, M., Gems, D., Hartley, R.C., Partridge, L. and Murphy, M.P. (2011) 'Measurement of H₂O₂ within living *Drosophila* during aging using a ratiometric mass spectrometry probe targeted to the mitochondrial matrix', *Cell Metab*, 13(3), pp. 340-50.

Cogliati, S., Enriquez, J.A. and Scorrano, L. (2016) 'Mitochondrial Cristae: Where Beauty Meets Functionality', *Trends Biochem Sci*, 41(3), pp. 261-273.

- Cogliati, S., Frezza, C., Soriano, M.E., Varanita, T., Quintana-Cabrera, R., Corrado, M., Cipolat, S., Costa, V., Casarin, A., Gomes, L.C., Perales-Clemente, E., Salviati, L., Fernandez-Silva, P., Enriquez, J.A. and Scorrano, L. (2013) 'Mitochondrial cristae shape determines respiratory chain supercomplexes assembly and respiratory efficiency', *Cell*, 155(1), pp. 160-71.
- Cooley, L., Kelley, R. and Spradling, A. (1988) 'Insertional mutagenesis of the *Drosophila* genome with single P elements', *Science*, 239(4844), pp. 1121-8.
- Cooper, A.J., Pinto, J.T. and Callery, P.S. (2011) 'Reversible and irreversible protein glutathionylation: biological and clinical aspects', *Expert Opin Drug Metab Toxicol*, 7(7), pp. 891-910.
- Cooper, J.M., Mann, V.M. and Schapira, A.H. (1992) 'Analyses of mitochondrial respiratory chain function and mitochondrial DNA deletion in human skeletal muscle: effect of ageing', *J Neurol Sci*, 113(1), pp. 91-8.
- Crofts, A.R. (2004) 'The cytochrome bc1 complex: function in the context of structure', *Annu Rev Physiol*, 66, pp. 689-733.
- Crompton, M. (1999) 'The mitochondrial permeability transition pore and its role in cell death', *Biochem J*, 341 (Pt 2), pp. 233-49.
- Cui, H., Kong, Y. and Zhang, H. (2012) 'Oxidative stress, mitochondrial dysfunction, and aging', *J Signal Transduct*, 2012, p. 646354.
- D'Amico, E., Factor-Litvak, P., Santella, R.M. and Mitsumoto, H. (2013) 'Clinical perspective on oxidative stress in sporadic amyotrophic lateral sclerosis', *Free Radic Biol Med*, 65, pp. 509-527.
- Da-Re, C., von Stockum, S., Biscontin, A., Millino, C., Cisotto, P., Zordan, M.A., Zeviani, M., Bernardi, P., De Pitta, C. and Costa, R. (2014) 'Leigh syndrome in *Drosophila melanogaster*: morphological and biochemical characterization of Surf1 post-transcriptional silencing', *J Biol Chem*, 289(42), pp. 29235-46.
- Dar, A.C., Das, T.K., Shokat, K.M. and Cagan, R.L. (2012) 'Chemical genetic discovery of targets and anti-targets for cancer polypharmacology', *Nature*, 486(7401), pp. 80-4.
- Dhalla, N.S., Temsah, R.M. and Netticadan, T. (2000) 'Role of oxidative stress in cardiovascular diseases', *J Hypertens*, 18(6), pp. 655-73.
- Dhillon, A.S., Hagan, S., Rath, O. and Kolch, W. (2007) 'MAP kinase signalling pathways in cancer', *Oncogene*, 26(22), pp. 3279-90.
- Diebold, L. and Chandel, N.S. (2016) 'Mitochondrial ROS regulation of proliferating cells', *Free Radic Biol Med*, 100, pp. 86-93.
- Diebold, L.P., Gil, H.J., Gao, P., Martinez, C.A., Weinberg, S.E. and Chandel, N.S. (2019) 'Mitochondrial complex III is necessary for endothelial cell proliferation during angiogenesis', *Nat Metab*, 1(1), pp. 158-171.

- Dietzl, G., Chen, D., Schnorrer, F., Su, K.C., Barinova, Y., Fellner, M., Gasser, B., Kinsey, K., Oppel, S., Scheiblaue, S., Couto, A., Marra, V., Keleman, K. and Dickson, B.J. (2007) 'A genome-wide transgenic RNAi library for conditional gene inactivation in *Drosophila*', *Nature*, 448(7150), pp. 151-6.
- Dillon, M.E., Wang, G., Garrity, P.A. and Huey, R.B. (2009) 'Review: Thermal preference in *Drosophila*', *J Therm Biol*, 34(3), pp. 109-119.
- DiMauro, S., Tanji, K. and Schon, E.A. (2012) 'The many clinical faces of cytochrome c oxidase deficiency', *Adv Exp Med Biol*, 748, pp. 341-57.
- Dogan, S.A., Cerutti, R., Beninca, C., Brea-Calvo, G., Jacobs, H.T., Zeviani, M., Szibor, M. and Viscomi, C. (2018) 'Perturbed Redox Signaling Exacerbates a Mitochondrial Myopathy', *Cell Metab*, 28(5), pp. 764-775 e5.
- Doonan, R., McElwee, J.J., Matthijssens, F., Walker, G.A., Houthoofd, K., Back, P., Matscheski, A., Vanfleteren, J.R. and Gems, D. (2008) 'Against the oxidative damage theory of aging: superoxide dismutases protect against oxidative stress but have little or no effect on life span in *Caenorhabditis elegans*', *Genes Dev*, 22(23), pp. 3236-41.
- Dorman, D.C., Moulin, F.J., McManus, B.E., Mahle, K.C., James, R.A. and Struve, M.F. (2002) 'Cytochrome oxidase inhibition induced by acute hydrogen sulfide inhalation: correlation with tissue sulfide concentrations in the rat brain, liver, lung, and nasal epithelium', *Toxicol Sci*, 65(1), pp. 18-25.
- Dorn, G.W., 2nd, Clark, C.F., Eschenbacher, W.H., Kang, M.Y., Engelhard, J.T., Warner, S.J., Matkovich, S.J. and Jowdy, C.C. (2011) 'MARF and Opa1 control mitochondrial and cardiac function in *Drosophila*', *Circ Res*, 108(1), pp. 12-7.
- Drew, B., Phaneuf, S., Dirks, A., Selman, C., Gredilla, R., Lezza, A., Barja, G. and Leeuwenburgh, C. (2003) 'Effects of aging and caloric restriction on mitochondrial energy production in gastrocnemius muscle and heart', *Am J Physiol Regul Integr Comp Physiol*, 284(2), pp. R474-80.
- Drose, S. (2013) 'Differential effects of complex II on mitochondrial ROS production and their relation to cardioprotective pre- and postconditioning', *Biochim Biophys Acta*, 1827(5), pp. 578-87.
- Drummond, G.R., Selemidis, S., Griendling, K.K. and Sobey, C.G. (2011) 'Combating oxidative stress in vascular disease: NADPH oxidases as therapeutic targets', *Nat Rev Drug Discov*, 10(6), pp. 453-71.
- Du, Y., Wooten, M.C., Gearing, M. and Wooten, M.W. (2009) 'Age-associated oxidative damage to the p62 promoter: implications for Alzheimer disease', *Free Radic Biol Med*, 46(4), pp. 492-501.
- Duong, A., Che, Y., Ceylan, D., Pinguelo, A., Andreatza, A.C., Trevor Young, L. and Berk, M. (2016) 'Regulators of mitochondrial complex I activity: A review of literature and evaluation in postmortem prefrontal cortex from patients with bipolar disorder', *Psychiatry Res*, 236, pp. 148-157.

- Edmondson, D.E. (2014) 'Hydrogen peroxide produced by mitochondrial monoamine oxidase catalysis: biological implications', *Curr Pharm Des*, 20(2), pp. 155-60.
- Eghbal, M.A., Pennefather, P.S. and O'Brien, P.J. (2004) 'H₂S cytotoxicity mechanism involves reactive oxygen species formation and mitochondrial depolarisation', *Toxicology*, 203(1-3), pp. 69-76.
- El-Khoury, R., Dufour, E., Rak, M., Ramanantsoa, N., Grandchamp, N., Csaba, Z., Duvillie, B., Benit, P., Gallego, J., Gressens, P., Sarkis, C., Jacobs, H.T. and Rustin, P. (2013) 'Alternative oxidase expression in the mouse enables bypassing cytochrome c oxidase blockade and limits mitochondrial ROS overproduction', *PLoS Genet*, 9(1), p. e1003182.
- El-Khoury, R., Kaulio, E., Lassila, K.A., Crowther, D.C., Jacobs, H.T. and Rustin, P. (2016) 'Expression of the alternative oxidase mitigates beta-amyloid production and toxicity in model systems', *Free Radic Biol Med*, 96, pp. 57-66.
- Elchuri, S., Oberley, T.D., Qi, W., Eisenstein, R.S., Jackson Roberts, L., Van Remmen, H., Epstein, C.J. and Huang, T.T. (2005) 'CuZnSOD deficiency leads to persistent and widespread oxidative damage and hepatocarcinogenesis later in life', *Oncogene*, 24(3), pp. 367-80.
- Endo, T. and Yamano, K. (2010) 'Transport of proteins across or into the mitochondrial outer membrane', *Biochim Biophys Acta*, 1803(6), pp. 706-14.
- Ernst, I.M., Pallauf, K., Bendall, J.K., Paulsen, L., Nikolai, S., Huebbe, P., Roeder, T. and Rimbach, G. (2013) 'Vitamin E supplementation and lifespan in model organisms', *Ageing Res Rev*, 12(1), pp. 365-75.
- Esparza-Molto, P.B., Nuevo-Tapioles, C. and Cuezva, J.M. (2017) 'Regulation of the H(+)-ATP synthase by IF1: a role in mitohormesis', *Cell Mol Life Sci*, 74(12), pp. 2151-2166.
- Esposito, G., Vos, M., Vilain, S., Swerts, J., De Sousa Valadas, J., Van Meensel, S., Schaap, O. and Verstreken, P. (2013) 'Aconitase causes iron toxicity in *Drosophila* pink1 mutants', *PLoS Genet*, 9(4), p. e1003478.
- Esterhazy, D., King, M.S., Yakovlev, G. and Hirst, J. (2008) 'Production of reactive oxygen species by complex I (NADH:ubiquinone oxidoreductase) from *Escherichia coli* and comparison to the enzyme from mitochondria', *Biochemistry*, 47(12), pp. 3964-71.
- Fernandez-Aguera, M.C., Gao, L., Gonzalez-Rodriguez, P., Pintado, C.O., Arias-Mayenco, I., Garcia-Flores, P., Garcia-Perganeda, A., Pascual, A., Ortega-Saenz, P. and Lopez-Barneo, J. (2015) 'Oxygen Sensing by Arterial Chemoreceptors Depends on Mitochondrial Complex I Signaling', *Cell Metab*, 22(5), pp. 825-37.
- Fernandez-Ayala, D.J., Sanz, A., Vartiainen, S., Kemppainen, K.K., Babusiak, M., Mustalahti, E., Costa, R., Tuomela, T., Zeviani, M., Chung, J., O'Dell, K.M., Rustin, P. and Jacobs, H.T. (2009) 'Expression of the *Ciona intestinalis* alternative oxidase (AOX) in *Drosophila* complements defects in mitochondrial oxidative phosphorylation', *Cell Metab*, 9(5), pp. 449-60.

- Fernandez-Moreno, M.A., Farr, C.L., Kaguni, L.S. and Garesse, R. (2007) 'Drosophila melanogaster as a model system to study mitochondrial biology', *Methods Mol Biol*, 372, pp. 33-49.
- Fessler, J.H., Kramerova, I., Kramerov, A., Chen, Y. and Fessler, L.I. (2004) 'Papilin, a novel component of basement membranes, in relation to ADAMTS metalloproteases and ECM development', *Int J Biochem Cell Biol*, 36(6), pp. 1079-84.
- Fitzgerald, J.C., Ugun-Klusek, A., Allen, G., De Girolamo, L.A., Hargreaves, I., Ufer, C., Abramov, A.Y. and Billett, E.E. (2014) 'Monoamine oxidase-A knockdown in human neuroblastoma cells reveals protection against mitochondrial toxins', *FASEB J*, 28(1), pp. 218-29.
- Foley, E. and O'Farrell, P.H. (2004) 'Functional dissection of an innate immune response by a genome-wide RNAi screen', *PLoS Biol*, 2(8), p. E203.
- Foriel, S., Willems, P., Smeitink, J., Schenck, A. and Beyrath, J. (2015) 'Mitochondrial diseases: Drosophila melanogaster as a model to evaluate potential therapeutics', *Int J Biochem Cell Biol*, 63, pp. 60-5.
- Formentini, L., Sanchez-Arago, M., Sanchez-Cenizo, L. and Cuezva, J.M. (2012) 'The mitochondrial ATPase inhibitory factor 1 triggers a ROS-mediated retrograde prosurvival and proliferative response', *Mol Cell*, 45(6), pp. 731-42.
- Forster, M.J., Dubey, A., Dawson, K.M., Stutts, W.A., Lal, H. and Sohal, R.S. (1996) 'Age-related losses of cognitive function and motor skills in mice are associated with oxidative protein damage in the brain', *Proc Natl Acad Sci U S A*, 93(10), pp. 4765-9.
- Foster, M.W., Hess, D.T. and Stamler, J.S. (2009) 'Protein S-nitrosylation in health and disease: a current perspective', *Trends Mol Med*, 15(9), pp. 391-404.
- Frolov, M.V., Benevolenskaya, E.V. and Birchler, J.A. (2000) 'The oxen gene of Drosophila encodes a homolog of subunit 9 of yeast ubiquinol-cytochrome c oxidoreductase complex: evidence for modulation of gene expression in response to mitochondrial activity', *Genetics*, 156(4), pp. 1727-36.
- Fukuoh, A., Cannino, G., Gerards, M., Buckley, S., Kazancioglu, S., Scialo, F., Lihavainen, E., Ribeiro, A., Dufour, E. and Jacobs, H.T. (2014) 'Screen for mitochondrial DNA copy number maintenance genes reveals essential role for ATP synthase', *Mol Syst Biol*, 10, p. 734.
- Gabbita, S.P., Butterfield, D.A., Hensley, K., Shaw, W. and Carney, J.M. (1997) 'Aging and caloric restriction affect mitochondrial respiration and lipid membrane status: an electron paramagnetic resonance investigation', *Free Radic Biol Med*, 23(2), pp. 191-201.
- Galanis, A., Pappa, A., Giannakakis, A., Lanitis, E., Dangaj, D. and Sandaltzopoulos, R. (2008) 'Reactive oxygen species and HIF-1 signalling in cancer', *Cancer Lett*, 266(1), pp. 12-20.

- Gan, W., Nie, B., Shi, F., Xu, X.M., Qian, J.C., Takagi, Y., Hayakawa, H., Sekiguchi, M. and Cai, J.P. (2012) 'Age-dependent increases in the oxidative damage of DNA, RNA, and their metabolites in normal and senescence-accelerated mice analyzed by LC-MS/MS: urinary 8-oxoguanosine as a novel biomarker of aging', *Free Radic Biol Med*, 52(9), pp. 1700-7.
- Gao, G., McMahon, C., Chen, J. and Rong, Y.S. (2008) 'A powerful method combining homologous recombination and site-specific recombination for targeted mutagenesis in *Drosophila*', *Proc Natl Acad Sci U S A*, 105(37), pp. 13999-4004.
- Garaude, J., Acin-Perez, R., Martinez-Cano, S., Enamorado, M., Ugolini, M., Nistal-Villan, E., Hervas-Stubbs, S., Pelegrin, P., Sander, L.E., Enriquez, J.A. and Sancho, D. (2016) 'Mitochondrial respiratory-chain adaptations in macrophages contribute to antibacterial host defense', *Nat Immunol*, 17(9), pp. 1037-1045.
- Garcia-Aguilar, A. and Cuezva, J.M. (2018) 'A Review of the Inhibition of the Mitochondrial ATP Synthase by IF1 in vivo: Reprogramming Energy Metabolism and Inducing Mitohormesis', *Front Physiol*, 9, p. 1322.
- Garcia-Bermudez, J. and Cuezva, J.M. (2016) 'The ATPase Inhibitory Factor 1 (IF1): A master regulator of energy metabolism and of cell survival', *Biochim Biophys Acta*. Garcia, C.J., Khajeh, J., Coulanges, E., Chen, E.I. and Owusu-Ansah, E. (2017a) 'Regulation of Mitochondrial Complex I Biogenesis in *Drosophila* Flight Muscles', *Cell Rep*, 20(1), pp. 264-278.
- Garcia, N., Zazueta, C. and Aguilera-Aguirre, L. (2017b) 'Oxidative Stress and Inflammation in Cardiovascular Disease', *Oxid Med Cell Longev*, 2017, p. 5853238.
- Gaude, E. and Frezza, C. (2014) 'Defects in mitochondrial metabolism and cancer', *Cancer Metab*, 2, p. 10.
- Genova, M.L., Ventura, B., Giuliano, G., Bovina, C., Formiggini, G., Parenti Castelli, G. and Lenaz, G. (2001) 'The site of production of superoxide radical in mitochondrial Complex I is not a bound ubiquinone but presumably iron-sulfur cluster N2', *FEBS Lett*, 505(3), pp. 364-8.
- Giorgio, M., Migliaccio, E., Orsini, F., Paolucci, D., Moroni, M., Contursi, C., Pelliccia, G., Luzi, L., Minucci, S., Marcaccio, M., Pinton, P., Rizzuto, R., Bernardi, P., Paolucci, F. and Pelicci, P.G. (2005) 'Electron transfer between cytochrome c and p66Shc generates reactive oxygen species that trigger mitochondrial apoptosis', *Cell*, 122(2), pp. 221-33.
- Goldberg, J., Currais, A., Prior, M., Fischer, W., Chiruta, C., Ratliff, E., Daugherty, D., Dargusch, R., Finley, K., Esparza-Molto, P.B., Cuezva, J.M., Maher, P., Petrascheck, M. and Schubert, D. (2018) 'The mitochondrial ATP synthase is a shared drug target for aging and dementia', *Aging Cell*, 17(2).
- Gospodaryov, D.V., Lushchak, O.V., Rovenko, B.M., Perkhulyan, N.V., Gerards, M., Tuomela, T. and Jacobs, H.T. (2014) 'Ciona intestinalis NADH dehydrogenase NDX confers stress-resistance and extended lifespan on *Drosophila*', *Biochim Biophys Acta*, 1837(11), pp. 1861-1869.

- Greaves, L.C., Reeve, A.K., Taylor, R.W. and Turnbull, D.M. (2012) 'Mitochondrial DNA and disease', *J Pathol*, 226(2), pp. 274-86.
- Green, E.W., Fedele, G., Giorgini, F. and Kyriacou, C.P. (2014) 'A Drosophila RNAi collection is subject to dominant phenotypic effects', *Nat Methods*, 11(3), pp. 222-3.
- Gristick, H.B., Rao, M., Chartron, J.W., Rome, M.E., Shan, S.O. and Clemons, W.M., Jr. (2014) 'Crystal structure of ATP-bound Get3-Get4-Get5 complex reveals regulation of Get3 by Get4', *Nat Struct Mol Biol*, 21(5), pp. 437-42.
- Guaras, A., Perales-Clemente, E., Calvo, E., Acin-Perez, R., Loureiro-Lopez, M., Pujol, C., Martinez-Carrascoso, I., Nunez, E., Garcia-Marques, F., Rodriguez-Hernandez, M.A., Cortes, A., Diaz, F., Perez-Martos, A., Moraes, C.T., Fernandez-Silva, P., Trifunovic, A., Navas, P., Vazquez, J. and Enriquez, J.A. (2016) 'The CoQH2/CoQ Ratio Serves as a Sensor of Respiratory Chain Efficiency', *Cell Rep*, 15(1), pp. 197-209.
- Guerin, C.L., Rossi, E., Saubamea, B., Cras, A., Mignon, V., Silvestre, J.S. and Smadja, D.M. (2017) 'Human very Small Embryonic-like Cells Support Vascular Maturation and Therapeutic Revascularization Induced by Endothelial Progenitor Cells', *Stem Cell Rev Rep*, 13(4), pp. 552-560.
- Gui, D.Y., Sullivan, L.B., Luengo, A., Hosios, A.M., Bush, L.N., Gitego, N., Davidson, S.M., Freinkman, E., Thomas, C.J. and Vander Heiden, M.G. (2016) 'Environment Dictates Dependence on Mitochondrial Complex I for NAD⁺ and Aspartate Production and Determines Cancer Cell Sensitivity to Metformin', *Cell Metab*, 24(5), pp. 716-727.
- Guo, F., Yu, J., Jung, H.J., Abruzzi, K.C., Luo, W., Griffith, L.C. and Rosbash, M. (2016) 'Circadian neuron feedback controls the Drosophila sleep--activity profile', *Nature*, 536(7616), pp. 292-7.
- Guo, M. (2012) 'Drosophila as a model to study mitochondrial dysfunction in Parkinson's disease', *Cold Spring Harb Perspect Med*, 2(11).
- Hagerhall, C. (1997) 'Succinate: quinone oxidoreductases. Variations on a conserved theme', *Biochim Biophys Acta*, 1320(2), pp. 107-41.
- Hakkaart, G.A., Dassa, E.P., Jacobs, H.T. and Rustin, P. (2006) 'Allotopic expression of a mitochondrial alternative oxidase confers cyanide resistance to human cell respiration', *EMBO Rep*, 7(3), pp. 341-5.
- Handy, D.E. and Loscalzo, J. (2012) 'Redox regulation of mitochondrial function', *Antioxid Redox Signal*, 16(11), pp. 1323-67.
- Harman, D. (1956) 'Aging: a theory based on free radical and radiation chemistry', *J Gerontol*, 11(3), pp. 298-300.
- Harman, D. (1972) 'The biologic clock: the mitochondria?', *J Am Geriatr Soc*, 20(4), pp. 145-7.
- Hayyan, M., Hashim, M.A. and AlNashef, I.M. (2016) 'Superoxide Ion: Generation and Chemical Implications', *Chem Rev*, 116(5), pp. 3029-85.

- He, Y. and Jasper, H. (2014) 'Studying aging in *Drosophila*', *Methods*, 68(1), pp. 129-33.
- Heigwer, F., Port, F. and Boutros, M. (2018) 'RNA Interference (RNAi) Screening in *Drosophila*', *Genetics*, 208(3), pp. 853-874.
- Hekimi, S., Lapointe, J. and Wen, Y. (2011) 'Taking a "good" look at free radicals in the aging process', *Trends Cell Biol*, 21(10), pp. 569-76.
- Held, J.M. and Gibson, B.W. (2012) 'Regulatory control or oxidative damage? Proteomic approaches to interrogate the role of cysteine oxidation status in biological processes', *Mol Cell Proteomics*, 11(4), p. R111 013037.
- Hernandez-Camacho, J.D., Bernier, M., Lopez-Lluch, G. and Navas, P. (2018) 'Coenzyme Q10 Supplementation in Aging and Disease', *Front Physiol*, 9, p. 44.
- Herrero, A. and Barja, G. (2000) 'Localization of the site of oxygen radical generation inside the complex I of heart and nonsynaptic brain mammalian mitochondria', *J Bioenerg Biomembr*, 32(6), pp. 609-15.
- Hey-Mogensen, M., Goncalves, R.L., Orr, A.L. and Brand, M.D. (2014) 'Production of superoxide/H₂O₂ by dihydroorotate dehydrogenase in rat skeletal muscle mitochondria', *Free Radic Biol Med*, 72, pp. 149-55.
- Higuchi-Sanabria, R., Frankino, P.A., Paul, J.W., 3rd, Tronnes, S.U. and Dillin, A. (2018) 'A Futile Battle? Protein Quality Control and the Stress of Aging', *Dev Cell*, 44(2), pp. 139-163.
- Hill, K., Model, K., Ryan, M.T., Dietmeier, K., Martin, F., Wagner, R. and Pfanner, N. (1998) 'Tom40 forms the hydrophilic channel of the mitochondrial import pore for preproteins [see comment]', *Nature*, 395(6701), pp. 516-21.
- Hirata, R., Graham, L.A., Takatsuki, A., Stevens, T.H. and Anraku, Y. (1997) 'VMA11 and VMA16 encode second and third proteolipid subunits of the *Saccharomyces cerevisiae* vacuolar membrane H⁺-ATPase', *J Biol Chem*, 272(8), pp. 4795-803.
- Hirth, F. (2010) '*Drosophila melanogaster* in the study of human neurodegeneration', *CNS Neurol Disord Drug Targets*, 9(4), pp. 504-23.
- Hofer, T., Marzetti, E., Xu, J., Seo, A.Y., Gulec, S., Knutson, M.D., Leeuwenburgh, C. and Dupont-Versteegden, E.E. (2008) 'Increased iron content and RNA oxidative damage in skeletal muscle with aging and disuse atrophy', *Exp Gerontol*, 43(6), pp. 563-70.
- Holmstrom, K.M. and Finkel, T. (2014) 'Cellular mechanisms and physiological consequences of redox-dependent signalling', *Nat Rev Mol Cell Biol*, 15(6), pp. 411-21.
- Huang da, W., Sherman, B.T. and Lempicki, R.A. (2009) 'Systematic and integrative analysis of large gene lists using DAVID bioinformatics resources', *Nat Protoc*, 4(1), pp. 44-57.

Huang, Q., Zhan, L., Cao, H., Li, J., Lyu, Y., Guo, X., Zhang, J., Ji, L., Ren, T., An, J., Liu, B., Nie, Y. and Xing, J. (2016) 'Increased mitochondrial fission promotes autophagy and hepatocellular carcinoma cell survival through the ROS-modulated coordinated regulation of the NFKB and TP53 pathways', *Autophagy*, 12(6), pp. 999-1014.

Humphrey, D.M., Parsons, R.B., Ludlow, Z.N., Riemensperger, T., Esposito, G., Verstreken, P., Jacobs, H.T., Birman, S. and Hirth, F. (2012) 'Alternative oxidase rescues mitochondria-mediated dopaminergic cell loss in *Drosophila*', *Hum Mol Genet*, 21(12), pp. 2698-712.

Humphrey, D.M., Toivonen, J.M., Giannakou, M., Partridge, L. and Brand, M.D. (2009) 'Expression of human uncoupling protein-3 in *Drosophila* insulin-producing cells increases insulin-like peptide (DILP) levels and shortens lifespan', *Exp Gerontol*, 44(5), pp. 316-27.

Hur, J.H., Bahadorani, S., Graniel, J., Koehler, C.L., Ulgherait, M., Rera, M., Jones, D.L. and Walker, D.W. (2013) 'Increased longevity mediated by yeast NDI1 expression in *Drosophila* intestinal stem and progenitor cells', *Aging (Albany NY)*, 5(9), pp. 662-81.

Hutter, E., Unterluggauer, H., Garedew, A., Jansen-Durr, P. and Gnaiger, E. (2006) 'High-resolution respirometry--a modern tool in aging research', *Exp Gerontol*, 41(1), pp. 103-9.

Idelchik, M., Begley, U., Begley, T.J. and Melendez, J.A. (2017) 'Mitochondrial ROS control of cancer', *Semin Cancer Biol*, 47, pp. 57-66.

Imlay, J.A. (2006) 'Iron-sulphur clusters and the problem with oxygen', *Mol Microbiol*, 59(4), pp. 1073-82.

Ishii, T., Yasuda, K., Akatsuka, A., Hino, O., Hartman, P.S. and Ishii, N. (2005) 'A mutation in the SDHC gene of complex II increases oxidative stress, resulting in apoptosis and tumorigenesis', *Cancer Res*, 65(1), pp. 203-9.

Jacobs, H.T., Fernandez-Ayala, D.J., Manjiry, S., Kemppainen, E., Toivonen, J.M. and O'Dell, K.M. (2004) 'Mitochondrial disease in flies', *Biochim Biophys Acta*, 1659(2-3), pp. 190-6.

Jacobson, J., Duchon, M.R., Hothersall, J., Clark, J.B. and Heales, S.J. (2005) 'Induction of mitochondrial oxidative stress in astrocytes by nitric oxide precedes disruption of energy metabolism', *J Neurochem*, 95(2), pp. 388-95.

Jacobson, J., Lambert, A.J., Portero-Otin, M., Pamplona, R., Magwere, T., Miwa, S., Driege, Y., Brand, M.D. and Partridge, L. (2010) 'Biomarkers of aging in *Drosophila*', *Aging Cell*, 9(4), pp. 466-477.

Jain, M., Rivera, S., Monclus, E.A., Synenki, L., Zirk, A., Eisenbart, J., Feghali-Bostwick, C., Mutlu, G.M., Budinger, G.R. and Chandel, N.S. (2013) 'Mitochondrial reactive oxygen species regulate transforming growth factor-beta signaling', *J Biol Chem*, 288(2), pp. 770-7.

- Jensen, P., Wilson, M.T., Aasa, R. and Malmstrom, B.G. (1984) 'Cyanide inhibition of cytochrome c oxidase. A rapid-freeze e.p.r. investigation', *Biochem J*, 224(3), pp. 829-37.
- Jonckheere, A.I., Smeitink, J.A. and Rodenburg, R.J. (2012) 'Mitochondrial ATP synthase: architecture, function and pathology', *J Inherit Metab Dis*, 35(2), pp. 211-25.
- Jung, S.N., Yang, W.K., Kim, J., Kim, H.S., Kim, E.J., Yun, H., Park, H., Kim, S.S., Choe, W., Kang, I. and Ha, J. (2008) 'Reactive oxygen species stabilize hypoxia-inducible factor-1 alpha protein and stimulate transcriptional activity via AMP-activated protein kinase in DU145 human prostate cancer cells', *Carcinogenesis*, 29(4), pp. 713-21.
- Kaiserova, K., Srivastava, S., Hoetker, J.D., Awe, S.O., Tang, X.L., Cai, J. and Bhatnagar, A. (2006) 'Redox activation of aldose reductase in the ischemic heart', *J Biol Chem*, 281(22), pp. 15110-20.
- Kaludercic, N. and Giorgio, V. (2016) 'The Dual Function of Reactive Oxygen/Nitrogen Species in Bioenergetics and Cell Death: The Role of ATP Synthase', *Oxid Med Cell Longev*, 2016, p. 3869610.
- Kalyanaraman, B., Darley-Usmar, V., Davies, K.J., Dennery, P.A., Forman, H.J., Grisham, M.B., Mann, G.E., Moore, K., Roberts, L.J., 2nd and Ischiropoulos, H. (2012) 'Measuring reactive oxygen and nitrogen species with fluorescent probes: challenges and limitations', *Free Radic Biol Med*, 52(1), pp. 1-6.
- Kang, Y., Fielden, L.F. and Stojanovski, D. (2018) 'Mitochondrial protein transport in health and disease', *Semin Cell Dev Biol*, 76, pp. 142-153.
- Kategaya, L.S., Changkakoty, B., Biechele, T., Conrad, W.H., Kaykas, A., Dasgupta, R. and Moon, R.T. (2009) 'Bili inhibits Wnt/beta-catenin signaling by regulating the recruitment of axin to LRP6', *PLoS One*, 4(7), p. e6129.
- Kauffman, M.E., Kauffman, M.K., Traore, K., Zhu, H., Trush, M.A., Jia, Z. and Li, Y.R. (2016) 'MitoSOX-Based Flow Cytometry for Detecting Mitochondrial ROS', *React Oxyg Species (Apex)*, 2(5), pp. 361-370.
- Kaufman, T.C. (2017) 'A Short History and Description of Drosophila melanogaster Classical Genetics: Chromosome Aberrations, Forward Genetic Screens, and the Nature of Mutations', *Genetics*, 206(2), pp. 665-689.
- Kaupilla, J.H.K., Bonekamp, N.A., Mourier, A., Isokallio, M.A., Just, A., Kaupilla, T.E.S., Stewart, J.B. and Larsson, N.G. (2018) 'Base-excision repair deficiency alone or combined with increased oxidative stress does not increase mtDNA point mutations in mice', *Nucleic Acids Res*, 46(13), pp. 6642-6669.
- Kempf, A., Song, S.M., Talbot, C.B. and Miesenbock, G. (2019) 'A potassium channel beta-subunit couples mitochondrial electron transport to sleep', *Nature*, 568(7751), pp. 230-234.

- Kemppainen, K.K., Rinne, J., Sriram, A., Lakanmaa, M., Zeb, A., Tuomela, T., Popplestone, A., Singh, S., Sanz, A., Rustin, P. and Jacobs, H.T. (2014) 'Expression of alternative oxidase in *Drosophila* ameliorates diverse phenotypes due to cytochrome oxidase deficiency', *Hum Mol Genet*, 23(8), pp. 2078-93.
- Kettenhofen, N.J. and Wood, M.J. (2010) 'Formation, reactivity, and detection of protein sulfenic acids', *Chem Res Toxicol*, 23(11), pp. 1633-46.
- Kim, G.H., Kim, J.E., Rhie, S.J. and Yoon, S. (2015) 'The Role of Oxidative Stress in Neurodegenerative Diseases', *Exp Neurobiol*, 24(4), pp. 325-40.
- Kim, Y.C., Wikstrom, M. and Hummer, G. (2009) 'Kinetic gating of the proton pump in cytochrome c oxidase', *Proc Natl Acad Sci U S A*, 106(33), pp. 13707-12.
- Kim, Y.S. (2002) 'Malonate metabolism: biochemistry, molecular biology, physiology, and industrial application', *J Biochem Mol Biol*, 35(5), pp. 443-51.
- Kirkinezos, I.G. and Moraes, C.T. (2001) 'Reactive oxygen species and mitochondrial diseases', *Semin Cell Dev Biol*, 12(6), pp. 449-57.
- Kluck, R.M., Bossy-Wetzell, E., Green, D.R. and Newmeyer, D.D. (1997) 'The release of cytochrome c from mitochondria: a primary site for Bcl-2 regulation of apoptosis', *Science*, 275(5303), pp. 1132-6.
- Kramerova, I.A., Kawaguchi, N., Fessler, L.I., Nelson, R.E., Chen, Y., Kramerov, A.A., Kusche-Gullberg, M., Kramer, J.M., Ackley, B.D., Sieron, A.L., Prockop, D.J. and Fessler, J.H. (2000) 'Papilin in development; a pericellular protein with a homology to the ADAMTS metalloproteinases', *Development*, 127(24), pp. 5475-85.
- Krause, K.H. (2004) 'Tissue distribution and putative physiological function of NOX family NADPH oxidases', *Jpn J Infect Dis*, 57(5), pp. S28-9.
- Kudryavtseva, A.V., Krasnov, G.S., Dmitriev, A.A., Alekseev, B.Y., Kardymon, O.L., Sadritdinova, A.F., Fedorova, M.S., Pokrovsky, A.V., Melnikova, N.V., Kaprin, A.D., Moskalev, A.A. and Snezhkina, A.V. (2016) 'Mitochondrial dysfunction and oxidative stress in aging and cancer', *Oncotarget*, 7(29), pp. 44879-44905.
- Kwong, L.K., Mockett, R.J., Bayne, A.C., Orr, W.C. and Sohal, R.S. (2000) 'Decreased mitochondrial hydrogen peroxide release in transgenic *Drosophila melanogaster* expressing intramitochondrial catalase', *Arch Biochem Biophys*, 383(2), pp. 303-8.
- Ladoukakis, E.D. and Zouros, E. (2017) 'Evolution and inheritance of animal mitochondrial DNA: rules and exceptions', *J Biol Res (Thessalon)*, 24, p. 2.
- Lambert, A.J. and Brand, M.D. (2009) 'Reactive oxygen species production by mitochondria', *Methods Mol Biol*, 554, pp. 165-81.
- Lane, R.K., Hilsabeck, T. and Rea, S.L. (2015) 'The role of mitochondrial dysfunction in age-related diseases', *Biochim Biophys Acta*, 1847(11), pp. 1387-400.
- Lapointe, J. and Hekimi, S. (2010) 'When a theory of aging ages badly', *Cell Mol Life Sci*, 67(1), pp. 1-8.

Larosa, V. and Remacle, C. (2018) 'Insights into the respiratory chain and oxidative stress', *Biosci Rep*, 38(5).

Larsson, N.G. (2010) 'Somatic mitochondrial DNA mutations in mammalian aging', *Annu Rev Biochem*, 79, pp. 683-706.

LeBrasseur, N.K., Tchkonina, T. and Kirkland, J.L. (2015) 'Cellular Senescence and the Biology of Aging, Disease, and Frailty', *Nestle Nutr Inst Workshop Ser*, 83, pp. 11-8.

Lee, S., Tak, E., Lee, J., Rashid, M.A., Murphy, M.P., Ha, J. and Kim, S.S. (2011) 'Mitochondrial H₂O₂ generated from electron transport chain complex I stimulates muscle differentiation', *Cell Res*, 21(5), pp. 817-34.

Lee, S.R. and Han, J. (2017) 'Mitochondrial Nucleoid: Shield and Switch of the Mitochondrial Genome', *Oxid Med Cell Longev*, 2017, p. 8060949.

Lefevre-Borg, F., Mathias, O. and Cavero, I. (1988) 'Role of the sympathetic nervous system in blood pressure maintenance and in the antihypertensive effects of calcium antagonists in spontaneously hypertensive rats', *Hypertension*, 11(4), pp. 360-70.
Lenaz, G. (2001) 'A critical appraisal of the mitochondrial coenzyme Q pool', *FEBS Lett*, 509(2), pp. 151-5.

Lesnefsky, E.J., Chen, Q., Moghaddas, S., Hassan, M.O., Tandler, B. and Hoppel, C.L. (2004) 'Blockade of electron transport during ischemia protects cardiac mitochondria', *J Biol Chem*, 279(46), pp. 47961-7.

Li, Y., Park, J.S., Deng, J.H. and Bai, Y. (2006) 'Cytochrome c oxidase subunit IV is essential for assembly and respiratory function of the enzyme complex', *J Bioenerg Biomembr*, 38(5-6), pp. 283-91.

Lill, R. (2009) 'Function and biogenesis of iron-sulphur proteins', *Nature*, 460(7257), pp. 831-8.

Lipinski, B. (2011) 'Hydroxyl radical and its scavengers in health and disease', *Oxid Med Cell Longev*, 2011, p. 809696.

Liu, W., Gnanasambandam, R., Benjamin, J., Kaur, G., Getman, P.B., Siegel, A.J., Shortridge, R.D. and Singh, S. (2007) 'Mutations in cytochrome c oxidase subunit VIa cause neurodegeneration and motor dysfunction in *Drosophila*', *Genetics*, 176(2), pp. 937-46.

Liu, Y. and Schubert, D.R. (2009) 'The specificity of neuroprotection by antioxidants', *J Biomed Sci*, 16, p. 98.

Liu, Z.Q. (2014) 'Antioxidants may not always be beneficial to health', *Nutrition*, 30(2), pp. 131-3.

Logan, A., Pell, V.R., Shaffer, K.J., Evans, C., Stanley, N.J., Robb, E.L., Prime, T.A., Chouchani, E.T., Cocheme, H.M., Fearnley, I.M., Vidoni, S., James, A.M., Porteous, C.M., Partridge, L., Krieg, T., Smith, R.A. and Murphy, M.P. (2016) 'Assessing the

Mitochondrial Membrane Potential in Cells and In Vivo using Targeted Click Chemistry and Mass Spectrometry', *Cell Metab*, 23(2), pp. 379-85.

Lopez-Otin, C., Blasco, M.A., Partridge, L., Serrano, M. and Kroemer, G. (2013) 'The hallmarks of aging', *Cell*, 153(6), pp. 1194-217.

Lu, J. and Gunner, M.R. (2014) 'Characterizing the proton loading site in cytochrome c oxidase', *Proc Natl Acad Sci U S A*, 111(34), pp. 12414-9.

Lu, X.L., Zhao, C.H., Yao, X.L. and Zhang, H. (2017) 'Quercetin attenuates high fructose feeding-induced atherosclerosis by suppressing inflammation and apoptosis via ROS-regulated PI3K/AKT signaling pathway', *Biomed Pharmacother*, 85, pp. 658-671.

Luna-Lopez, A., Gonzalez-Puertos, V.Y., Lopez-Diazguerrero, N.E. and Konigsberg, M. (2014) 'New considerations on hormetic response against oxidative stress', *J Cell Commun Signal*, 8(4), pp. 323-31.

Ma, L., Johns, L.A. and Allen, M.J. (2009) 'A modifier screen in the Drosophila eye reveals that aPKC interacts with Glued during central synapse formation', *BMC Genet*, 10, p. 77.

Magder, S. (2006) 'Reactive oxygen species: toxic molecules or spark of life?', *Crit Care*, 10(1), p. 208.

Magwere, T., Pamplona, R., Miwa, S., Martinez-Diaz, P., Portero-Otin, M., Brand, M.D. and Partridge, L. (2006) 'Flight activity, mortality rates, and lipoxidative damage in Drosophila', *J Gerontol A Biol Sci Med Sci*, 61(2), pp. 136-45.

Mai, N., Chrzanowska-Lightowlers, Z.M. and Lightowlers, R.N. (2017) 'The process of mammalian mitochondrial protein synthesis', *Cell Tissue Res*, 367(1), pp. 5-20.

Mailloux, R.J. (2018) 'Mitochondrial Antioxidants and the Maintenance of Cellular Hydrogen Peroxide Levels', *Oxid Med Cell Longev*, 2018, p. 7857251.

Mailloux, R.J., Gardiner, D. and O'Brien, M. (2016) '2-Oxoglutarate dehydrogenase is a more significant source of O₂(.)-/H₂O₂ than pyruvate dehydrogenase in cardiac and liver tissue', *Free Radic Biol Med*, 97, pp. 501-512.

Malina, C., Larsson, C. and Nielsen, J. (2018) 'Yeast mitochondria: an overview of mitochondrial biology and the potential of mitochondrial systems biology', *FEMS Yeast Res*, 18(5).

Mannella, C.A., Pfeiffer, D.R., Bradshaw, P.C., Moraru, I., Slepchenko, B., Loew, L.M., Hsieh, C.E., Buttle, K. and Marko, M. (2001) 'Topology of the mitochondrial inner membrane: dynamics and bioenergetic implications', *IUBMB Life*, 52(3-5), pp. 93-100.

Marella, M., Seo, B.B., Thomas, B.B., Matsuno-Yagi, A. and Yagi, T. (2010) 'Successful amelioration of mitochondrial optic neuropathy using the yeast NDI1 gene in a rat animal model', *PLoS One*, 5(7), p. e11472.

Margulis, L. (1975) 'Symbiotic theory of the origin of eukaryotic organelles; criteria for proof', *Symp Soc Exp Biol*, (29), pp. 21-38.

Martin, I., Jones, M.A., Rhodenizer, D., Zheng, J., Warrick, J.M., Seroude, L. and Grotewiel, M. (2009) 'Sod2 knockdown in the musculature has whole-organism consequences in *Drosophila*', *Free Radic Biol Med*, 47(6), pp. 803-13.

Massie, H.R., Aiello, V.R. and Banziger, V. (1983) 'Iron accumulation and lipid peroxidation in aging C57BL/6J mice', *Exp Gerontol*, 18(4), pp. 277-85.

Massie, H.R., Aiello, V.R. and Williams, T.R. (1985) 'Iron accumulation during development and ageing of *Drosophila*', *Mech Ageing Dev*, 29(2), pp. 215-20.

Matus-Ortega, M.G., Cardenas-Monroy, C.A., Flores-Herrera, O., Mendoza-Hernandez, G., Miranda, M., Gonzalez-Pedrajo, B., Vazquez-Meza, H. and Pardo, J.P. (2015) 'New complexes containing the internal alternative NADH dehydrogenase (Ndi1) in mitochondria of *Saccharomyces cerevisiae*', *Yeast*, 32(10), pp. 629-41.

McCarron, J.G., Wilson, C., Sandison, M.E., Olson, M.L., Girkin, J.M., Saunter, C. and Chalmers, S. (2013) 'From structure to function: mitochondrial morphology, motion and shaping in vascular smooth muscle', *J Vasc Res*, 50(5), pp. 357-71.

McCord, J.M. and Fridovich, I. (1969) 'Superoxide dismutase. An enzymic function for erythrocyte hemocuprein (hemocuprein)', *J Biol Chem*, 244(22), pp. 6049-55.

McDonald, A.E. (2009) 'Alternative oxidase: what information can protein sequence comparisons give us?', *Physiol Plant*, 137(4), pp. 328-41.

McDonald, A.E. and Gospodaryov, D.V. (2019) 'Alternative NAD(P)H dehydrogenase and alternative oxidase: Proposed physiological roles in animals', *Mitochondrion*, 45, pp. 7-17.

McDonald, A.E., Vanlerberghe, G.C. and Staples, J.F. (2009) 'Alternative oxidase in animals: unique characteristics and taxonomic distribution', *J Exp Biol*, 212(Pt 16), pp. 2627-34.

McKenzie, M. and Ryan, M.T. (2010) 'Assembly factors of human mitochondrial complex I and their defects in disease', *IUBMB Life*, 62(7), pp. 497-502.

Menezes, M.J., Guo, Y., Zhang, J., Riley, L.G., Cooper, S.T., Thorburn, D.R., Li, J., Dong, D., Li, Z., Glessner, J., Davis, R.L., Sue, C.M., Alexander, S.I., Arbuckle, S., Kirwan, P., Keating, B.J., Xu, X., Hakonarson, H. and Christodoulou, J. (2015) 'Mutation in mitochondrial ribosomal protein S7 (MRPS7) causes congenital sensorineural deafness, progressive hepatic and renal failure and lactic acidemia', *Hum Mol Genet*, 24(8), pp. 2297-307.

Menger, K.E., James, A.M., Cocheme, H.M., Harbour, M.E., Chouchani, E.T., Ding, S., Fearnley, I.M., Partridge, L. and Murphy, M.P. (2015) 'Fasting, but Not Aging, Dramatically Alters the Redox Status of Cysteine Residues on Proteins in *Drosophila melanogaster*', *Cell Rep*, 11(12), pp. 1856-65.

- Metzen, E., Zhou, J., Jelkmann, W., Fandrey, J. and Brune, B. (2003) 'Nitric oxide impairs normoxic degradation of HIF-1alpha by inhibition of prolyl hydroxylases', *Mol Biol Cell*, 14(8), pp. 3470-81.
- Michalek, R.D., Nelson, K.J., Holbrook, B.C., Yi, J.S., Stridiron, D., Daniel, L.W., Fetrow, J.S., King, S.B., Poole, L.B. and Grayson, J.M. (2007) 'The requirement of reversible cysteine sulfenic acid formation for T cell activation and function', *J Immunol*, 179(10), pp. 6456-67.
- Mills, E.L., Kelly, B., Logan, A., Costa, A.S., Varma, M., Bryant, C.E., Toulomousis, P., Dabritz, J.H., Gottlieb, E., Latorre, I., Corr, S.C., McManus, G., Ryan, D., Jacobs, H.T., Szibor, M., Xavier, R.J., Braun, T., Frezza, C., Murphy, M.P. and O'Neill, L.A. (2016a) 'Succinate Dehydrogenase Supports Metabolic Repurposing of Mitochondria to Drive Inflammatory Macrophages', *Cell*, 167(2), pp. 457-470 e13.
- Mills, E.L., Kelly, B., Logan, A., Costa, A.S.H., Varma, M., Bryant, C.E., Toulomousis, P., Dabritz, J.H.M., Gottlieb, E., Latorre, I., Corr, S.C., McManus, G., Ryan, D., Jacobs, H.T., Szibor, M., Xavier, R.J., Braun, T., Frezza, C., Murphy, M.P. and O'Neill, L.A. (2016b) 'Succinate Dehydrogenase Supports Metabolic Repurposing of Mitochondria to Drive Inflammatory Macrophages', *Cell*, 167(2), pp. 457-470 e13.
- Mimaki, M., Wang, X., McKenzie, M., Thorburn, D.R. and Ryan, M.T. (2012) 'Understanding mitochondrial complex I assembly in health and disease', *Biochim Biophys Acta*, 1817(6), pp. 851-62.
- Mitchell, P. (1961) 'Coupling of phosphorylation to electron and hydrogen transfer by a chemi-osmotic type of mechanism', *Nature*, 191, pp. 144-8.
- Miwa, S., St-Pierre, J., Partridge, L. and Brand, M.D. (2003) 'Superoxide and hydrogen peroxide production by Drosophila mitochondria', *Free Radic Biol Med*, 35(8), pp. 938-48.
- Mockett, R.J., Sohal, B.H. and Sohal, R.S. (2010) 'Expression of multiple copies of mitochondrially targeted catalase or genomic Mn superoxide dismutase transgenes does not extend the life span of Drosophila melanogaster', *Free Radic Biol Med*, 49(12), pp. 2028-31.
- Mohr, S., Bakal, C. and Perrimon, N. (2010) 'Genomic screening with RNAi: results and challenges', *Annu Rev Biochem*, 79, pp. 37-64.
- Mohr, S.E. (2014) 'RNAi screening in Drosophila cells and in vivo', *Methods*, 68(1), pp. 82-8.
- Mohr, S.E. and Perrimon, N. (2012) 'RNAi screening: new approaches, understandings, and organisms', *Wiley Interdiscip Rev RNA*, 3(2), pp. 145-58.
- Moloney, J.N. and Cotter, T.G. (2018) 'ROS signalling in the biology of cancer', *Semin Cell Dev Biol*, 80, pp. 50-64.
- Monteuuis, G., Miscicka, A., Swirski, M., Zenad, L., Niemitalo, O., Wrobel, L., Alam, J., Chacinska, A., Kastaniotis, A.J. and Kufel, J. (2019) 'Non-canonical translation

initiation in yeast generates a cryptic pool of mitochondrial proteins', *Nucleic Acids Res*, 47(11), pp. 5777-5791.

Mookerjee, S.A., Gerencser, A.A., Nicholls, D.G. and Brand, M.D. (2017) 'Quantifying intracellular rates of glycolytic and oxidative ATP production and consumption using extracellular flux measurements', *J Biol Chem*, 292(17), pp. 7189-7207.

Morelli, A.M., Ravera, S., Calzia, D. and Panfoli, I. (2019) 'An update of the chemiosmotic theory as suggested by possible proton currents inside the coupling membrane', *Open Biol*, 9(4), p. 180221.

Morgan, B., Van Laer, K., Owusu, T.N., Ezerina, D., Pastor-Flores, D., Amponsah, P.S., Tursch, A. and Dick, T.P. (2016) 'Real-time monitoring of basal H₂O₂ levels with peroxiredoxin-based probes', *Nat Chem Biol*, 12(6), pp. 437-43.

Morgan, T.H. (1910) 'Sex Limited Inheritance in *Drosophila*', *Science*, 32(812), pp. 120-2.

Mracek, T., Drahota, Z. and Houstek, J. (2013) 'The function and the role of the mitochondrial glycerol-3-phosphate dehydrogenase in mammalian tissues', *Biochim Biophys Acta*, 1827(3), pp. 401-10.

Mracek, T., Holzerova, E., Drahota, Z., Kovarova, N., Vrbacky, M., Jesina, P. and Houstek, J. (2014) 'ROS generation and multiple forms of mammalian mitochondrial glycerol-3-phosphate dehydrogenase', *Biochim Biophys Acta*, 1837(1), pp. 98-111.
Muller, F.L. (2009) 'A critical evaluation of cpYFP as a probe for superoxide', *Free Radic Biol Med*, 47(12), pp. 1779-80.

Muller, F.L., Liu, Y. and Van Remmen, H. (2004) 'Complex III releases superoxide to both sides of the inner mitochondrial membrane', *J Biol Chem*, 279(47), pp. 49064-73.

Muller, F.L., Roberts, A.G., Bowman, M.K. and Kramer, D.M. (2003) 'Architecture of the Qo site of the cytochrome bc₁ complex probed by superoxide production', *Biochemistry*, 42(21), pp. 6493-9.

Murphy, E., Kohr, M., Sun, J., Nguyen, T. and Steenbergen, C. (2012) 'S-nitrosylation: a radical way to protect the heart', *J Mol Cell Cardiol*, 52(3), pp. 568-77.
Murphy, M.P. (2009) 'How mitochondria produce reactive oxygen species', *Biochem J*, 417(1), pp. 1-13.

Navarro, A., Boveris, A., Bandez, M.J., Sanchez-Pino, M.J., Gomez, C., Muntane, G. and Ferrer, I. (2009) 'Human brain cortex: mitochondrial oxidative damage and adaptive response in Parkinson disease and in dementia with Lewy bodies', *Free Radic Biol Med*, 46(12), pp. 1574-80.

Nelson, G., Kucheryavenko, O., Wordsworth, J. and von Zglinicki, T. (2018) 'The senescent bystander effect is caused by ROS-activated NF- κ B signalling', *Mech Ageing Dev*, 170, pp. 30-36.

Netto, L.E. and Antunes, F. (2016) 'The Roles of Peroxiredoxin and Thioredoxin in Hydrogen Peroxide Sensing and in Signal Transduction', *Mol Cells*, 39(1), pp. 65-71.

Neupane, P., Bhujju, S., Thapa, N. and Bhattarai, H.K. (2019) 'ATP Synthase: Structure, Function and Inhibition', *Biomol Concepts*, 10(1), pp. 1-10.

Ni, Z. and Lee, S.S. (2010) 'RNAi screens to identify components of gene networks that modulate aging in *Caenorhabditis elegans*', *Brief Funct Genomics*, 9(1), pp. 53-64.

Nicholson, L., Singh, G.K., Osterwalder, T., Roman, G.W., Davis, R.L. and Keshishian, H. (2008) 'Spatial and temporal control of gene expression in *Drosophila* using the inducible GeneSwitch GAL4 system. I. Screen for Irval nervous system drivers', *Genetics*, 178(1), pp. 215-34.

Olahova, M., Yoon, W.H., Thompson, K., Jangam, S., Fernandez, L., Davidson, J.M., Kyle, J.E., Grove, M.E., Fisk, D.G., Kohler, J.N., Holmes, M., Dries, A.M., Huang, Y., Zhao, C., Contrepois, K., Zappala, Z., Fresard, L., Waggott, D., Zink, E.M., Kim, Y.M., Heyman, H.M., Stratton, K.G., Webb-Robertson, B.M., Undiagnosed Diseases, N., Snyder, M., Merker, J.D., Montgomery, S.B., Fisher, P.G., Feichtinger, R.G., Mayr, J.A., Hall, J., Barbosa, I.A., Simpson, M.A., Deshpande, C., Waters, K.M., Koeller, D.M., Metz, T.O., Morris, A.A., Schelley, S., Cowan, T., Friederich, M.W., McFarland, R., Van Hove, J.L.K., Enns, G.M., Yamamoto, S., Ashley, E.A., Wangler, M.F., Taylor, R.W., Bellen, H.J., Bernstein, J.A. and Wheeler, M.T. (2018) 'Biallelic Mutations in ATP5F1D, which Encodes a Subunit of ATP Synthase, Cause a Metabolic Disorder', *Am J Hum Genet*, 102(3), pp. 494-504.

Owusu-Ansah, E., Song, W. and Perrimon, N. (2013) 'Muscle mitohormesis promotes longevity via systemic repression of insulin signaling', *Cell*, 155(3), pp. 699-712.
Pacher, P., Beckman, J.S. and Liaudet, L. (2007) 'Nitric oxide and peroxynitrite in health and disease', *Physiol Rev*, 87(1), pp. 315-424.

Pamplona, R. (2011) 'Advanced lipoxidation end-products', *Chem Biol Interact*, 192(1-2), pp. 14-20.

Pamplona, R. and Barja, G. (2007) 'Highly resistant macromolecular components and low rate of generation of endogenous damage: two key traits of longevity', *Ageing Res Rev*, 6(3), pp. 189-210.

Pamplona, R. and Costantini, D. (2011) 'Molecular and structural antioxidant defenses against oxidative stress in animals', *Am J Physiol Regul Integr Comp Physiol*, 301(4), pp. R843-63.

Pamplona, R., Prat, J., Cadenas, S., Rojas, C., Perez-Campo, R., Lopez Torres, M. and Barja, G. (1996) 'Low fatty acid unsaturation protects against lipid peroxidation in liver mitochondria from long-lived species: the pigeon and human case', *Mech Ageing Dev*, 86(1), pp. 53-66.

Pan, Z., Voehringer, D.W. and Meyn, R.E. (1999) 'Analysis of redox regulation of cytochrome c-induced apoptosis in a cell-free system', *Cell Death Differ*, 6(7), pp. 683-8.

- Panday, A., Sahoo, M.K., Osorio, D. and Batra, S. (2015) 'NADPH oxidases: an overview from structure to innate immunity-associated pathologies', *Cell Mol Immunol*, 12(1), pp. 5-23.
- Pandey, U.B. and Nichols, C.D. (2011) 'Human disease models in *Drosophila melanogaster* and the role of the fly in therapeutic drug discovery', *Pharmacol Rev*, 63(2), pp. 411-36.
- Panth, N., Paudel, K.R. and Parajuli, K. (2016) 'Reactive Oxygen Species: A Key Hallmark of Cardiovascular Disease', *Adv Med*, 2016, p. 9152732.
- Papa, S., Martino, P.L., Capitanio, G., Gaballo, A., De Rasmio, D., Signorile, A. and Petruzzella, V. (2012) 'The oxidative phosphorylation system in mammalian mitochondria', *Adv Exp Med Biol*, 942, pp. 3-37.
- Paraidathathu, T., de Groot, H. and Kehrer, J.P. (1992) 'Production of reactive oxygen by mitochondria from normoxic and hypoxic rat heart tissue', *Free Radic Biol Med*, 13(4), pp. 289-97.
- Parey, K., Brandt, U., Xie, H., Mills, D.J., Siegmund, K., Vonck, J., Kuhlbrandt, W. and Zickermann, V. (2018) 'Cryo-EM structure of respiratory complex I at work', *Elife*, 7.
- Park, J., Lee, S.B., Lee, S., Kim, Y., Song, S., Kim, S., Bae, E., Kim, J., Shong, M., Kim, J.M. and Chung, J. (2006) 'Mitochondrial dysfunction in *Drosophila* PINK1 mutants is complemented by parkin', *Nature*, 441(7097), pp. 1157-61.
- Park, J.S., Li, Y.F. and Bai, Y. (2007) 'Yeast NDI1 improves oxidative phosphorylation capacity and increases protection against oxidative stress and cell death in cells carrying a Leber's hereditary optic neuropathy mutation', *Biochim Biophys Acta*, 1772(5), pp. 533-42.
- Pasdois, P., Parker, J.E., Griffiths, E.J. and Halestrap, A.P. (2011) 'The role of oxidized cytochrome c in regulating mitochondrial reactive oxygen species production and its perturbation in ischaemia', *Biochem J*, 436(2), pp. 493-505.
- Passos, J.F., Saretzki, G., Ahmed, S., Nelson, G., Richter, T., Peters, H., Wappler, I., Birket, M.J., Harold, G., Schaeuble, K., Birch-Machin, M.A., Kirkwood, T.B. and von Zglinicki, T. (2007) 'Mitochondrial dysfunction accounts for the stochastic heterogeneity in telomere-dependent senescence', *PLoS Biol*, 5(5), p. e110.
- Paulsen, C.E. and Carroll, K.S. (2010) 'Orchestrating redox signaling networks through regulatory cysteine switches', *ACS Chem Biol*, 5(1), pp. 47-62.
- Pavelescu, L.A. (2015) 'On reactive oxygen species measurement in living systems', *J Med Life*, 8 Spec Issue, pp. 38-42.
- Pearce, L.L., Lopez Manzano, E., Martinez-Bosch, S. and Peterson, J. (2008) 'Antagonism of nitric oxide toward the inhibition of cytochrome c oxidase by carbon monoxide and cyanide', *Chem Res Toxicol*, 21(11), pp. 2073-81.

- Perales-Clemente, E., Bayona-Bafaluy, M.P., Perez-Martos, A., Barrientos, A., Fernandez-Silva, P. and Enriquez, J.A. (2008) 'Restoration of electron transport without proton pumping in mammalian mitochondria', *Proc Natl Acad Sci U S A*, 105(48), pp. 18735-9.
- Perrimon, N., Ni, J.Q. and Perkins, L. (2010) 'In vivo RNAi: today and tomorrow', *Cold Spring Harb Perspect Biol*, 2(8), p. a003640.
- Perry, S.W., Norman, J.P., Barbieri, J., Brown, E.B. and Gelbard, H.A. (2011) 'Mitochondrial membrane potential probes and the proton gradient: a practical usage guide', *Biotechniques*, 50(2), pp. 98-115.
- Phillips, J.P., Campbell, S.D., Michaud, D., Charbonneau, M. and Hilliker, A.J. (1989) 'Null mutation of copper/zinc superoxide dismutase in *Drosophila* confers hypersensitivity to paraquat and reduced longevity', *Proc Natl Acad Sci U S A*, 86(8), pp. 2761-5.
- Picard, M., Wallace, D.C. and Burrelle, Y. (2016) 'The rise of mitochondria in medicine', *Mitochondrion*, 30, pp. 105-16.
- Pineda-Molina, E., Klatt, P., Vazquez, J., Marina, A., Garcia de Lacoba, M., Perez-Sala, D. and Lamas, S. (2001) 'Glutathionylation of the p50 subunit of NF-kappaB: a mechanism for redox-induced inhibition of DNA binding', *Biochemistry*, 40(47), pp. 14134-42.
- Pirastu, M., Ristaldi, M.S., Loudianos, G., Murru, S., Sciarratta, G.V., Parodi, M.I., Leone, D., Agosti, S. and Cao, A. (1990) 'Molecular analysis of atypical beta-thalassemia heterozygotes', *Ann N Y Acad Sci*, 612, pp. 90-7.
- Pogson, J.H., Ivatt, R.M., Sanchez-Martinez, A., Tufi, R., Wilson, E., Mortiboys, H. and Whitworth, A.J. (2014) 'The complex I subunit NDUFA10 selectively rescues *Drosophila* pink1 mutants through a mechanism independent of mitophagy', *PLoS Genet*, 10(11), p. e1004815.
- Poirier, L., Shane, A., Zheng, J. and Seroude, L. (2008) 'Characterization of the *Drosophila* gene-switch system in aging studies: a cautionary tale', *Aging Cell*, 7(5), pp. 758-70.
- Pollard, A.K., Craig, E.L. and Chakrabarti, L. (2016) 'Mitochondrial Complex 1 Activity Measured by Spectrophotometry Is Reduced across All Brain Regions in Ageing and More Specifically in Neurodegeneration', *PLoS One*, 11(6), p. e0157405.
- Poole, L.B., Karplus, P.A. and Claiborne, A. (2004) 'Protein sulfenic acids in redox signaling', *Annu Rev Pharmacol Toxicol*, 44, pp. 325-47.
- Porcelli, A.M., Ghelli, A., Zanna, C., Pinton, P., Rizzuto, R. and Rugolo, M. (2005) 'pH difference across the outer mitochondrial membrane measured with a green fluorescent protein mutant', *Biochem Biophys Res Commun*, 326(4), pp. 799-804.
- Pryde, K.R. and Hirst, J. (2011) 'Superoxide is produced by the reduced flavin in mitochondrial complex I: a single, unified mechanism that applies during both forward and reverse electron transfer', *J Biol Chem*, 286(20), pp. 18056-65.

Puca, A.A., Carrizzo, A., Villa, F., Ferrario, A., Casaburo, M., Maciag, A. and Vecchione, C. (2013) 'Vascular ageing: the role of oxidative stress', *Int J Biochem Cell Biol*, 45(3), pp. 556-9.

Quinlan, C.L., Goncalves, R.L., Hey-Mogensen, M., Yadava, N., Bunik, V.I. and Brand, M.D. (2014) 'The 2-oxoacid dehydrogenase complexes in mitochondria can produce superoxide/hydrogen peroxide at much higher rates than complex I', *J Biol Chem*, 289(12), pp. 8312-25.

Quinlan, C.L., Orr, A.L., Perevoshchikova, I.V., Treberg, J.R., Ackrell, B.A. and Brand, M.D. (2012) 'Mitochondrial complex II can generate reactive oxygen species at high rates in both the forward and reverse reactions', *J Biol Chem*, 287(32), pp. 27255-64.

Quinlan, C.L., Perevoshchikova, I.V., Hey-Mogensen, M., Orr, A.L. and Brand, M.D. (2013) 'Sites of reactive oxygen species generation by mitochondria oxidizing different substrates', *Redox Biol*, 1, pp. 304-12.

Quinzii, C.M. and Hirano, M. (2010) 'Coenzyme Q and mitochondrial disease', *Dev Disabil Res Rev*, 16(2), pp. 183-8.

Rajendran, J., Purhonen, J., Tegelberg, S., Smolander, O.P., Morgelin, M., Rozman, J., Gailus-Durner, V., Fuchs, H., Hrabe de Angelis, M., Auvinen, P., Mervaala, E., Jacobs, H.T., Szibor, M., Fellman, V. and Kallijarvi, J. (2019) 'Alternative oxidase-mediated respiration prevents lethal mitochondrial cardiomyopathy', *EMBO Mol Med*, 11(1).

Rana, A., Oliveira, M.P., Khamoui, A.V., Aparicio, R., Rera, M., Rossiter, H.B. and Walker, D.W. (2017) 'Promoting Drp1-mediated mitochondrial fission in midlife prolongs healthy lifespan of *Drosophila melanogaster*', *Nat Commun*, 8(1), p. 448.

Ray, P.D., Huang, B.W. and Tsuji, Y. (2012) 'Reactive oxygen species (ROS) homeostasis and redox regulation in cellular signaling', *Cell Signal*, 24(5), pp. 981-90.

Reynaert, N.L., van der Vliet, A., Guala, A.S., McGovern, T., Hristova, M., Pantano, C., Heintz, N.H., Heim, J., Ho, Y.S., Matthews, D.E., Wouters, E.F. and Janssen-Heininger, Y.M. (2006) 'Dynamic redox control of NF-kappaB through glutaredoxin-regulated S-glutathionylation of inhibitory kappaB kinase beta', *Proc Natl Acad Sci U S A*, 103(35), pp. 13086-91.

Rhooms, S.K., Murari, A., Goparaju, N.S.V., Vilanueva, M. and Owusu-Ansah, E. (2019) 'Insights from *Drosophila* on mitochondrial complex I', *Cell Mol Life Sci*.

Richter, C., Park, J.W. and Ames, B.N. (1988) 'Normal oxidative damage to mitochondrial and nuclear DNA is extensive', *Proc Natl Acad Sci U S A*, 85(17), pp. 6465-7.

Ristow, M. and Schmeisser, S. (2011) 'Extending life span by increasing oxidative stress', *Free Radic Biol Med*, 51(2), pp. 327-36.

Rival, T., Page, R.M., Chandraratna, D.S., Sendall, T.J., Ryder, E., Liu, B., Lewis, H., Rosahl, T., Hider, R., Camargo, L.M., Shearman, M.S., Crowther, D.C. and Lomas, D.A. (2009) 'Fenton chemistry and oxidative stress mediate the toxicity of the beta-

amyloid peptide in a Drosophila model of Alzheimer's disease', *Eur J Neurosci*, 29(7), pp. 1335-47.

Rizzuto, R., De Stefani, D., Raffaello, A. and Mammucari, C. (2012) 'Mitochondria as sensors and regulators of calcium signalling', *Nat Rev Mol Cell Biol*, 13(9), pp. 566-78.

Robb, E.L., Hall, A.R., Prime, T.A., Eaton, S., Szibor, M., Viscomi, C., James, A.M. and Murphy, M.P. (2018) 'Control of mitochondrial superoxide production by reverse electron transport at complex I', *J Biol Chem*, 293(25), pp. 9869-9879.

Robinson, K.M., Janes, M.S., Pehar, M., Monette, J.S., Ross, M.F., Hagen, T.M., Murphy, M.P. and Beckman, J.S. (2006) 'Selective fluorescent imaging of superoxide in vivo using ethidium-based probes', *Proc Natl Acad Sci U S A*, 103(41), pp. 15038-43.

Rodenburg, R.J. (2011) 'Biochemical diagnosis of mitochondrial disorders', *J Inherit Metab Dis*, 34(2), pp. 283-92.

Rodic, S. and Vincent, M.D. (2018) 'Reactive oxygen species (ROS) are a key determinant of cancer's metabolic phenotype', *Int J Cancer*, 142(3), pp. 440-448.

Roelofs, B.A., Ge, S.X., Studlack, P.E. and Polster, B.M. (2015) 'Low micromolar concentrations of the superoxide probe MitoSOX uncouple neural mitochondria and inhibit complex IV', *Free Radic Biol Med*, 86, pp. 250-8.

Roger, A.J., Munoz-Gomez, S.A. and Kamikawa, R. (2017) 'The Origin and Diversification of Mitochondria', *Curr Biol*, 27(21), pp. R1177-R1192.

Rutter, J., Winge, D.R. and Schiffman, J.D. (2010) 'Succinate dehydrogenase - Assembly, regulation and role in human disease', *Mitochondrion*, 10(4), pp. 393-401.

Saari, S., Garcia, G.S., Bremer, K., Chioda, M.M., Andjelkovic, A., Debes, P.V., Nikinmaa, M., Szibor, M., Dufour, E., Rustin, P., Oliveira, M.T. and Jacobs, H.T. (2019) 'Alternative respiratory chain enzymes: Therapeutic potential and possible pitfalls', *Biochim Biophys Acta Mol Basis Dis*, 1865(4), pp. 854-866.

Sajnani, K., Islam, F., Smith, R.A., Gopalan, V. and Lam, A.K. (2017) 'Genetic alterations in Krebs cycle and its impact on cancer pathogenesis', *Biochimie*, 135, pp. 164-172.

Sanchez-Caballero, L., Guerrero-Castillo, S. and Nijtmans, L. (2016) 'Unraveling the complexity of mitochondrial complex I assembly: A dynamic process', *Biochim Biophys Acta*.

Sandalio, L.M., Rodriguez-Serrano, M., Romero-Puertas, M.C. and del Rio, L.A. (2013) 'Role of peroxisomes as a source of reactive oxygen species (ROS) signaling molecules', *Subcell Biochem*, 69, pp. 231-55.

Santamaria, G., Martinez-Diez, M., Fabregat, I. and Cuezva, J.M. (2006) 'Efficient execution of cell death in non-glycolytic cells requires the generation of ROS controlled by the activity of mitochondrial H⁺-ATP synthase', *Carcinogenesis*, 27(5), pp. 925-35.

- Sanz, A. (2016) 'Mitochondrial reactive oxygen species: Do they extend or shorten animal lifespan?', *Biochim Biophys Acta*.
- Sanz, A., Fernandez-Ayala, D.J., Stefanatos, R.K. and Jacobs, H.T. (2010a) 'Mitochondrial ROS production correlates with, but does not directly regulate lifespan in *Drosophila*', *Aging (Albany NY)*, 2(4), pp. 200-23.
- Sanz, A., Pamplona, R. and Barja, G. (2006) 'Is the mitochondrial free radical theory of aging intact?', *Antioxid Redox Signal*, 8(3-4), pp. 582-99.
- Sanz, A., Soikkeli, M., Portero-Otin, M., Wilson, A., Kemppainen, E., McIlroy, G., Ellila, S., Kemppainen, K.K., Tuomela, T., Lakanmaa, M., Kiviranta, E., Stefanatos, R., Dufour, E., Hutz, B., Naudi, A., Jove, M., Zeb, A., Vartiainen, S., Matsuno-Yagi, A., Yagi, T., Rustin, P., Pamplona, R. and Jacobs, H.T. (2010b) 'Expression of the yeast NADH dehydrogenase Ndi1 in *Drosophila* confers increased lifespan independently of dietary restriction', *Proc Natl Acad Sci U S A*, 107(20), pp. 9105-10.
- Sanz, A., Stefanatos, R. and McIlroy, G. (2010c) 'Production of reactive oxygen species by the mitochondrial electron transport chain in *Drosophila melanogaster*', *J Bioenerg Biomembr*, 42(2), pp. 135-42.
- Sanz, A. and Stefanatos, R.K. (2008) 'The mitochondrial free radical theory of aging: a critical view', *Curr Aging Sci*, 1(1), pp. 10-21.
- Sathyanarayanan, S., Zheng, X., Kumar, S., Chen, C.H., Chen, D., Hay, B. and Sehgal, A. (2008) 'Identification of novel genes involved in light-dependent CRY degradation through a genome-wide RNAi screen', *Genes Dev*, 22(11), pp. 1522-33.
- Sato, K., Torimoto, Y., Hosoki, T., Ikuta, K., Takahashi, H., Yamamoto, M., Ito, S., Okamura, N., Ichiki, K., Tanaka, H., Shindo, M., Hirai, K., Mizukami, Y., Otake, T., Fujiya, M., Sasaki, K. and Kohgo, Y. (2011) 'Loss of ABCB7 gene: pathogenesis of mitochondrial iron accumulation in erythroblasts in refractory anemia with ringed sideroblast with isodicentric (X)(q13)', *Int J Hematol*, 93(3), pp. 311-318.
- Sazanov, L.A. (2014) 'The mechanism of coupling between electron transfer and proton translocation in respiratory complex I', *J Bioenerg Biomembr*, 46(4), pp. 247-53.
- Schapira, A.H. (2008) 'Mitochondria in the aetiology and pathogenesis of Parkinson's disease', *Lancet Neurol*, 7(1), pp. 97-109.
- Schapira, A.H., Cooper, J.M., Dexter, D., Clark, J.B., Jenner, P. and Marsden, C.D. (1990) 'Mitochondrial complex I deficiency in Parkinson's disease', *J Neurochem*, 54(3), pp. 823-7.
- Scherz-Shouval, R., Shvets, E., Fass, E., Shorer, H., Gil, L. and Elazar, Z. (2007) 'Reactive oxygen species are essential for autophagy and specifically regulate the activity of Atg4', *EMBO J*, 26(7), pp. 1749-60.
- Schieber, M. and Chandel, N.S. (2014) 'ROS function in redox signaling and oxidative stress', *Curr Biol*, 24(10), pp. R453-62.

- Schiff, M., Benit, P., Jacobs, H.T., Vockley, J. and Rustin, P. (2012) 'Therapies in inborn errors of oxidative metabolism', *Trends Endocrinol Metab*, 23(9), pp. 488-95.
- Schmeisser, S., Zarse, K. and Ristow, M. (2011) 'Lonidamine extends lifespan of adult *Caenorhabditis elegans* by increasing the formation of mitochondrial reactive oxygen species', *Horm Metab Res*, 43(10), pp. 687-92.
- Schrader, M. and Fahimi, H.D. (2006) 'Peroxisomes and oxidative stress', *Biochim Biophys Acta*, 1763(12), pp. 1755-66.
- Schreck, R., Rieber, P. and Baeuerle, P.A. (1991) 'Reactive oxygen intermediates as apparently widely used messengers in the activation of the NF-kappa B transcription factor and HIV-1', *EMBO J*, 10(8), pp. 2247-58.
- Schulz, T.J., Zarse, K., Voigt, A., Urban, N., Birringer, M. and Ristow, M. (2007) 'Glucose restriction extends *Caenorhabditis elegans* life span by inducing mitochondrial respiration and increasing oxidative stress', *Cell Metab*, 6(4), pp. 280-93.
- Scialo, F., Fernandez-Ayala, D.J. and Sanz, A. (2017) 'Role of Mitochondrial Reverse Electron Transport in ROS Signaling: Potential Roles in Health and Disease', *Front Physiol*, 8, p. 428.
- Scialo, F., Mallikarjun, V., Stefanatos, R. and Sanz, A. (2013) 'Regulation of lifespan by the mitochondrial electron transport chain: reactive oxygen species-dependent and reactive oxygen species-independent mechanisms', *Antioxid Redox Signal*, 19(16), pp. 1953-69.
- Scialo, F., Sriram, A., Fernandez-Ayala, D., Gubina, N., Lohmus, M., Nelson, G., Logan, A., Cooper, H.M., Navas, P., Enriquez, J.A., Murphy, M.P. and Sanz, A. (2016a) 'Mitochondrial ROS Produced via Reverse Electron Transport Extend Animal Lifespan', *Cell Metab*, 23(4), pp. 725-34.
- Scialo, F., Sriram, A., Stefanatos, R. and Sanz, A. (2016b) 'Practical Recommendations for the Use of the GeneSwitch Gal4 System to Knock-Down Genes in *Drosophila melanogaster*', *PLoS One*, 11(8), p. e0161817.
- Sena, L.A. and Chandel, N.S. (2012) 'Physiological roles of mitochondrial reactive oxygen species', *Mol Cell*, 48(2), pp. 158-67.
- Sena, L.A., Li, S., Jairaman, A., Prakriya, M., Ezponda, T., Hildeman, D.A., Wang, C.R., Schumacker, P.T., Licht, J.D., Perlman, H., Bryce, P.J. and Chandel, N.S. (2013) 'Mitochondria are required for antigen-specific T cell activation through reactive oxygen species signaling', *Immunity*, 38(2), pp. 225-36.
- Senior, A.E., Nadanaciva, S. and Weber, J. (2002) 'The molecular mechanism of ATP synthesis by F1F0-ATP synthase', *Biochim Biophys Acta*, 1553(3), pp. 188-211.
- Seo, A.Y., Xu, J., Servais, S., Hofer, T., Marzetti, E., Wohlgemuth, S.E., Knutson, M.D., Chung, H.Y. and Leeuwenburgh, C. (2008) 'Mitochondrial iron accumulation with age and functional consequences', *Aging Cell*, 7(5), pp. 706-16.

- Seo, B.B., Kitajima-Ihara, T., Chan, E.K., Scheffler, I.E., Matsuno-Yagi, A. and Yagi, T. (1998) 'Molecular remedy of complex I defects: rotenone-insensitive internal NADH-quinone oxidoreductase of *Saccharomyces cerevisiae* mitochondria restores the NADH oxidase activity of complex I-deficient mammalian cells', *Proc Natl Acad Sci U S A*, 95(16), pp. 9167-71.
- Seo, B.B., Nakamaru-Ogiso, E., Cruz, P., Flotte, T.R., Yagi, T. and Matsuno-Yagi, A. (2004) 'Functional expression of the single subunit NADH dehydrogenase in mitochondria in vivo: a potential therapy for complex I deficiencies', *Hum Gene Ther*, 15(9), pp. 887-95.
- Seo, B.B., Nakamaru-Ogiso, E., Flotte, T.R., Matsuno-Yagi, A. and Yagi, T. (2006) 'In vivo complementation of complex I by the yeast Ndi1 enzyme. Possible application for treatment of Parkinson disease', *J Biol Chem*, 281(20), pp. 14250-5.
- Sgraja, T., Ulschmid, J., Becker, K., Schneuwly, S., Klebe, G., Reuter, K. and Heine, A. (2004) 'Structural insights into the neuroprotective-acting carbonyl reductase Sniffer of *Drosophila melanogaster*', *J Mol Biol*, 342(5), pp. 1613-24.
- Shadel, G.S. and Horvath, T.L. (2015) 'Mitochondrial ROS signaling in organismal homeostasis', *Cell*, 163(3), pp. 560-9.
- Sharma, L.K., Lu, J. and Bai, Y. (2009) 'Mitochondrial respiratory complex I: structure, function and implication in human diseases', *Curr Med Chem*, 16(10), pp. 1266-77.
- Shchepinova, M.M., Cairns, A.G., Prime, T.A., Logan, A., James, A.M., Hall, A.R., Vidoni, S., Arndt, S., Caldwell, S.T., Prag, H.A., Pell, V.R., Krieg, T., Mulvey, J.F., Yadav, P., Cobley, J.N., Bright, T.P., Senn, H.M., Anderson, R.F., Murphy, M.P. and Hartley, R.C. (2017) 'MitoNeoD: A Mitochondria-Targeted Superoxide Probe', *Cell Chem Biol*, 24(10), pp. 1285-1298 e12.
- Sheng, Y., Abreu, I.A., Cabelli, D.E., Maroney, M.J., Miller, A.F., Teixeira, M. and Valentine, J.S. (2014) 'Superoxide dismutases and superoxide reductases', *Chem Rev*, 114(7), pp. 3854-918.
- Shimada, S., Shinzawa-Itoh, K., Baba, J., Aoe, S., Shimada, A., Yamashita, E., Kang, J., Tateno, M., Yoshikawa, S. and Tsukihara, T. (2017) 'Complex structure of cytochrome c-cytochrome c oxidase reveals a novel protein-protein interaction mode', *EMBO J*, 36(3), pp. 291-300.
- Sies, H. (1997) 'Oxidative stress: oxidants and antioxidants', *Exp Physiol*, 82(2), pp. 291-5.
- Simonsen, A., Cumming, R.C., Brech, A., Isakson, P., Schubert, D.R. and Finley, K.D. (2008) 'Promoting basal levels of autophagy in the nervous system enhances longevity and oxidant resistance in adult *Drosophila*', *Autophagy*, 4(2), pp. 176-84.
- Singh, A., Maqbool, M., Mobashir, M. and Hoda, N. (2017) 'Dihydroorotate dehydrogenase: A drug target for the development of antimalarials', *Eur J Med Chem*, 125, pp. 640-651.

- Soberanes, S., Misharin, A.V., Jairaman, A., Morales-Nebreda, L., McQuattie-Pimentel, A.C., Cho, T., Hamanaka, R.B., Meliton, A.Y., Reyfman, P.A., Walter, J.M., Chen, C.I., Chi, M., Chiu, S., Gonzalez-Gonzalez, F.J., Antalek, M., Abdala-Valencia, H., Chiarella, S.E., Sun, K.A., Woods, P.S., Ghio, A.J., Jain, M., Perlman, H., Ridge, K.M., Morimoto, R.I., Sznajder, J.I., Balch, W.E., Bhorade, S.M., Bharat, A., Prakriya, M., Chandel, N.S., Mutlu, G.M. and Budinger, G.R.S. (2019) 'Metformin Targets Mitochondrial Electron Transport to Reduce Air-Pollution-Induced Thrombosis', *Cell Metab*, 29(2), pp. 335-347 e5.
- Soberanes, S., Urich, D., Baker, C.M., Burgess, Z., Chiarella, S.E., Bell, E.L., Ghio, A.J., De Vizcaya-Ruiz, A., Liu, J., Ridge, K.M., Kamp, D.W., Chandel, N.S., Schumacker, P.T., Mutlu, G.M. and Budinger, G.R. (2009) 'Mitochondrial complex III-generated oxidants activate ASK1 and JNK to induce alveolar epithelial cell death following exposure to particulate matter air pollution', *J Biol Chem*, 284(4), pp. 2176-86.
- Sohal, R.S. and Weindruch, R. (1996) 'Oxidative stress, caloric restriction, and aging', *Science*, 273(5271), pp. 59-63.
- Sousa, J.S., D'Imprima, E. and Vonck, J. (2018) 'Mitochondrial Respiratory Chain Complexes', *Subcell Biochem*, 87, pp. 167-227.
- Sperl, W., Skladal, D., Gnaiger, E., Wyss, M., Mayr, U., Hager, J. and Gellerich, F.N. (1997) 'High resolution respirometry of permeabilized skeletal muscle fibers in the diagnosis of neuromuscular disorders', *Mol Cell Biochem*, 174(1-2), pp. 71-8.
- Srinivasan, S. and Avadhani, N.G. (2012) 'Cytochrome c oxidase dysfunction in oxidative stress', *Free Radic Biol Med*, 53(6), pp. 1252-63.
- St-Pierre, J., Buckingham, J.A., Roebuck, S.J. and Brand, M.D. (2002) 'Topology of superoxide production from different sites in the mitochondrial electron transport chain', *J Biol Chem*, 277(47), pp. 44784-90.
- Stadtman, E.R. (2006) 'Protein oxidation and aging', *Free Radic Res*, 40(12), pp. 1250-8.
- Stadtman, E.R. and Levine, R.L. (2003) 'Free radical-mediated oxidation of free amino acids and amino acid residues in proteins', *Amino Acids*, 25(3-4), pp. 207-18.
- Stadtman, E.R., Moskovitz, J. and Levine, R.L. (2003) 'Oxidation of methionine residues of proteins: biological consequences', *Antioxid Redox Signal*, 5(5), pp. 577-82.
- Stefanatos, R. and Sanz, A. (2011) 'Mitochondrial complex I: a central regulator of the aging process', *Cell Cycle*, 10(10), pp. 1528-32.
- Stefanatos, R. and Sanz, A. (2018) 'The role of mitochondrial ROS in the aging brain', *FEBS Lett*, 592(5), pp. 743-758.
- Stehling, O. and Lill, R. (2013) 'The role of mitochondria in cellular iron-sulfur protein biogenesis: mechanisms, connected processes, and diseases', *Cold Spring Harb Perspect Biol*, 5(8), p. a011312.

Stock, D., Leslie, A.G. and Walker, J.E. (1999) 'Molecular architecture of the rotary motor in ATP synthase', *Science*, 286(5445), pp. 1700-5.

Stroud, D.A., Surgenor, E.E., Formosa, L.E., Reljic, B., Frazier, A.E., Dibley, M.G., Osellame, L.D., Stait, T., Beilharz, T.H., Thorburn, D.R., Salim, A. and Ryan, M.T. (2016) 'Accessory subunits are integral for assembly and function of human mitochondrial complex I', *Nature*, 538(7623), pp. 123-126.

Su, T., Turnbull, D.M. and Greaves, L.C. (2018) 'Roles of Mitochondrial DNA Mutations in Stem Cell Ageing', *Genes (Basel)*, 9(4).

Sun, J., Druhan, L.J. and Zweier, J.L. (2010) 'Reactive oxygen and nitrogen species regulate inducible nitric oxide synthase function shifting the balance of nitric oxide and superoxide production', *Arch Biochem Biophys*, 494(2), pp. 130-7.

Sun, J., Morgan, M., Shen, R.F., Steenbergen, C. and Murphy, E. (2007) 'Preconditioning results in S-nitrosylation of proteins involved in regulation of mitochondrial energetics and calcium transport', *Circ Res*, 101(11), pp. 1155-63.

Sun, N., Youle, R.J. and Finkel, T. (2016) 'The Mitochondrial Basis of Aging', *Mol Cell*, 61(5), pp. 654-666.

Sun, W.H., Liu, F., Chen, Y. and Zhu, Y.C. (2012) 'Hydrogen sulfide decreases the levels of ROS by inhibiting mitochondrial complex IV and increasing SOD activities in cardiomyocytes under ischemia/reperfusion', *Biochem Biophys Res Commun*, 421(2), pp. 164-9.

Sun, Y., Yolitz, J., Wang, C., Spangler, E., Zhan, M. and Zou, S. (2013) 'Aging studies in *Drosophila melanogaster*', *Methods Mol Biol*, 1048, pp. 77-93.

Symersky, J., Osowski, D., Walters, D.E. and Mueller, D.M. (2012) 'Oligomycin frames a common drug-binding site in the ATP synthase', *Proc Natl Acad Sci U S A*, 109(35), pp. 13961-5.

Szibor, M., Dhandapani, P.K., Dufour, E., Holmstrom, K.M., Zhuang, Y., Salwig, I., Wittig, I., Heidler, J., Gizatullina, Z., Gainutdinov, T., German Mouse Clinic, C., Fuchs, H., Gailus-Durner, V., de Angelis, M.H., Nandania, J., Velagapudi, V., Wietelmann, A., Rustin, P., Gellerich, F.N., Jacobs, H.T. and Braun, T. (2017) 'Broad AOX expression in a genetically tractable mouse model does not disturb normal physiology', *Dis Model Mech*, 10(2), pp. 163-171.

Szklarczyk, D., Morris, J.H., Cook, H., Kuhn, M., Wyder, S., Simonovic, M., Santos, A., Doncheva, N.T., Roth, A., Bork, P., Jensen, L.J. and von Mering, C. (2017) 'The STRING database in 2017: quality-controlled protein-protein association networks, made broadly accessible', *Nucleic Acids Res*, 45(D1), pp. D362-D368.

Tain, L.S., Sehlke, R., Jain, C., Chokkalingam, M., Nagaraj, N., Essers, P., Rassner, M., Gronke, S., Froelich, J., Dieterich, C., Mann, M., Alic, N., Beyer, A. and Partridge, L. (2017) 'A proteomic atlas of insulin signalling reveals tissue-specific mechanisms of longevity assurance', *Mol Syst Biol*, 13(9), p. 939.

Tait, S.W. and Green, D.R. (2012) 'Mitochondria and cell signalling', *J Cell Sci*, 125(Pt 4), pp. 807-15.

Tan, S., Sagara, Y., Liu, Y., Maher, P. and Schubert, D. (1998) 'The regulation of reactive oxygen species production during programmed cell death', *J Cell Biol*, 141(6), pp. 1423-32.

Tan, Y., Ci, Y., Dai, X., Wu, F., Guo, J., Liu, D., North, B.J., Huo, J. and Zhang, J. (2017) 'Cullin 3SPOP ubiquitin E3 ligase promotes the poly-ubiquitination and degradation of HDAC6', *Oncotarget*, 8(29), pp. 47890-47901.

Tanner, C.M., Kamel, F., Ross, G.W., Hoppin, J.A., Goldman, S.M., Korell, M., Marras, C., Bhudhikanok, G.S., Kasten, M., Chade, A.R., Comyns, K., Richards, M.B., Meng, C., Priestley, B., Fernandez, H.H., Cambi, F., Umbach, D.M., Blair, A., Sandler, D.P. and Langston, J.W. (2011) 'Rotenone, paraquat, and Parkinson's disease', *Environ Health Perspect*, 119(6), pp. 866-72.

Tatarkova, Z., Kovalska, M., Timkova, V., Racay, P., Lehotsky, J. and Kaplan, P. (2016) 'The Effect of Aging on Mitochondrial Complex I and the Extent of Oxidative Stress in the Rat Brain Cortex', *Neurochem Res*, 41(8), pp. 2160-72.

Taylor, C.T. and Moncada, S. (2010) 'Nitric oxide, cytochrome C oxidase, and the cellular response to hypoxia', *Arterioscler Thromb Vasc Biol*, 30(4), pp. 643-7.

Templeton, D.J., Aye, M.S., Rady, J., Xu, F. and Cross, J.V. (2010) 'Purification of reversibly oxidized proteins (PROP) reveals a redox switch controlling p38 MAP kinase activity', *PLoS One*, 5(11), p. e15012.

Theodosiou, N.A. and Xu, T. (1998) 'Use of FLP/FRT system to study Drosophila development', *Methods*, 14(4), pp. 355-65.

Thierbach, G. and Reichenbach, H. (1981) 'Myxothiazol, a new antibiotic interfering with respiration', *Antimicrob Agents Chemother*, 19(4), pp. 504-7.

Timon-Gomez, A., Nyvltova, E., Abriata, L.A., Vila, A.J., Hosler, J. and Barrientos, A. (2018) 'Mitochondrial cytochrome c oxidase biogenesis: Recent developments', *Semin Cell Dev Biol*, 76, pp. 163-178.

Tormos, K.V., Anso, E., Hamanaka, R.B., Eisenbart, J., Joseph, J., Kalyanaraman, B. and Chandel, N.S. (2011) 'Mitochondrial complex III ROS regulate adipocyte differentiation', *Cell Metab*, 14(4), pp. 537-44.

Toroser, D., Orr, W.C. and Sohal, R.S. (2007) 'Carbonylation of mitochondrial proteins in Drosophila melanogaster during aging', *Biochem Biophys Res Commun*, 363(2), pp. 418-24.

Treberg, J.R., Quinlan, C.L. and Brand, M.D. (2010) 'Hydrogen peroxide efflux from muscle mitochondria underestimates matrix superoxide production--a correction using glutathione depletion', *FEBS J*, 277(13), pp. 2766-78.

Treberg, J.R., Quinlan, C.L. and Brand, M.D. (2011) 'Evidence for two sites of superoxide production by mitochondrial NADH-ubiquinone oxidoreductase (complex I)', *J Biol Chem*, 286(31), pp. 27103-10.

Tufi, R., Gandhi, S., de Castro, I.P., Lehmann, S., Angelova, P.R., Dinsdale, D., Deas, E., Plun-Favreau, H., Nicotera, P., Abramov, A.Y., Willis, A.E., Mallucci, G.R., Loh, S.H. and Martins, L.M. (2014) 'Enhancing nucleotide metabolism protects against mitochondrial dysfunction and neurodegeneration in a PINK1 model of Parkinson's disease', *Nat Cell Biol*, 16(2), pp. 157-66.

Untergasser, A., Cutcutache, I., Koressaar, T., Ye, J., Faircloth, B.C., Remm, M. and Rozen, S.G. (2012) 'Primer3--new capabilities and interfaces', *Nucleic Acids Res*, 40(15), p. e115.

Ursini, F. and Bindoli, A. (1987) 'The role of selenium peroxidases in the protection against oxidative damage of membranes', *Chem Phys Lipids*, 44(2-4), pp. 255-76.

Vajro, P., Zielinska, K., Ng, B.G., Maccarana, M., Bengtson, P., Poeta, M., Mandato, C., D'Acunto, E., Freeze, H.H. and Eklund, E.A. (2018) 'Three unreported cases of TMEM199-CDG, a rare genetic liver disease with abnormal glycosylation', *Orphanet J Rare Dis*, 13(1), p. 4.

Valentini, S., Cabreiro, F., Ackerman, D., Alam, M.M., Kunze, M.B., Kay, C.W. and Gems, D. (2012) 'Manipulation of in vivo iron levels can alter resistance to oxidative stress without affecting ageing in the nematode *C. elegans*', *Mech Ageing Dev*, 133(5), pp. 282-90.

van der Blik, A.M., Sedensky, M.M. and Morgan, P.G. (2017) 'Cell Biology of the Mitochondrion', *Genetics*, 207(3), pp. 843-871.

Van Raamsdonk, J.M. and Hekimi, S. (2009) 'Deletion of the mitochondrial superoxide dismutase *sod-2* extends lifespan in *Caenorhabditis elegans*', *PLoS Genet*, 5(2), p. e1000361.

Van Raamsdonk, J.M. and Hekimi, S. (2012) 'Superoxide dismutase is dispensable for normal animal lifespan', *Proc Natl Acad Sci U S A*, 109(15), pp. 5785-90.

Van Remmen, H., Ikeno, Y., Hamilton, M., Pahlavani, M., Wolf, N., Thorpe, S.R., Alderson, N.L., Baynes, J.W., Epstein, C.J., Huang, T.T., Nelson, J., Strong, R. and Richardson, A. (2003) 'Life-long reduction in MnSOD activity results in increased DNA damage and higher incidence of cancer but does not accelerate aging', *Physiol Genomics*, 16(1), pp. 29-37.

Vanlerberghe, G.C. (2013) 'Alternative oxidase: a mitochondrial respiratory pathway to maintain metabolic and signaling homeostasis during abiotic and biotic stress in plants', *Int J Mol Sci*, 14(4), pp. 6805-47.

Veal, E.A., Day, A.M. and Morgan, B.A. (2007) 'Hydrogen peroxide sensing and signaling', *Mol Cell*, 26(1), pp. 1-14.

Veltri, R.W., Sprinkle, P.M., Maxim, P.E., Theofilopoulos, A.N., Rodman, S.M. and Kinney, C.L. (1978) 'Immune monitoring protocol for patients with carcinoma of the

head and neck. Preliminary report', *Ann Otol Rhinol Laryngol*, 87(5 Pt 1), pp. 692-700.

Vilain, S., Esposito, G., Haddad, D., Schaap, O., Dobрева, M.P., Vos, M., Van Meensel, S., Morais, V.A., De Strooper, B. and Verstreken, P. (2012) 'The yeast complex I equivalent NADH dehydrogenase rescues pink1 mutants', *PLoS Genet*, 8(1), p. e1002456.

Vissers, J.H., Manning, S.A., Kulkarni, A. and Harvey, K.F. (2016) 'A Drosophila RNAi library modulates Hippo pathway-dependent tissue growth', *Nat Commun*, 7, p. 10368.

von Mering, C., Jensen, L.J., Snel, B., Hooper, S.D., Krupp, M., Foglierini, M., Jouffre, N., Huynen, M.A. and Bork, P. (2005) 'STRING: known and predicted protein-protein associations, integrated and transferred across organisms', *Nucleic Acids Res*, 33(Database issue), pp. D433-7.

Vos, M., Lauwers, E. and Verstreken, P. (2010) 'Synaptic mitochondria in synaptic transmission and organization of vesicle pools in health and disease', *Front Synaptic Neurosci*, 2, p. 139.

Walker, D.W., Hajek, P., Muffat, J., Knoepfle, D., Cornelison, S., Attardi, G. and Benzer, S. (2006) 'Hypersensitivity to oxygen and shortened lifespan in a Drosophila mitochondrial complex II mutant', *Proc Natl Acad Sci U S A*, 103(44), pp. 16382-7.

Walker, J.E. (2013) 'The ATP synthase: the understood, the uncertain and the unknown', *Biochem Soc Trans*, 41(1), pp. 1-16.

Wallace, D.C. (1999) 'Mitochondrial diseases in man and mouse', *Science*, 283(5407), pp. 1482-8.

Wallace, D.C. (2005) 'A mitochondrial paradigm of metabolic and degenerative diseases, aging, and cancer: a dawn for evolutionary medicine', *Annu Rev Genet*, 39, pp. 359-407.

Wang, C., Li, P., Xuan, J., Zhu, C., Liu, J., Shan, L., Du, Q., Ren, Y. and Ye, J. (2017) 'Cholesterol Enhances Colorectal Cancer Progression via ROS Elevation and MAPK Signaling Pathway Activation', *Cell Physiol Biochem*, 42(2), pp. 729-742.

Wang, W., Fang, H., Groom, L., Cheng, A., Zhang, W., Liu, J., Wang, X., Li, K., Han, P., Zheng, M., Yin, J., Wang, W., Mattson, M.P., Kao, J.P., Lakatta, E.G., Sheu, S.S., Ouyang, K., Chen, J., Dirksen, R.T. and Cheng, H. (2008) 'Superoxide flashes in single mitochondria', *Cell*, 134(2), pp. 279-90.

Wang, X., Fang, H., Huang, Z., Shang, W., Hou, T., Cheng, A. and Cheng, H. (2013) 'Imaging ROS signaling in cells and animals', *J Mol Med (Berl)*, 91(8), pp. 917-27.
Wang, X. and Quinn, P.J. (2000) 'The location and function of vitamin E in membranes (review)', *Mol Membr Biol*, 17(3), pp. 143-56.

Wang, X., Wang, W., Li, L., Perry, G., Lee, H.G. and Zhu, X. (2014) 'Oxidative stress and mitochondrial dysfunction in Alzheimer's disease', *Biochim Biophys Acta*, 1842(8), pp. 1240-7.

Wang, Y., Branicky, R., Noe, A. and Hekimi, S. (2018) 'Superoxide dismutases: Dual roles in controlling ROS damage and regulating ROS signaling', *J Cell Biol*, 217(6), pp. 1915-1928.

Wang, Y., Nartiss, Y., Steipe, B., McQuibban, G.A. and Kim, P.K. (2012) 'ROS-induced mitochondrial depolarization initiates PARK2/PARKIN-dependent mitochondrial degradation by autophagy', *Autophagy*, 8(10), pp. 1462-76.

Watmough, N.J. and Frerman, F.E. (2010) 'The electron transfer flavoprotein: ubiquinone oxidoreductases', *Biochim Biophys Acta*, 1797(12), pp. 1910-6.

Weeber, E.J., Levy, M., Sampson, M.J., Anflous, K., Armstrong, D.L., Brown, S.E., Sweatt, J.D. and Craigen, W.J. (2002) 'The role of mitochondrial porins and the permeability transition pore in learning and synaptic plasticity', *J Biol Chem*, 277(21), pp. 18891-7.

Weinberg, F., Hamanaka, R., Wheaton, W.W., Weinberg, S., Joseph, J., Lopez, M., Kalyanaraman, B., Mutlu, G.M., Budinger, G.R. and Chandel, N.S. (2010) 'Mitochondrial metabolism and ROS generation are essential for Kras-mediated tumorigenicity', *Proc Natl Acad Sci U S A*, 107(19), pp. 8788-93.

Weinberg, S.E., Sena, L.A. and Chandel, N.S. (2015) 'Mitochondria in the regulation of innate and adaptive immunity', *Immunity*, 42(3), pp. 406-17.

West, A.P., Brodsky, I.E., Rahner, C., Woo, D.K., Erdjument-Bromage, H., Tempst, P., Walsh, M.C., Choi, Y., Shadel, G.S. and Ghosh, S. (2011) 'TLR signalling augments macrophage bactericidal activity through mitochondrial ROS', *Nature*, 472(7344), pp. 476-80.

Wheaton, W.W., Weinberg, S.E., Hamanaka, R.B., Soberanes, S., Sullivan, L.B., Anso, E., Glasauer, A., Dufour, E., Mutlu, G.M., Budigner, G.S. and Chandel, N.S. (2014) 'Metformin inhibits mitochondrial complex I of cancer cells to reduce tumorigenesis', *Elife*, 3, p. e02242.

Wiedemann, N. and Pfanner, N. (2017) 'Mitochondrial Machineries for Protein Import and Assembly', *Annu Rev Biochem*, 86, pp. 685-714.

Wirth, C., Brandt, U., Hunte, C. and Zickermann, V. (2016) 'Structure and function of mitochondrial complex I', *Biochim Biophys Acta*, 1857(7), pp. 902-14.

Wong, A., Boutis, P. and Hekimi, S. (1995) 'Mutations in the clk-1 gene of *Caenorhabditis elegans* affect developmental and behavioral timing', *Genetics*, 139(3), pp. 1247-59.

Wong, H.S., Benoit, B. and Brand, M.D. (2019) 'Mitochondrial and cytosolic sources of hydrogen peroxide in resting C2C12 myoblasts', *Free Radic Biol Med*, 130, pp. 140-150.

Wong, H.S., Dighe, P.A., Mezera, V., Monternier, P.A. and Brand, M.D. (2017) 'Production of superoxide and hydrogen peroxide from specific mitochondrial sites under different bioenergetic conditions', *J Biol Chem*, 292(41), pp. 16804-16809.

- Wong, H.S., Monternier, P.A., Orr, A.L. and Brand, M.D. (2018) 'Plate-Based Measurement of Superoxide and Hydrogen Peroxide Production by Isolated Mitochondria', *Methods Mol Biol*, 1782, pp. 287-299.
- Xia, D., Esser, L., Tang, W.K., Zhou, F., Zhou, Y., Yu, L. and Yu, C.A. (2013) 'Structural analysis of cytochrome bc1 complexes: implications to the mechanism of function', *Biochim Biophys Acta*, 1827(11-12), pp. 1278-94.
- Xia, Y. and Zweier, J.L. (1997) 'Superoxide and peroxynitrite generation from inducible nitric oxide synthase in macrophages', *Proc Natl Acad Sci U S A*, 94(13), pp. 6954-8.
- Xu, T., Pagadala, V. and Mueller, D.M. (2015) 'Understanding structure, function, and mutations in the mitochondrial ATP synthase', *Microb Cell*, 2(4), pp. 105-125.
- Xu, Z. and Xu, L. (2016) 'Fluorescent probes for the selective detection of chemical species inside mitochondria', *Chem Commun (Camb)*, 52(6), pp. 1094-119.
- Yagi, T., Seo, B.B., Nakamaru-Ogiso, E., Marella, M., Barber-Singh, J., Yamashita, T. and Matsuno-Yagi, A. (2006) 'Possibility of transkingdom gene therapy for complex I diseases', *Biochim Biophys Acta*, 1757(5-6), pp. 708-14.
- Yang, W. and Hekimi, S. (2010) 'A mitochondrial superoxide signal triggers increased longevity in *Caenorhabditis elegans*', *PLoS Biol*, 8(12), p. e1000556.
- Yang, W., Li, J. and Hekimi, S. (2007) 'A Measurable increase in oxidative damage due to reduction in superoxide detoxification fails to shorten the life span of long-lived mitochondrial mutants of *Caenorhabditis elegans*', *Genetics*, 177(4), pp. 2063-74.
- Yoboue, E.D., Sitia, R. and Simmen, T. (2018) 'Redox crosstalk at endoplasmic reticulum (ER) membrane contact sites (MCS) uses toxic waste to deliver messages', *Cell Death Dis*, 9(3), p. 331.
- Yubero, D., Montero, R., Martin, M.A., Montoya, J., Ribes, A., Grazina, M., Trevisson, E., Rodriguez-Aguilera, J.C., Hargreaves, I.P., Salviati, L., Navas, P., Artuch, R., Co, Q.d.s.g., Jou, C., Jimenez-Mallebrera, C., Nascimento, A., Perez-Duenas, B., Ortez, C., Ramos, F., Colomer, J., O'Callaghan, M., Pineda, M., Garcia-Cazorla, A., Espinos, C., Ruiz, A., Macaya, A., Marce-Grau, A., Garcia-Villoria, J., Arias, A., Emperador, S., Ruiz-Pesini, E., Lopez-Gallardo, E., Neergheen, V., Simoes, M., Diogo, L., Blazquez, A., Gonzalez-Quintana, A., Delmiro, A., Dominguez-Gonzalez, C., Arenas, J., Garcia-Silva, M.T., Martin, E., Quijada, P., Hernandez-Lain, A., Moran, M., Rivas Infante, E., Avila Polo, R., Paradas Lope, C., Bautista Lorite, J., Martinez Fernandez, E.M., Cortes, A.B., Sanchez-Cuesta, A., Cascajo, M.V., Alcazar, M. and Brea-Calvo, G. (2016) 'Secondary coenzyme Q10 deficiencies in oxidative phosphorylation (OXPHOS) and non-OXPHOS disorders', *Mitochondrion*, 30, pp. 51-8.
- Yun, J. and Finkel, T. (2014) 'Mitohormesis', *Cell Metab*, 19(5), pp. 757-66.

- Zangar, R.C., Davydov, D.R. and Verma, S. (2004) 'Mechanisms that regulate production of reactive oxygen species by cytochrome P450', *Toxicol Appl Pharmacol*, 199(3), pp. 316-31.
- Zhang, G., Luo, Y., Li, G., Wang, L., Na, D., Wu, X., Zhang, Y., Mo, X. and Wang, L. (2014) 'DHRSX, a novel non-classical secretory protein associated with starvation induced autophagy', *Int J Med Sci*, 11(9), pp. 962-70.
- Zhang, J., Perry, G., Smith, M.A., Robertson, D., Olson, S.J., Graham, D.G. and Montine, T.J. (1999) 'Parkinson's disease is associated with oxidative damage to cytoplasmic DNA and RNA in substantia nigra neurons', *Am J Pathol*, 154(5), pp. 1423-9.
- Zhang, J., Wang, X., Vikash, V., Ye, Q., Wu, D., Liu, Y. and Dong, W. (2016) 'ROS and ROS-Mediated Cellular Signaling', *Oxid Med Cell Longev*, 2016, p. 4350965.
- Zhang, L., Lu, P., Yan, L., Yang, L., Wang, Y., Chen, J., Dai, J., Li, Y., Kang, Z., Bai, T., Xi, Y., Xu, J., Sun, G. and Yang, T. (2019) 'MRPL35 Is Up-Regulated in Colorectal Cancer and Regulates Colorectal Cancer Cell Growth and Apoptosis', *Am J Pathol*, 189(5), pp. 1105-1120.
- Zhang, Z., Huang, L., Shulmeister, V.M., Chi, Y.I., Kim, K.K., Hung, L.W., Crofts, A.R., Berry, E.A. and Kim, S.H. (1998) 'Electron transfer by domain movement in cytochrome bc1', *Nature*, 392(6677), pp. 677-84.
- Zhao, H., Kalivendi, S., Zhang, H., Joseph, J., Nithipatikom, K., Vasquez-Vivar, J. and Kalyanaraman, B. (2003) 'Superoxide reacts with hydroethidine but forms a fluorescent product that is distinctly different from ethidium: potential implications in intracellular fluorescence detection of superoxide', *Free Radic Biol Med*, 34(11), pp. 1359-68.
- Zhao, R.Z., Jiang, S., Zhang, L. and Yu, Z.B. (2019) 'Mitochondrial electron transport chain, ROS generation and uncoupling (Review)', *Int J Mol Med*.
- Zhao, Y. and Zhao, B. (2013) 'Oxidative stress and the pathogenesis of Alzheimer's disease', *Oxid Med Cell Longev*, 2013, p. 316523.
- Zhou, Y., Wang, L., Ban, X., Zeng, T., Zhu, Y., Li, M., Guan, X.Y. and Li, Y. (2018) 'DHRS2 inhibits cell growth and motility in esophageal squamous cell carcinoma', *Oncogene*, 37(8), pp. 1086-1094.
- Zhu, J., Vinothkumar, K.R. and Hirst, J. (2016) 'Structure of mammalian respiratory complex I', *Nature*, 536(7616), pp. 354-358.
- Zielonka, J., Hardy, M. and Kalyanaraman, B. (2009) 'HPLC study of oxidation products of hydroethidine in chemical and biological systems: ramifications in superoxide measurements', *Free Radic Biol Med*, 46(3), pp. 329-38.
- Zielonka, J. and Kalyanaraman, B. (2010) 'Hydroethidine- and MitoSOX-derived red fluorescence is not a reliable indicator of intracellular superoxide formation: another inconvenient truth', *Free Radic Biol Med*, 48(8), pp. 983-1001.

Zuckerbraun, B.S., Chin, B.Y., Bilban, M., d'Avila, J.C., Rao, J., Billiar, T.R. and Otterbein, L.E. (2007) 'Carbon monoxide signals via inhibition of cytochrome c oxidase and generation of mitochondrial reactive oxygen species', *FASEB J*, 21(4), pp. 1099-106.